



UNIVERSITAT POLITÈCNICA  
DE CATALUNYA  
BARCELONATECH

## ***Protection and Fault Management in Active Distribution Systems***

**Mehdi Monadi**

**ADVERTIMENT** La consulta d'aquesta tesi queda condicionada a l'acceptació de les següents condicions d'ús: La difusió d'aquesta tesi per mitjà del repositori institucional UPCommons (<http://upcommons.upc.edu/tesis>) i el repositori cooperatiu TDX (<http://www.tdx.cat/>) ha estat autoritzada pels titulars dels drets de propietat intel·lectual **únicament per a usos privats** emmarcats en activitats d'investigació i docència. No s'autoritza la seva reproducció amb finalitats de lucre ni la seva difusió i posada a disposició des d'un lloc aliè al servei UPCommons o TDX. No s'autoritza la presentació del seu contingut en una finestra o marc aliè a UPCommons (*framing*). Aquesta reserva de drets afecta tant al resum de presentació de la tesi com als seus continguts. En la utilització o cita de parts de la tesi és obligat indicar el nom de la persona autora.

**ADVERTENCIA** La consulta de esta tesis queda condicionada a la aceptación de las siguientes condiciones de uso: La difusión de esta tesis por medio del repositorio institucional UPCommons (<http://upcommons.upc.edu/tesis>) y el repositorio cooperativo TDR (<http://www.tdx.cat/?locale-attribute=es>) ha sido autorizada por los titulares de los derechos de propiedad intelectual **únicamente para usos privados enmarcados** en actividades de investigación y docencia. No se autoriza su reproducción con finalidades de lucro ni su difusión y puesta a disposición desde un sitio ajeno al servicio UPCommons. No se autoriza la presentación de su contenido en una ventana o marco ajeno a UPCommons (*framing*). Esta reserva de derechos afecta tanto al resumen de presentación de la tesis como a sus contenidos. En la utilización o cita de partes de la tesis es obligado indicar el nombre de la persona autora.

**WARNING** On having consulted this thesis you're accepting the following use conditions: Spreading this thesis by the institutional repository UPCommons (<http://upcommons.upc.edu/tesis>) and the cooperative repository TDX (<http://www.tdx.cat/?locale-attribute=en>) has been authorized by the titular of the intellectual property rights **only for private uses** placed in investigation and teaching activities. Reproduction with lucrative aims is not authorized neither its spreading nor availability from a site foreign to the UPCommons service. Introducing its content in a window or frame foreign to the UPCommons service is not authorized (*framing*). These rights affect to the presentation summary of the thesis as well as to its contents. In the using or citation of parts of the thesis it's obliged to indicate the name of the author.



UNIVERSITAT POLITÈCNICA  
DE CATALUNYA  
BARCELONATECH

**PhD Thesis**

**Protection and Fault  
Management in Active  
Distribution Systems**

*Mehdi Monadi*

Barcelona, October 2016

# **Protection and Fault Management in Active Distribution Systems**

***Mehdi Monadi***

Dissertation submitted to the Doctorate Office  
of the Universitat Politècnica de Catalunya in  
partial fulfillment of the requirements for the  
degree of Doctor of Philosophy by the

**UNIVERSITAT POLITÈCNICA DE  
CATALUNYA**

**Electrical Engineering Department  
Research Center on  
Renewable Electrical Energy Systems**

Barcelona, October 2016



**UNIVERSITAT POLITÈCNICA  
DE CATALUNYA  
BARCELONATECH**

## Protection and Fault Management in Active Distribution Systems

Copyright © Mehdi Monadi, 2016

Printed by the UPC

Barcelona, September 2016

Research Projects: ENE 2011-29041-C02-01,  
ENE2013-48428-C2-2-R,  
ENE2014-60228-R.

UNIVERSITAT POLITÈCNICA DE CATALUNYA (UPC)

Electrical Engineering Department (DEE)

Research Center on

Renewable Electrical Energy Systems (SEER)

Rambla Sant Nebridi s/n, GAIA Research Building, UPC Campus,  
08222-Terrassa, Barcelona, Spain.

Web: <http://seer.upc.edu>

<http://www.upc.edu>

بسم الله الرحمن الرحيم



## ACKNOWLEDGEMENTS

---

First and foremost I express my gratitude to Allah, the Almighty, for enlightening my path and guiding me in each stage of life and every success I have or may reach.

I would like to express my sincere gratitude to my supervisors Prof. Pedro Rodriguez for giving me this opportunity to pursue my PhD at UPC. I would also like to thank my second supervisor Prof. Jose Ignacio Candela for his kindly supports during my study.

It is a pleasure to thank my colleagues in the research center on Renewable Electrical Energy Systems (SEER). I would like to thank all of them specially Dr. Alvaro Luna for their cooperation and valuable discussions. I also acknowledge my supervisor and colleagues in the SmarTs Lab, for their collaboration during my stay in KTH University as a visitor, especially Prof. Luigi Vanfretti and Dr. Hossein Hooshyar.

During my study I was supported by the Ministry of Science, Research and Technology of Iran. This financial support is acknowledged.

Finally, I would like to thank my family for their love, patience, and continuous supports.



The employment of renewable energy systems (RES), as a type of distributed generation (DG) units, is increasing in distribution systems. This integration changes the topology, performance and the operational aspects of conventional distribution systems. Protection is one of the main issues that are affected after the high penetration of DGs. Therefore, new protection methods are necessary to guarantee the safety and the reliability of active distribution systems.

On the other hand, most of the RESs are interfaced with the AC grids through power-electronic devices. These interfaces consist of at least one AC/DC conversion units. Hence, using DC distribution systems can contribute to the loss/cost reduction, as some power conversion stages are eliminated. Enhancement in system stability, reduction of power losses, and power quality improvement are other advantages of DC networks. For these reasons, as well as the simple integration of electronic loads that are supplied by DC power, the concept of DC distribution systems has attracted a considerable attention over the last years. In fact, MVDC and LVDC grids can be an important part of the future distribution systems. Furthermore, AC and DC system can contribute to construct hybrid AC/DC distribution systems.

According to these significant changes in the distribution systems, it is necessary to modify the algorithm of existing protection methods or to propose new protection schemes for both active AC and DC distribution systems.

Moreover, in conventional distribution systems, loads are supplied by upstream grid, i.e., transmission lines; therefore, when a fault impacts the upstream grid and the faulty part disconnected by the protection system, all loads connected to distribution systems are disconnected as well. However, in active distribution systems, DGs can support the on-outage zones if the grid equipped with an appropriate fault management system. Therefore, automatic self-healing methods can increase the network reliability and power supply continuity.

On the other hand, smart grid is a new concept that provides new capabilities for distribution systems to enhance network performance and reliability. Using the features of smart grids can provide more information from the various sections of the grid and then adapt the protection systems according to the operational conditions of the grid. Furthermore, network self-healing is introduced as one of the features of the future smart distribution grids which can increase the network reliability. To provide the self-healing capability, distribution grids should be equipped with adequate algorithms that are able to guarantee the continuous and optimal operation for the isolated section of the grid.

In this thesis, differences between protection issues in DC and AC systems are investigated and analyzed. Then, based on this analysis, effective protection and fault management methods are presented for DC distribution systems and microgrids. In the other part of this thesis, a fault management and self-healing algorithm is proposed for active distribution systems. The proposed methods have been evaluated by the hardware-in-the-loop (HIL) approach using real-time simulators and suitable controllers.

| <b>CONTENTS</b>   |    |
|---|----|
| Introduction.....   | 1  |
| 1.1. Background and motivation .....                              | 1  |
| 1.2. Challenges of protection.....                                | 4  |
| 1.3. Challenge of self-healing and fault management .....         | 5  |
| 1.4. Objectives of the thesis .....                               | 7  |
| 1.5. Thesis outline and contributions.....                        | 8  |
| 1.6. List of publications.....                                    | 9  |
| Protection of AC and DC systems. Comparison and analysis.....     | 13 |
| 2.1. Introduction .....   | 13 |
| 2.2. Fault Characteristics in AC and DC Distribution Systems..... | 16 |
| 2.2.1. Fault Characteristics in AC Systems.....                   | 16 |
| 2.2.2. Fault Characteristics in DC Systems.....                   | 17 |
| 2.2.2.1. DC-Link Capacitor Discharge Component.....               | 18 |
| 2.2.2.2. Cable-Discharge Component.....                           | 19 |
| 2.2.2.3. Grid-Side Component.....                                 | 20 |
| 2.3. Comparison of AC and DC Fault Current Characteristics .....  | 21 |
| 2.4. Protection Challenges in AC and DC Systems.....              | 23 |
| 2.4.1. Protection Challenges in AC Systems.....                   | 23 |
| 2.4.1.1. Change in the fault current level.....                   | 23 |
| 2.4.1.2. Change in the power flow direction.....                  | 24 |
| 2.4.2. Protection Challenges in DC Systems.....                   | 24 |
| 2.4.2.1. Difficulties in the coordination of O/C relays.....      | 24 |
| 2.4.2.2. Inadequacy of AC circuit breakers (ACCBs).....           | 25 |
| 2.5. Protection Methods For AC Systems Embedding DGs.....         | 26 |
| 2.5.1. Classical Alternative Methods.....                         | 26 |
| 2.5.1.1. Voltage-Based Protection .....                           | 26 |

|  |    |
|--|----|
| 2.5.1.2. Distance Protection.....  | 26 |
| 2.5.1.3. Differential Protection.....                                      | 26 |
| 2.5.1.4. Directional O/C-Based Protection.....                             | 27 |
| 2.5.2. Fault Current Limiting Methods.....                                 | 28 |
| 2.5.2.1. Application of Fault Current Limiters (FCLs).....                 | 28 |
| 2.5.2.2. Immediate Disconnection of DGs Subsequent to the Fault.....       | 29 |
| 2.5.3. Adaptive Protection Schemes.....                                    | 29 |
| 2.5.4. Communication-Based Methods.....                                    | 30 |
| 2.6. Protection Methods For DC Systems.....                                | 32 |
| 2.6.1. Fault Interruption Schemes.....                                     | 32 |
| 2.6.1.1. Converter Blocking Schemes.....                                   | 32 |
| 2.6.1.2. Converter Blocking with AC-Side CBs.....                          | 33 |
| 2.6.1.3. Converter Blocking with AC-side CBS and DC Isolator Switches..... | 33 |
| 2.6.1.4. Fault Current Limiting Methods.....                               | 34 |
| 2.6.1.5. Employment of DC Circuit Breakers.....                            | 35 |
| 2.6.2. Fault Detection Methods.....  | 36 |
| 2.6.2.1. Current-Based Protection.....                                     | 36 |
| 2.6.2.2. Distance Protection.....  | 37 |
| 2.6.2.3. Differential Protection.....                                      | 38 |
| 2.6.2.4. Signal-Processing Based Methods.....                              | 38 |
| 2.7. Comparison of Protection Methods in AC and DC Networks.....           | 39 |
| Differential- based protection for DC distribution systems.....            | 41 |
| 3.1. Fault Current in VSC-based DC Networks.....                           | 42 |
| 3.1.1. Characteristics.....  | 42 |
| 3.1.2. Choice an adequate fault current interruption method.....           | 44 |
| 3.2. Fault location using local measured quantities.....                   | 45 |
| 3.2.1. Pole to pole solid faults location.....                             | 45 |
| 3.2.2. Pole to ground faults location.....                                 | 48 |
| 3.2.2.1. Fault location in radial distribution feeders with DGs.....       | 48 |
| 3.2.2.2. Fault location in multi-terminal DC systems.....                  | 51 |
| 3.2.3. Discussion.....   | 56 |
| 3.3. Components of the proposed protection method.....                     | 57 |

---

|   |     |
|---|-----|
| 3.3.1. Main differential protection .....   | 57  |
| 3.3.2. Main and backup protection zones .....   | 58  |
| 3.3.2.1. Differential-based protection zones .....                                      | 58  |
| 3.3.2.2. Overcurrent-directional-based backup zones .....                               | 60  |
| 3.4. Proposed protection strategy .....   | 63  |
| 3.5. Real Time Simulation Results .....   | 65  |
| Protection and fault management in multi-terminal DC systems .....                      | 75  |
| 4.1. MVDC distribution system study case .....  | 76  |
| 4.2. Requirements of the proposed protection strategy .....                             | 77  |
| 4.2.1. Fault clearance using hybrid DCCBs .....   | 77  |
| 4.2.2. Fault detection by overcurrent-based local protection unit (LPU) .....           | 78  |
| 4.2.3. Fault isolation using isolator switches .....                                    | 78  |
| 4.2.4. Fault location using the proposed communication-assisted relay .....             | 78  |
| 4.3. Proposed protection strategy .....   | 82  |
| 4.3.1. Main Protection .....  | 82  |
| 4.3.2. Backup protection .....  | 84  |
| 4.3.3. Busbar protection .....  | 86  |
| 4.4. Adapting the relays threshold .....  | 87  |
| 4.5. Real-time verification and case studies .....                                      | 88  |
| 4.6. Discussion about the network operation .....                                       | 95  |
| 4.6.3. Voltage at the Microgrids's busses .....   | 100 |
| Centralized Protection and Self-Healing for DC Distribution Systems and Microgrid ..... | 103 |
| 5.1. Study Case System .....  | 104 |
| 5.2. Components of the proposed protection scheme .....                                 | 105 |
| 5.2.1. Fault interruption and isolation .....   | 105 |
| 5.2.2. Forming sub-microgrids (SMGs) .....  | 105 |
| 5.2.3. Fault detection and location .....   | 106 |
| 5.2.4. Centralized Protection Unit (CPU) .....  | 110 |
| 5.3. Proposed Protection Scheme .....   | 110 |
| 5.3.1. Main Protection .....  | 110 |
| 5.3.2. Backup protection .....  | 113 |
| 5.4. Self-healing and adapting unit .....   | 115 |
| 5.4.1. Re-calculating the SMRs setting .....  | 116 |
| 5.5. HIL verification and case studies .....  | 118 |

|   |     |
|---|-----|
| Fault management and self-healing in active distribution systems.....                 | 123 |
| 6.1. Introduction .....   | 123 |
| 6.2. Study Case .....   | 125 |
| 6.3. Requirements of the proposed ONC method .....                                    | 127 |
| 6.3.1. Network assumptions .....  | 127 |
| 6.4. Proposed Optimized-Network-Clustering (ONC) algorithm .....                      | 127 |
| 6.4.1. Constraints for successful operation of an isolated microgrid.....             | 127 |
| 6.4.2. Objective Functions for Optimal network clustering .....                       | 130 |
| 6.4.2.1. To minimize the total losses .....   | 130 |
| 6.4.2.2. To minimize the voltage deviations.....                                      | 130 |
| 6.4.2.3. To minimize the disconnected loads and enhance the reliability indices ..... | 131 |
| 6.5. Calculation of the optimization functions.....                                   | 132 |
| 6.5.1. Using network parameters.....  | 132 |
| 6.5.2. PMU-based equivalent circuit.....  | 133 |
| 6.5.3. Calculation of the PMU-based equivalent circuit.....                           | 134 |
| 6.6. Steps of the proposed method.....  | 136 |
| 6.6.1. Method Explanation.....  | 142 |
| 6.7. Converting the study grid to a hybrid AC/DC grid.....                            | 144 |
| 6.8. HIL validation and Simulation Results.....                                       | 145 |
| 6.8.1. Implementation of the proposed ONC.....  | 145 |
| Conclusions and future work .....   | 151 |
| 7.1. Conclusions .....  | 151 |
| 7.2. Future works:.....   | 153 |
| Laboratory Setup .....  | 167 |
| A. The Setup of the SEER Research Center.....   | 167 |
| B. The setup of the SmarTS group.....   | 169 |
| A Conventional ONC method.....  | 171 |

|   |    |
|---|----|
| Fig. 1.1. A conceptual scheme of the future hybrid AC/DC distribution systems.....  | 2  |
| Fig. 1.2. The concept of network-clustering.....  | 6  |
| Fig. 2.1. The structure of a prototype DC distribution system.....  | 15 |
| Fig. 2.2. Equivalent circuit for LLLG fault in AC systems.....  | 16 |
| Fig. 2.3. A simplified schematic diagram for a PP fault in a VSC-based DC grid.....   | 18 |
| Fig. 2.4. Differential protection scheme for distribution feeders.....  | 27 |
| Fig. 2.5. Directional O/C based protection.....   | 28 |
| Fig. 3.1. Equivalent circuit of a PP fault in a VSC-based DC feeder.....  | 43 |
| Fig. 3.2. Waveforms of a typical DC fault current.....  | 44 |
| Fig. 3.3. Equivalent circuit for a PP fault.....  | 45 |
| Fig. 3.4. Simplified equivalent circuit of a PP fault.....  | 46 |
| Fig. 3.5. Equivalent circuit of a PG fault in a radial DC feeder.....   | 49 |
| Fig. 3.6. Fault current from both side of a faulty line; $m=0.3$ .....  | 50 |
| Fig. 3.7. A typical mutli-terminal DC grid.....   | 52 |
| Fig. 3.8. The equivalent circuit of a PG fault occurred in Line12.....  | 52 |
| Fig. 3.9. The equivalent circuit of a PG fault occurred in Line12.....  | 53 |
| Fig. 3.10. Fault current from both side of the protected line.....  | 55 |
| Fig. 3.11. Differential protection scheme for a distribution line.....  | 58 |
| Fig. 3.13. Typical time frames for fault detection and sending the trip command.....  | 59 |
| Fig. 3.14. Symbolic logic circuit for the backup protection.....  | 61 |
| Fig. 3.15. Coordination of O/C directional relays for the backup protection scheme.....                                       | 62 |
| Fig. 3.16. Flowchart of the proposed protection strategy.....   | 64 |
| Fig. 3.17. The schematic diagram of the HIL setup.....  | 65 |
| Fig. 3.18. Single-line diagram of the study distribution system.....  | 66 |
| Fig. 3.19. Waveforms of (a) differential current seen by R34, and (b) converter current and scaled trip signal to DCCB34..... | 68 |
| Fig. 3.20. Time delay in the fault detection and sending trip signal.....   | 68 |
| Fig. 3.21. The protection zones of R34, R45, and R54.....   | 69 |

|  |     |
|--|-----|
| Fig. 3.22. The differential current and trip signals issued by (a) R54 (Zone1), and (b) R45 (Zone1). .....   | 70  |
| Fig.3.23. Trip signals of the main and backup protection for a PP fault at F2.....   | 70  |
| Fig. 3.24. Waveforms of (a) the fault and differential currents of the faulty line, and (b) the converter current for two fault resistances. ....  | 71  |
| Fig. 3.25. Trip signals send to the DCCBs.....   | 71  |
| Fig. 3.26. Backup protection zones (communication network failure). ....   | 73  |
| Fig. 4.1. A prototype multi-terminal DC distribution system. ....  | 77  |
| Fig. 4.2. The logic circuit of the CIRs.....   | 79  |
| Fig. 4.3. The fault current direction for different faults in a loop feeder; a) fault inside the protected zone; b and c) fault outside of the protected zone. ....  | 80  |
| Fig. 4.4. Flowchart of the proposed algorithm for the CIRs. ....   | 81  |
| Fig. 4.5. Study network with the protection elements.....  | 82  |
| Fig. 4.6. The time sequence of the main protection. ....   | 84  |
| Fig. 4.7. Flowchart of the LPUs algorithm. ....  | 86  |
| Fig. 4.8. Fault Current with and without operation of DCCBs. ....  | 89  |
| Fig. 4.9. Fault detection time of LPU1 and fault location time of CIR23.....   | 90  |
| Fig. 4.10. The status of DCCB1, DCCB6, DIS23, DIS32, and the open signal of CIR23.....   | 90  |
| Fig. 4.11. Fault currents seen by LPU1 and CIR23 and the pickup current of these relays..  | 91  |
| Fig. 4.12. The status of DCCB1, DIS23; the open signal of CIR23 and the trip signal of LPU1.....   | 91  |
| Fig. 4.13. Fault currents flowing through isolators of different buses. a) Bus1. Maximum positive current flows from DIS12, b) Bus2. Maximum positive current flows from DIS23, c) Bus4. Maximum positive current flows from DIS43, d) Bus6. Maximum positive current flows from DIS64. .... | 93  |
| Fig. 4.14. The status of DCCB2, DIS23, DIS32, and DIS64. ....  | 94  |
| Fig. 4.15. The status of DCCB1, DCCB2, DIS21 and the signals of CIR23 to DIS23 and CIR21.....  | 95  |
| Fig. 4.16. Simplified diagram of the study system.....   | 96  |
| Fig. 4.17. AC network voltage (Vac).....   | 96  |
| Fig. 4.18. AC network current to VSC1 (Iac).....   | 97  |
| Fig. 4.20. a) Voltage of the AC network; b) total current (Itotal).....  | 98  |
| Fig. 4.21. a) Current of the AC load (ILoad); b) current to VSC1(Iac).....   | 98  |
| Fig. 4.22. AC side voltage (Vac) during the backup protection for the network of Fig. 4.16 .   | 99  |
| Fig. 4.23. Current (Iac) during the backup protection for network of Fig. 4.16. ....   | 99  |
| Fig. 4.24. AC side voltage (Vac) and the total current (Itotal) during the backup protection for network of Fig. 4.19. ....  | 100 |
| Fig. 4.25. PCC voltage of the Microgrid-1 of the study system: three phase voltages. ....  | 101 |

---

|  |     |
|--|-----|
| Fig. 4.26. PCC voltage of the Microgrid-1 of the study system: the RMS value of phase A.       | 102 |
| Fig. 5.1. DC microgrid study case  | 104 |
| Fig. 5.2. Required data for differential and multi-terminal differential protection for a SMG. | 107 |
| Fig. 5.3. The logic circuit of the SMR.  | 108 |
| Fig. 5.4. Study microgrid equipped with the protection elements.                               | 109 |
| Fig. 5.5. The proposed algorithm for the SPRs.   | 112 |
| Fig. 5.6. The proposed algorithm of the SHA.   | 117 |
| Fig. 5.7. The operation time of the protection elements for case study1.                       | 119 |
| Fig. 5.8. The operation time of the protection elements for case study 2.                      | 120 |
| Fig. 6.1. The study distribution network and location of PMUs.                                 | 126 |
| Fig. 6.2. a. A typical FMG, and b. its equivalent circuit estimated by n PMUs [158].           | 134 |
| Fig. 6.3. A possible arrangement for FMGs of the study system.                                 | 138 |
| Fig. 6.4. Fundamental Microgrids and a possible arrangement for CMSs.                          | 139 |
| Fig. 6.5. Fundamental Microgrids and another possible arrangement for CMSs.                    | 140 |
| Fig. 6.6. The flowchart of the proposed ONC method.  | 143 |
| Fig. 6.7. The modified study grid with DC feeders to operate as a hybrid AC/DC system.         | 144 |
| Fig. 6.8. The structure of the HIL test-bed.   | 145 |
| Fig. 6.9. The front-panel of the Lab-View application designed to implement the ONC.           | 148 |
| Fig. A.1. The HIL test-bed at the SEER Research Center (UPC)                                   | 168 |
| Fig. B.1. Fundamental Microgrids and a possible arrangement for CMSs.                          | 172 |



---

|  |     |
|--|-----|
| Table 2.1. Comparison of AC and DC fault currents characteristics.....   | 22  |
| Table 2.2. Main issues associated with the use of conventional protection.....                                 | 25  |
| Table 2.3. Advantages and disadvantages of protection methods in AC distribution systems<br>embedding DGs..... | 31  |
| Table 2.4. Performance of fault interruption schemes for MVDC system of Fig. 2.1.....                          | 35  |
| Table 2.5. A summary of protection methods in AC and DC networks.....  | 40  |
| Table 3.1. The parameters of the simulated feeder.....   | 54  |
| Table 3.2. Operating times of the main and backup protection for selected fault scenarios...                   | 74  |
| Table 4.1. Meaning of the exchanged signals among CIRs.....  | 80  |
| Table 5.1. Operating times of the main and backup protection for selected fault scenarios.                     | 121 |
| Table 6.1. The rated power of DGs.....   | 126 |
| Table 6.2. Information exchange between the network elements.....  | 128 |
| Table 6.3. Data reported by the ZCUs.....  | 146 |
| Table 6.4. Various states according to the optimization function.....  | 147 |
| Table 6.5. The objective functions for various CMS cases.....  | 149 |



---

|       |  |
|-------|--|
| AC    | alternating current.                   |
| ACCB  | AC circuit breaker.                    |
| AC/DC | AC to DC conversion.                   |
| AIE   | active impedance estimation.           |
| ANN   | artificial neural network.             |
| CAU   | centralized adapting unit.             |
| CB    | circuit breaker.                       |
| CIR   | communication-assisted isolator relay. |
| CMU   | central management unit.               |
| CMS   | candidate microgrid set.               |
| CT    | current transducer.                    |
| CPU   | centralized protection unit.           |
| cRIO  | compact reconfigurable IO systems.     |
| DC    | direct current.                        |
| DC/AC | DC to AC conversion.                   |
| DCCB  | DC circuit breaker.                    |
| DG    | distributed generator.                 |
| DDG   | dispatchable DG.                       |
| DIG   | diesel generator.                      |
| FCL   | fault current limiter.                 |
| FMG   | fundamental microgrid.                 |
| HIL   | hardware-in-the-loop.                  |
| HIF   | high impedance fault.                  |
| IEDs  | intelligent electronic devices.        |
| Inst. | instantaneously.                       |
| LCC   | line-commutated converters.            |
| LG    | single-phase-to-ground faults.         |
| LLG   | double-phase-to-ground faults.         |
| LLLG  | three-phase faults.                    |
| LPU   | local protection unit.                 |

|        |  |
|--------|--|
| MRA    | multi-resolution analysis.                         |
| MVDC   | medium-voltage DC.                                 |
| MT     | micro turbine.                                     |
| O/C    | over current.                                      |
| OF     | objective function.                                |
| ONC    | optimized network-clustering.                      |
| PCC    | point of common coupling.                          |
| PG     | pole to ground.                                    |
| PMU    | phasor measurement unit.                           |
| PP     | pole to pole.                                      |
| PV     | Photovoltaic.                                      |
| RES    | renewable energy system.                           |
| RSG    | restrictive signal generator.                      |
| SHA    | self-healing and adapting.                         |
| SMG    | sub microgrid.                                     |
| SMR    | sub microgrid relay.                               |
| SPR    | source protection relay.                           |
| SSCB   | solid-state circuit breaker.                       |
| $TD_F$ | time delay for forward faults.                     |
| $TD_R$ | time delay for reverse faults.                     |
| TM     | time margin.                                       |
| TMD    | time margin of the differential-based backup zone. |
| VSC    | voltage source converter.                          |
| WTC    | wavelet transform coefficients.                    |
| ZCU    | zone control unit.                                 |

---

# Introduction

## 1.1. Background and motivation

Due to the multiple advantages of the renewable energy resources (RES), the penetration and employment of these distributed generation (DG) units is increasing in distribution systems. Although the greatest amount of electrical power is still generated by centralized conventional power plants, RESs are the world's fastest growing energy market [1]. The depletion of the fossil-fuel resources, their increasing costs, and the environmental concerns about the effects of using conventional power plants are of the main reasons that have contributed to the worldwide attention to the RESs. The worldwide commitment to reduce greenhouse emissions give a substantial support for RESs; while conventional power plants with fossil-based fuel have a significant negative effects on global warming due to their greenhouse emission, the RESs are clean resources of energy [2].

From the technical perspective, most RESs are interfaced to AC grids through power-electronic converters. These interfaces consist of at least one DC/AC conversion unit. Therefore, using DC distribution systems can contribute to the loss/cost reduction, as some power conversion stages are eliminated [3]. Decreasing the number of power conversion stages can also enhance the reliability of the system. Enhancement in system stability, reduction of power losses, and power quality improvement are other advantages of DC networks. For these reasons, as well as the simple integration of electronic loads that are supplied by DC power, the concept of DC distribution systems has attracted a considerable attention over the last years. In fact, DC grids can be introduced as an alternative for AC systems and have been considered as an important part of the future hybrid AC/DC

distribution systems. Moreover, AC and DC system can contribute to construct hybrid distribution systems in which both AC and DC grids are used simultaneously. Fig. 1.1 shows a conceptual scheme for future hybrid networks, where AC and DC systems work together in HV and MV levels for transmission and distribution grids of a city.

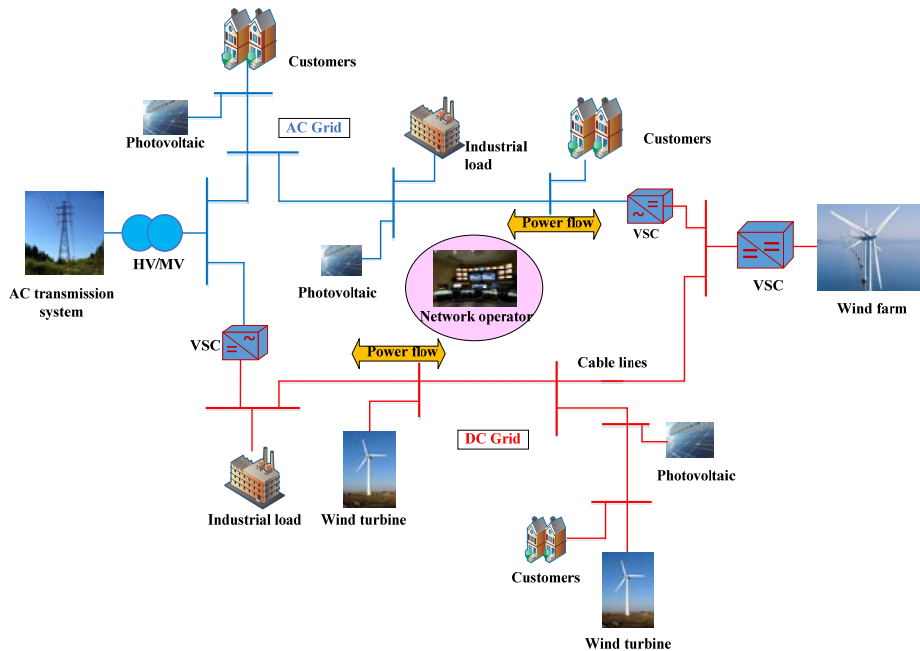


Fig. 1.1. A conceptual scheme of the future hybrid AC/DC distribution systems.

It is also worth mentioning that after the new technical developments in the power-electronic technologies, DC systems had benefited by increased attention. Due to these developments, voltage source converters (VSC), that provide more flexible operation than line-commutated converters (LCC), are available in various rated voltages and powers [4, 5]. This factor facilitates the implementation and worldwide usage of DC distribution systems. These converters can also provide control on active and reactive power and they are a suitable choice for DC distribution systems that need to be interfaced to AC systems and various types of DGs by making use of bidirectional AC/DC converter.

Another important operational aspect of active distribution systems is the possibility of autonomous and isolated operation. In conventional distribution systems, loads are supplied from upstream grid, i.e., transmission lines; therefore, following a disturbance or a fault occurrence, all of the connected loads of distribution systems, or a section of them, are

disconnected from the main grid. However, due to the presence of DGs in active distribution systems, these networks are more flexible than conventional grid. In these systems, DGs can supply and support the on-outage zones if the grid is equipped with the appropriate control and management systems. Accordingly, the implementation of adequate automatic self-healing methods can increase the network reliability and power supply continuity when a part of the grid is isolated from the rest of the network.

On the other hand, due to the variable and intermittent behavior of DGs, the recently proposed distribution systems are more dynamic and complex than conventional ones. Therefore, these systems need more complex and smart protection, control and management methods to guarantee their reliable, stable and safe operation. Thus, smart grids have been introduced as a new concept/paradigm that provides new capabilities to enhance the performance and reliability of distribution systems. Communication is one of the foundations and bedrocks of smart grids; as it can be seen in [6] provided by IEEE: “At its most basic level, the Smart Grid should be inextricably dependent on a pervasive information and communication infrastructure that overlays the electric grid itself. This infrastructure would enable collection of information—including state, sensor, demand, market pricing, and anomaly data—as well as control grid operations.”. Accordingly, when addressing the subject of smart grids, it is realistic to assume that the required communication system has already been constructed and communication-assisted protection, control and management methods can be implemented in the existing communication infrastructures.

The capabilities of smart grids make possible to collect required information from the various sections of the grid and then adapt the protection systems according to the operational conditions of the grid. Communication-based protection and network self-healing methods are introduced as important features of smart distribution grids which can increase the network reliability. A communication-assisted protection not only detect and locate faults by making use of the local measured quantities, but also is able to use the measured quantities at the other sections of the grid. Therefore, these methods normally can provide a more stable and selective protection. Furthermore, a self-healing system can divide the on-outage section into a set of microgrids that operate individually and continue the reliable supply for the maximum possible loads [7].

According to the above mentioned explanations, issues and challenges around the following two subjects are investigated in thesis in the context of smart active distribution systems:

- Protection of emerging DC distribution systems
- Self-healing and fault management in active distribution systems (AC and DC)

More explanations about the challenges related to these two subjects and specific objectives of the thesis are explained in the following sections.

### 1.2. Challenges of protection

Despite the aforementioned incentives of active distribution systems, the integration of renewable-energy-based DGs into power systems has dramatic effects on the energy supply and the service continuity of the distribution network. This integration also causes fundamental changes in the topology performance and the operational aspects of the conventional distribution systems.

Conventional distribution systems normally are supplied by the upstream transmission systems that are connected to large centralized conventional power plants. These grids are passive systems presenting mostly a radial topology. Thus, protection and control systems of these networks are typically designed based on the assumption that the power flow is unidirectional; however, integration of DGs changes this basic characteristic of the conventional distribution systems.

Furthermore, conventional power plants, such as steam power plants, have a continuous operation and consequently can supply their connected load regardless to the environment conditions; however, most of the RES-based DGs have intermittent behavior. On the other hand, DG units do not present this continuous generation profile due to technical, legal or economic constraints and consequently, networks including these units do not have a constant structure and their topology will be changed any time, according to the status of DG units. Although impacts of DGs on the distribution network depend on various parameters as size, type, location, and interconnection interface of DGs, the integration of DGs is forcing the passive distribution systems to evolve towards active networks and therefore change the traditional radial topology of the distribution feeders [8]. This operational behavior can affect the protective and control schemes and therefore, despite of the advantages of DG units, can impact negatively on the some aspects of the distribution system's operation. Coordination of the protective devices, stability, and power quality are important issues which may be affected by DG unit. Therefore, it is necessary to modify the algorithms of existing protection and control methods or propose new smart and effective protection schemes for active distribution systems.

In addition to the above mentioned issues, there are concerns about the performance of conventional protection systems in both AC and DC distributing systems; the protection of active DC distribution systems face with more challenges and issues due to the specific characteristics of fault current in VSC-based DC systems. Moreover, there are limited studies and experiences about protection issues for DC systems, and protection methods of VSC-based DC distribution systems with DGs are still in the early stages of development. Some of the main concerns about protection of DC grids are addressed here.

In AC systems, the fault impedance that consists of cable reactance and resistance, limits the fault current where the value of reactance is normally larger than its resistance. In DC networks, however, the value of reactance is quite negligible as compared to the network resistance. Moreover, following a fault occurrence, the DC-link capacitors of VSCs are discharged through the fault path and cause high transient current. Therefore, not only the peak value of the DC fault currents is higher than the peak value of the fault currents in counterpart AC systems, but also the lower value of the fault impedance gives rise to a higher rate of change of the DC fault currents. In other words, DC faults cause a high-raising-rate current, that develops faster than fault current in AC systems [9]. On the other hand, the withstand rating of semiconductor devices employed in VSCs is fairly lower than that in AC power generators [10]. Consequently, the protection systems in DC networks must operate relatively faster in order to prevent any damage to the converter's semiconductor (particularly, freewheeling diodes). The operating time of DC protection systems, which is in the range of several milliseconds, is typically less than the operating time of AC protection systems. Consequently, considering the high raising rate of DC fault current and the required faster operation of protection systems, it is difficult to coordinate conventional overcurrent relays in DC systems.

On the other hand, fault current interruption in DC systems presents other additional issues. For example, conventional AC circuit breakers (CBs) clear the fault during a zero crossing point of the current waveform; however, DC fault currents do not cross a zero point. Thus, ACCBs are not suitable for interrupting the fault current in DC grids. Although various type of DC circuit breakers (DCCB) are designed to operate related to the specification of DC fault current, in the medium and high level of voltage, DCCBs are more expensive than their counterpart AC. Consequently, is not economically feasible to equip all the feeders with this type of breakers for most distribution networks. Thus, using the minimum numbers of DCCBs should be considered as an important factor in designing and implementing protection methods of DC systems. In this regard, the global effects of the operation of DCCBs on the performance of other AC and DC feeders that are not in the faulty zone and the coordination between these CBs and other switches should be investigate as well.

### 1.3. Challenge of self-healing and fault management

The second main challenge that is considered in the thesis is related to the fault management and self-healing in active distribution systems.

Active distribution systems and microgrids can operate in grid-connected and islanded modes. Since the loads are supplied by the host network and DGs, the load-generation balance is always met in the grid-connected mode. Whereas, when following a disturbance or a fault occurrence, the entire of the distribution system, or a section of it, is disconnected from the main grid, so loads inside the on-outage section are supplied only by the DGs. In

this case, the supply-adequacy is the main concern about the successful operation of islanded grids; considering the total possible generated power of DGs, additional supervisory actions are needed to achieve the load-generation balance. In other words, supply-adequacy is the initial condition for the reliable operation of the isolated grids. Consequently, using the capabilities of smart grids, forming a supply-adequate microgrid by real-time balancing between the load and generation is known as one of the important features and essential requirements of the network self-healing process [7].

The supply-adequacy can not necessarily guarantee the optimal operation of the on-outage section. For example, supply-adequacy may need to apply a load shedding process; however, using well-designed self-healing algorithm can result in minimizing the disconnected loads. Furthermore, an optimized self-healing method can enhance the efficiency and reliability of the on-outage grid by improving some of the operational features of the grid; for instance, by minimizing the energy losses or minimizing the voltage deviations.

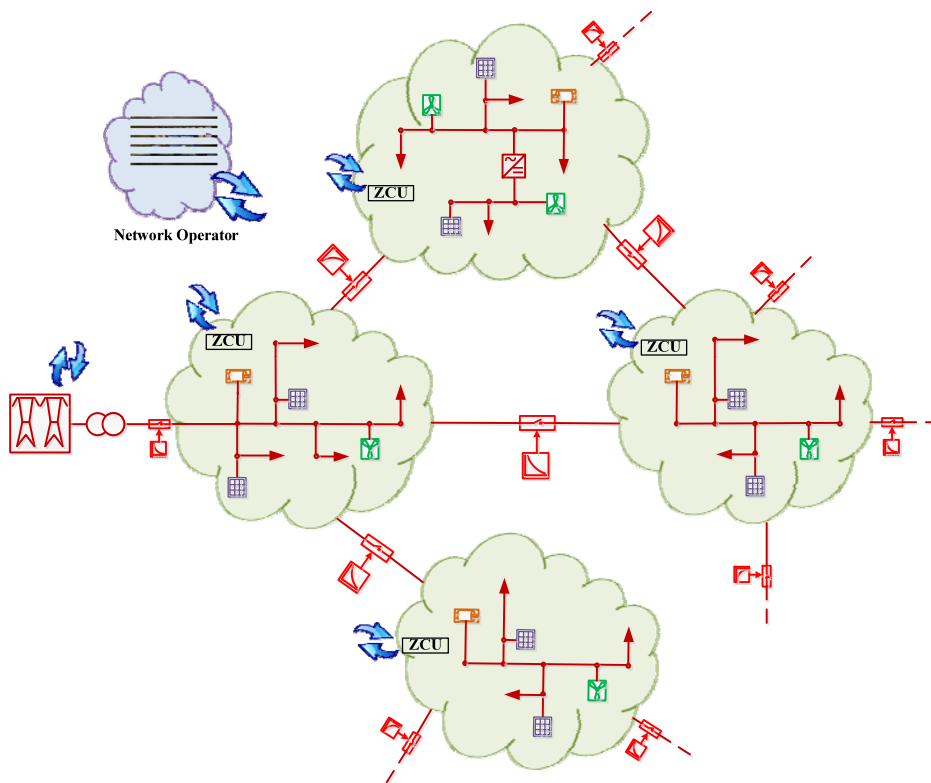


Fig. 1.2. The concept of network-clustering.

Microgrid-based network clustering was introduced as a self-healing action to continue the reliable supply for the maximum possible loads of the isolated section of active distribution systems. In this method, as it is shown in Fig. 1.2, the on-outage section is sectionalized into a set of microgrids that are able to operate individually and consequently improve the overall network operation and reliability [11]. Optimized network-clustering (ONC) in turn is a self-healing task to divide the on-outage zone to a set of microgrids considering different factors such as minimizing the total loss, power quality issues, and DG characteristics. In other words, the main goal of ONC is finding the best arrangement for network clusters (microgrids) of the on-outage zone. Although some of the previous methods, like works presented in [7, 12-14], determined the borders of each microgrid regardless to the position of existing CBs, a realistic ONC should consider the location of existing CBs as a limitation of the optimization process.

Most of the advanced network-clustering methods need to have enough information about the network topology and components (e.g. line impedance, etc.) [7, 13, 14]; however, such information is not always available; therefore, measurement-based clustering methods can be consider as a solution for providing a general ONC based on the analysis of the measured quantities from various locations of the on-outage zones. Due to the independency of the measurement-based ONC on the network topology, DGs connection/ disconnection, network reconfiguration and adding new feeders, these factors do not impact the method's accuracy. In measurement-based methods, the model/ behavior of the study grid is estimated by the use of the measured quantities. Therefore, employing the emerging measurement devices, which has been presented based on the capabilities of smart grids, provides more accurate estimation and consequently enhance the effectiveness and reliability of the ONC.

#### 1.4. Objectives of the thesis

In the previous sections the advantages and opportunities of the integration of active distribution systems and DC grids and also concerns about the protection and fault-management in these system has been addressed. Considering these challenges and according to the research policy of the SEER research center, which is focused on the development of methods and algorithms that facilitate the connection of RESs to power systems, the objectives of this thesis have been focused on two general subjects: in the first part of the thesis, tried to investigate the protection issues in the emerging DC systems, determine the weaknesses of the conventional protection methods for these networks, and present the effective protection methods for these grids; in the second part of the thesis, automatic self-healing methods for active distribution systems have been investigated and a measurement-based ONC has been presented considering the features of smart grids.

The main objectives of this thesis are the following:

- To investigate differences between the protection issues in AC and DC distribution systems and to analyze the effectiveness of the existing protection methods for active distribution systems to identify the advantages and disadvantages of these methods when they are used for VSC-based DC systems.
- To propose effective communication-based fault detection/location methods for DC distribution systems considering the specification behavior of fault current in these grids.
- To present efficient backup for the proposed communication-based protection method in order to manage the communication failure.
- To present the fault isolation methods considering the economic challenges of using the DCCBs and to complement the operation of the fault isolation methods in DC distribution systems and microgrid with fault management schemes to facilitate the network restoration, power continuously, and to enhance the network reliability.
- To develop measurement-based self-healing methods for active AC distribution systems based on the optimized-network-clustering method in order to reach to reliable and optimum operation for the on-outage zones of distribution systems.
- To evaluate the proposed methods by using the hardware-in-the-loop (HIL) approach to consider some of the practical concerns, like communication delay, that are not taken into account in off-line simulations leading to a more accurate verification.

### 1.5. Thesis outline and contributions

The rest of this thesis is organized as follows:

**Chapter 2** provides a comparison between protection issues and methods in AC and DC systems. This chapter also presents a review on the existing protection methods (state of the art) for AC and DC systems. The main parts of this chapter have been published in the first journal paper (JP1); see Section 1.6.

**Chapter 3** presents a multi-zone differential protection for DC distribution systems. The proposed multi-zone differential relay provides backup differential protections, besides the conventional differential protection, to improve the reliability of the overall protection system. The proposed method also provides a directional overcurrent-based backup protection to manage communication failures. The efficacy of the proposed technique is demonstrated through real-time HIL testing conducted in the OPAL-RT. The main parts of this chapter have been published in the second journal paper (JP2); see Section 1.6.

**Chapter 4** proposes an adaptive-communication-assisted fault location method based on the overcurrent protection. In this fast and selective protection scheme, faults are located by using the exchanged signals among the relays installed at both sides of lines. Accordingly, the fault location method does not rely on the synchronized measured current from both sides of the protected line. Moreover, the proposed scheme is equipped with a backup fault location method that is activated if communication system fails. Similar to the previous chapter, the proposed protection scheme has been implemented and tested in real-time using the OPAL-RT real-time simulator. The main parts of this chapter have been published in the third journal paper (JP3); see Section 1.6.

**Chapter 5** presents a centralized protection strategy for MVDC distribution systems and microgrids. The proposed strategy consists of a communication-assisted fault detection method with a centralized protection coordinator and a fault isolation technique that provides an economic, fast, and selective protection by using the minimum number of DCCBs. This chapter also introduces a centralized self-healing strategy that guarantees successful operation of zones that are separated from the main grid after the operation of the protection devices. Furthermore, to provide a more reliable protection, thresholds of the protection devices are adapted according to the operational modes of the microgrid and the status of DGs. The main parts of this chapter have been published in the fourth journal paper (JP4); see Section 1.6.

**Chapter 6** proposes an optimized network clustering for active distribution system. In this method after a fault occurrence, the on-outage section of the active distribution network is divided into some supply-adequacy microgrids. To achieve the optimum operation, the borders of microgrids are determined considering the total losses, voltage deviations and minimum load shedding. On the other hand, the equivalent circuit of each zone of the network is calculated based on the measured data by PMUs; therefore, the proposed clustering method determines the optimum microgrids without requirement to the information about the network topology and components. The performance of the proposed method has evaluated for AC and hybrid AC/DC grids. The proposed method and the related results of this chapter are also presented in fifth journal paper (JP5) which is under preparation as is explained in Section 1.6.

### 1.6. List of publications

This thesis has resulted in the following publications:

#### A. Journal Papers

- JP1.** M. Monadi, M.A. Zamani, A. Luna, J.I. Candela, P.Rodriguez, "Protection of AC and DC distribution systems Embedding distributed energy resources: A

comparative review and analysis”, *Renewable & Sustainable Energy Reviews*, Elsevier, vol. 51, pp. 1578-1593, 2015

- JP2.** M. Monadi, M.A. Zamani, C. Koch-Ciobotaru, J.I. Candela, P. Rodriguez, “A Communication-Assisted Protection Scheme for Direct-current Distribution Networks”, *Energy*, Elsevier, vol. 109, pp. 578-591, 2016.
- JP3.** M. Monadi, C. Koch-Ciobotaru, A. Luna, J.I. Candela, P. Rodriguez, “Multi-Terminal MVDC Grids Fault Location and Isolation”, accepted for publication in *IET Generation, Transmission & Distribution*, June 2016
- JP4.** M. Monadi, C. Gavriluta, J.I. A. Luna, Candela, P. Rodriguez, “Centralized Protection Strategy for Medium Voltage DC Microgrids”, accepted for publication in *IEEE Transactions on Power Delivery*, July 2016.
- JP5.** M. Monadi, H. Hooshyar, F. Mahmood, J.I. Candela, L. Vanfretti, P. Rodriguez, “Measurement-based Optimized Network Clustering and Restoration for Active Distribution Systems”, Under preparation; scheduled to be submitted to *IEEE Transactions on Power Systems*.

### **B. Book Chapter**

- BC1.** M. Monadi, K. Rouzbehi, J.I. Candela, P. Rodriguez, “DC Distribution Systems; a Solution for Integration of Distributed Generation Systems”, Elsevier, Accepted for publication after addressing all the comments of reviewers.

### **C. Conference papers**

- CP1.** M. Monadi, A. Luna, J.I. Candela, M. Fayezizadeh, P. Rodriguez, “Analysis of Ferroresonance Effects in Distribution Networks with Distributed Source Units” , *IECON 2013 Conference*, Austria
- CP2.** C. Koch-Ciobotaru, M. Monadi, A. Luna, P. Rodriguez, “Distributed FLISR Algorithm for Smart Grid self-Reconfiguration based on IEC61850”, *ICREA2014*, IEEE Conference
- CP3.** M. Monadi, C. Koch-Ciobotaru, A. Luna, J.I. Candela, P. Rodriguez, “A Protection Strategy for Fault Detection and Location for Multi-Terminal MVDC Distribution Systems with Renewable Energy Systems”, *ICREA 2014*, IEEE Conference
- CP4.** M. Monadi, C. Gavriluta, J.I. Candela, P. Rodriguez, “A Communication-Assisted Protection for MVDC Distribution Systems with Distributed Generation”, *PES General Meeting 2015*, IEEE Conference
- CP5.** M. Monadi, C. Koch-Ciobotaru, A. Luna, J.I. Candela, P. Rodriguez, “Implementation of Differential Relay for MVDC Distribution Systems Using Real Time Simulation and Hardware-in-the-Loop”, *ECCE 2015*, IEEE Conference

- CP6.** M. Monadi, C. Koch-Ciobotaru, A. Luna, J.I. Candela, P. Rodriguez, “Design of a Centralized Protection Technique for Medium Voltage DC Microgrids”, EPE (ECCE Europe) 2015, IEEE Conference
- CP7.** H. Ghorbani, M. Monadi, A. Luna, J.I. Candela, P. Rodriguez, “Enhanced Performance of SVC via Using Rotor Speed Deviation Signal (RSDS)”, EPE (ECCE Europe) 2015, IEEE Conference
- CP8.** A. Bidadfar, H. Hooshyar, M. Monadi, L. Vanfretti, “Decoupled Voltage Stability Assessment of Distribution Networks using Synchrophasors”, presented at IEEE PES General Meeting, 2016.
- CP9.** L. Vanfretti, H. Hooshyar, F. Mahmood, R.S. Singh, A. Bidadfar, N. Singh, M. Monadi, “Synchrophasor applications for distribution networks enhancing T&D operation and information exchange”, presented at *ISGAN-NASPI Symposium*, Atlanta, 2016.



---

## Protection of AC and DC systems. Comparison and analysis

### 2.1. Introduction

The integration of Renewable Energy Systems (RESs) such as wind energy systems, Photovoltaic (PV) systems, biomass power plants, and small hydro turbines is increasing in electric networks. These resources, which constitutes one of the most relevant technologies among DGs, are typically smaller, in terms of installed power, than conventional power plants and more distributed from a geographic point of view [15, 16]. Although the main part of electrical power is still generated by conventional power plants, RESs are the world's fastest growing energy market [1]. Moreover, deregulation of electric utilities based on the liberalism of power markets, increases the opportunity for further deployment of RESs and other types of DGs [2]. One of the main reasons for this worldwide attention is the environmental concerns about the effects of using conventional power plant. While conventional power plants with fossil-based fuel have a significant impact on the greenhouse emission and global warming, RESs stand out as clean resources of energy [2, 17]. On the other hand, the limitation of fossil fuels and their increasing costs, along with the limited investment on constructing new large power plants and transmission lines, are the other reasons that have contributed to the deployment of small power plants. These power plants can be connected at strategic points of distribution systems or close to load centers [16].

Despite the aforementioned incentives, the integration of renewable-energy-based DGs into power systems has dramatic effects on the energy supply in distribution network; it also

causes fundamental changes in the topology and operation of these networks [18]. Traditionally, distribution systems behaves as passive grids [19], which deliver the electrical power from upper voltage levels down to the loads connected to medium/low-voltage networks without generation facilities. The topology of these systems is selected based on the required consumer reliability and economic considerations. Although loop topology has been used in distribution systems, most distribution feeders have a radial structure [20, 21]. The integration of RESs into distribution networks changes the operational philosophy of conventional power systems, especially those with radial and passive nature [22, 23]. In other words, RESs converts the distribution system to an active network [19]. In addition, the intermittent nature of most RESs can adversely impact the operational aspects of power systems. Protection coordination, voltage control, system stability, and power quality are the major issues associated with DGs [24-26]. Particularly, the protection of active distribution networks may not be adequately achieved by conventional methods, and new techniques are required [21, 27, 28].

Most RESs are interfaced with the grid through power-electronic converters [16, 29]. Therefore, using DC distribution systems can contribute to the loss/cost reduction, as some power conversion stages are eliminated [3, 30]. Moreover, compared to AC systems, DC networks can transmit higher power over longer distances. The enhancement in the system's safety, reduction of electromagnetic fields, and power quality improvement are other advantages of DC networks [30]. In addition to the simple integration of most modern electronic loads, which are supplied by DC power, has attracted a lot of attention towards DC distribution systems. It is worth mentioning that almost all voltage and current levels can be currently obtained by series or parallel combination of new power electronic devices [4, 5].

The employment of medium-voltage DC (MVDC) distribution systems has so far remained as a research topic, although they had limited application such as electrical ships [31]. However, due to their advantages, they are introduced as an alternative for AC systems in future commercial and industrial grids [32-38]. The creation of multi-microgrids [39], providing a collection of grids for off-shore wind farms and wide-area solar power plants [4, 40, 41], increasing the power transmission capacity of existing AC lines [35, 42], and simple integration of industrial DC loads, [33] are some of the applications of MVDC systems. Fig. 2.1 shows a typical multi-terminal DC distribution system. Although MVDC systems can be considered as a future alternative to AC distribution networks, there are serious concerns about their application. In this regard, protection is one of the main issues associated with the application of DC grids [1, 4, 9, 43]. The differences between the characteristics of AC and DC fault currents, inadequacy of conventional protection methods for fault detection, fault location, and fault interruption devices/methods are some of the protection challenges in these grids.

No matter the type of the distribution system, it must be effectively protected against different types of faults. An effective protection scheme shall provide adequate sensitivity, redundancy, selectivity, and security [44]. Therefore, it must be designed based on the characteristics of the system as well as on the applicable standards/regulations. This means that the following main protection issues should be addressed in emerging AC and DC distribution systems:

- 1) The impacts of DGs on the protection schemes in existing AC distribution systems, requires the proposal of new effective protection methods.
- 2) The identification of the protection requirements for emerging DC distribution networks.

The main objective of this chapter is to provide a comprehensive and up-to-date review of the latest protection methods employed in AC and DC distribution systems embedding DGs. The study also identifies the differences between the protection schemes in AC and DC systems.

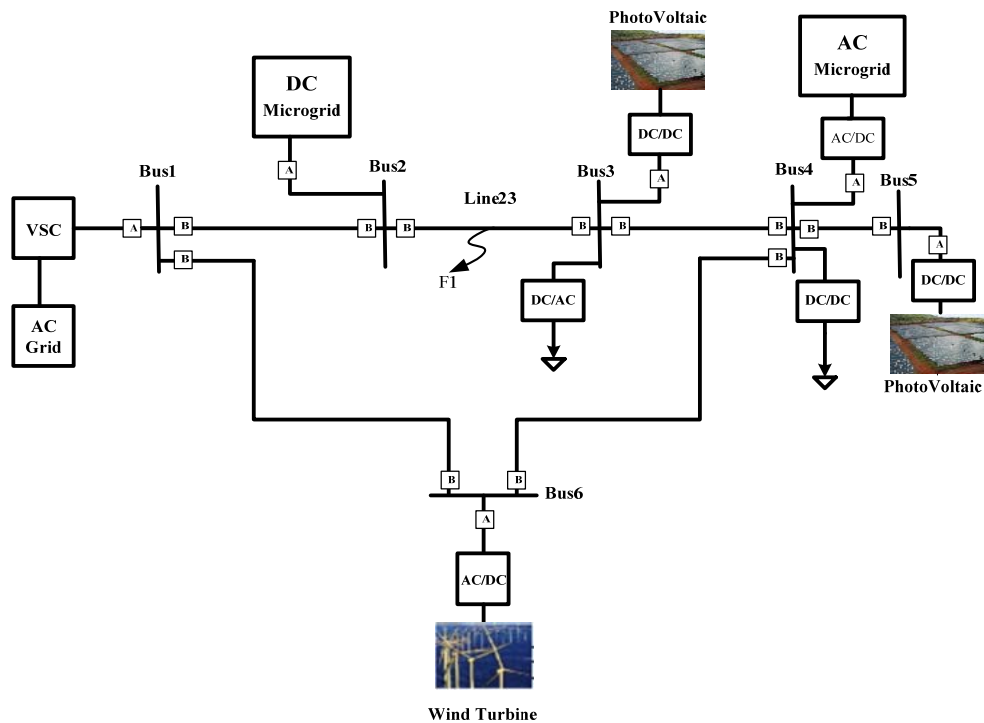


Fig. 2.1. The structure of a prototype DC distribution system.

## 2.2. Fault Characteristics in AC and DC Distribution Systems

The design of a proper fault detection method requires some knowledge of the fault current characteristics. In addition, to coordinate protective devices and to determine the type and rating of fault interrupting and/or measuring devices, the features of the fault current should be known. In this section, the main characteristics of short-circuit currents in AC and DC systems are briefly discussed while the DG impacts are ignored; the effects of DGs will be discussed in Section 3.

### 2.2.1. Fault Characteristics in AC Systems

Fault types vary from network to network. However, their classifications are universally accepted. They can generally be categorized into symmetrical faults, that is, three-phase faults (LLL, LLLG), and asymmetrical faults, that is, single-phase-to-ground faults (LG), phase-to-phase faults (LL), and double-phase-to-ground faults (LLG). The magnitude of the fault current depends on the type, location, and impedance of the fault. Typically, three-phase faults create maximum fault currents; Fig. 2.2 shows a simplified equivalent circuit of a power system when a three-phase fault impacts the network.

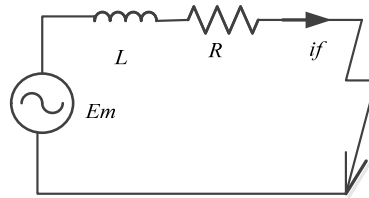


Fig. 2.2. Equivalent circuit for LLLG fault in AC systems

AC power systems are typically energized by three-phase synchronous generators, which can be modeled by a voltage source in series with an impedance. Considering the equivalent circuit of Fig. 2.3, the three-phase fault current can be obtained as [44]:

$$i_f(t) = \frac{E_m}{Z} \sin(\omega t + \beta - \theta) + \left[ \frac{E_m}{Z} \sin(\theta - \beta) + i(0^+) \right] e^{-\frac{t}{\tau}} \quad (2.1)$$

where  $E_m$  denotes the nominal source voltage;  $Z = |Z| \angle \theta$  that is the equivalent impedance, which consists of the generator impedance and the impedance from the generators terminal to the fault point, ( $Z = R + jX$ );  $\omega$  signifies the network nominal frequency (in rad/s);  $\beta$  is the phase angle (point of wave) at which the fault is initiated;  $i(0^+)$  is the pre-fault current, and  $\tau = X/R\omega$  denotes the circuit time constant.

As the equation (2.1) shows, the fault current in AC networks has two components: *i*) a decaying DC component and *ii*) a steady-state AC component [45, 46]. Although the term steady-state is commonly used, it should be noted that the magnitude of this component is not constant during the first few cycles following the fault. Therefore, subsequent to a fault, the AC component will have different magnitudes during the three following periods [47] :

1) Sub-transient period, during which the magnitude of the AC component is calculated using the generator sub-transient reactance ( $x_d''$ ); this period typically lasts less than 50ms.

2) Transient period, during which the generator transient reactance ( $x_d' > x_d''$ ) is used to obtain the fault current level; based on the transient reactance value, fault currents during the transient period (50ms-1s) are smaller than those experienced during the sub-transient period.

3) Steady-state period, during which the fault current settles at its steady-state value; the fault current at this period is calculated using the generator synchronous reactance ( $x_d > x_d'$ ) and is smaller than the sub-transient and transient fault currents.

### 2.2.2. Fault Characteristics in DC Systems

In bipolar DC systems, short circuit faults are divided into two main categories, namely, pole to pole faults and pole to ground faults. In pole to pole faults, the positive pole is directly connected to the negative pole (PP) or simultaneously connects to the negative pole and ground/neutral point (PPG). These faults are often of low-impedance type and, thus, endanger the system very seriously. Pole to ground (PG) faults, on the other hand, occur when either the positive or negative pole are connected to the ground or the neutral point. This type of faults, which usually occur due to insulation degradation, are the most common types of short circuits in DC grids; however, they are not as critical as pole to pole faults [10, 48, 49].

Different types of Voltage Source Converters (VSCs) are widely employed to connect DGs to DC grids and to construct DC switchgears. For instance, a multi-level VSC is used to interface an MVDC grid with an existing AC system [50]. The connection of PV systems and/or wind farms to DC networks also requires an energy conversion mechanism, including a medium-frequency interconnection transformer [51]. The transformer is particularly necessary for the connection of low-voltage DGs. It is important to note that, in addition to the network impedance, the operational characteristics of VSCs affect the behavior of DC faults and must be considered in the design of a proper protection system. This thesis mainly focuses on VSC-based DC distribution systems. The fault characteristics of PP faults are discussed in the following paragraphs.

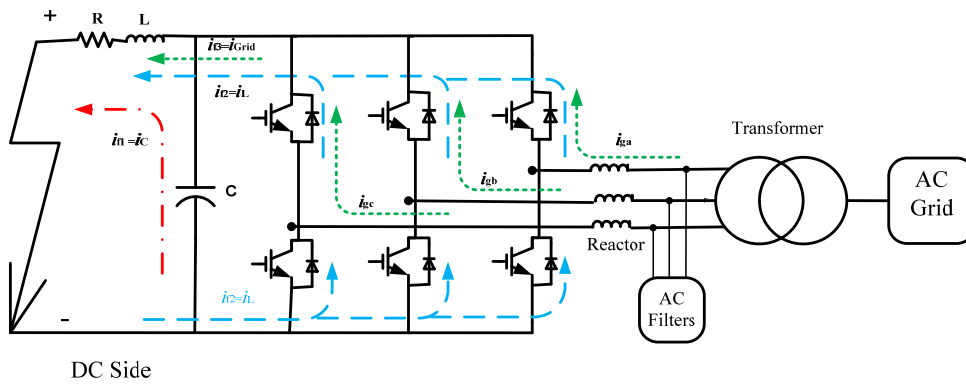


Fig. 2.3. A simplified schematic diagram for a PP fault in a VSC-based DC grid.

Fig. 2.3 shows a simplified schematic diagram of a typical PP fault assuming that a two-level VSC is used as an interface. In this figure, R and L represent the resistance and inductance of the DC line between the main DC bus (location of DC-link capacitor) and the fault location. The analysis of the equivalent circuit of Fig. 2.3 indicates that the fault current is supplied by three sources, that is, i) DC-link capacitor, ii) cable inductance (discharged through freewheeling diodes), and iii) utility grid [52, 53]. Therefore, DC fault currents are constituted of three different components with different behavior, which will be analyzed in the following.

### 2.2.2.1. DC-Link Capacitor Discharge Component

Following the occurrence of the fault in DC grids, the DC-link capacitor is discharged, mainly due to the voltage drop of the main DC bus. Using the equivalent circuit of Fig. 2.3 (see also Table 2.1), the DC-link capacitor component,  $i_c$ , can be obtained by solving the following second-order differential equation:

$$\frac{d^2 i_c}{dt^2} + \frac{R}{L} \frac{di_c}{dt} + \frac{1}{LC} i_c = 0 \quad (2.2)$$

where R and L denote the DC line resistance and inductance, respectively; and C represents the capacitance of the DC-link capacitor. Depending on the damping factor (i.e.,  $\xi$ ) of the RLC circuit (see Table 2.1), three different kind of responses can be considered for the DC-link capacitor current, namely, i) under-damped response ( $\xi < 1$ ), ii) critically damped

response ( $\xi = 1$ ), and iii) Over-damped response ( $\xi > 1$ ). The damping factor, in turn, is given by:

$$\xi = \frac{R}{2} \sqrt{\frac{C}{L}} \quad (2.3)$$

As the equation (2.3) shows, the waveform of the DC-link capacitor current depends on the system impedance (R and L) as well as on the DC-link capacitor (C). For example, in a short distribution feeder, if a solid fault impacts the DC line, the fault current will have most of the times an under-damped behavior which can be mathematically described as [52]:

$$i_c(t) = -\frac{V_0}{L\omega_d} e^{-\frac{R}{2L}t} \sin(\omega_d t) + I_0 e^{-\frac{R}{2L}t} \left[ \cos(\omega_d t) + \frac{R}{2L\omega_d} \sin(\omega_d t) \right] \quad (2.4)$$

Where

$$\omega_d = \sqrt{\frac{4L - R^2C}{4L^2C}} \quad (2.5)$$

and  $V_0$  and  $I_0$  are the initial values of the capacitor voltage and the cable current.

The above discussion shows that the fault impedance can significantly affect the characteristics of the DC-link capacitor component of the fault current. In particular, the fault resistance changes both the magnitude and transient response of the fault current. It should be also pointed out that the DC-link capacitor current appears subsequent to a fault in all VSC-based DC grids, whereas the existence of the two other fault current components depends on other factors including the type and control of the VSC supplying the DC bus.

### 2.2.2.2. Cable-Discharge Component

Fig. 2.3 shows a typical VSC whose DC side is affected by a fault. Subsequent to the fault, the control scheme of the converter turns off the VSC switches (e.g., IGBTs) to protect them against the overcurrent condition. Once the switches are blocked and the DC-link capacitor is discharged ( $V_c(t) = 0$ ), the energy stored in the cable inductance will be discharged through the antiparallel freewheeling diodes. Using the equivalent circuit of this phase (see Table 2.1), the cable-discharge component,  $i_L$ , can be obtained by solving the following first-order differential equation:

$$L \frac{di_L}{dt} + i_L \cdot R = 0 \quad (2.6)$$

Solving (5), the cable-discharge current is calculated as:

$$i_L(t) = I_0 e^{-\frac{R}{L}t} \quad (2.7)$$

### 2.2.2.3. Grid-Side Component

Following the blocking of the main converter switches, the VSC operates as an uncontrolled full-bridge rectifier; thus, it continues to feed the fault from the AC grid through the freewheeling diode paths [54, 55]. In case of a three-phase AC-to-DC converter, this rectified current is obtained by:

$$i_{Grid}(t) = i_{ga'}(> 0) + i_{gb'}(> 0) + i_{gc'}(> 0), \quad (2.8)$$

where  $i_{gx'}(> 0)$  denotes the positive value of the phase-x current ( $i_{gx}$ ) which contributes to the fault current through the freewheeling diodes. For example, the phase-a part  $i_{ga'}(> 0)$  is calculated as [53] :

$$i(t) = K_1 \sin(\omega_s t + \gamma) + K_2 e^{-\frac{R}{L_T}t} + \frac{K_3}{\omega_d} \omega_0 e^{-\frac{R}{L}t} \sin(\omega_d t + \beta) \quad (2.9)$$

$$+ \frac{K_4}{\omega_d} \omega_0 e^{-\frac{R}{L}t} \sin(\omega_d t)$$

where  $K_1 = I_g [(1 - \omega_s^2 LC)^2 + (RC \omega_s)^2]^{-\frac{1}{2}}$ ;  $L_T = L_{Reactor} + L$ ;  $\gamma = \alpha - \arctan\left(\frac{RC \omega_s}{1 - \omega_s^2 LC}\right) - \arctan\left(\frac{\omega_s L_T}{R}\right)$ ;  $K_3 = -(K_1 \sin \gamma + K_2)$ ;  $K_4 = \frac{K_2 L_T}{R} - \omega_s K_1 \cos \gamma$ ;  $I_g$  is the maximum grid current amplitude; and  $\omega_s$  and  $\alpha$  are the angular frequency and phase voltage angle of phase-a.

It should be noted that, except the DC-link capacitor current, the other two fault current components flow through the freewheeling diodes; thus, these diodes may get damaged quickly if proper provisions are not put in place [54, 56].

#### 2.3. Comparison of AC and DC Fault Current Characteristics

Based on the discussion of Sections 2.1 and 2.2, it is evident that AC and DC fault currents have different characteristics. From the point of view of the system protection, the main differences are:

- Since the AC fault current has a sinusoidal shape, it has two zero crossing points in each period. Hence, the fault interrupting devices can break the currents during a zero crossing of the current waveform. However, DC fault currents do not cross a zero point. Consequently, AC breakers are not suitable for breaking DC fault currents.
- In AC power systems, the fault impedance consists of a reactance and a resistance, where the value of reactance is normally larger than its resistance, that limit the fault current. In DC networks, however, the value of reactance is quite negligible if compared with the network resistance. Consequently, not only the peak value of DC fault currents is higher than the peak value of the faulty currents in counterpart AC systems, but also the lower value of the fault impedance gives rise to a higher rate of change of the DC fault currents [57].
- Since DC faults cause a high-raising-rate currents, faults in VSC-based DC systems develops faster than AC systems [9, 58]. On the other hand, the withstand rating of semiconductor devices employed in VSCs is fairly lower than that in AC power generators [10]. Consequently, the protection systems in DC networks must operate relatively faster in order to prevent any damage on the converter's semiconductors (particularly, freewheeling diodes). The operating time of DC protection systems, which is in the range of several milliseconds, is typically less than the operating time of AC protection systems and it is given by [53]:

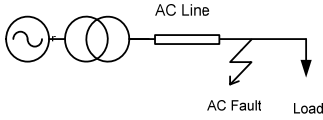
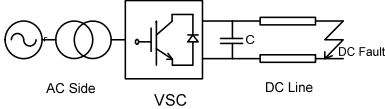
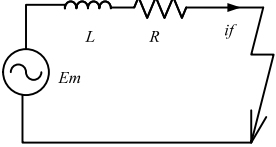
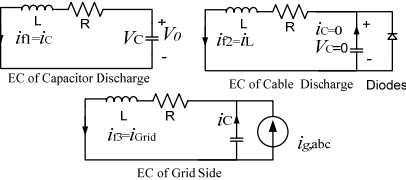
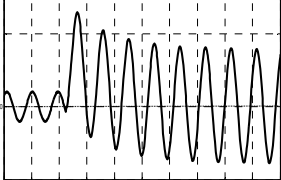
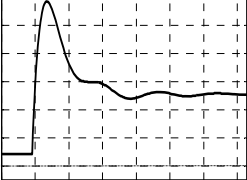
$$t_1 = (\pi - \arctan((V_0 C \omega_0 \sin \frac{\beta}{V_0 C \omega_0 \cos \beta - I_0}) / \omega)) / \omega \quad (2.10)$$

where  $\omega_0 = \frac{1}{\sqrt{LC}}$ .

It can be concluded from Equation (2.10) that many conventional protection methods for AC systems are not suitable for DC systems as they are not fast enough. Thus, conventional protection schemes in AC grids should be modified to fulfill the fault detection/isolation requirements in DC systems. To provide a better understanding of issues, Table 2.1 has summarized the main differences between the characteristics of AC (LLLG) and DC (PP) fault currents.

## Chapter2. Protection of AC and DC systems. Comparison and analysis

Table 2.1. Comparison of AC and DC fault currents characteristics.

|  | AC Fault (LLG)  | DC Fault (PP)   |
|--|---|---|
| Schematic of faulty feeder               |  |   |
| Equivalent circuit (EC) of faulty feeder |  |   |
| Fault Current waveform                   |  |   |
| First stage of fault current             | Sub-transient stage:<br>$I_f'' = \frac{V_F}{(Z_{net} + x_d'')}$                   | Capacitor discharge current (for under-damping condition):<br>$i_c(t) = \frac{V_0}{L\omega_d} e^{-\alpha t} \sin(\omega_d t) + I_0 e^{-\alpha t} [\cos(\omega_d t) - \frac{\alpha}{\omega_d} \sin(\omega_d t)]$ |
| Second stage of fault current            | Transient stage:<br>$I_f' = \frac{V_F}{(Z_{net} + x_d')}$                         | Cable discharge current:<br>$i_L(t) = I_0 e^{-\frac{R}{L}t}$  |
| Final stage of fault current             | Steady state current:<br>$I_f = \frac{V_F}{(Z_{net} + x_d)}$                      | The rectified grid side current:<br>$i_{grid}(t) = i_{ga} (> 0) + i_{gb} (> 0) + i_{gc} (> 0)$  |
| Zero crossing time                       | Based on the rated frequency.   | No zero crossing point (direct current).  |
| Maximum value of fault current           | Is related to voltage and equivalent fault impedance.                             | Is according to the size of DC-link capacitor, DC voltage and equivalent fault impedance.   |
| Effect of fault impedance                | Change the amplitude of fault current.  | Change in the fault current characteristics. (Under/over/critical damping).   |
| Ideal fault clearing time                | The first possible zero crossing point.   | Before finishing the capacitor discharge stage.   |

### 2.4. Protection Challenges in AC and DC Systems

Conventional distribution systems are passive networks which are mostly arranged in radial topology [20]. These networks are normally protected by current-based devices such as O/C relays, fuses, reclosers, and sectionalizers. The O/C protective relays monitor the current flowing through a protected circuit/element and trip the CB if the current exceeds a threshold value for a specific period of times. The operating time of the relay is determined by the current magnitude measured by the relay, the relay settings, and the employed time-current characteristic (definite-time or inverse-time). The O/C relays provide a non-unit protection in which the physical borders of the protected zone are not specified. The main feature of the non-unit protection is that the upstream relays can provide remote backup for downstream ones. However, the coordination between the main and backup relays should be performed very accurately so that an adequate selectivity and sensitivity are achieved. Conventional protection systems are designed based on the assumption that there is a unidirectional flow of power within the network, which may be affected in the presence of DGs. With the increasing penetration of DGs, the fundamentals of distribution system protection have been challenged. In the following paragraphs, the main issues associated with the protection of AC distribution system embedding DGs as well as the protection challenges of DC grids are discussed.

#### 2.4.1. Protection Challenges in AC Systems

As discussed in the previous section, the introduction of DGs has affected several operational aspects of AC power systems including their protection philosophy [20, 59]. Although the impacts of DGs on the distribution network depend on factors such as: size, type, location, and interconnection interface of DGs [59-62], they can potentially change the following: *i*) fault current level of the feeder and *ii*) power flow direction on the feeder. These changes, in turn, can impact the performance of current-based protection schemes as described below.

##### 2.4.1.1. Change in the fault current level

DGs can change the fault current seen by a protective device depending on their size, type, location, and interconnection medium [63]. The increment in current can cause nuisance tripping if the measured current by the relay exceeds its pick-up setting. On the other hand, O/C protective devices of a distribution feeder are coordinated for a range between the minimum and maximum fault currents of that feeder. Therefore, any change in the fault current may lead to the protection mis-coordination amongst relays, fuses, and reclosers [28, 64]. Moreover, in the presence of DGs, both DG and the main grid will contribute to the fault and hence, the fault current will be shared between them. This can reduce the fault contribution of the main grid and cause a delayed operation (or non-operation) of the

corresponding relays, which is known as “blinding of protection”[47]. The severity of protection blinding depends on the local short-circuit level, grid impedance, and DG capacity and location [28].

### 2.4.1.2. Change in the power flow direction

Connection of a DG to a distribution feeder can also change the power flow and fault current direction in the corresponding feeder [62]. Therefore, the coordination amongst current based devices can be disrupted as most of them are non-directional units. On the other hand, when a DG is installed on a feeder, it can contribute to faults located on adjacent radial feeders. In this case, due to the change of the fault current direction (i.e., from feeder to main bus), the non-directional relays may incorrectly operate for a fault in the neighboring feeder. This issue, which is referred to as the “false tripping” in the technical literature [47], can decrease the system reliability. It should be pointed out that, with the addition of DGs to distribution networks, the demands will play a more active role in power systems. Thus, the system operational condition may regularly change. This requires the protection system to adapt itself to the new operational situation in order to ensure the system reliability.

### 2.4.2. Protection Challenges in DC Systems

In addition to the aforementioned issues which may happen in both AC and DC systems with DGs, there are specific challenges which are related to the use of conventional protection devices in DC systems. These issues, which can exist with or without the presence of DGs, are described in the following subsections.

#### 2.4.2.1. Difficulties in the coordination of O/C relays

The key point in the coordination of time-inverse O/C protective devices is the discrepancy between the fault currents measured by them. Due to the low value of the line reactance and the high rising rate of DC fault currents, the coordination of O/C relays in DC systems is a challenging task [65, 66]. As mentioned before, the rising rate of DC fault currents is relatively higher than in AC fault currents. Therefore, subsequent to the fault, all the in-series O/C relays simultaneously measure a high  $I_{\text{Fault}}/I_{\text{Setting}}$  ratio. This may lead them to operate on instantaneous mode. Moreover, O/C relays must be able to effectively detect both PP and PG faults, whereas there is a significant difference between the current magnitudes of these two types of fault. If the relay settings are selected based on the PP fault currents, it may result in the delayed operation of the protection scheme for PG faults. On the other hand, selection of a low pick-up for the relay may cause protection mis-coordination for PP faults. In the work presented in [3] various fault scenarios for a typical DC feeder have been analyzed. The results of the study show that O/C relays cannot protect DC systems in a coordinated manner, leading to a decreased selectivity. Although definite-time O/C relays

can be used as an option to achieve selectivity in DC systems, the coordination of definite-time relays may result in a long fault clearance in large DC systems with several radial lines [67].

**2.4.2.2. Inadequacy of AC circuit breakers (ACCBs)**

ACCBs are conventional fault current interrupters in distribution systems; they typically have a mechanical operating mechanism which is capable of clearing the fault in several tens of milliseconds [68]. ACCBs interrupt the fault current during a zero crossing of the current waveform. DC fault currents, however, do not cross zero point. Moreover, DC systems require a relatively faster protection system capable of operating in several milliseconds to prevent any damage to the freewheeling diodes of VSCs [3, 56, 69]. Therefore, conventional ACCBs are not suitable for fault current interruption in DC systems. Different types of solid-state and hybrid DC breakers have been proposed/implemented [70, 71]. However, due to the economic and technical issues associated with these CBs, fault interrupting devices are still one of the main challenges in the development of DC systems. Table 2.2 provides a summary of the main protection issues in AC distribution systems embedding DGs as well as MVDC grids.

Table 2.2. Main issues associated with the use of conventional protection.

| Method                           | AC distribution systems  | DC distribution systems  |
|----------------------------------|--|--|
| <b>O/C based fault detection</b> | Without DG: <ul style="list-style-type: none"> <li>• Coordination of protection devices.</li> <li>• Detection of High-Impedance Faults (HIF)</li> </ul>  | Without DG: <ul style="list-style-type: none"> <li>• Difficult relay coordination due to the high raising rate of DC fault currents.</li> <li>• Fault resistance changes not only the peak value of the fault current, but also changes its specifications.</li> </ul>   |
|                                  | With DG: <ul style="list-style-type: none"> <li>• Change in the current of the feeder which can cause nuisance tripping.</li> <li>• Mis-coordination between current based devices due to the change in the minimum and maximum level of fault and also current direction.</li> <li>• False tripping. Blinding of the protection. Need of relays with flexible settings</li> </ul> | With DG: <ul style="list-style-type: none"> <li>• Similar issues as AC systems.</li> <li>• Requirement for a fast action protection limits obtaining of the useful information for fault location [56].</li> </ul>   |
| <b>AC circuit breakers</b>       |  | <ul style="list-style-type: none"> <li>• ACCBs interrupt the fault current at zero-crossing points which do not exist in DC fault currents.</li> <li>• ACCBs are not fast enough to prevent damages on the freewheeling diodes of the VSC.</li> <li>• Major economic and technological challenges around production of solid-state or hybrid DCCBs.</li> </ul> |

### 2.5. Protection Methods For AC Systems Embedding DGs

As discussed above, the integration of DGs in the distribution systems results in the inefficiency of traditional O/C protection schemes. Therefore, in this section, various protection methods that have been proposed for AC distribution systems with DGs are studied.

#### 2.5.1. Classical Alternative Methods

Due to the inadequacy of O/C relays, other traditional methods such as voltage-based methods, impedance-based methods, differential relays, and directional relays have been proposed as the first alternatives to address the protection issues associated with the DG penetration in distribution feeders. These methods are described below.

##### 2.5.1.1. Voltage-Based Protection

A voltage-based method has been proposed in [72] in which the RMS value of the DG terminal voltage is measured continuously. If this value is above 88% of the rated voltage, it is considered as normal condition (or an out-of-zone fault). However, when this value drops below 88% of its nominal rating, it is interpreted as a fault close to the DG; thus, the DG has to limit its output current through the intervention of the control system. The main advantage of the voltage-based methods is that their performance is independent of the value/direction of the current, which may change in the existence of DGs. However, the network voltage can be affected by various transient incidents other than faults. Therefore, this type of protection would be vulnerable to transient cases such as load switching and/or energization of dynamic loads. On the other hand, voltage-based methods cannot provide an adequate selective protection.

##### 2.5.1.2. Distance Protection

Distance or impedance-based protection is one of the traditional protection schemes for transmission lines. Introduction of DGs to distribution systems have made them similar to transmission networks where power can flow in both directions. Therefore, distance relays can be used for active distribution systems [73] where protection zones are defined based on the DG location. The main issue about using impedance-based relays is the effect of fault resistance on the calculated impedance. The effect is particularly important in distribution system where the lines are short and the feeders are more likely to experience high-impedance faults. In addition, the measured current by distance relay depends on the DG status which, in turn, impacts the impedance measured by the relay.

##### 2.5.1.3. Differential Protection

Differential relays offer a sensitive unit protection capable of detecting faults in a short period of time; moreover, the protection scheme is not affected by the DG type, location, and size. Therefore, differential relays can be used to overcome the limitation of non-unit protections in the existence of DGs [74]. As shown in Fig. 2.4, the relay located at one end of the line receives the current measurements from the other end via the communication link; the relay monitors the current difference between the two ends of the line and issues a trip signal if this differential current exceeds a threshold. Since unit protections cannot provide backup for other neighboring relays, differential relays should be equipped with a backup protection scheme. For example, wide area backup protection has been proposed in [75]. The implementation of this backup method in distribution feeder requires additional communication links. However, due to the requirement of communication infrastructure, this method is not an economic solution for some types of small distribution system. It is noted that a synchronizing mechanism may also be needed in case the line is long [76].

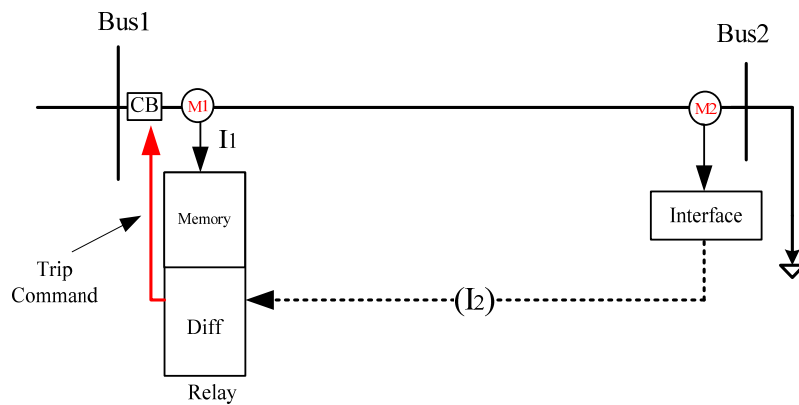


Fig. 2.4. Differential protection scheme for distribution feeders.

#### 2.5.1.4. Directional O/C-Based Protection

In active distribution systems, fault current can be supplied by more than one source and fed from more than one direction. Therefore, directional overcurrent units have been used to determine the faulty feeder when each feeder embeds several DGs [27, 77]. Fig. 2.5 shows a simple three-feeder distribution system with directional O/C relays. Once a fault occurs in a feeder, it is fed by all DGs in the system as well as the main utility grid. Therefore, the O/C relays installed at the beginning of healthy feeders may measure large current in reverse direction. If non-directional relays are used, there is a possibility of protection mal-operation. Using directional units, only the protective relay of the faulty feeder operates, after  $t_{fwd}$ , and other devices work as backup for this relay. It should be noted that O/C elements are coordinated considering the presence of DGs [27]. Moreover, in addition to distribution

feeders with high penetration of DGs, this method can be applied to collector grid of wind-power plants [78].

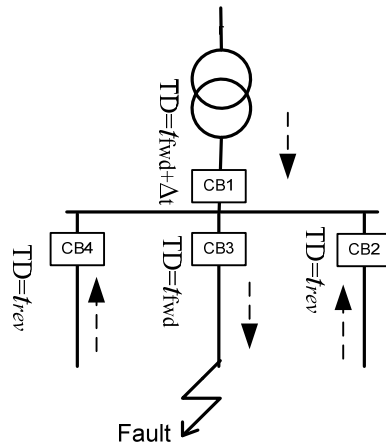


Fig. 2.5. Directional O/C based protection.

### 2.5.2. Fault Current Limiting Methods

The protection issues in active distribution systems are mainly caused by the contribution of DGs to fault currents. Therefore, several methods have been proposed to decrease/eliminate the contribution of DGs to the fault without using adaptive techniques. These methods rely on either Fault Current Limiters (FCLs) or DG disconnection subsequent to the fault; they are discussed below.

#### 2.5.2.1. Application of Fault Current Limiters (FCLs)

FCL is a devices that has no effect on the normal operation of the distribution system, but insert a high impedance in series with the DGs (immediately after the fault inception) to limit the magnitude of the fault current [64]. These devices are used to decrease/eliminate the fault current contribution of DGs in order to prevent mis-coordination amongst O/C relays [79, 80]. Typically, FCL have a constant impedance although the use of variable-impedance FLCs has also been proposed in the literature [64]. In these types of FCL, the impedance of the FCL is adapted according to the system operating condition. Using FCLs, the fault current level will not significantly change in different operational modes of distribution systems and, hence, protection coordination is maintained. However, the application of FLC-based methods in typical distribution systems requires more experience with these devices [81]. In addition, the performance of FCLs for transient incidents, suddenly change in load current, and high-impedance faults should be thoroughly studied[82].

### 2.5.2.2. Immediate Disconnection of DGs Subsequent to the Fault

In this method, all the DGs connected to the faulty feeder will be disconnected from the network once a fault is detected. As such, the conventional protection will not be disrupted by the DG contributions [83]. In some of the already presented technical documents, it was recommended that, subsequent to abnormal voltages/frequencies caused by network faults, DGs must be disconnected in a pre-specified period of time [84]. The temporary/permanent disconnection of DGs in response to faults is a simple method to preserve coordination between protective devices. The main disadvantage of this method is that all DGs that experience the voltage drop will be tripped, even if they are not directly connected to the faulty feeder. Thus, the use of communication media has been proposed to prevent unnecessary tripping of DGs. For example, Reference [85], has proposed to divide the distribution system into several zones controlled by a central relay. The boundaries of the zones are determined based on the location of the CBs. The proposed method is able to detect the faulty zone and send the trip signals, via communication links, to the corresponding CBs and DGs in order to isolate the faulty zone. Consequently, only the DGs inside the faulty zone are disconnected in response to the fault. A similar method has been proposed in [86] where Artificial Neural Network (ANN) has been used to detect the faulty zone. It should, however, be noted that recent standards make some allowance for DGs to remain connected during faults in order to mitigate voltage drops, improve system stability, and increase network reliability [87].

### 2.5.3. Adaptive Protection Schemes

As discussed earlier, fixed relay settings may not provide adequate protection for distribution systems with DGs. Therefore, adaptive protection schemes have been introduced in such a way that the relay settings/characteristics are adapted based on the operational condition of the power system [88]. Most of the adaptive methods have the following common elements [63]:

- 1) A central unit for continuous monitoring of the operational parameters of the protected system such as current and voltage.
- 2) An algorithm developed in the central unit to recognize the structure of the network by analyzing vital data such as status of CBs and/or DGs.
- 3) An effective method to calculate/select new protection settings based on the system operating conditions. All the required settings can be calculated off-line and stored in a look-up table or be calculated on line.
- 4) An efficient communication medium amongst protective devices and central controller.

Although the aforementioned elements are necessary for an effective adaptive scheme, they may not be sufficient. The main difference between various adaptive methods is the algorithms used to determine protection settings. Therefore, based on the complexity level of

the power system, the central controller must be equipped with the proper relay coordination algorithms. The proposed methods for the calculation of relay settings in distribution systems with high penetration of DGs can be broadly divided into the following categories:

- 1) Mathematical methods: various mathematical methods such as graph analysis [89] and optimization methods [90] are used for relay coordination in loop networks. These methods can also be applied to active distribution systems; however, they are typically time consuming and must be executed after any change in the topology of the distribution system.
- 2) Intelligent methods: Genetic Algorithm (GA) [91], ANN [92-94], and fuzzy systems are some of the intelligent-based techniques that have been proposed for relay coordination in the presence of DGs.

Although adaptive methods can provide acceptable protection for active distribution systems, they are normally expensive due to the communication requirements. Moreover, after any fundamental change in the distribution system (e.g., addition of new feeder), it is necessary to update the relay coordination algorithm [95].

### 2.5.4. Communication-Based Methods

With the recent advances in communication technologies, it has become possible to employ accurate, secure, and safe protection methods using network-wide information. Various types of data can be transferred to different elements of protection systems through communication links. For instance, an agent-based method has been proposed in [96] to coordinate relays in the presence of DGs. In this method, to coordinate the relay settings by using a pair-to-pair method, the adjacent relays exchange their current through communication link. A multi-agent based protection method has also been presented in [21], where the current of adjacent and remote buses are analyzed using the wavelet transform to detect the fault. Reference [85] proposed an adaptive communication-based scheme in which transfer trip signals are sent from a central relay to all CBs. In the communication-assisted method proposed in [97], the current directional information is used to detect the faulty section. Once the faulty zone is detected, a trip signal is sent out to the corresponding CB(s) to isolate the section. In [98], by using the signs of the wavelet transform coefficients (WTC), the relay of each bus recognizes that fault is inside the bus or not. If the fault is recognized to be external, each busbar relay exchanges the direction of the fault current with the neighboring busbar relay(s) to determine the faulty feeder. The reliability of the communication media is the main concern associated with communication-based protection methods. In addition, it is costly to establish a high-speed communication link within the electric network.

## 2.5. Protection Methods For AC Systems Embedding DGs

Table 2.3. Advantages and disadvantages of protection methods in AC distribution systems embedding DGs

| Protection method       | Advantage   | Disadvantage  |
|-------------------------|---|---|
| Voltage based           | <ul style="list-style-type: none"> <li>Stable performance against change in the value/direction of current, due to DG connection.</li> </ul>  | <ul style="list-style-type: none"> <li>Operation for transient incidents and disturbances.</li> <li>Vulnerability to HIFs.</li> <li>Cannot provide adequate selectivity.</li> </ul>   |
| Distance                | <ul style="list-style-type: none"> <li>Providing backup for neighbor protection devices.</li> </ul>   | <ul style="list-style-type: none"> <li>Fault impedance impacts measured impedance and cause mis-operation.</li> <li>Limited accuracy for distribution systems with short lines.</li> <li>The reach of the relay can be reduced due to the installed DG.</li> </ul>                                |
| Differential            | <ul style="list-style-type: none"> <li>Better sensitivity</li> <li>Lower dependency to fault impedance.</li> <li>Provide selective protection.</li> <li>The current direction does not impact the fault detection.</li> </ul> | <ul style="list-style-type: none"> <li>Requirement to communication link which increase the cost of the implementation.</li> <li>No backup protection is provided.</li> <li>Dependency on communication.</li> </ul>   |
| Directional O/C         | <ul style="list-style-type: none"> <li>Applicable for networks with different type of DGs</li> <li></li> </ul>  | <ul style="list-style-type: none"> <li>Long delay on the operation of backup protections for large-scale power systems due to using time constant relays.</li> <li>Applicable for small scale distribution systems with radial configurations.</li> </ul>   |
| Fault current limiting. | <ul style="list-style-type: none"> <li>No need to protection audit (DGs do not affect protection coordination).</li> </ul>  | <ul style="list-style-type: none"> <li>No systematic method to find the exact values of FCL impedance.</li> <li>Requires more experience and development to provide reliable devices especially for networks with high short circuit level.</li> <li>Dependency operation time of FCL.</li> </ul> |
| DG disconnection        | <ul style="list-style-type: none"> <li>Relays coordination is simply preserved without any external devices.</li> </ul>   | <ul style="list-style-type: none"> <li>Negative network-wide impacts (e.g., on the voltage stability)</li> <li>Impacts on the sound loads and reduced selectivity/security</li> <li>Increased outage time due to the delay on returning the system to normal condition.</li> </ul>                |
| Communication based     | <ul style="list-style-type: none"> <li>Can provide a fast and selective protection without any complex algorithm.</li> </ul>  | <ul style="list-style-type: none"> <li>Requirement to a backup protection during the communication failures.</li> <li>Costly method due to the requirement to high speed and reliable communication.</li> </ul>   |
| Adaptive protection     | <ul style="list-style-type: none"> <li>Providing accurate setting for various operating conditions.</li> <li>Possibility of using effective algorithms for detection of such special faults as HIFs.</li> </ul>               | <ul style="list-style-type: none"> <li>Communication requirements which impact system cost and reliability.</li> <li>Need to complex methods for relay setting calculations, especially in a high- DG penetrated environment.</li> </ul>  |

IEC61850 is one of the standard protocols which is used in substation automation applications in order to meet the increasing demand of modern power systems [99]. It is an Ethernet-based protocol which has the capability to be translated for the future communication networks [100]. In this protocol, the data is represented in an object-oriented manner and is transmitted multiple times to ensure its receipt. Moreover, IEC61850 can be used for time-critical applications where a fast protection scheme is required [101, 102]. According to this protocol, a standard format is used for the data format which is communicated between Intelligent Electronic Devices (IEDs). Some of the advanced communication-based methods for distribution systems relay on this protocol. In [103], for example, the information of different IEDs within the network is transferred to a centralized controller using the IEC61850 protocol. The method uses multi-setting microprocessor-based relays whose settings are selected based on the network operating conditions. Reference [23] proposes a centralized protection scheme based on the standard transferred variables (data/attribute) defined by the IEC61850-7-420 protocol, that is, the recent version of IEC61850 developed for DGs. IEC 61850 has also been proposed for fault location based on the positive-sequence of voltage and current phasors of the two ends of the feeder [104].

### 2.6. Protection Methods For DC Systems

Due to the specific characteristics of DC systems, they cannot be effectively protected by conventional protection methods, at least in the same manner that they are used in AC systems. Thus, modified or new fault detection/interruption methods are needed for these systems. This section describes some of the proposed methods for DC systems. It should be noted that the protection methods which can be applied to both HVDC networks and MVDC distribution systems are also discussed in this section.

#### 2.6.1. Fault Interruption Schemes

As mentioned before, one of the main protection challenges in DC distribution networks is the choice for performing fast and cost-effective fault interrupting schemes [105]. This is in contrast to AC networks where the fault interrupting technology has been well developed. In the following subsections, some of the proposed methods for fault clearance in DC grids are discussed.

##### 2.6.1.1. Converter Blocking Schemes

All the conventional and RES-based sources are interfaced with DC grids through an energy conversion system. Therefore, the controller of the converter can turn off the main converter switches subsequent to a fault occurrence to provide protection for the network. This type of protection, known as “converter blocking”, causes a complete shut-down of the

entire system and is normally used for HVDC lines [44, 106]. Although blocking the converter can break the fault current in line commutated converters (LCC), this method is not useful for VSC-based DC networks. Furthermore, once the main switches of the VSC are blocked, the VSC will lose its control and the fault can be still fed through the freewheeling diodes [51]. Therefore, to provide an adequate protection for VSC-based multi-terminal DC systems, revising the converter topology has been proposed [10, 69, 107]. Replacing the IGBT-Diode configuration of VSC by a structure consisting on two Emitter Turn Off (ETO) has been used in [69], while [10] suggests using thyristor switches to eliminate the freewheeling effect of diodes. These methods, however, increase the initial investment on the converters. In addition, they may cause unnecessary outage of healthy load and sources, especially in multi-terminal DC systems. In addition, for a typical two-terminal DC line, it is acceptable to de-energize the line once a fault takes place within the line; however, for multi-terminal distribution systems such as the one shown in Fig. 2.1, this option does not provide an adequate selectivity and system reliability.

### 2.6.1.2. Converter Blocking with AC-Side CBs

The operation of the AC-side CBs introduced in [54] along with the converter blocking scheme can provide an economic protection method for VSC-based DC networks. In this method, after the fault occurrence and blocking the VSCs, the ACCBs, located on the AC-side of the VSCs, operate to prevent the fault to be fed through the freewheeling diodes. Although this method can interrupt the fault current contribution from the AC side, it is not fast enough to prevent damages to the freewheeling diodes of the VSCs; this is due to the fact that the operation time of medium-voltage ACCBs is in the range of several tens of milliseconds [68]. Moreover, AC-side CBs cannot break the discharge current of DC-link capacitors. Also, selectivity issues remains as the main weakness of these methods [48].

### 2.6.1.3. Converter Blocking with AC-side CBS and DC Isolator Switches

To provide a selective protection, the use of fast DC isolator switches has been suggested by researchers. Although these switches cannot extinguish the fault current, they can be used to de-energize low-current and/or no-load DC feeders. The work presented in [108] suggested that each DC feeder could be equipped by a DC isolator switch, e.g. DC contactor, which operate in coordination with the fully controllable converters. In this method, once a fault impacts a feeder, all the converters are blocked to de-energize the DC bus. While the fault current decay to a low value, less than the nominal current of the DC switch, the switch of the faulty feeder operates and isolates the faulty part. Subsequently, the converter re-energizes the DC bus. The method also proposes to equip each load with a capacitor in order to prevent any interruption of the supply during the temporary de-energizing of the DC bus. This method can provide a selective protection and prevent unnecessary outage of healthy feeders. However, the efficiency of the method for VSC-based MVDC systems is still a

question under investigation; this is because the discharge current of capacitors is allowed to flow in the faulty circuit, consisting of a DC busbar and the faulty feeder. Moreover, this method is not applicable to general structures of VSCs in which the converter is not able to interrupt the fault current.

In [109], another method is proposed, which provides selective protection for looped DC networks using DC switches. The method, which has been named ‘Hand Shaking’ method, is based on the coordinated operation of high-speed DC switches, converter controllers, and AC-side CBs. For a typical looped DC distribution system with DGs, as shown in Fig. 2.1, the switches of all the converters are blocked once a fault takes place within the system. The AC-side CBs are then tripped to clear the fault. After the fault current interruption, the corresponding DC switches of the faulty feeder, labeled by “B” in Fig. 2.1, will operate to isolate the fault. Finally, the rest of the system is re-energized by closing the ACCBs and unblocking the VSCs.

These methods do not consider the requirements for the equipment that should break/reduce the capacitor discharge current; it should be borne in mind that the capacitor discharge current is the most hazardous part of DC fault current and can seriously damage the system’s equipment. On the other hand, as mentioned in Section 2.5.1.2, AC-side CBs are not fast enough to prevent damages at freewheeling diodes. Moreover, the operation of AC-side CBs can impact negatively on the AC network. To that end, such methods, which are based on ‘cut and try’ process, can potentially threaten the system reliability [4].

### 2.6.1.4. Fault Current Limiting Methods

Limiting the fault current can protect sensitive elements employed in VSC and DC grids. For example, using a well-designed inductor at the terminal of converters has been suggested in [51]. The employment of active DC fault current limiters (FCLs) which consist of superconducting windings has been proposed in order to reduce the short-circuit level in DC systems [110]. The installation of FCLs in series with VSCs, see locations labeled by “A” in Fig. 2.1, contribute to protect the freewheeling diodes against the fault current and mitigate the impacts of DGs on the protection coordination. On the other hand, multi-mode control schemes can also be used for special designed converters to limit the fault current in DC distribution systems; this is done by switching between different control mode as the system operating conditions changes [43, 111]. Such techniques have also been proposed for a prototype MVDC distribution network used in a shipboard [43]. In this method, the distribution system divided into various zones, and each zone is protected by Power Electronics Building Blocks (PEBB) converters. Therefore, applying this method to distribution systems requires replacing all switches (locations “A” and “B” in Figs. 2.1) with PEBB-based converters, resulting in a costly approach.

2.6.1.5. Employment of DC Circuit Breakers

DC circuit breakers (DCCBs) are designed to operate based on the specification of DC fault currents, and various applications have been proposed for them. For instance, employing a solid-state DCCB in series with the DC-link capacitor can prevent the appearance of fast discharging currents [58, 69]. Although this type of CBs can interrupt the main part of the DC fault current, i.e., capacitor discharge part, they also affect the voltage of the main bus and sound feeders. Furthermore, switching the DC-link capacitors may have a destructive effect on the system’s power quality [52].

Table 2.4. Performance of fault interruption schemes for MVDC system of Fig. 2.1.

| Fault interruption method                          | Protection system description  | parts which loss the supply after fault at FI (see Fig. 2.1)             | Remarks   |
|--|--|--|---|
| Converter blocking                                 | <ul style="list-style-type: none"> <li>Blocking the converter</li> <li>No switch in points A and B</li> </ul>                                      | Entire DC system.  | <ul style="list-style-type: none"> <li>No selective protection and reduce the reliability.</li> <li>Incapability in breaking capacitor discharge current.</li> <li>No backup protection.</li> <li>Incapability in breaking fault current feeding from AC-side (for typical VSCs).</li> </ul>  |
| Converter blocking with AC-side CB                 | <ul style="list-style-type: none"> <li>Blocking the converters</li> <li>AC-side CB</li> <li>No switch in points A and B</li> </ul>                 | Entire DC system.  | <ul style="list-style-type: none"> <li>No selective protection.</li> <li>No fast enough method to prevent damage on freewheeling diodes.</li> <li>Incapability in breaking capacitor discharge current.</li> <li>Negative impact on AC side network.</li> </ul>   |
| Converter blocking with DC switches and AC-side CB | <ul style="list-style-type: none"> <li>Blocking the converter</li> <li>AC-side CB</li> <li>Fast isolating DC switches in points A and B</li> </ul> | Temporary overall blackout during ‘cut and try’ process and then Line23. | <ul style="list-style-type: none"> <li>Provide selectivity after a ‘cut and try’ process.</li> <li>No fast enough method to prevent damage on freewheeling diodes.</li> <li>Incapability in breaking capacitor discharge current.</li> <li>Impacts on the operation of sensitive loads.</li> <li>Negative impact on AC side network.</li> </ul> |
| Employment of DCCB [58, 69]                        | <ul style="list-style-type: none"> <li>DCCB for main capacitor</li> </ul>  | Based on the existence of switches in points B.                          | <ul style="list-style-type: none"> <li>No backup protection.</li> <li>Destructive impacts on DC-bus voltage and power quality.</li> </ul>   |
| Employment of DCCB [112, 113]                      | <ul style="list-style-type: none"> <li>DCCBs in point A</li> <li>Fast isolating DC switches in point B</li> </ul>                                  | Temporary overall blackout during ‘cut and try’ process and then Line23. | <ul style="list-style-type: none"> <li>Provide selectivity after an overall blackout.</li> <li>Can impact on the operation of sensitive loads.</li> </ul>   |
| Employment of DCCB [53, 114]                       | <ul style="list-style-type: none"> <li>DCCBs in both A and B Points</li> </ul>   | Only the faulty line (Line23).   | <ul style="list-style-type: none"> <li>Costly.</li> <li>Selective protection.</li> <li>Requirement to effective fault detection and location methods.</li> </ul>  |

The work presented in [112] has proposed to use hybrid DCCBs at the connection point of VSCs and DC grids (locations “A” in Fig. 2.1), while fast DC isolating switches are recommended in other locations within the network (locations “B” in Fig. 2.1). In this method, when a fault impacts the DC grid, all the DCCBs operate to interrupt the fault current. Then, DC switches located at both sides of the faulty part isolate the fault and, finally, the healthy parts of the network are re-energized by reclosing the proper DCCBs. A similar method was also presented for DC microgrids [113], where the fault is first cleared by DCCBs, at the same time that the converters are disconnected; then, the healthy parts are disconnected by the operation of disconnecter switches. Although these methods can provide selectivity, their operating time should be verified according to the power quality standards. Moreover, the application of these switching-based methods in DC systems should be investigated if industrial and sensitive loads are used in the network; this is because they may adversely impact on the reliability of DC systems [9].

Based on the above discussion, it has been proposed to use independent CBs and relays for each feeder of the DC network (both locations labeled by “A” and “B” in Fig. 2.1) to increase the reliability of complex DC grids embedding DGs [114]. It is, however, acknowledged that economic and technical issues associated with the widespread use of DCCBs require further investigations. Table 2.4 summarizes the operational aspects of DC fault clearance methods in the context of the system of Fig. 2.1, when a fault occurs in the line between Bus2 and Bus3 (i.e., Fault F1 on LineL23).

### 2.6.2. Fault Detection Methods

Although different types of fault detection techniques have been proposed for AC systems, protective methods in DC systems are still in the early stage of development [65]. Moreover, the characteristics of DC systems limit the variety of the methods that can be employed to detect faults in these systems. For instance, a number of fault location methods are designed for AC systems, which work based on the phasor and harmonic analysis. However, due to the lack of frequency and phasor information, these methods are unlikely to be applied to DC systems [56]. Moreover, the lack of information in time domain limits the use of digital-signal-processing-based methods, such as DFT-based methods [65]. On the other hand, the need for a fast protection in DC networks prevents the application of those methods that extract fault data from the voltage and current waveforms [3, 56]. In the following section, the most important proposed methods for protection of active MVDC system are discussed.

#### 2.6.2.1. Current-Based Protection

Due to the simplicity of O/C protection, they are always the first choice for the protection of AC distribution systems. However, as explained in Section 2.3.2., this type of protection does not provide adequate selectivity for multi-terminal DC systems. Nonetheless, these

relays can be used along with other types of protective functions to protect small DC grids. For instance, the work referenced in [34] has proposed to analyze the magnitude of DC-link voltage along with the fault current in order to locate the fault in low-voltage DC microgrids. Likewise in [69], a hybrid relay has been devised which is based on overcurrent and under-voltage elements; once both the overcurrent and under-voltage element pick up, the relay confirms the occurrence of the fault. The methodology proposed in [115] and the O/C-based relay suggested in [116] have been designed based on the slope of the current in DC networks. However, as discussed in Section 2.3.1., the O/C-based methods can potentially fail when DGs are integrated into the network.

Establishing communications between O/C relays has been proposed to improve the protection selectivity. For instance, the work presented in [117] suggests using the current magnitude, current direction, and voltage of the DC bus to provide a fast and reliable protection for low-voltage DC networks. In this method, faults are detected by monitoring the DC current of the individual feeders and the voltage of the DC bus. Then, the faulty feeder is determined based on the direction of the DC fault currents. It should be noted that the feeder relays exchange the information of fault current directions via a suitable communication link. If a relay detects the fault with a forward current direction, its corresponding feeder is recognized as the faulty feeder and is disconnected from the DC bus.

### 2.6.2.2. Distance Protection

In [53], a distance protection scheme was proposed for MVDC networks. The salient difference between the proposed method and the conventional distance protection in AC system is on the calculation of the fault location. If compared to AC systems, the method shown in [53] employs a simpler formulation to achieve a fast fault detection. According to the proposed methodology, the fault distance is estimated using two DC measuring elements installed on the protected line, and it is given by:

$$x = \frac{v(n)}{v(n) - v(r)} d \quad (2.11)$$

where  $v(n)$  and  $v(r)$  are the measured voltages by the two DC measuring elements, and  $d$  denotes the distance between these two measuring devices. This method has a favorable fast detecting time and also is applicable for DC systems with DGs. Active impedance estimation (AIE) has also been suggested in [118], where a current with a wide-range frequency is injected to the DC feeder while the resultant voltage is recorded. Then, using the measured voltage and current, the equivalent system impedance is estimated. The main challenge associated with the distance protection is that it is vulnerable to the fault impedance. Also,

the choice of a proper frequency range for injected current is an important shortcoming of the AIE method.

### 2.6.2.3. Differential Protection

As discussed in Section 2.4.1.3, differential protection has an accurately defined protection zone. The fault current level, the rate-of-change-of the current, existence of DGs, and fault resistance have relatively low impact on the performance of differential protection, making differential protection one of the best options for the protection of DC systems [3]. The work presented in [48] has proposed a protection methods for DC systems in which each section of the system is protected by a master controller; the controller, in turn, operates based on the difference between the measured currents at two ends of the protected section. If the current difference is more than a threshold, it is considered as a fault and trip commands are sent to the solid-state switches located at both ends of the faulty section. The works presented in [119, 120] suggested that a telecommunication link should be used between the protective devices in the both sides of each DC feeder. Then, each differential relay, which is installed on one side of the line, will only send the trip command to its corresponding CB. It is worth to remember that the protection system must be very fast for DC systems and, thus, differential protection is a proper choice. The results shown in [121] evidence that differential-based protection methods can detect DC faults in less than  $40\mu\text{s}$  while the operating time of differential protection in AC networks is more than 20ms; these times are without considering the communication delay. It is worth noting that most of differential relays in AC systems have to compare both the magnitude and the phase-angle of 3phase currents, whereas only the current magnitude are compared in DC systems; therefore, it can operate faster. It should be pointed out that communication delay and/or failure must also be taken into consideration when differential protection systems are designed, especially in case of MVDC feeders. For example, Reference [114] has employed O/C relays to provide backup protection if the communication network fails. Nonetheless, providing remote backup for adjacent protections, dependency on the communication network, and potential need for synchronized measurements in large systems are some of the challenges associated with differential protection in DC systems.

### 2.6.2.4. Signal-Processing Based Methods

To overcome the challenges about the fault location in DC grids and provide a selective protection for these systems, wavelet-transform-based methods have been suggested in [9, 122, 123]. In these methods, the criteria of fault location are defined based on the analysis of DC voltage and currents through wavelet transform (WT). For instance, a fault detection/location technique has been proposed in [9], which is based on the wavelet-transform coefficients of voltage and current as well as magnitude and derivative of the voltage. On the other hand, the work in [123] used complex-wavelet coefficients of transient

currents to detect DC faults. The use of a feature vector containing the energy of wavelet coefficients has been suggested in [122]; the proposed vector is generated based on the multi-resolution analysis (MRA) and compared with a predefined threshold to detect the fault. The method proposed in [122] has also shown satisfactory results for the DC systems in the presence of DGs. However, since the fault location criteria and settings vary from network to network, the application of feature network may not provide a generic method for DC systems.

Artificial Neural Networks (ANNs) have widely been used in AC power system. In most cases, the input data to ANN is obtained from the analysis of post-fault waveforms. For instance, Fourier transform has been used in [124] to extract the harmonic contents of voltages/currents in order to feed an ANN. However, as mentioned before, FFT cannot be easily used in DC systems due to the lack of time-domain information as well as required time for the process. Therefore, it has been suggested in [125] that the sampled value of DC current and voltage be fed to ANN directly. The main concerns about the direct use of voltage and current samples include noise and incorrect sampling [9]. Therefore, the use of wavelet transform and multi-resolution analysis (MRA) has respectively been suggested in [65, 126] in order to extract the feature vector of faults and feed them to an ANN. It is worth mentioning that the ANN-based protection schemes have the capability of both detection and classification of DC faults. The travelling-waves-based protection methods are also proposed for DC systems [127-129]. Following the fault occurrence in a line, the travelling waves are propagated from the fault point to both sides of the line. By using the synchronized measurements, the accurate difference in arrival times of the travelling waves to each end of the line is determined. This means, if the velocity of travelling waves is known, that the fault location can be calculated. In [127] a travelling-wave-based method was used to protect multi-terminal DC systems with DGs. However, due to the small length of distribution feeders, it is very difficult to obtain the exact time difference and locate the faulty feeder. Moreover, since the travelling waves propagate along the lines of a multi-terminal system, most of the measurement devices installed within the DC network may receive these waves. As such, the travelling wave boundary method shown in [129] may not find the exact location of the fault [123]. The abovementioned issues should be added to the concerns associated with the use of some sort of synchronizing mechanism for travelling waves in long lines.

## 2.7. Comparison of Protection Methods in AC and DC Networks

Different protection methods for AC and DC distribution networks were explained in Sections 2.4 and 2.5, respectively. The main features of these methods are summarized and compared in Table 2.5.

## Chapter2. Protection of AC and DC systems. Comparison and analysis

Table 2.5. A summary of protection methods in AC and DC networks.

| Fault detection method                 | AC distribution systems   | DC distribution systems  |
|--|---|--|
| Over current                           | <ul style="list-style-type: none"> <li>Simple algorithm.</li> <li>Inefficient in the presence of DGs.</li> </ul>  | <ul style="list-style-type: none"> <li>Fast method.</li> <li>Should be used with other methods or equipped with communication links to provide selectivity.</li> <li>Applicable in fault interrupt methods based on blocking the converters when selectivity is not desired.</li> </ul>  |
| Differential                           | <ul style="list-style-type: none"> <li>Mostly, phase and Magnitude of three-phase currents are compared.</li> <li>Detects faults in 20-50ms.</li> </ul>   | <ul style="list-style-type: none"> <li>Only the magnitudes of DC currents are compared.</li> <li>Faster than AC differential relays.</li> <li>Insensitive to high raising rate of DC currents and fault resistance.</li> </ul>   |
| Distance                               | <ul style="list-style-type: none"> <li>The measured current and voltage are used for distance estimation.</li> <li>Use of symmetrical components analysis to avoid the impact of fault resistance.</li> </ul>   | <ul style="list-style-type: none"> <li>Simple algorithm (use simpler fault location estimator).</li> <li>Faster than AC relays.</li> <li>More sensitivity to fault resistance (as compared to AC systems).</li> </ul>  |
| Fault current limiting                 | <ul style="list-style-type: none"> <li>Typically consists of constant or variable inductors.</li> </ul>   | <ul style="list-style-type: none"> <li>Can be done by external inductors, or the current limiting modes of especial converter.</li> <li>Requires high-speed semiconductor switches.</li> <li>Requires devices with higher withstand rating DC current with high raising rate.</li> </ul>   |
| Intelligent methods such as ANN, Fuzzy | <ul style="list-style-type: none"> <li>Fast methods for fault detection, classification, and location without requirement to complex mathematical equations.</li> <li>Requirements for analysis of the post-fault waveforms to input proper data to the ANN.</li> </ul> | <ul style="list-style-type: none"> <li>Frequency based transformations are not applicable for obtaining the input data.</li> <li>Direct use of sampled data to the ANN increases the complexity of its structure and its training time.</li> <li>Direct use of measured data increases the impact of noises and reduces the accuracy.</li> </ul> |
| Wavelet transform                      | <ul style="list-style-type: none"> <li>Effective for fault detection and location with or without other methods, e.g. wavelet-ANN, wavelet-Fuzzy, etc.</li> </ul>   | <ul style="list-style-type: none"> <li>Applicable for the analysis post-fault waveforms.</li> <li>Can be used with intelligent methods for the protection of DC systems with DGs.</li> </ul>   |
| Communication Based                    | <ul style="list-style-type: none"> <li>Is increasing in distribution systems and smart grids due to the providing a fast, accurate and selective protection.</li> </ul>   | <ul style="list-style-type: none"> <li>Can be applicable for coordination of O/C relays instead of using time grading methods.</li> <li>Delay on the communication link can be a major concern.</li> </ul>   |
| Directional O/C                        | <ul style="list-style-type: none"> <li>Detects the fault current direction according to the relative phases of the voltage and current.</li> </ul>  | <ul style="list-style-type: none"> <li>Requirement to accurate and fast methods for detecting the current direction.</li> </ul>  |

---

## Differential- based protection for DC distribution systems

As explained in Chapter 2, differential protection, as a communication-assisted method, has been proposed as an effective and fast method for the protection of DC distribution systems [121]. Since the fault current level, the rate-of-change-of the current, status of DGs, and fault resistance have relatively low impact on the performance of differential protection, they are one of the best options for the protection of DC systems embedding DGs [130]. Therefore, in [120] current differential relays have been used to provide a selective protection for multi-terminal DC systems. Also, a differential-based protection has been used in [131] where, in order to ensure the accurate decision of the relay, the relay is equipped with operating and restraining signals. However, as opposed to non-unit protection schemes such as O/C and distance protection, conventional differential scheme cannot provide backup protection for adjacent protection zones. Moreover, since the effectiveness of differential protection heavily relies on the existence of a reliable communication medium, any communication failure can substantially affect the performance of the protection. Therefore, it is important to apply some modifications to the conventional differential protection in order to deal with these issues.

In this chapter, after analyzing the fault location method based on the local measured quantities, a multi-zone differential-based protection method is proposed for MVDC distribution systems. The proposed communication-assisted method employs a simple and solid algorithm that does not require time-consuming processes, while providing second and

third differential zones that operate as a backup for the main zone. More importantly, the proposed method is equipped with directional O/C relays which provide a selective backup protection if the communication system fails. The contributions of this chapter can be summarized as:

- 1) The proposed multi-zone differential relay provides backup differential protections, besides the conventional differential protection, to improve the reliability of the overall protection system.
- 2) The proposed method also provides a directional overcurrent-based backup protection to manage communication failures.
- 3) The effectiveness of the proposed method is independent of the network's operation mode, fault current levels, and status of DGs. Therefore, it is a suitable performance for distribution systems with a high penetration of DG.
- 4) The efficacy of the proposed technique is demonstrated through real-time HIL testing conducted in the OPAL-RT, where the impact of communication delays is also considered.

### 3.1. Fault Current in VSC-based DC Networks

#### 3.1.1. Characteristics

To design an effective protection scheme for DC distribution systems, it is imperative to analyze the characteristics of DC fault currents. Fig. 1 shows a simplified schematic diagram of a typical pole -to-pole (PP) fault in a VSC-based DC feeder; in this figure, R and L represent the resistance and inductance of the line located between the main DC bus (DC-link capacitor) and the fault location respectively. Subsequent to the fault in the DC grid, the DC-link capacitor is discharged due to the voltage drop of the main DC bus. Once the DC-link capacitor is discharged, the energy stored in the cable inductance is discharged through the freewheeling diodes of the VSC. On the other hand, the control of the converter turns off the VSC switches to protect them against the over-current condition caused by the fault; this causes the VSC to operate as an uncontrolled full-bridge rectifier and continue feeding the fault from the AC side through the freewheeling diodes [130].

Based on the above discussion, the DC fault current includes three different components, namely, *i*) the DC-link capacitor discharging current ( $i_C$ ), *ii*) the cable inductance discharging current ( $i_L$ ), and *iii*) the AC grid current ( $i_{Grid}$ ). A typical DC fault current is shown in Fig. 3.2. During the capacitor discharging period ( $t_0 \leq t \leq t_c$ ), there is no fault current contribution from the converter side. However, for  $t > t_c$ , the inductor discharging current and the AC grid current flow through the converter freewheeling diodes (see Fig. 3.2(b)); this may damage the freewheeling diodes of the VSC [56]. Therefore, the protection of DC

distribution systems should operate during the capacitor discharging component ( $t_0 \leq t \leq t_c$ ) to prevent any damage to the converter [132]. This is based on the assumption that, after the fault occurs, the converter remains in-service in order to give a chance to the protection system to isolate the fault; this also ensures that the smallest possible area of the system is de-energized in response to the fault.

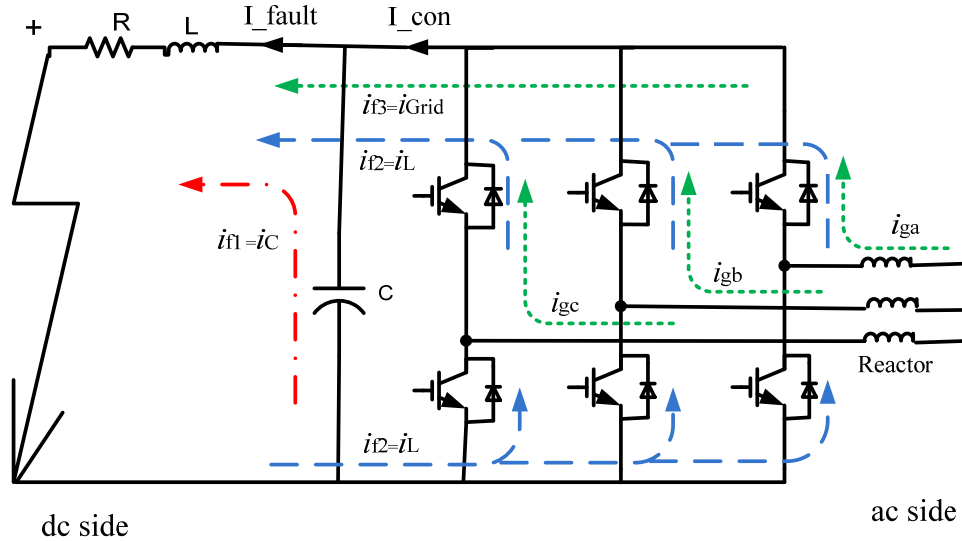


Fig. 3.1. Equivalent circuit of a PP fault in a VSC-based DC feeder.

The critical time for the operation of the DC protection systems, that is,  $\Delta t_c = t_c - t_0$ , depends on several factors such as fault type, fault location, and fault resistance. For a typical PP fault, the critical time can be obtained as [4]:

$$\Delta t_c = (\pi - \arctan((V_0 C \omega_0 \sin \beta / (V_0 C \omega_0 \cos \beta - I_0)) / \omega)) \quad (3.1)$$

where  $\omega = \sqrt{\frac{4L - R^2 C}{4L^2 C}}$ ;  $\beta = \arctan(\frac{2\omega L}{R})$ ;  $I_0 = i_{cable}(0)$ ;  $V_0 = v_c(0)$ ;  $\omega_0 = \frac{1}{\sqrt{LC}}$ .

It should be pointed out that, for pole-to-ground (PG) faults, the critical time increases; this is also the case for faults that include higher impedances. In addition, although the fault

current characteristics of a two-level converter have been studied in this study, the analyze is the same for multi-level converters and half-bridge modular multilevel converters [131].

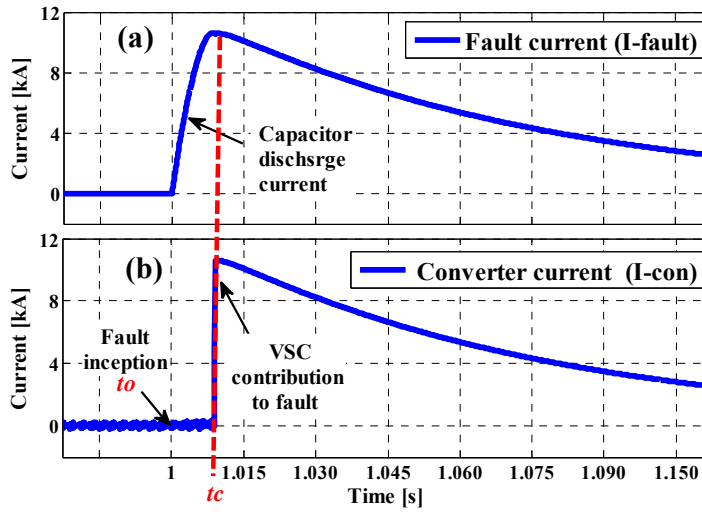


Fig. 3.2. Waveforms of a typical DC fault current.

### 3.1.2. Choice an adequate fault current interruption method

It is well known that conventional AC circuit breakers (ACCBs) interrupt the fault current at the zero crossing point. Since DC fault currents do not cross zero, ACCBs are not suitable for interrupting these fault currents. The use of AC-side CBs along with the converter blocking scheme and DC isolating switches have been proposed for fault interruption in multi-terminal DC systems [109]. The main disadvantage of this method is that ACCBs may not operate fast enough to prevent damages to freewheeling diodes of the converter. Moreover, ACCBs are not capable of breaking the DC-link capacitor discharging current,  $i_c$ . It should also be noted that the aforementioned methods isolate the faulty parts of the network based on a “cut-and-try” process, which can significantly affect the reliability of the DC and AC-side network. Therefore, this chapter assumes that all feeders are equipped with DC circuit breakers (DCCBs), as suggested in [3], [9], [133]. The solid-state DCCBs are capable of fault clearance in sub-millisecond [134]; however, it is known that the economic aspects related to the widespread use of these CBs are still under investigation.

3.2. Fault location using local measured quantities

In conventional power systems, the primary protection systems operate based on the local measured quantities. The “primary protection” is defined as a protection systems that operates based on the local measured quantities. In fact, such protection systems do not need communication networks. In conventional power systems, to provide a selective protection, a relay installed at one side of the faulty should be able to discriminate between faults that occur inside the corresponding line and the ones that occur outside.

In this section, the behaviors of different types of fault in DC systems are explained. Then the possibility of fault location based on local measured quantities (voltage and current measured at the location of the corresponding relay) is investigated. In fact, according to the explanations of Section 3.2.1, it is difficult to coordinate Overcurrent relays in MVDC feeders, here tried to investigate the possibility estimation of the fault location using the voltage and current of one side of the line.

3.2.1. Pole to pole solid faults location

PP faults often have low fault impedance [113]; accordingly, Fig. 3.3 shows the equivalent circuit of the faulty line of a multi-terminal DC grid (e.g. Fig. 2.1 ) when a PP fault occurs. It is should be noted that, although the grounding capacitors of the DC distribution lines are negligible, in the equivalent circuit of Fig. 3.3 it is assumed that these capacitors are considered into DC-link capacitors of both sides of the line. The equivalent circuit of Fig. 3.3 can be simplified as shown in Fig. 3.4.

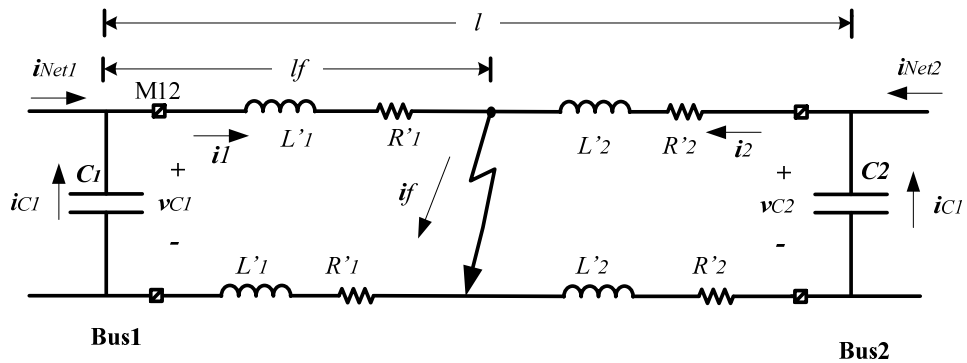


Fig. 3.3. Equivalent circuit for a PP fault.

As mentioned above, a primary relay should be equipped with the effective algorithm to receive and analyze the current and the voltage from the local measurement devices, e.g.

M12 in Fig. 3.3, and send the trip command to the related CBs if a fault occurs inside the main protected zone (corresponding DC line). For this reason, the algorithm of the primary relay can be designed according to the relation between the fault location and measured quantities by the local measurement devices.

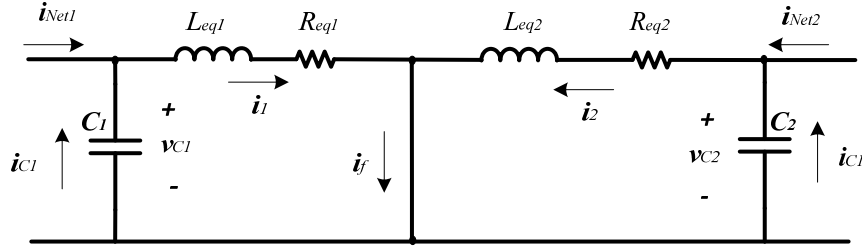


Fig. 3.4. Simplified equivalent circuit of a PP fault.

In some previous works like the ones presented in [56, 113, 135], the fault location has been calculated by solving the differential equations obtained from the KVL when applied to the loop created by the fault. The related equation is:

$$\frac{d^2 i_1(t)}{dt^2} + \frac{R_{eq1}}{L_{eq1}} \frac{di_1(t)}{dt} + \frac{1}{L_{eq1} C_1} i_1(t) = 0 \quad (3.2)$$

Where  $R_{eq1} = 2mR$ ,  $L_{eq1} = 2(L_s + mL)$ ,  $R$  and  $L$  denote the line resistance and inductance,  $L_s$  is a small inductance that is used to limit the rising-rate of the fault currents, and  $m$  determines the fault location, which can be found as:

$$m = \frac{l_f}{l} \quad (3.3)$$

Where  $l$  is the total length of the line and  $l_f$  determines the fault position. Moreover, in (2.2) the damping factor (i.e.,  $\xi$ ) is defined as

$$\xi = \frac{R_{eq1}}{2} \sqrt{\frac{C_1}{L_{eq1}}} \quad (3.4)$$

According to (3.2) it is clear that in the case of PP fault occurrence (and when  $R_f$  is negligible) the current coming from other side of the line do not play any role in the

equivalent circuit of the faulty section seen from the point of view of a relay installed at the connection point of Line12 and Bus1. Therefore, (3.2) can provide an acceptable relation between the local measured value, the fault point and the fault resistance. However, as explained in Section 2.2.1, the fault current corresponding to the line relay, measured by M12, can be overdamped ( $\xi < 1$ ), critically damped ( $\xi = 1$ ) or under damped ( $\xi > 1$ ).

The methods presented in [135] assumed that (3.2) always has the overdamped response. However, it is clear that the values of  $C_1$ ,  $L_{eq1}$ , and  $L_{eq1}$  influence the fault current behavior; therefore, assuming the “underdamp” behavior for the fault current, it cannot provide a general solution. Accordingly, a numerical solution is used for the differential equation that represents the behavior of the equivalent circuit of Fig. 3.4. In this method the voltage of Bus1 is considered as well. If again the KVL is applied at the abovementioned loop, at the instant  $t_k$ , we can write:

$$v_c(t_k) = R_{eq1}i(t_k) + L_{eq1} \frac{di_1(t_k)}{dt} \quad (3.5)$$

If it is assumed that  $i_1'(t_k) = \frac{di_1(t_k)}{dt}$ , (3.5) can be expressed as:

$$v_c(t_k) = R_{eq1}i(t_k) + L_{eq1}i_1'(t_k) \quad (3.6)$$

Moreover, the numerical derivatives are calculated as:

$$i_1'(t_k) = \frac{i(t_{k+1}) - i(t_{k-1}))}{2\Delta t} \quad (3.7)$$

Where  $\Delta t$  is the sampling time period of the relay.

Thus, (3.6) can be written as:

$$v_c(t_k) = 2mRi(t_k) + 2(L_s + mL) \left( \frac{i(t_{k+1}) - i(t_{k-1}))}{2\Delta t} \right) \quad (3.8)$$

The only unknown parameter in (3.8) is  $m$  which can be obtained as:

$$m = \frac{v_c(t_k) - L_s \left( \frac{i(t_{k+1}) - i(t_{k-1})}{2\Delta t} \right)}{2 \left( Ri(t_k) + L \left( \frac{i(t_{k+1}) - i(t_{k-1})}{2\Delta t} \right) \right)} \quad (3.9)$$

If  $m < 1$ , it means that the fault has occurred inside the corresponding line and hence the relay will send the trip command immediately. Otherwise, the fault has been detected out of the main protected line. In this case, the relay can operate as a backup for the corresponding relay; thus, it will send the trip command if the fault current is not cleared after a predetermined time delay. If compared with the method presented in [136] for the solid (short circuit) faults, the method presented here estimates the fault location only with one measurement device. Indeed, in [136], the author, suggested to use two measurement sensors in each protected line and estimate the fault location by using two voltage divider.

In order to achieve to an accurate value for  $m$ , its value will be estimated by using several samples of the measured voltage and current and least squared error (LSQ) technique.

It is worth noting that since the method needs continuous measured values, the accuracy of the measurement device impacts directly on the accuracy of the proposed method. Therefore, reliable measurement devices are needed to reach an acceptable performance for this method.

### **3.2.2. Pole to ground faults location**

Most of the faults in DC systems involves only one of the poles and are known as PG faults. This type of faults usually happen due to the damage on the insulators or mechanical stress on the cables. Therefore, in most cases, PG faults happen through a fault resistance. The existence of fault resistance impacts on the accuracy of the fault location method using (3.2) and (3.5). This section investigates the effects of the fault resistance on the performance of the primary relays in radial and loop distribution systems.

#### **3.2.2.1. Fault location in radial distribution feeders with DGs**

Most of the distribution feeders have a radial structure. Although in the conventional radial feeders, current flows only in one direction, after the DG integration, the bidirectional currents may appear in radial feeders. Moreover, due to the existence of the DC-link capacitors of DGs' VSC, the first stage of the fault current can be supplied from both sides of the faulty line (See Fig. 3.5).

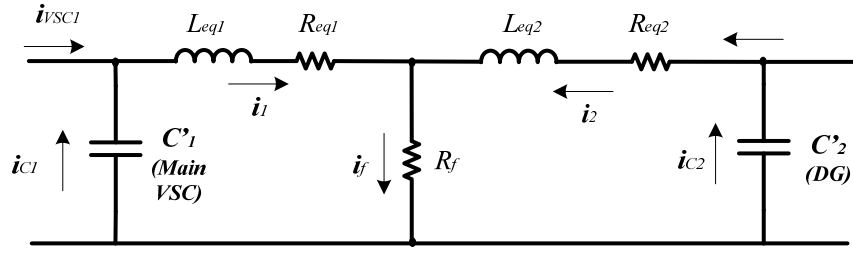


Fig. 3.5. Equivalent circuit of a PG fault in a radial DC feeder.

Since the first stage of the fault current is caused by the discharge of the DC-link capacitors, the values of these capacitors have an important role on the values of the fault current flowing from each side of the line. On the other hand, normally in radial feeders, loads are mainly supplied by the utility grid and through the main converter; hence the rated power of this converter is significantly larger than converters of DGs. Considering the relation between the capacity of the DC-link capacitor and the rated power of the related converter, explained in [137], the DC-link capacitor of the main VSC is normally selected to be much larger than the capacitors of DGs' converters. Therefore, during the first transient stage, the fault current flowing from the  $C'_1$  is normally much larger than current coming from the other side of the faulty line.

Fig. 3.6 shows the capacitor discharge currents from both sides of a line for the different values of fault resistance and  $C'_1/C'_2$  ratio. This figure illustrates that when  $C'_1$  is significantly larger than  $C'_2$ , the values of the total fault current ( $i_f$ ) is pretty much close to the measured value in Bus1 ( $i_1$ ). Accordingly, by ignoring the capacitor discharge current from other side of the radial feeder, the following equations can describe the fault behavior:

$$v_{c1}(t_k) = (R_{eq1} + R_f)i(t_k) + L_{eq1} \frac{di_1(t_k)}{dt} \quad (3.10)$$

Where  $R_{eq1} = mR$  and  $L_{eq1} = L_s + mL$ . Hence:

$$v_{c1}(t_k) = (mR + R_f)i(t_k) + (L_s + mL)i'(t_k) \quad (3.11)$$

In (3.11),  $v_{c1}(t_k)$ ,  $i(t_k)$  and  $i'(t_k)$  are measured by the local sensors and  $m$  and  $R_f$  are unknown. Since two equations are necessary to calculate these two unknown variables, the required equations are generated by applying KVL in two different instant [138].

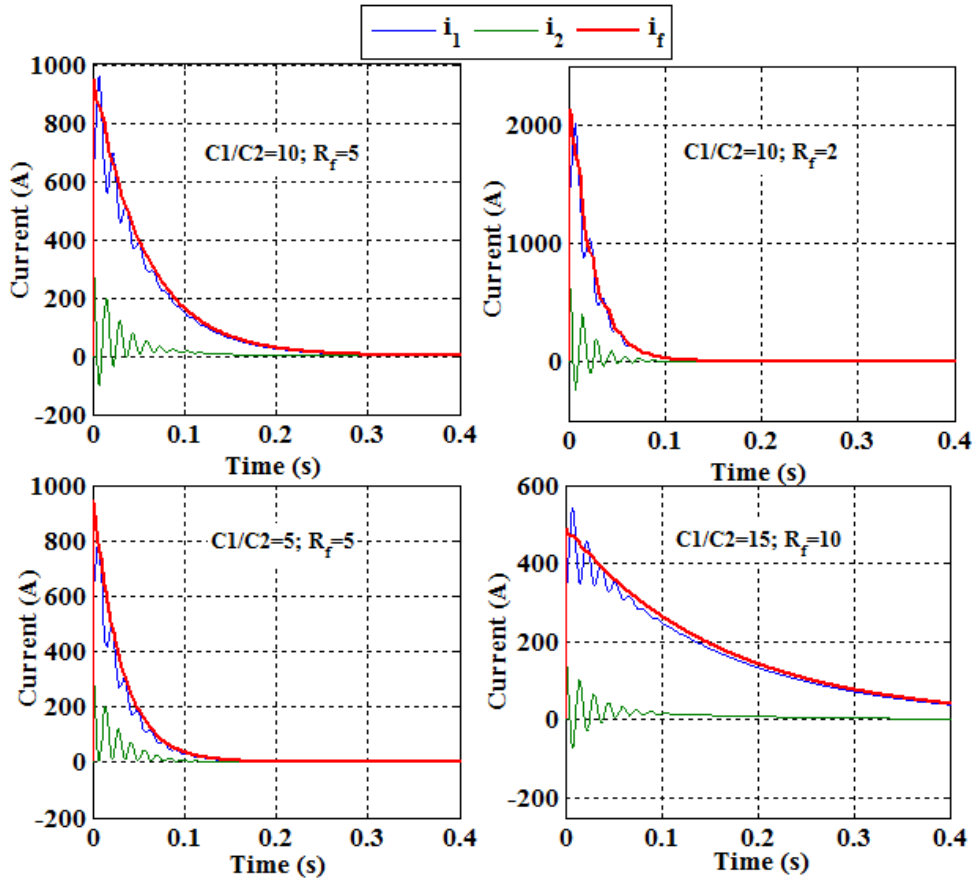


Fig. 3.6. Fault current from both side of a faulty line;  $m=0.3$ .

Indeed, in this case, two measured values are used to form the following equations:

$$\begin{aligned}
 v_{C'1}(t_k) &= (mR + R_f)i(t_k) + (L_s + mL)i'(t_k) \\
 v_{C'1}(t_{k+1}) &= (mR + R_f)i(t_{k+1}) + (L_s + mL)i'(t_{k+1})
 \end{aligned}
 \tag{3.12}$$

$i'(t_k)$  and  $i'(t_{k+1})$  are calculated as described in (3.7). Solving the above equations the following system is found:

$$\begin{bmatrix} m \\ R_f \end{bmatrix} = \begin{bmatrix} Ri(t_k) + Li'(t_k) & i(t_k) \\ Ri(t_{k+1}) + Li'(t_k + 1) & i(t_{k+1}) \end{bmatrix}^{-1} \begin{bmatrix} v_{C'1}(t_k) - L_s i'(t_k) \\ v_{C'1}(t_{k+1}) - L_s i'(t_{k+1}) \end{bmatrix} \quad (3.13)$$

It is worth to outstand that (3.13) can provide an accurate estimation for  $m$  and  $R_f$  only if the first stage of the fault current flowing from the other side of the line ( $i_2$ ) is significantly smaller than the measured value in the relay location (i.e.,  $i_1 \gg i_2$ ). Therefore, this analysis is valid if: 1)  $C'_1 \gg C'_2$ , or 2) if fast enough DCCBs are located at the DG stations and disconnect DGs' stations immediately after the fault occurrence and hence the only current is fed from the main VSC.

### 3.2.2.2. Fault location in multi-terminal DC systems

Fig. 3.7 shows a multi-terminal DC system. In this system, since different type of sources and microgrids are connected together, the DC-link capacitors of the VSC stations installed at all busses may have significant values. Thus, the fault current from the other side of the faulty line are not negligible during the first stage of the fault current. This is the main difference between this case and the previous one. In other words, the differential equations that describe the fault current behavior in such systems should consider both parts of the fault current flowing from both sides of the faulty line.

Fig. 3.8 and Fig. 3.9 present the equivalent circuit of the faulty line of Fig. 3.7 when a PG fault strikes Line12. Applying the KVL in the left-side loop formed by the fault resistance, the capacitor of Bus1 and the cable model the following equation is obtained:

$$v_{c'1}(t) = L_{eq1} \frac{di_1(t)}{dt} + R_{eq1} i_1(t) + R_f (i_1(t) + i_2(t)) \quad (3.14)$$

It this equation, in addition to the current and the voltage measured at the corresponding busbar, the fault current from the other side of the line is also considered. Since the local sensors cannot measure  $i_2(t)$ , it is necessary to form another equation and express  $i_2(t)$  through the measureable quantities at Bus1.

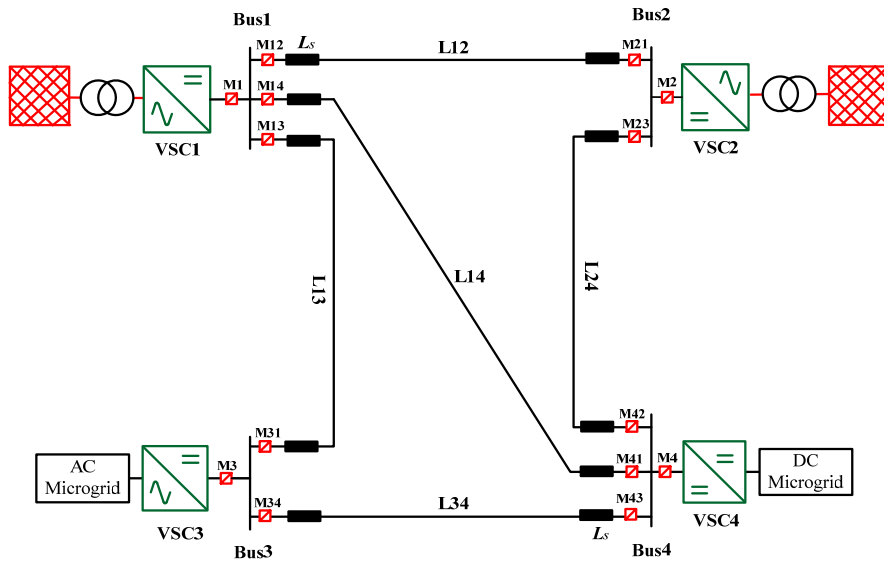


Fig. 3.7. A typical multi-terminal DC grid.

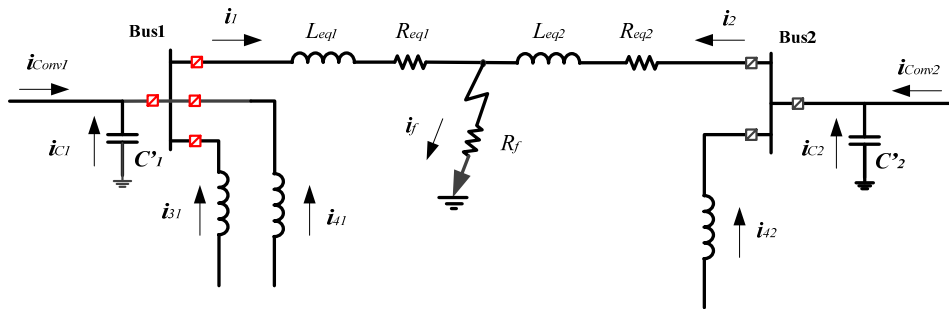


Fig. 3.8. The equivalent circuit of a PG fault occurred in Line12.

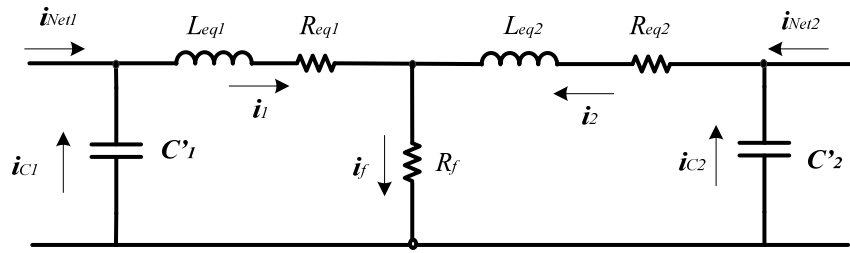


Fig. 3.9. The equivalent circuit of a PG fault occurred in Line12.

The required equation can be obtained from applying the KVL on the right-side loop formed by fault resistance, the second segment of the faulty line and the capacitor of the other end VSC (i.e.,  $C'_2$ ). Applying the KVL results in:

$$v_{C'2}(t) + L_{eq2} \frac{di_2(t)}{dt} + R_{eq2}i_2(t) + R_f (i_1(t) + i_2(t)) = 0 \quad (3.15)$$

and

$$i_2(t) = i_{C'2}(t) + i_{Net2}(t) \quad (3.16)$$

Where  $i_{Net2}(t)$  is the current flowing from Bus4 to Bus2 and the fault point.

Analyzing (3.15) and (3.16) it can be concluded that it is difficult to estimate the fault location and the fault resistance without knowing the measured value from the other side of the line. However, obtaining the accurate fault resistance and fault location is not the main goal of the fault location method. In fact, it is only enough to distinguish between faults that occurs inside the corresponding line or outside of that. Hence, by using reasonable assumptions and simplifications, it is possible to estimate the fault location.

When a fault happens at Line12, it will impact the voltage of all the busbars of Fig. 3.7. Therefore, the DC-link capacitors installed at each DC buses will start to discharge. The discharge circuit of each capacitor consist of resistances and inductances whose values are related to 1) the distance from the corresponding bus to the fault location; 2) the number and value of the current limiter inductances ( $L_s$ ) between the capacitor and the fault point.

Since the parameters of the discharge current are not the same for all the capacitors, these capacitors are not discharged exactly in the same time. For example, for a fault that occurs in Line12 the capacitors connected to Bus1 and Bus2 are discharged faster than the capacitors belonging to Bus3 and Bus5. Fig. 3.10 shows the simulation results for a MVDC line with

the parameters introduced in Table1. This figure determines that some millisecond after the fault occurrence,  $i_{Net2}$  is obviously smaller than  $i_1$  and  $i_2$ .

Table 3.1. The parameters of the simulated feeder.

| <b>Parameters</b>                |                   |
|----------------------------------|-------------------|
| <b>Line resistance (R)</b>       | 0.24 $\Omega$ /km |
| <b>Line inductance (L)</b>       | 2 mH              |
| <b>Series inductor (Ls)</b>      | 0.5 mH            |
| <b>D-link capacitor (C'1)</b>    | 10 mF             |
| <b>Line length (l)</b>           | 2 km              |
| <b>Rated voltage of the line</b> | V=5kV             |

According to the above explanations and considering the simulation results shown in Fig. 3.10, it can be expressed that during the first transient stage of the fault,  $i_{Net2}(t)$  can be neglected; therefore,  $i_2(t) = i_{c'2}(t)$ .

It is noted that due to use of the above assumption, the error of the fault location method is negligible only if faults are located during the capacitor discharge stage. Indeed, the fault should be located when  $v_c(t)$  is still larger than any phase value of the AC side of the corresponding VSC.

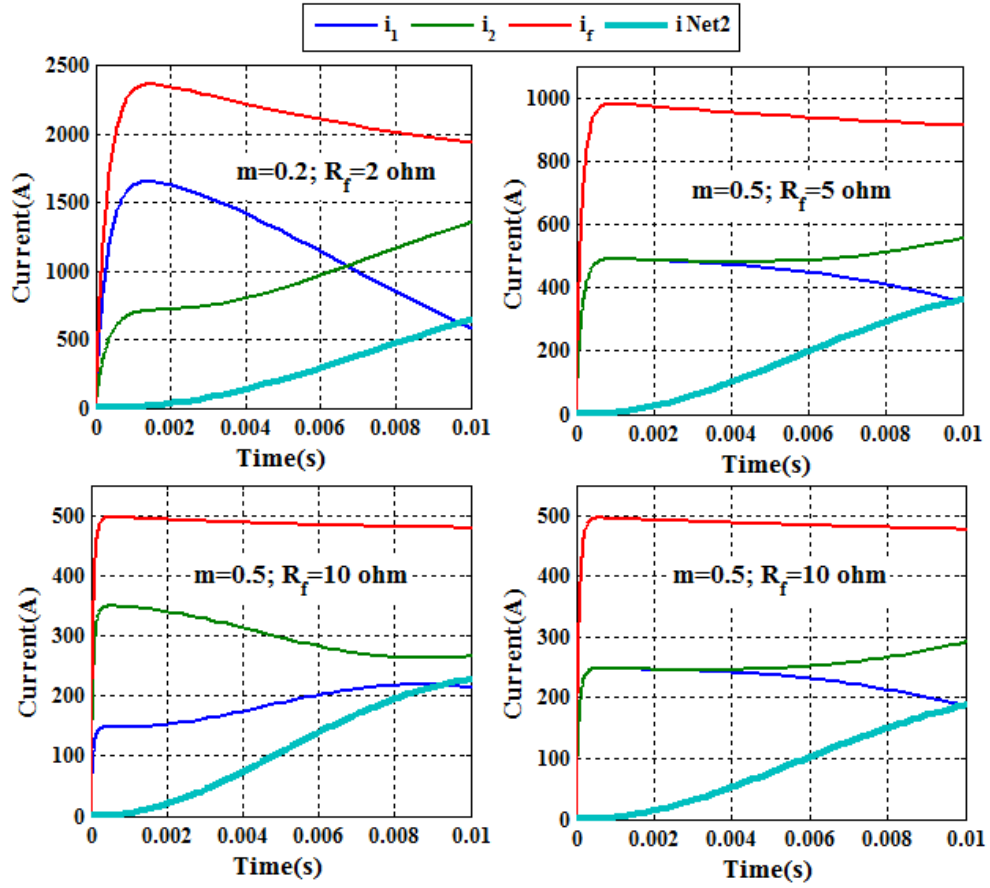


Fig. 3.10. Fault current from both side of the protected line.

Using this assumption, (3.15) is re-written as:

$$L_{eq2} \frac{d^2 i_2(t)}{dt^2} + (R_f + R_{eq2}) \frac{di_2(t)}{dt} + R_f \frac{di_1(t)}{dt} + \frac{1}{C_2'} i_2(t) = 0 \quad (3.17)$$

Where  $R_{eq2} = (1 - m)R$  and  $L_{eq2} = L_s + (1 - m)L$ .

Equations (14) and (17) describe the fault behaviour in MTDC system. To calculate  $m$  and  $R_f$ , these equation can be written as following:

$$v_{c'1} = L_{eq1}Di_1 + i_1(R_f + R_{eq1}) + R_f i_2 \quad (3.18)$$

$$\left( L_{eq2}D^2 + (R_f + R_{eq2})D + \frac{1}{C_2} \right) i_2 + R_f Di_1 = 0$$

Where  $D$  is the differentiation operator that is defined as  $D^n \equiv \frac{d^n i}{dt^n}$ . By using the elimination method for solving (3.18),  $i_2$  is eliminated and after applying the required manipulations, we can write:

$$B_1 D^2 v_{c'1} + B_2 D v_{c'1} + B_3 v_{c'1} = \quad (3.19)$$

$$A_1 D^3 i_1 + A_2 D^2 i_1 + A_3 D i_1 + A_4 i_1$$

Accordingly, (3.19) describes the relation between the local measured value in Bus1. In this equation,  $A_i$  and  $B_i$  are the functions of  $L_{eq1}$ ,  $L_{eq2}$ ,  $R_{eq1}$ ,  $R_{eq2}$ ,  $R_f$  and  $m$ . Therefore, the only unknown variables in (3.19) are  $R_f$  and  $m$ .

### 3.2.3. Discussion

According to the above explanations, (3.9), (3.13), and (3.19) can describe the fault current behavior and can provide an estimation for the fault location when a PG or a PP fault occurs in different types of DC systems. However, as it was previously explained, those equations, especially those presented for PG faults with significant fault resistance, have been obtained by applying simplifications linked to some assumption. Therefore, the fault detection algorithms using the above equations may cause protection mal-operation due to the following reasons:

- Normally distribution lines are not very long; thus, the line resistance and inductance are relatively low. Therefore, in most of the PG fault cases, the resistance of the equivalent circuit is very close to the fault resistance. Therefore, there is not a significant difference between the fault current caused by a fault occurred inside the corresponding line or outside of that line (especially for cases that fault resistance is high). That is why it is not straightforward to distinguish between the inside and outside faults in distribution lines.
- For multi-terminal systems, the behavior of the fault current is presented by a complex differential equation (see (3.19)). Moreover, in order to provide a more accurate fault location, faults in these systems should be detected very fast (just in the first several milliseconds). Due to the uncertainties in measurement devices, it is

not easy to calculate/estimate the fault location by use of the sampled values of the measured current and voltage.

Therefore, in the following sections of this chapter a more reliable protection for DC systems is presented using the communication infrastructures of smart grids.

### 3.3. Components of the proposed protection method

As explained in the first section of this chapter, although differential protection is a well proven technique for fast protection of DC distribution lines, it cannot operate as a backup for adjacent protection zones. Whereas, to provide a reliable protection, each protected zone should be protected by at least one backup protection [44]. The lack of backup protection and the need of a reliable communication link challenge the application of differential protection for MVDC distribution feeders. This chapter proposes a modified differential-based protection scheme which is capable of *i*) providing backup protection, *ii*) managing the communication network failure, and *iii*) operating correctly in the existence of DGs with various operational modes. In the following subsections, the main elements of the proposed method are introduced.

#### 3.3.1. Main differential protection

The proposed method is mainly based on the differential algorithm in which the difference between the currents at both sides of a protected feeder/zone is continuously measured. If the absolute value of this differential current is found to be greater than a threshold, a trip signal is sent to the corresponding DCCB at each end of the line. For the relay shown in Fig. 3.11, the absolute value of differential current is computed as:

$$i_{diff}[k] = |i_1[k] - i_2[k]| \quad (3.20)$$

Where  $i_1$  and  $i_2$  denote the measured current at both ends of the line, and  $k$  is the sample number. Equation (3.20) shows that bi-directional power flows caused by DGs cannot impact the performance of the differential scheme.

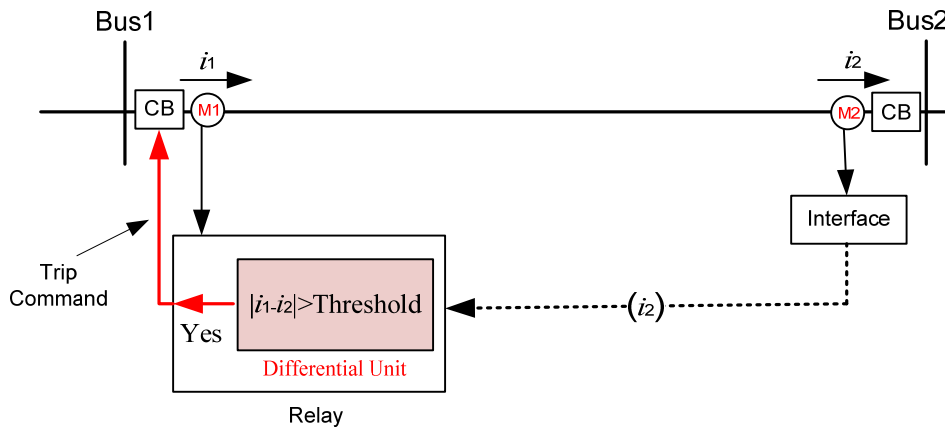


Fig. 3.11. Differential protection scheme for a distribution line

### 3.3.2. Main and backup protection zones

To ensure system reliability, the proposed protection strategy provides main and backup protection zones. These protection zones are divided into two groups as follows.

#### 3.3.2.1. Differential-based protection zones

In the proposed method, each relay provides main and backup differential-based protection zones. For example Relay R3 shown in Fig. 3.12, these protection zones are:

- 1- Zone1: It is the main protection zone covering the line whose current is monitored by the relay (i.e., Line23 in this example). Thus, the relay R3 operates instantaneously for any fault taking place in this line.
- 2- Zone2: It is a backup protection zone for the downstream line/busbar of the relay (i.e., Line34 and Bus3 in this example). Therefore, for any fault in this line/bus, the relay operates after a time delay, named as TMD, if the main protection of the line/bus fails to operate.

In other words, the proposed method not only provides a main differential zone (i.e., Zone1), but also offers a differential backup zone for the neighboring lines/busbars (i.e., Zone2). Consequently, adding a differential backup for the neighboring zones will enhance the reliability of the protection system. For example, let us consider fault F1 in Fig. 3.12. This fault will be detected by both Relays R5 (Zone 1) and R3 (Zone 2). If R5 fails to operate and isolate the fault within a predetermined time (i.e., TMD), the Relay R3 will operate in its backup zone.

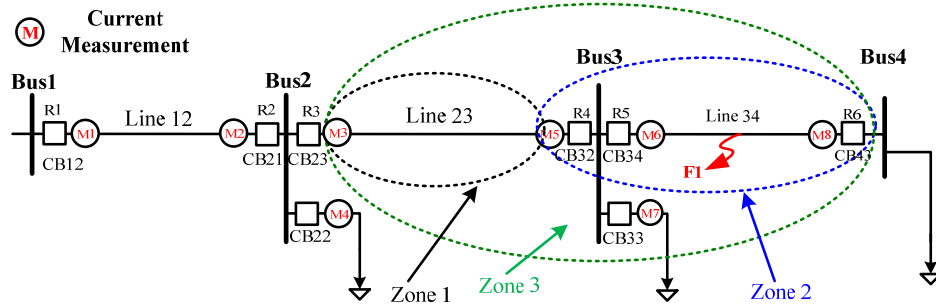


Fig. 3.12. Proposed differential-based protection zones (for Relay R3).

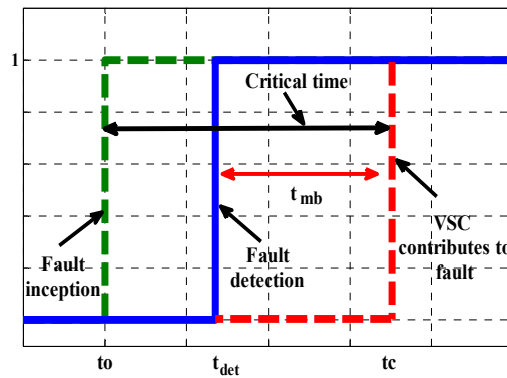


Fig. 3.13. Typical time frames for fault detection and sending the trip command.

On the other hand, to provide a selective protection without any interference between backup zones, it is necessary to ensure that Zone2 of each relay does not operate before the Zone1 of the downstream relay. Therefore, TMD is the key factor in the coordinated operation of the main and backup relays. As it was already explained, the fault current should be interrupted during the first stage of the fault current. Indeed, the main and backup zones should operate during the critical time of the VSC station (i.e.,  $\Delta t_c$ ). On the other hand, both Zone1 and Zone2 require communication links; hence, they detect faults after  $t_{det}$  which is heavily dependent on communication delay. Thus, as shown in Fig. 3.13, once the fault is

detected, both the main and backup differential protection should operate within  $t_{mb}$  time frame that can be calculated as:

$$t_{mb} \leq \Delta t_c - t_{det} \quad (3.21)$$

Where  $\Delta t_c$  is the critical time of the VSC station, and  $t_{det}$  is the fault detection time of the relays (including the communication delay and processing time). Since, the  $t_{mb}$  is the maximum time frame that both, main and backup zones, should operate, the maximum value of TMD can be calculated as:

$$TMD_{max} = t_{mb}/2 \quad (3.22)$$

On the other hand, the minimum value of TMD should be larger than the operating time of DCCBs and the delay associated with the current transducer. Thus, to provide a selective protection, the time margin between the main and backup zones should be selected as:

$$t_{Br} < TMD \leq t_{mb}/2 \quad (3.23)$$

Where  $t_{Br}$  is the summation of the operating time of DCCBs and the delay associated with the current transducer (CT) and its A/D converters. Equation (3.23) implies that if for a specific network,  $t_{mb}/2$  is less than the operating times of the SSCBs, there will be a high possibility of mis-coordination between the consecutive relays.

It should be also noted that, the proposed method also offers the possibility of a third zone consisting of Zone1 and Zone2. Zone3 can provide a backup protection for the main protection zone (i.e., Line23 in this example). Therefore, if the main protection of Line23 (Zone1 of R3) fails to operate, e.g., due to a deficiency in M5, Zone3 will provide backup for Zone1.

#### 3.3.2.2. Overcurrent-directional-based backup zones

Since the differential relays are vulnerable to communication failures, the proposed method employs O/C directional relays to back the differential protection up if the communication network fails. The O/C directional relays can be of either inverse-time type or definite-time type. Although inverse-time O/C relays provide a lower tripping time in large systems, their coordination in DC systems is challenging due to the high raising rate of DC fault currents [52]. The use of backup O/C directional protection has been proposed in [97]. However, this type of coordination may results in a relatively longer operation time in large distribution systems. Therefore, since a fast protection scheme is required for DC networks (to guarantee the safety of the converters), this strategy proposes to employ the backup O/C directional

elements for a selective number of relays within the DC network. Thus, each feeder of the network is divided into several protection zones in order to minimize the fault clearance time in large DC networks; the relay of each zone is then equipped with a directional definite-time O/C element. In addition, each protection zone will need to have a radial structure for the proper operation of the backup protection. Fig. 3.14 shows the logic circuit of the backup protection scheme where the O/C directional element have two operating times for forward and reverse faults, i.e.,  $TD_F$  and  $TD_R$ , respectively. As Fig. 3.14 indicates, if the communication network fails while a forward fault is detected, a trip signal is issued after a time delay ( $TD_F$ ).

Fig. 3.15 shows the coordination of O/C definite-time relays for the backup protection scheme in a DC distribution system with two feeders; in this figure, TM denotes a suitable time margin that enables coordination of relays in forward and reverse directions. It should be noted that since solid-state DCCB are used, TM is in the range of several milliseconds (see case study 4 of this chapter). The grading times for forward and reverse directions are chosen in a way that the smallest part of the network is de-energized subsequent to a fault.

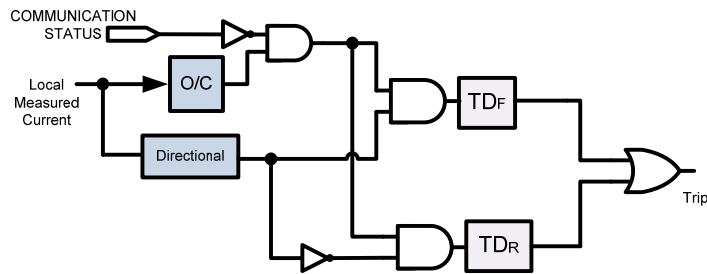


Fig. 3.14. Symbolic logic circuit for the backup protection.

In the network of Fig. 3.15 each feeder has been divided to 2 zones; therefore, to provide a selective protection, the operating time of the most upstream relay (i.e.,  $R_V$ ) is set on:

$$TD_F(R_V) = t_f + 2TM \quad (3.24)$$

Where  $t_f$  is the time delay of the operation of the most downstream relay of each feeder. In general case, if it is assumed that the maximum zone number of each feeder is denoted by  $n$ , the operating time of  $R_V$  can be expressed by:

$$TD_F(R_V) = t_f + nTM \quad (3.25)$$

On the other hand, to protect the VSC station, the maximum operating time of the most upstream relay, i.e.,  $R_V$  in Fig. 3.15, and its corresponding CB should be less than the critical time of the VSC station; that is:

$$\Delta t_c > TD_F(R_V) + t_{Br} \quad (3.26)$$

Substituting (3.25) in (3.26) results in:

$$\Delta t_c > t_f + nTM + t_{Br} \quad (3.27)$$

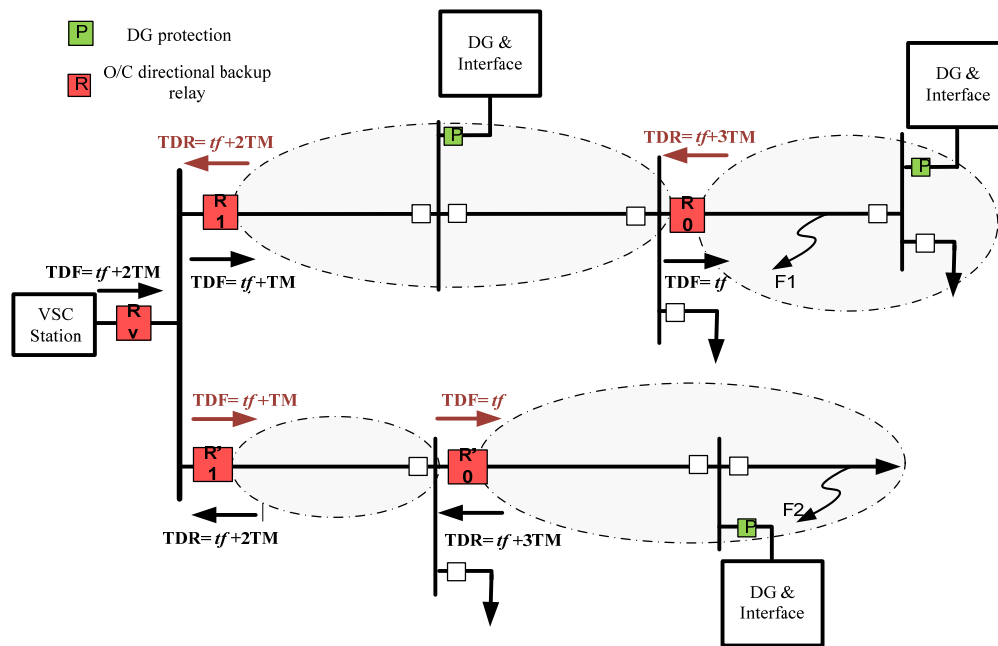


Fig. 3.15. Coordination of O/C directional relays for the backup protection scheme.

The equation (3.27) indicates that the maximum number of backup zones for each feeder can be calculated as:

$$n < \frac{\Delta t_c - t_{Br} - t_f}{TM} \quad (3.28)$$

If no time delay is assumed for the most downstream relays (i.e.,  $t_f = 0$  for  $R_0$  and  $R'_0$ ), then equation (3.28) can further be simplified as:

$$n < \frac{\Delta t_c - t_{Br}}{TM} \quad (3.29)$$

Base on the equation (3.29), the number of directional O/C backup zones is limited by  $\Delta t_c$  and  $TM$ , where  $TM$  is also determined by the operating time of DCCBs, fault detection time, and the delay associated with CT sensors. The Study Case 4 of this chapter provides more details about the operating times of directional O/C units proposed for the backup protection.

#### 3.4. Proposed protection strategy

The flowchart of Fig. 3.16 provides a graphical illustration of the proposed protection strategy. The current measurement units, i.e., M1 through M8 in Fig. 3.12, transmit their measured values to the corresponding relays via the communication network. The relay algorithm calculates the differential currents based on the defined differential-based protection zones (i.e., Zone1, Zone2, and Zone3). If a fault strikes the line, the differential current of Zone1 exceeds its respective threshold, and the relay will immediately send a trip signal to the associated DCCB. If a relay fails to properly detect a fault in its main protection zone (i.e., Zone1), the upstream relay will detect the fault in its backup differential protection zone (i.e., Zone2) and will operate after a time delay (TMD); the TMD, in turn, is defined in a way that the coordination between the main and backup protection is preserved.

Fig. 3.16 illustrates that the backup differential zone (i.e., Zone2) operates after the TMD, giving a chance to the main protection (i.e., Zone1) to detect and isolate the fault first. Finally, Zone3 provides a backup for Zone1 of the same relay, e.g., if the measurement device at the remote end of the line fails. It is noted that, considering the typical data propagation delays and a limited geographical span of a DC distribution system, all relays receive the current measurement and detect faults almost at the same time. The proposed strategy also considered the possibility of CB failure, that is, if the CB commanded by the main protection fails to operate, a breaker failure signal is sent to the adjacent CB(s) to de-energize the smallest possible area of the system.

The flowchart of Fig. 3.16 also demonstrates that the relay switches of the O/C directional-based backup protection will act if the communication network fails. In this case, the relay will also send an alarm signal to the control center to report the communication failure. It should be noted that, according to the specifications of the industrial protocols, the protective devices, are equipped with the communication failure detection capability and switch to the backup protection without requiring any signal from the external supervisory systems [139].

As mentioned in Section 3.2.2, only a selected number of relays are equipped with this backup protection scheme.

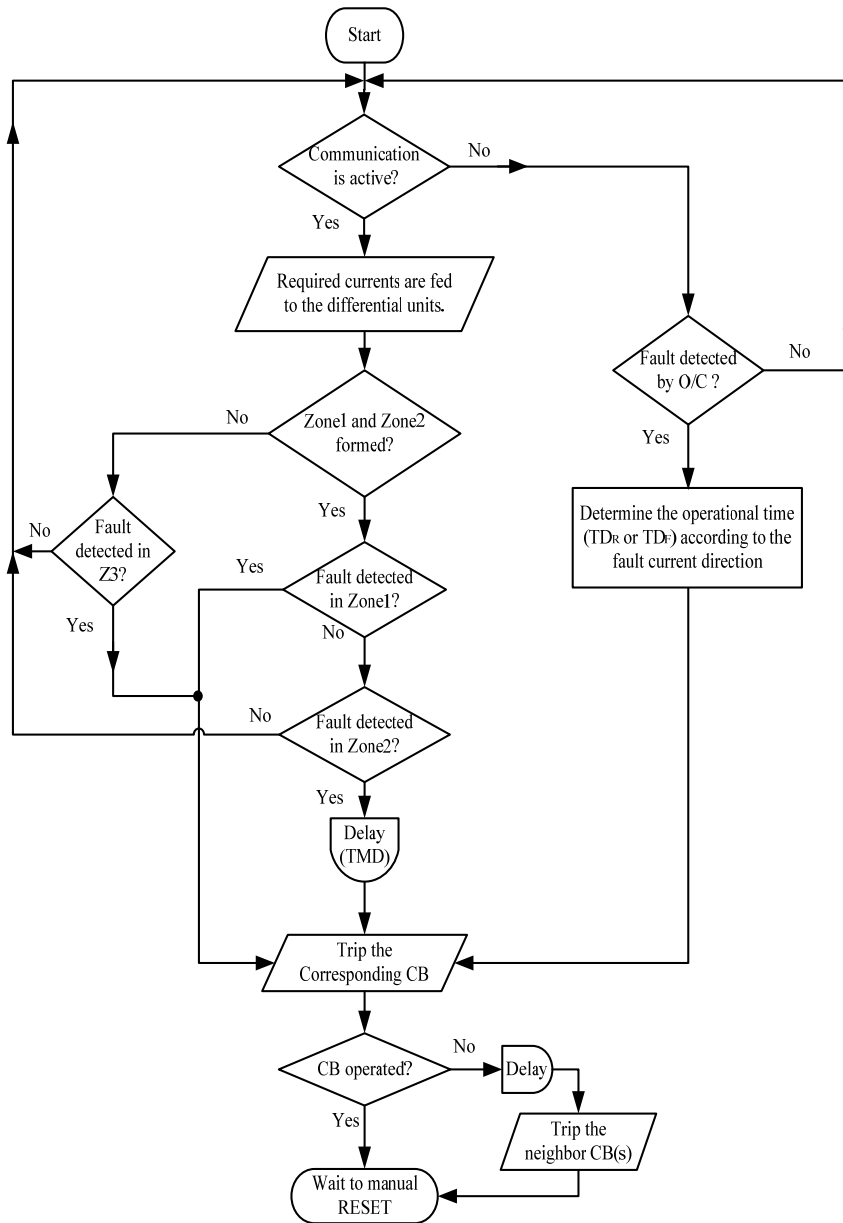


Fig. 3.16. Flowchart of the proposed protection strategy

### 3.5. Real Time Simulation Results

#### 3.5.1. Test Setup

To evaluate the effectiveness of the proposed protection strategy, a HIL approach has been used. Fig. 3.17 shows the schematic diagram of the HIL test-bed setup. The components of this setup are shown in Fig. 3.18, which include: 1) a real-time digital simulator (OPAL-RT) that simulates the behavior of the components in the study network under various operational conditions; 2) a PC that is used as a command station (programming host) to run the Matlab/Simulink models executed on the OPAL-RT; 3) a development board (DK60 from Beck company) which has been used to implement the proposed protection algorithm; and 4) a router that is used to connect all the setup devices in the same sub-network. In this test setup, the board operates as the protection brain and communicates with current measurements units simulated in the OPAL-RT, via Ethernet medium. Therefore, the HIL test setup considers the communication delays consisting of *i*) preparation of data (packaging) in the sending end and *ii*) opening the data package in the receiving node. Since the delay associated with data propagation between two nodes is relatively small (less than 0.1ms for most distribution feeders [74]), it is ignored in this study.

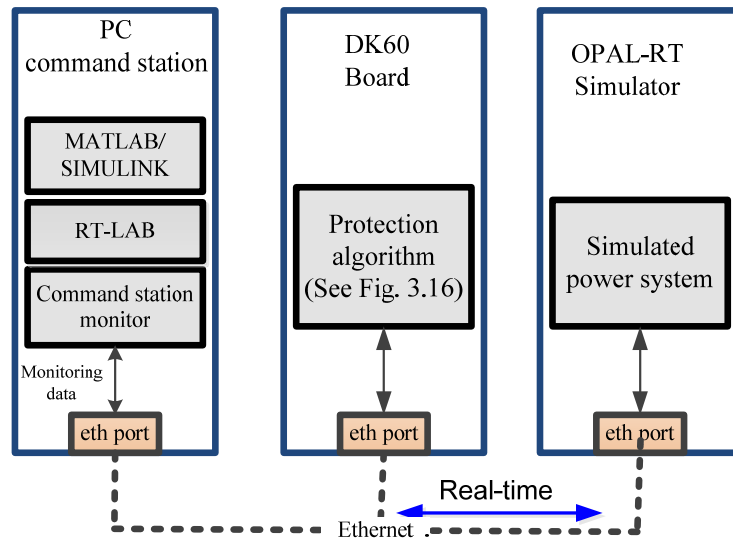


Fig. 3.17. The schematic diagram of the HIL setup.

#### 3.5.2. The study system

The effectiveness of the proposed method is demonstrated in the context of the distribution network of Fig. 3.18. The basic configuration and parameters of this network is extracted

from the benchmark proposed in [140]; however, some modifications have been done to enable its operation as a DC distribution system with DGs. Hereafter, the network of Fig. 3.18 is referred to as the “study system”.

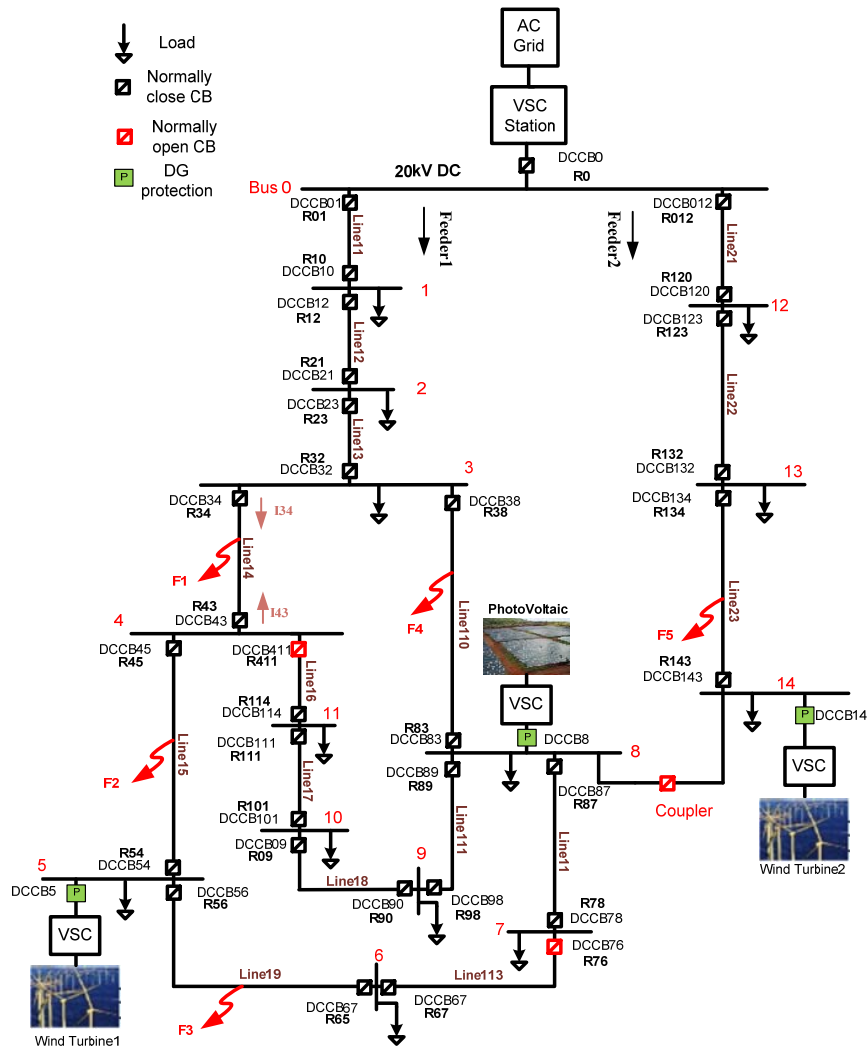


Fig. 3.18. Single-line diagram of the study distribution system.

The study system is a bipolar DC network which includes two main DC feeders connected through a normally open coupler circuit breaker. Therefore, the loads can be supplied by

radial or meshed lines depending on the status of DCCB411, DCCB76, and the coupler; these breakers normally are open. The two-level  $\pm 10$ -kV VSCs are used to interface the AC network and RESs with the DC network. The Hall-Effect CTs installed at both sides of the DC lines determine the borders of the protection zones. The data transfer between the DC buses is possible thanks to dedicated communication links.

Each DG is individually protected so that it will be disconnected from the network if a fault strikes the grid during a certain period of time. Fig. 3.18 shows the location of the DCCBs and the relays.

#### 3.5.3. The Study Cases

In the following paragraphs, several fault scenarios are simulated to demonstrate the efficacy of the proposed method, when communication delays are considered. In all the study cases, it is assumed that the fault is initiated at  $t = 1.0$ s.

##### 1) Study Case 1

The objective of this scenario is to evaluate the performance of the proposed strategy when the communication link operates correctly. In this case, a PP fault impacts the location F1 of the study system. Thus, the protection algorithm of the relay R34 detects the fault in this first zone and sends a signal to the OPAL-RT, via Ethernet ports, to trip its corresponding circuit breaker. Fig. 3.19(a) shows that, after the PP occurs at F1, the differential current seen by R34 increases rapidly. The fault current of the VSC station is shown in Fig. 3.19(b); the figure indicates that the trip signal is generated by R34 due to the discharging current of the capacitor (before the main converter can contribute to the fault); hence, the proposed protection is fast enough to prevent any damage to the converter while isolating the faulty section.

The timing for the fault detection and VSC contribution is shown in Fig. 20. The figure indicates that the relay R34 detects the fault in its main zone and sends the trip signal to DCCB34 almost 2.6ms after the fault inception; this delay is due to the communication and processing times. Although the delays caused by the measurement and interface devices are not considered in this study, it has been verified that such delays are less than  $10\mu$ s assuming that Hall-Effect current transducers and appropriate microprocessor-based relays are used [121].

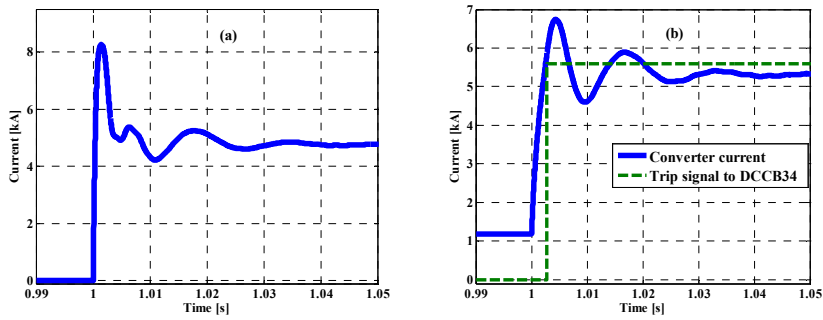


Fig. 3.19. Waveforms of (a) differential current seen by R34, and (b) converter current and scaled trip signal to DCCB34.

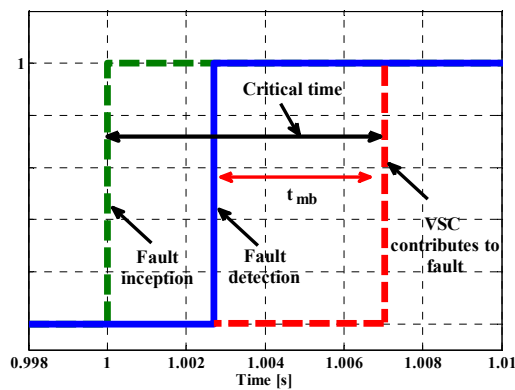


Fig. 3.20. Time delay in the fault detection and sending trip signal.

As shown in Fig. 3.20,  $t_{det}$  is around 2.6ms ( $\pm 0.3$ ms in different test cases). Moreover, the simulation results show that the critical time of the main converter of the study system is around 7.2ms. Therefore, once the fault is detected, it should be cleared in less than 4.6ms ( $\pm 0.3$ ms), which is the maximum time that fault current, must be interrupted by the main or the backup protection. Therefore, the maximum value of TMD can be calculated as [4]:

$$TMD = t_{mb} / 2 \approx 2.3ms \quad (3.30)$$

On the other hand, since DCCBs are assumed to be of solid-state type, their operating time is less than 1ms [134]. Therefore, considering some microseconds delay for the measurement

devices and the A/D conversion, as well as a marginal time, the time delay between the main and backup differential zones is set to be 2.0ms in this study.

2) Case Study 2

If it is assumed that a PP fault takes place at location F2, and Relay R45 fails to detect and isolate the fault. Thus, due to the R45 failure, the fault is detected by the backup protection, that is, Zone2 of R34. Fig. 3.21 illustrates the protection zones of R45, R54, and R34.

Fig. 3.22(a) shows that Zone1 of R54 detects the fault and sends the trip signal to DCCB54 in about 2.7ms. However, as shown in Fig. 3.22(b), Zone1 of R45 fails to issue the trip signal. Hence, Zone2 of R34 operates after a predefined time delay (i.e., TMD=2ms). The main and backup trip signals are shown in Fig. 3.23; the figure indicates that the backup trip is sent to DCCB34 in about 4.8ms from the fault initiation.

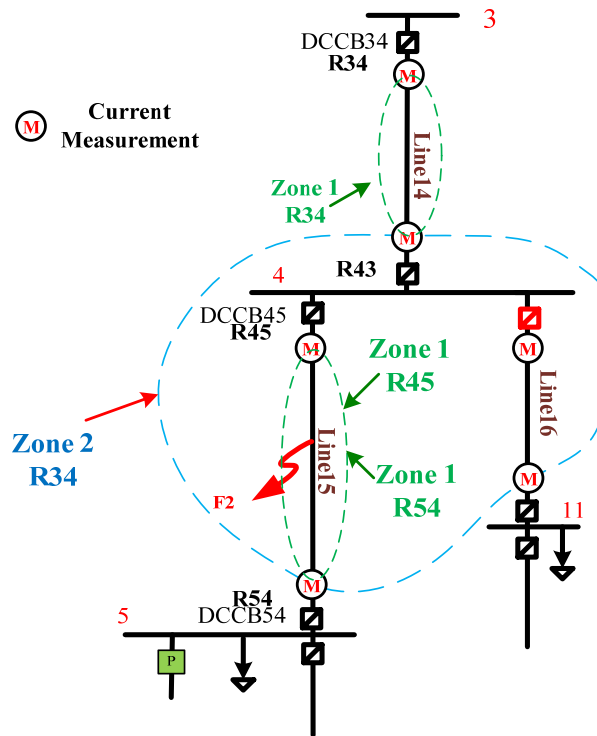


Fig. 3.21. The protection zones of R34, R45, and R54.

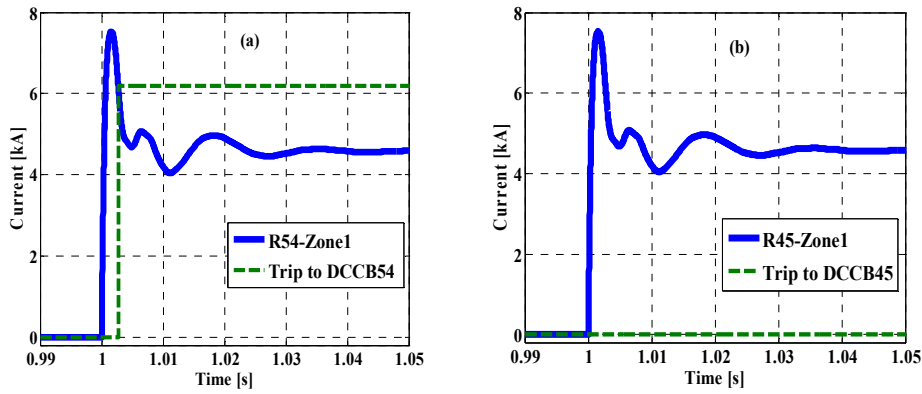


Fig. 3.22. The differential current and trip signals issued by (a) R54 (Zone1), and (b) R45 (Zone1).

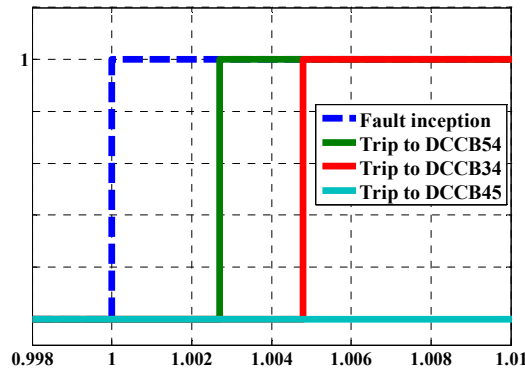


Fig.3.23. Trip signals of the main and backup protection for a PP fault at F2.

### 3) Study Case 3

To verify the effectiveness of the proposed method for high-impedance faults, it is assumed that a 100-Ω PP fault strikes the study system at F1. Fig. 3.24(a) shows the currents measured at both sides of the faulty line as well as the differential current at the Zone1 of R34. The effect of the fault resistance on the fault current measured at the VSC station is also shown in Fig. 3.24(b). As indicated in Fig. 3.25, the relay R34 detects the fault and issues the trip signal in about 4.7ms from the fault initiation. It is clear that, due to the impact of the fault resistance on the raising rate of the DC fault current, the relay operating time is

relatively higher in this case; however, it is still fast enough to ensure operation of the protection system before the critical time of VSC station.

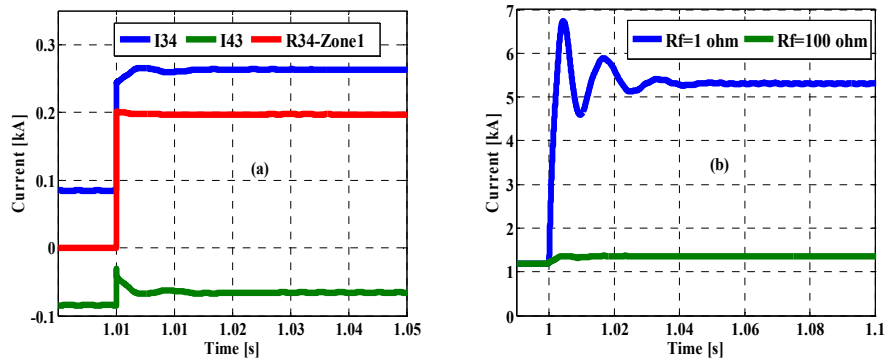


Fig. 3.24. Waveforms of (a) the fault and differential currents of the faulty line, and (b) the converter current for two fault resistances.

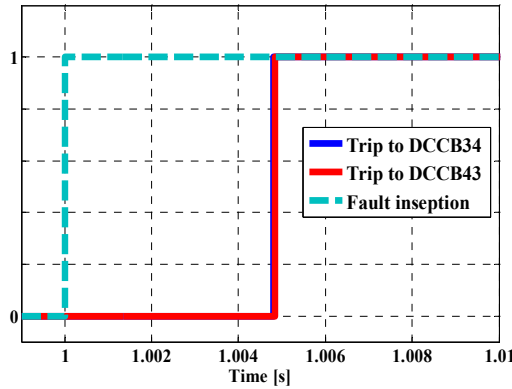


Fig. 3.25. Trip signals send to the DCCBs.

#### 4) Study Case 4

As discussed in Section 3.3.2.2, the O/C directional relays will provide backup protection if the communication network fails. Fig. 3.26 shows the protection zones of backup O/C directional relays which have been selected based on the position of normally open DCCBs. Considering the selected backup protection zones, relays R01, R32, R34, R38, R012, and R134 are equipped with O/C directional modules. It is, however, noted that R32 is equipped with the O/C directional unit only to prevent undesired power interruption, in case of R34,

R38 (or their associated DCCBs) failure. The remaining relays are disabled until the communication network is restored.

As illustrated in Fig. 3.18, the maximum operating time of the most upstream relay, i.e., R0, is 3TM; this time should be selected based on the critical time of the main VSC as well as on the constraints linked to the coordination with other relays. Therefore, since the critical time of the main VSC converter is 7.2ms, the maximum value of TM turns out to be 2.4ms. Furthermore, the operating time of the main protection of each zone can be expressed as:

$$t_{op} = t_{CB} + t_{det} + t_{CT} \quad (3.31)$$

where  $t_{CT}$  signifies the delay associated with current transducers and their corresponding A/D converters (several microseconds);  $t_{det}$  is the fault detection time of the relay algorithm (in the range of several microseconds); and  $t_{CB}$  denotes the operating time of DCCBs. Therefore, the main protection of each zone will operate in about 1ms, and considering an additional time margin, TM is set on 2ms in this study. This TM is used to coordinate the selected relays which operate in case of communication failure.

To further demonstrate the effectiveness of the proposed protection strategy, various fault scenarios have also been tested using the real-time simulation setup and their results have been reported in Table 3.2.

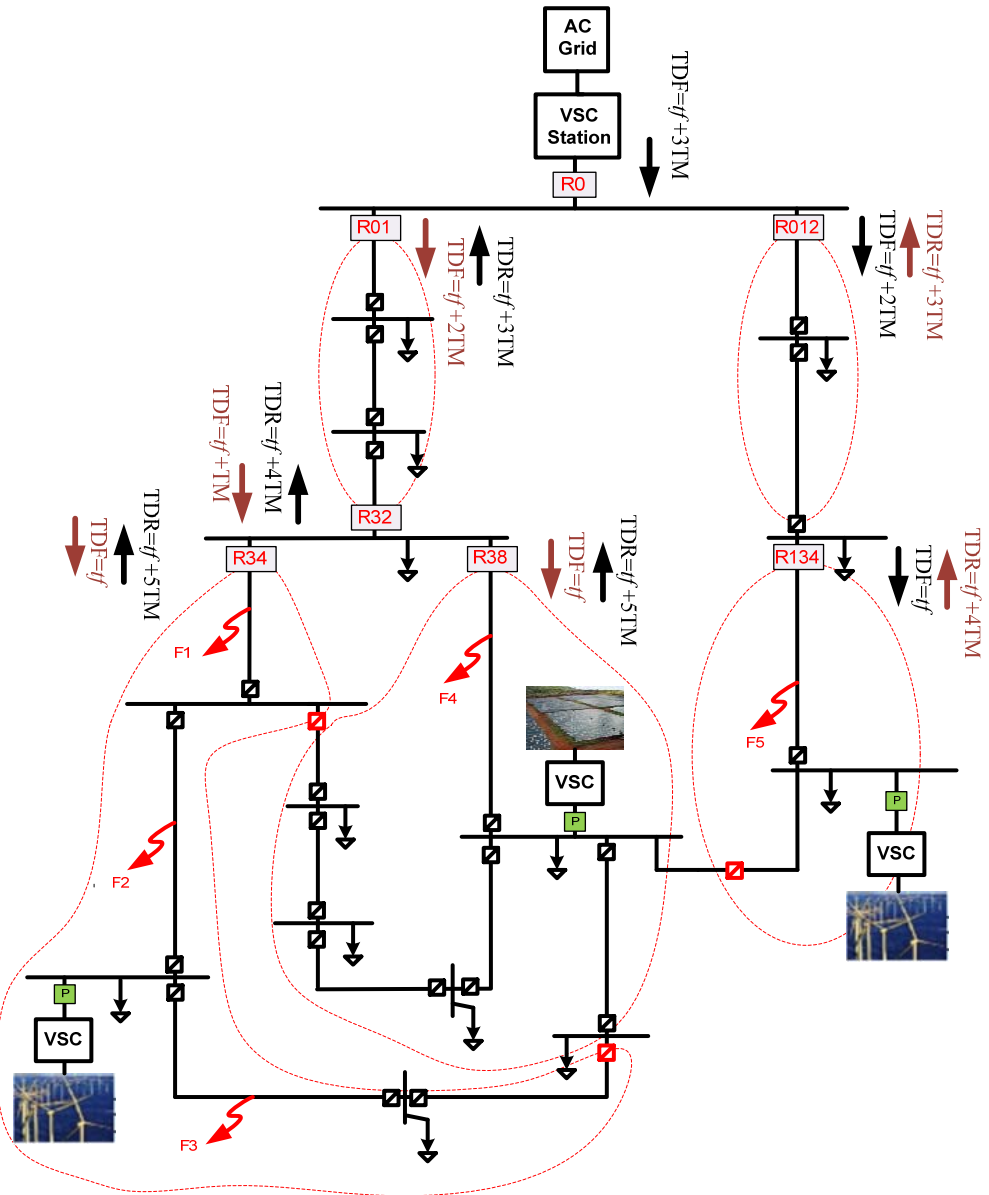


Fig. 3.26. Backup protection zones (communication network failure).

### Chapter3. Differential- based protection for DC distribution systems

Table 3.2. Operating times of the main and backup protection for selected fault scenarios.

| Fault Type            | Fault Location | Fault resistance ( $\Omega$ ) | Main Protection |        |                                 | Backup Protection |        |                                 |
|-----------------------|----------------|-------------------------------|-----------------|--------|---------------------------------|-------------------|--------|---------------------------------|
|                       |                |                               | Relay           | Zone   | Trip signal after ( <i>ms</i> ) | Relay             | Zone   | Trip signal after ( <i>ms</i> ) |
| <b>PP</b>             | F1             | 1.00                          | R34             | Zone 1 | 2.6                             | R2                | Zone 2 | 4.8                             |
|                       | F1             | 100                           | R34             | Zone 1 | 4.8                             | R2                | Zone 2 | 6.7                             |
|                       | F2             | 1.00                          | R45             | Zone 1 | 2.4                             | R34               | Zone 2 | 4.6                             |
|                       | F2             | 100                           | R45             | Zone 1 | 4.4                             | R34               | Zone 2 | 6.5                             |
|                       | F3             | 1.00                          | R56             | Zone 1 | 2.5                             | R45               | Zone 2 | 4.7                             |
|                       | F4             | 1.00                          | R38             | Zone 1 | 2.5                             | R2                | Zone 2 | 4.6                             |
| <b>PG</b>             | F1             | 1.00                          | R34             | Zone 1 | 2.3                             | R2                | Zone 2 | 4.5                             |
|                       | F2             | 1.00                          | R45             | Zone 1 | 2.7                             | R34               | Zone 2 | 4.8                             |
|                       | F3             | 1.00                          | R56             | Zone 1 | 2.6                             | R45               | Zone 2 | 4.7                             |
|                       | F3             | 100                           | R56             | Zone 1 | 4.5                             | R45               | Zone 2 | 6.6                             |
|                       | F4             | 1.00                          | R38             | Zone 1 | 2.3                             | R2                | Zone 2 | 4.6                             |
|                       | F4             | 100                           | R38             | Zone 1 | 3.7                             | R2                | Zone 2 | 6.0                             |
| Communication Failure |                |                               |                 |        |                                 |                   |        |                                 |
| PP                    | F1             | 1.00                          | R34             | -      | Inst.                           | R32               | -      | 2                               |
| PP                    | F2             | 1.00                          | R34             | -      | Inst.                           | R32               | -      | 2                               |
| PG                    | F5             | 1.00                          | R134            | -      | Inst.                           | R012              | -      | 2.4                             |

---

## Protection and fault management in multi-terminal DC systems

This chapter proposes an economic advantageous protection strategy which implies that DCCBs are placed only at the connection points of the active elements of the DC grid, i.e., at the connection points of the DC grid with renewable energy sources (RESs), microgrids and AC networks (points tagged as “A” in Fig. 4.1). Indeed, while in the previous chapter it was assumed that DCCBs are were located at all the DC lines, in this chapter the fault interruption is handled by the minimum possible amount of DCCBs. Moreover, in order to isolate the faulty line, DC isolator switches, which are cheaper than DCCBs, are placed on both sides of the DC lines.

On the other hand, in order to develop a fast and selective protection, a communication-assisted fault location method is introduced in which the faulty line is identified based on the exchanged signals among the relays installed on both ends of the DC lines. Compared with the differential protection, presented in the previous chapter, in which the measured current at one end of the line must be continuously transmitted to the other side, the transmitted data in the proposed method contain identification signals and are sent to the other end of the line only when a fault is detected.

The performance of the proposed protection strategy is demonstrated by means of experimental analysis performed using a hardware in the loop (HIL) platform. In this setup, the proposed algorithm is implemented in a development board (DK60) that emulates a relay. The board is connected to a real-time simulator (OPAL-RT) which is simulating a MVDC network in real time. The algorithm running on the DK60 board receives the signals

associated to the measured currents from the OPAL-RT environment and sends the operational signals to the protective devices simulated on OPAL-RT.

Compared to the methods already presented in the literature, the main features of the proposed strategy presented in this chapter can be summarized as follows:

- The proposed fault location is an adaptive-communication-assisted method based on the directional-overcurrent protection. In this fast and selective protection scheme, faults are located by using the exchanged signals among the relays installed at both sides of the lines. Accordingly, the fault location method does not rely on the synchronized measured current from both sides of the protected line.
- The proposed method can provide a generic protection method without using time-consuming and complex methods. Moreover, the high rising rate of DC fault currents change due to the network topology and the intermittent behavior of DGs cannot cause the mal-operation of protections.
- To manage communication failures, the proposed scheme is equipped with a backup fault location method which is activated if the communication system fails.
- The proposed protection scheme has been implemented and tested in a real-time simulation platform working as hardware in the loop (HIL). Therefore, some of the practical concerns, like communication delays, have been taken into account, leading to a more accurate verification.

### 4.1. MVDC distribution system study case

There are multiple interesting applications for multi-terminal DC networks such as: connection between several AC microgrids for creating a multiple-microgrid [39]; connection of RESs to the grid [16]; enhancing the transmission capacity of AC lines by conversion to DC (especially when there are bottlenecks for construction of new AC lines) [35, 42]; and, connection of DC loads (especially in industrial applications) [33]. Fig. 4.1 shows a hypothetical multi-terminal DC network which is designed to handle all these applications. Hereafter in this chapter, the network of Fig. 4.1 is referred to as the “study network”.

The study network is a bipolar DC system consisting of radial and loop lines. The two-level  $\pm 10\text{kV}$  VSCs are used to interface the AC network, microgrids, and RESs to the DC network. The Hall-Effect current measurements are installed at each side of the DC lines and busbars. The data transmission between all the DC busbars is performed by using a dedicated communication link. The appropriate protection devices that must be installed at the points A and B are described in the following sections. Loads are protected by fuses. The elements connected to the network, as well as the cable parameters, are reported in the Appendix of this chapter.

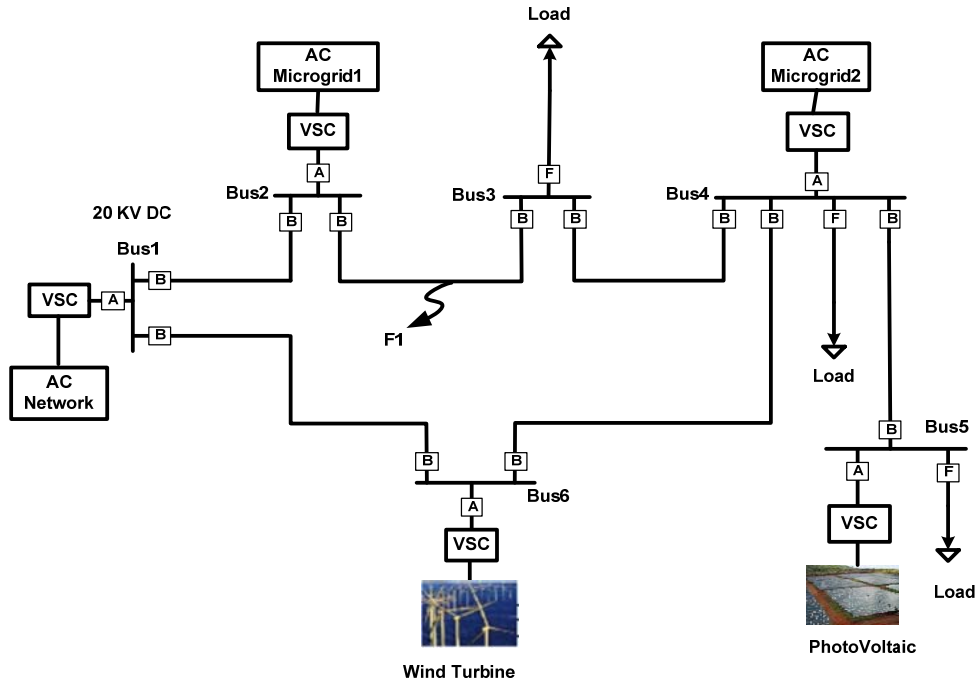


Fig. 4.1. A prototype multi-terminal DC distribution system.

#### 4.2. Requirements of the proposed protection strategy

Well-designed protection schemes are able to detect/locate the various types of faults, interrupt the fault current and isolate the faulty part before serious damages occur on vital devices. Thus, according to the characteristics of the DC fault current, the proposed protection strategy is designed to protect the MVDC distribution networks by using the components that are introduced in the following subsections.

##### 4.2.1. Fault clearance using hybrid DCCBs.

As mentioned above, DCCBs are necessary to interrupt the fault current and protect the converter components in the VSC-based DC networks. On the other hand, once a fault impacts a DC network, the fault current can be supplied by the AC-side sources, distributed generators (DGs), and microgrids. Therefore, the fault current can be interrupted if the DCCBs are located only at the connection points of these active elements to the network (points tagged as “A” in Fig. 4.1).

Solid state CBs are able to operate in less than 1 millisecond [134]; however, the use of SSCBs in the medium-voltage level implies increased costs and technological issues [51]. A hybrid-type CD CB which is able to interrupt the fault current in less than 5ms has been developed by ABB [70]. In the proposed strategy it is assumed that DCCBs of this type are installed at points A of Fig 4.1.

### 4.2.2. Fault detection by overcurrent-based local protection unit (LPU)

Due to the fast rising rate of DC fault currents, fast fault detection can be obtained by monitoring the current in the connection points of the network (points tagged as “A” in Fig. 4.1). Therefore, a local protection unit (LPU) is installed at each connection point where DCCBs are placed. The LPU includes an instantaneous overcurrent unit which operates according to a predetermined threshold and the current flowing through the connection point. The LPU detects the solid (low impedance) faults after several microseconds and sends the trip command to the corresponding DCCB, as its main function. The LPU also communicates with other protection devices to handle the other functions that are explained in Section 4.4.

### 4.2.3. Fault isolation using isolator switches

To isolate the faulty parts of the MVDC network and facilitate the network restoration, DC isolator switches are placed at each end of the DC lines (points tagged as “B” in Fig. 4.1). This type of switches, which are considerably cheaper than DCCBs, must be opened/ closed when their current is close to zero. Therefore, they are used to isolate faulty parts after the fault current has been already interrupted by the CBs. The conventional AC CBs can be an appropriate choice for this purpose. The operational time of the typical medium voltage AC breakers is less than 60ms [68].

### 4.2.4. Fault location using the proposed communication-assisted relay.

The fault detection and interruption by the LPUs and DCCBs results in the overall de-energizing of the DC network; thus, it cannot provide a selective protection. Hence, in the proposed strategy, the selective protection is achieved by exchanging data between the relays installed at both ends of each DC line. In this way, a “communication-assisted isolator relay” (CIR) is designed to locate the exact faulty line and to send the proper commands to the corresponding isolator switches. The CIRs are equipped with instantaneous overcurrent and directional units, as is shown in the logic circuit of Fig. 4.2. The figure also indicates that a CIR installed at each end of a DC line, receives two signals from another CIR installed at the other end. These signals are: *i*) the DET signal that determines the fault detection by the relay and *ii*) the DIR signal which determines the direction of the fault current. Table 1 represents the DET and the DIR signals in binary format. Each CIR sends the trip command to the

## 4.2. Requirements of the proposed protection strategy

associated isolator when the other end CIR confirms that the fault has occurred inside the protected line (i.e., when the CIR receives  $DET=1$  and  $DIR=1$ ). The flowchart of Fig. 4.4 provides a graphical illustration of the proposed algorithm for the CIRs. This figure shows that the trip command is sent to the corresponding DC isolators after the fault current has been interrupted by the DCCBs. The roles of the CIRs on the proposed strategy in explained in Section 4.4.

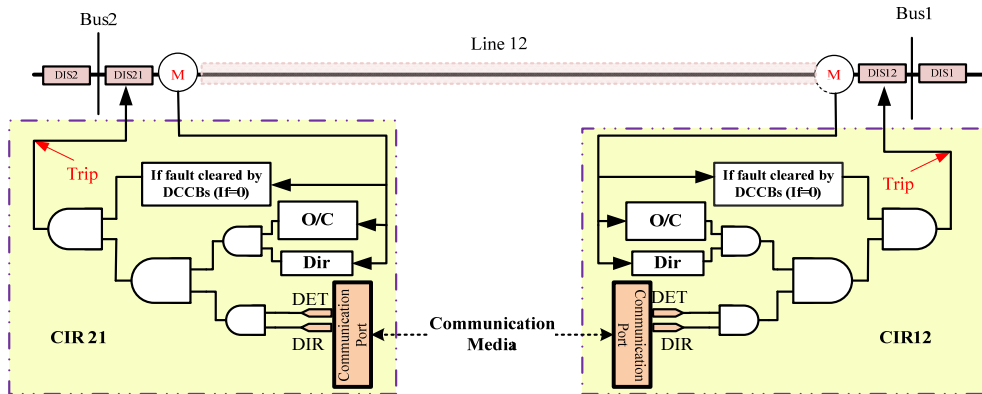


Fig. 4.2. The logic circuit of the CIRs.

Since the method is based on the direction of the fault current, more details are provided in Fig. 4.3 to illustrate the logic of the fault detection. This figure shows the direction of the fault current when the fault happens inside or outside of the protection zone of Relay 1.

It can be seen that only when the fault is happening inside the protected line, the fault current in both sides of the line flows from the bus to the line (the fault current flows inside the protection zone). In other words, when the fault is not inside the protection zone of a picked up relay, at least one of the CTs of the zone detects a current which is flowing outside of the zone.

Table 4.1. Meaning of the exchanged signals among CIRs

| Signal value            | 1                              | 0                         |
|-------------------------|--------------------------------|---------------------------|
| Signal name             |                                |                           |
| Fault Detection (DET)   | Fault detected by the O/C unit | Normal condition          |
| Current Direction (DIR) | Inside: from bus to line       | Outside: from line to bus |

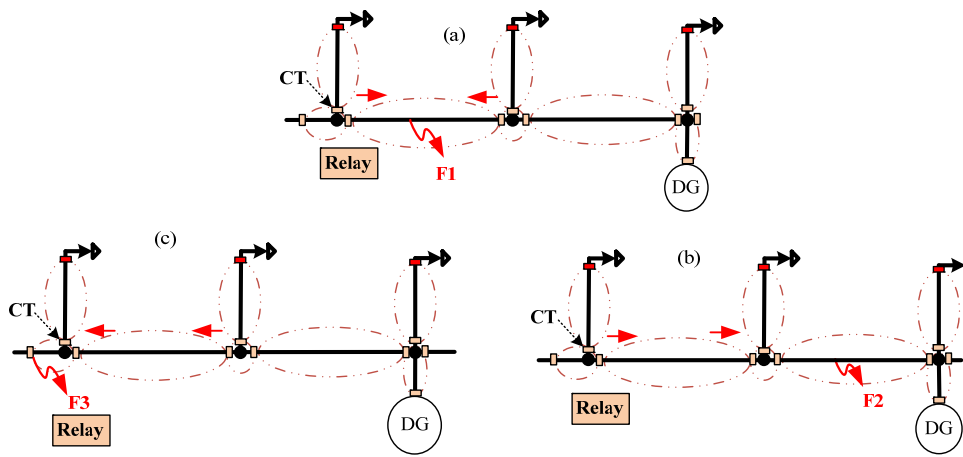


Fig. 4.3. The fault current direction for different faults in a loop feeder; a) fault inside the protected zone; b and c) fault outside of the protected zone.

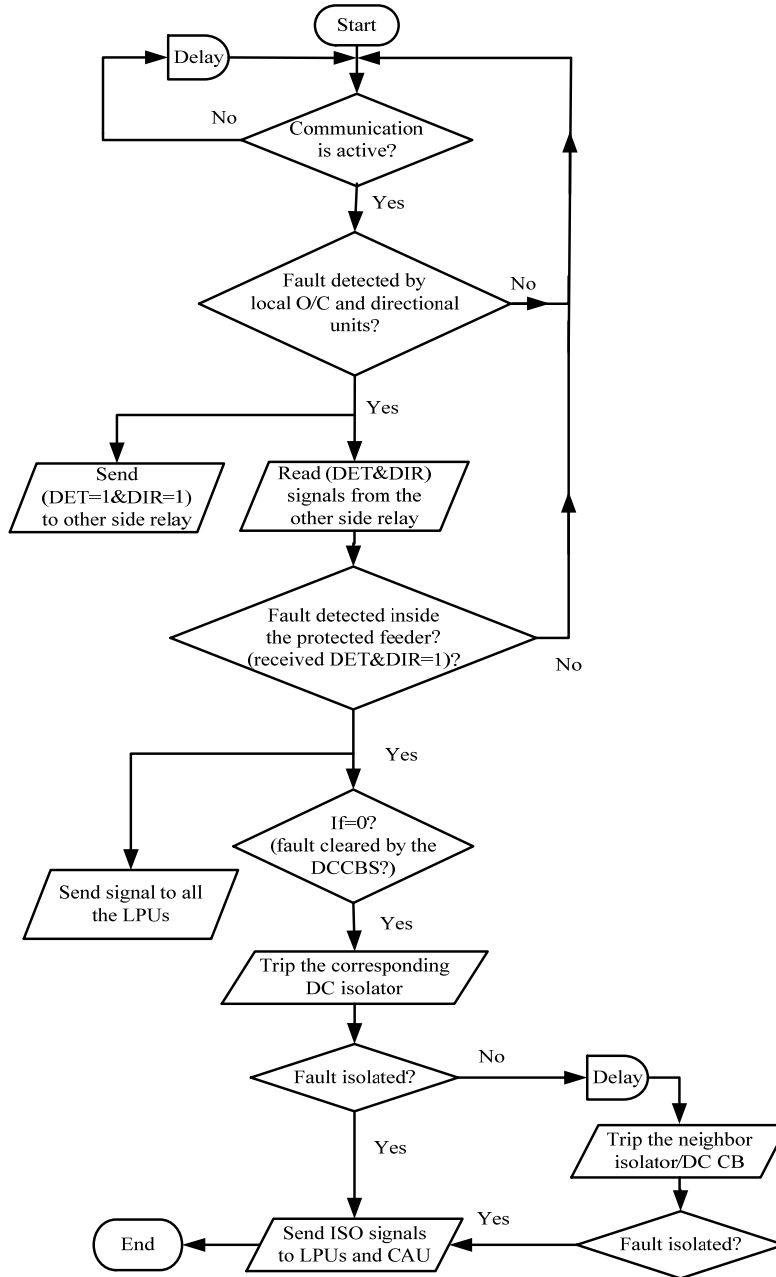


Fig. 4.4. Flowchart of the proposed algorithm for the CIRs.

### 4.3. Proposed protection strategy

This section explains the proposed protection strategy considering the protection elements described in the previous section. The proposed strategy includes both main and backup protections. The main protection is communication-assisted; whereas the backup protection is activated when the communication link fails.

#### 4.3.1. Main Protection

In this strategy, the connection points (points tagged as “A” in Fig. 4.1) are equipped with CBs and LPU. The DC isolator switches and the CIRs are also installed on the DC feeders (points tagged as “B” in Fig. 4.1), as shown in Fig. 4.5. The operation sequence of the main protection is explained here according to the time diagram shown in Fig. 4.6.

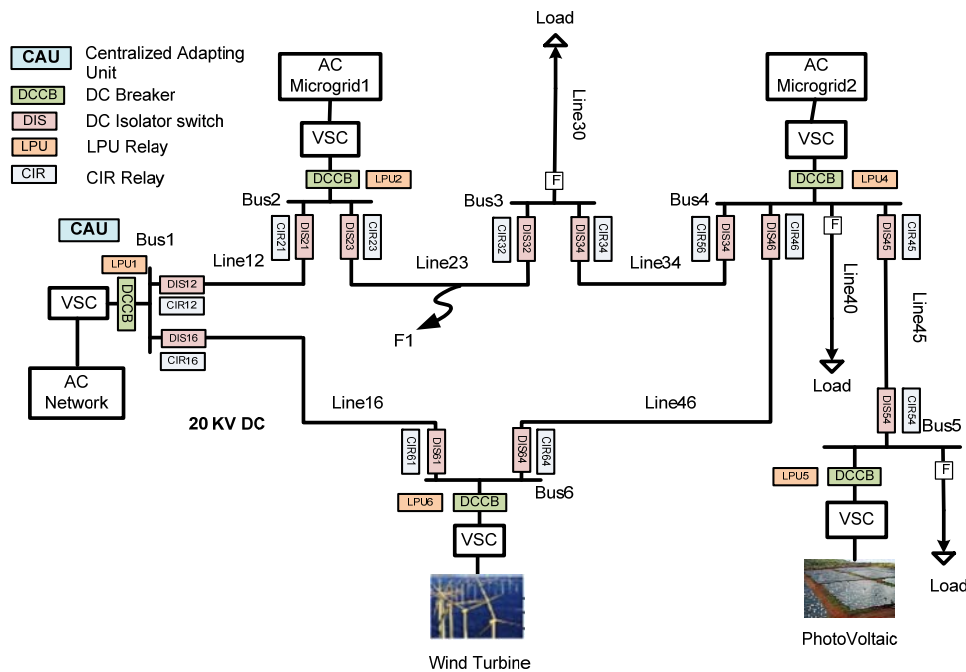


Fig. 4.5. Study network with the protection elements.

Subsequent to the fault occurrence, the LPUs detect the fault and send the trip command to the associated DCCBs. Then, the DCCBs operates and interrupts the fault at  $t_3$ . The time interval ( $t_1 - t_3$ ) is related to the operation time of the hybrid DCCBs which is around 5ms

[70]. Simultaneously to the operation of the DCCBs, the DET and the DIR signals are transmitted between the CIRs of the DC lines; therefore, considering the communication time delay of the, i.e.,  $t_1 - t_2$ , the faulty line is detected at  $t_2$ . Then, the CIR, installed at each end of the faulty line, monitors the line current and sends the open command to the associated isolator when the fault current decays to zero.

During ( $t_4 - t_5$ ) the DC isolator switches operate and finally the faulty line is isolated at  $t_5$ . Once an isolator switch operates, the associated CIR sends a signal (named ISO signal) to all the LPUs. The LPU of each busbar monitors the status of the isolators and sends the close command to the DCCB when the faulty feeder is completely isolated. By re-closing the DCCBs, the healthy parts of the network are re-energized. The proposed algorithm for the LPUs, which can be implemented on a microprocessor-based relay, is shown in Fig. 4.7.

It is worth to mention that the pickup settings of the LPUs,  $I_{LPU}$ , are set according to the nominal current of the corresponding connection points,  $I_{CP}$ , (e.g.,  $I_{LPU} = 1.2 I_{CP}$ ); while, the pickup settings of the CIRs are set based on the nominal current of the associated line. Therefore, the pickup current of the LPUs is typically larger than the CIRs pickup current. On the other hand, when a fault has occurred through significant impedance, the fault current does not increase dramatically and the current at the connection points may remain below the LPUs pickup current. In this case, the possibility of the detecting the fault through the CIRs is higher than the fault detection probability of the LPUs. Thus, to increase the high impedance fault (HIF) detection possibility, the CIRs send the appropriate signals to the LPUs, when they detect a fault. Moreover, as shown in Fig. 4.7, the LPUs send the trip command if they receive the signals from the CIRs even if they do not detect the fault.

The proposed protection strategy can be in the following steps:

1. The fault is detected by the LPUs and the trip command is sent to the DCCBs.
2. The DCCBs interrupt the fault current.
3. The fault location is determined by the CIRs.
4. The faulty line is isolated by opening the corresponding isolator switches.
5. The DCCBs are re-closed and the rest of the network is restored.

It should be noted that during the steps of the proposed strategy, microgrids can operate in grid-isolated mode. Therefore, if there is a power balance between the generation of the internal DGs and the connected loads inside the microgrid, these loads will not sense any interruption. For other critical loads it is possible to connect energy storage devices close to the load, in order to prevent any power shortage that would damage the normal operation.

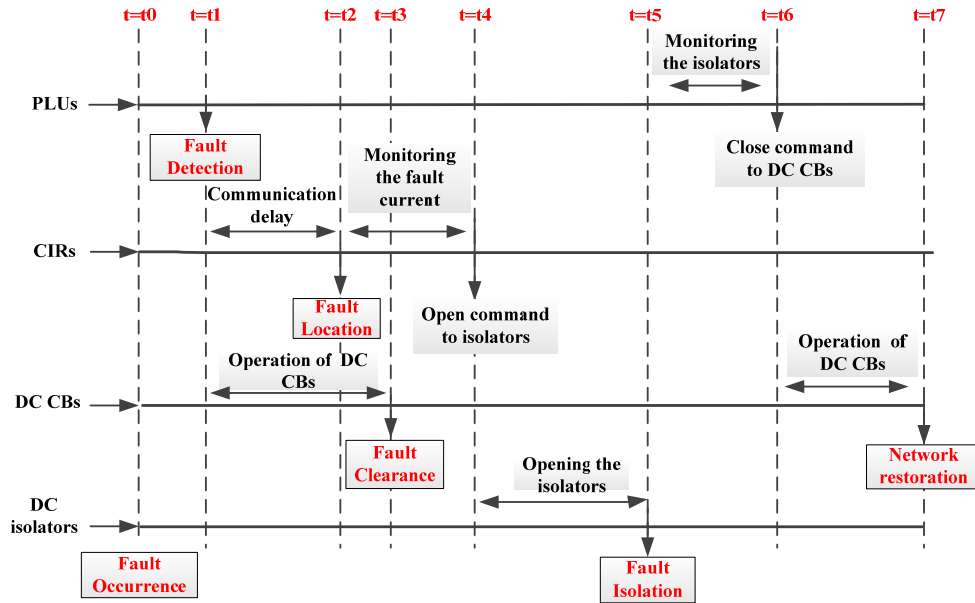


Fig. 4.6. The time sequence of the main protection.

#### 4.3.2. Backup protection

When the communication link is interrupted, the CIRs cannot locate the fault; hence, their operation is blocked. On the other hand, as shown in Fig. 4.7, the LPUs are switched to the backup strategy, which does not require communications. The algorithm of the backup strategy is designed based on the handshaking method presented in [109] with some modifications in order to improve its weakness. The proposed backup protection, which can be named as modified handshaking method, is explained here in the context of the study network, shown previously in Fig. 4.5.

Let us assume that fault F1, affecting Line23, impacts the study network when the communication link has failed. In this case, the LPUs detect the fault and send the trip commands to the DCCBs. Furthermore, before the fault current interruption, the LPU of each active bus determines the isolator switch that carries the maximum fault current flowing from the bus to the lines (i.e., maximum positive fault current); these isolators are named “selected isolator”. When the fault current is interrupted, the selected isolator of each active bus is opened. For example, in the study network, DIS23, DIS12, DIS61, DIS54 and DIS43 are opened after the fault clearance.

By opening the selected isolators, the faulty part is isolated; however, in order to provide a selective protection, most of these switches must be re-closed. To recognize the candidates

for re-closing, the DCCBs are re-closed whereas the opened switches are still open. At this stage, the opened switches that have both of their poles connected to the energized bus, i.e., DIS12, DIS61, DIS54 are selected; these switches are allowed to be re-closed. To guarantee the safety of the isolator switches, these switches are re-closed when the distribution system is de-energized. Therefore, once the candidate for re-closing is selected, the LPUs send the open commands to the DCCBs, again. Consequent to the opening of the DCCBs and de-energizing the network, the selected switches are re-closed. Finally, the DCCBs receive the close commands and re-energize the rest of the network.

The steps of the backup method are:

1. The fault is detected by the LPUs and the trip command is sent to the DCCBs.
2. The LPU of each bus detects the isolator that carries the maximum positive fault current.
3. The DCCBs interrupt the fault current.
4. The open command is sent to the isolators selected in Step (2), when the current flowing through the isolator decays to zero.
5. The isolator switches selected in step (2) are opened.
6. The DCCBs are re-closed when the selected isolators are opened.
7. Isolators that should be reclosed are selected.
8. The DCCBs are re-opened.
9. The isolators selected in step (7) are re-closed.
10. The DCCBs are re-closed and the rest of the network is restored.

If compared to the main protection, the backup causes a larger time delay in the network restoration; this issue is explained in the Case study2 of this chapter.

As mentioned above, in the second step of the backup method, the LPU of each bus selects the isolator that carries the maximum positive current. In special conditions, if the measured currents at two isolators of a bus are equal, both of them should be selected in Step (2). Therefore, after opening the DCCBs, both isolators are opened. The remaining steps are executed as mentioned above. Indeed, even for this special case, the method is still stable. It is worth to remarks that both isolators can be re-closed in Step (9) if the fault is not located inside their corresponding line.

It is also notable that, after the activation of the backup protection, the isolator failure backup is handled by the LPUs. For example, after the fault occurrence in Line16, the LPU6 sends the open command to DIS61 (Step 4). If DIS61 fails to open, the LPU6 will detect this

failure and sends the open command to DIS64 after a time interval. In this case, after the fault isolation, the LPU6 will not send the “close” command to the DCCB6.

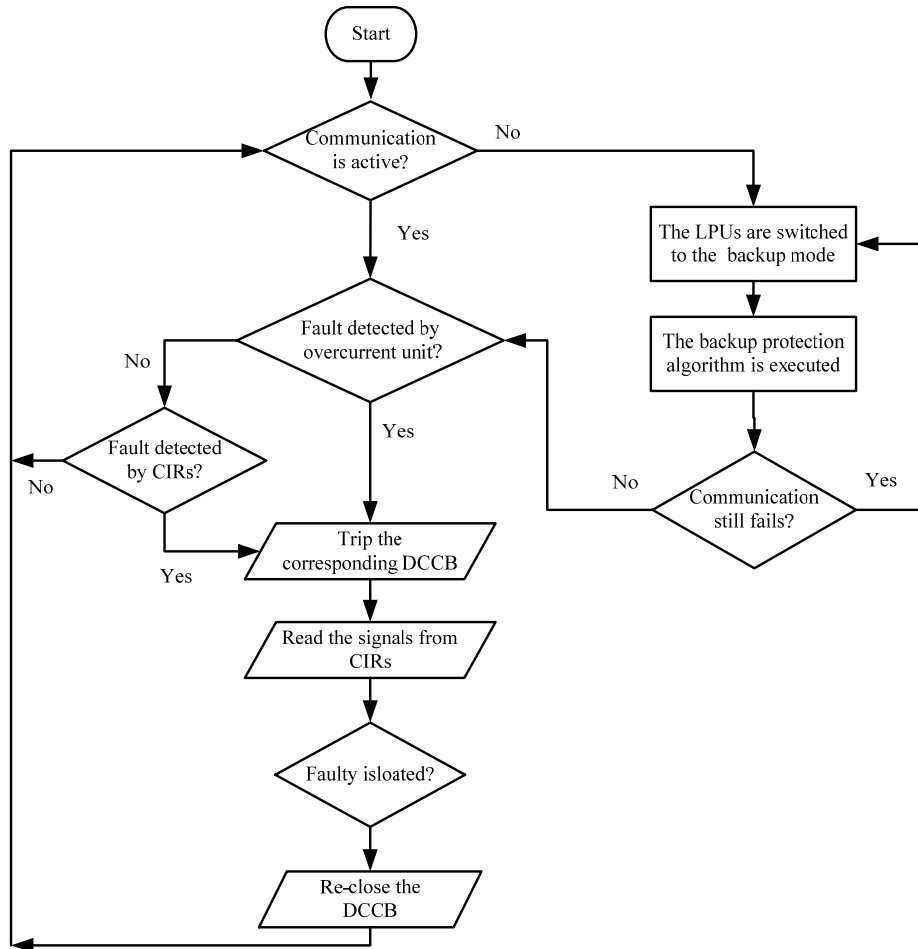


Fig. 4.7. Flowchart of the LPUs algorithm.

### 4.3.3. Busbar protection

Once a fault occurs at a DC bus, the fault currents flow from the feeders to the faulty bus; thus, the CIRs cannot locate the fault. For this reason and also due to the requirement of having a more sensitive protection, the busbar protection is designed based on the differential current method. The differential protection is used typically for busbar protection due to its

high selectivity and fast operation [141]. In this chapter, the busbar protection is considered a function of the LPUs; however, for the buses without the LPU, an independent relay should be allocated. The busbar protection sends the notification signals to the corresponding CIRs in order to separate the faulty bus.

#### 4.4. Adapting the relays threshold

The LPUs and the CIRs detect faults based on the overcurrent method. The operation of the overcurrent-based relays is related to the time-dial and the pickup current settings; the pickup current ( $I_p$ ) is defined as the minimum value of the current at which the relay starts to operate. Considering the use of the instantaneous overcurrent units, the proposed relays operate without time delay. Meanwhile, the pickup current must be defined according to the largest nominal current flowing through the protected element. On the other hand, in active distribution networks, the magnitude/direction of the lines current would be changed based on the variations of the operational conditions of the network. Therefore, a Centralized Adapting Unit (CAU) has been designed to re-calculate the relays pickup currents according to the network operating conditions. The CAU calculates the new pickup currents based on the power flow equations of the DC systems presented in [142]. In a multi-terminal DC network, the power flow from the DC buses to the DC grid is given by:

$$\mathbf{P} = \mathbf{U} \otimes (\mathbf{Y}\mathbf{U}) \quad (4.1)$$

where the vector  $\mathbf{U}$  denotes the DC busses voltages,  $\mathbf{Y}$  denotes the admittance matrix of the DC grid, and  $\otimes$  is the Hadamard product operator. The vectors  $\mathbf{P}$  and  $\mathbf{U}$  are introduced in (4.2).

$$\mathbf{P} = \begin{bmatrix} P_1 \\ \cdot \\ \cdot \\ \cdot \\ P_n \end{bmatrix}, \quad \mathbf{U} = \begin{bmatrix} U_1 \\ \cdot \\ \cdot \\ \cdot \\ U_n \end{bmatrix} \quad (4.2)$$

Consequent to the change in the injected power to the DC busses, the DC voltage variation of the network can be obtained by:

$$\Delta\mathbf{U} = \mathbf{J}_{DC}^{-1} \Delta\mathbf{P} \quad (4.3)$$

Where  $\Delta\mathbf{P}$  denotes the nodal power variation and  $\mathbf{J}_{DC}$  is the Jacobian matrix of the DC grid that is given by:

$$J_{DC} = \text{diag}(\mathbf{U}) \cdot \mathbf{V} + \text{diag}(\mathbf{YU}) \quad (4.4)$$

Where *diag* refers to the mathematical operator which converts a vector into a diagonal matrix. Substituting (4.4) into (4.3), the voltages of the DC busses after the change in the injected power at the nodes can be calculated as:

$$\mathbf{U}_2 = \mathbf{U}_1 + J_{DC}^{-1} \Delta \mathbf{P} \quad (4.5)$$

Where, vectors  $\mathbf{U}_1$  and  $\mathbf{U}_2$  denote the voltages at the DC busses before and after any event, respectively. Finally, the current of each DC feeder could be found as:

$$\mathbf{I} = \mathbf{Y} \cdot \mathbf{U}_2 = \mathbf{Y} \cdot (\mathbf{U}_1 + J_{DC}^{-1} \Delta \mathbf{P}) \quad (4.6)$$

The equation (4.6) shows that any change in the network topology, reflected in  $\mathbf{Y}$  matrix, may impact the direction and/or the magnitude of the distribution line currents. Furthermore, this equation illustrates that the connection/disconnection of DGs or change in their generated power, reflected in  $\Delta \mathbf{P}$ , may also result in significant changes in the feeders currents. Thus, in order to calculate the new pickup currents, the CAU monitors: 1) the status of the DCCBs and isolators to estimate the network topology and to update the  $\mathbf{Y}$  matrix; 2) the injected power by DGs; and 3) the voltage at the DC busses. Then, the CAU calculates the new pickup currents and communicates with CIRs and LPUs to apply the new settings.

#### **4.5. Real-time verification and case studies**

In order to evaluate the effectiveness of the proposed protection strategy, considering the communication delay, a HIL approach has been used. Further explanations about the setup test-bed are presented in the first Appendix of this thesis.

The performance of the proposed strategy is studied here considering five study cases, where different operating conditions in the network under study are considered, in the presence of different type of DC faults. For the study cases defined and presented in this work, it is assumed that the fault is triggered at  $t = 1\text{s}$ .

##### **Case study1**

###### **Occurrence of a PP fault at F1.**

This case study is introduced to evaluate the performance of the proposed strategy when the communication link is active. In this case, the protection algorithm of CIR23 has been implemented on the DK60 board. Once the fault occurs, the LPUs detect the fault and send

the trip command to the corresponding DCCBs. The plot in Fig. 4.8 compares the fault current when it is interrupted by the operation of the DCCBs with the fault current without any interruption.

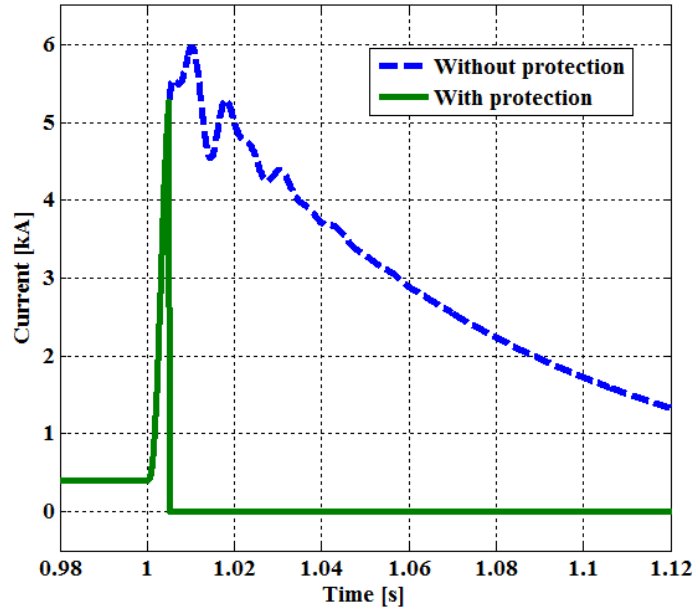


Fig. 4.8. Fault Current with and without operation of DCCBs.

Fig. 4.9 shows the fault detection and location time of LPU1 and CIR23, respectively. CIR23 relay, implemented on the board, locates the fault using the messages sent by CIR32. As measured from our experiments, CIR23 locates the faults after around 2.7ms. This relay, however, sends the trip (open) command to DIS23 when the current of this isolator decays to zero. Indeed, this test demonstrates that the time delay in fault location using the exchanged data between relays is approximately 2.7ms; hereafter, this time delay is referred as  $T_D$ . Fig. 4.10 shows the operational status of DCCB1 and DCCB6. The figure illustrates that although DCCB6 is located further away from the faulty point, their corresponding LPUs detect the fault and send the trip command almost simultaneously. Fig. 4.10 also illustrates that 10ms after the fault clearance, DIS23 and DIS32 receive the open command from their CIRs. These two switches isolate the fault after 55-60ms, considering the use of conventional AC CBs as DC isolators.

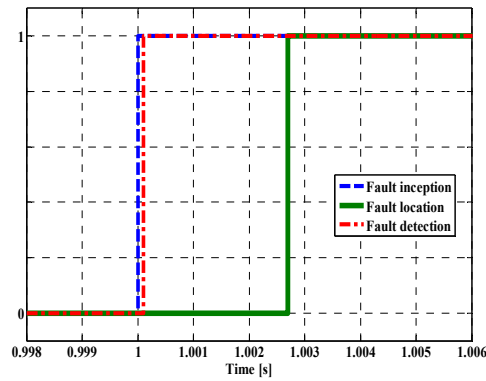


Fig.. 4.9. Fault detection time of LPU1 and fault location time of CIR23.

Once DIS23 and DIS32 are opened, CIR23 and CIR32 send the ISO signal to all the LPUs. In this test, the CIR23 sends the message after  $T_D$ . Finally, the DCCBs are re-closed, when the LPUs received the ISO signals from CIR23 and CIR32. Fig. 4.10 demonstrates that the rest of the study network is restored 85ms after the fault occurrence.

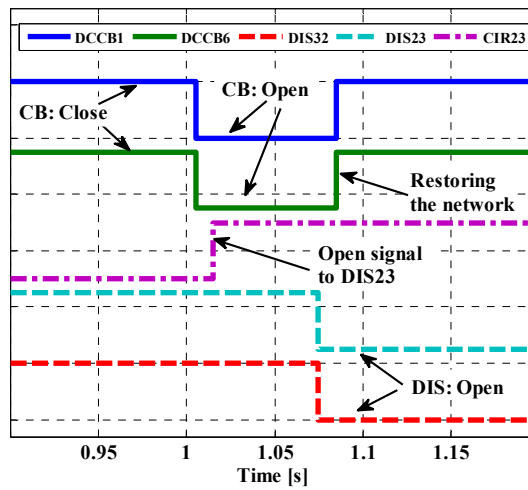


Fig. 4.10. The status of DCCB1, DCCB6, DIS23, DIS32, and the open signal of CIR23

### Case study 2

#### Occurrence of a pole to ground high impedance fault (HIF) at F1.

In this study, a high impedance fault is applied to the study network when the generated power of the DGs inside the Microgrid1 is only 25% of their installed capacity and the DGs inside the Microgrid2 have been disconnected. According to the DGs status, the CAU has set the pickup current of CIR23 and LPU1 on 275A and 960A respectively (20% more than the nominal current). Similar to the previous case, the algorithm of CIR23 has been implemented on the board. Fig. 4.11 shows the fault currents seen by LPU1 and CIR23 and the pickup current of these relays. This figure demonstrates that the LPU1 does not detect the fault, whereas the fault is detectable by CIR23. Therefore, as shown in Fig. 4.12, the CIR23 which detects the fault after 5.2ms, reports the fault detection to the LPUs.

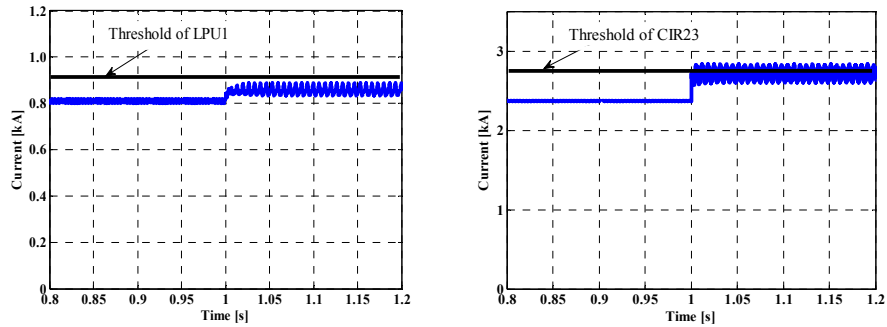


Fig. 4.11. Fault currents seen by LPU1 and CIR23 and the pickup current of these relays.

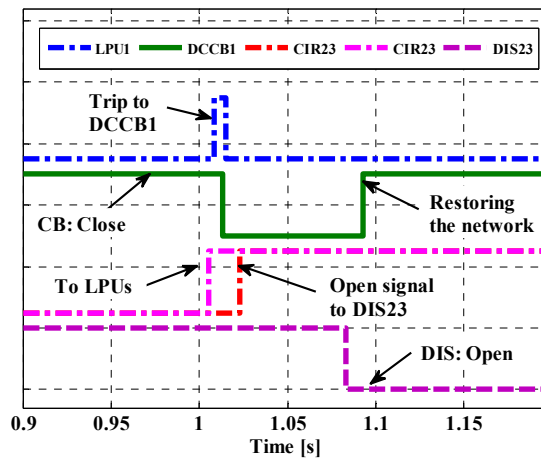


Fig. 4.12. The status of DCCB1, DIS23; the open signal of CIR23 and the trip signal of LPU1.

Fig. 4.12 also illustrates that the fault current is interrupted 13ms after the fault occurrence. It can be noticed that, although the fault is cleared 8ms later than the case 1, due to the limited increment in the flowing current, the VSCs components still remain safe. Moreover, Fig. 4.12 demonstrates that the rest of the protection steps are similar to the Case study1 and the healthy parts of the network are restored 93ms after the fault occurrence.

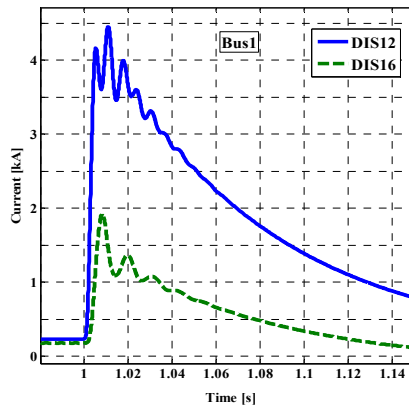
### Case study 3

#### Occurrence of a PP fault at F1, when communication systems are interrupted.

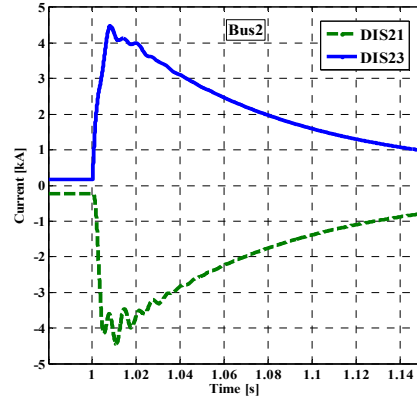
In order to evaluate the backup protection, it is assumed that a PP fault impacts the network when the communication link between the protection relays is interrupted. In this case, the operation of the CIRs has been blocked and the algorithm for LPU2 has been implemented on the board. Similar to the first case study, at the first steps, the fault is detected by LPUs and is cleared by the operation of the DCCBs. During the opening event/operation of the DCCB, the associated LPUs select the isolators to be opened. Since Bus3 does not have any LPU relay the isolators connected to this bus remain closed. Moreover, only one isolator has been connected to Bus5; thus, this isolator (DIS54) is selected for this bus. For the other busses, which have more than one isolators connected, the one that carries the maximum positive current (from bus to line) is selected. Fig. 4.13 demonstrates that according to the fault current flowing through the isolators, DIS12, DIS21, DIS43, and DIS64 are the candidate isolators in Bus1, Bus2, Bus4, and Bus6, respectively. The selected isolators are opened when the fault current is interrupted by the DCCBs.

Fig. 4.14 shows that DIS23 and DIS64 are completely opened almost 75ms after the fault occurrence; whereas, the status of DIS32 is not changed. To determine which isolators can be reclosed, the DCCBs are reclosed again and remain closed during 100ms. During this time interval, DIS12 and DIS are selected as the isolators which can be closed. The DCCBs are opened again 185ms after the fault occurrence, however the selected isolator, must be reclosed after the rated reclosing time (RRT). The RRT is related to the operational limitation of the conventional AC CBs and is 300ms for the fast-reclosing devices [143]. Therefore, the re-close command is applied to the selected isolators at  $t = 1.375s$ . Fig. 14 shows that the study network is restored 470ms after the fault occurrence.

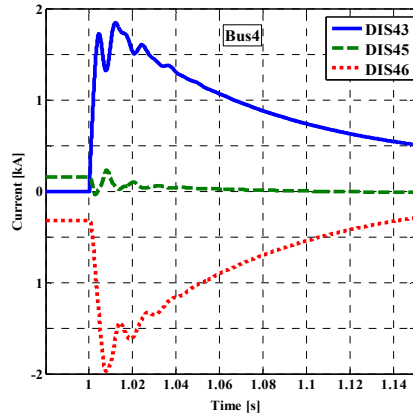
This backup, however, adds more time delay for the network restoration (mainly due to the RRT); and requires a repeated operation of the DCCBs and DC isolators. Another issue is that it cannot provide complete selectivity. In this study case, although the fault has occurred at Line23, the Line32 remained de-energized as well.



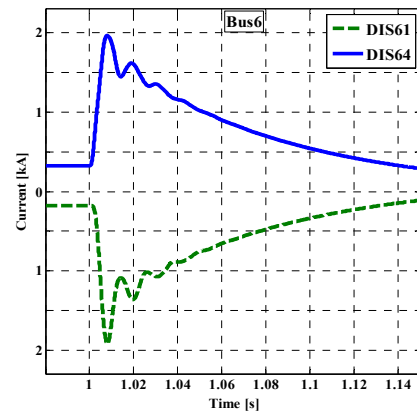
a.



b.



c.



d.

Fig. 4.13. Fault currents flowing through isolators of different buses. a) Bus1. Maximum positive current flows from DIS12, b) Bus2. Maximum positive current flows from DIS23, c) Bus4. Maximum positive current flows from DIS43, d) Bus6. Maximum positive current flows from DIS64.

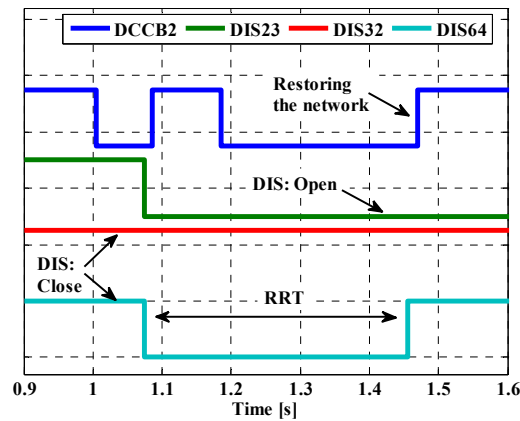


Fig. 4.14. The status of DCCB2, DIS23, DIS32, and DIS64.

**Case Study 4**

**Occurrence of a pole to pole fault at F1, when DC isolator fails to operate.**

To study the performance of the isolator failure backup protection, this case study assumed that after the fault occurrence in Line23 and the operation of DCCBs, DIS23 fails to open. In this case, once CIR23, which is implemented on the board, detects that the DIS23 cannot isolate the fault, sends the open command to the DIS12 through the CIR12. Moreover CIR23 sends a message to LPU2 to block the re-closing operation of the DCCB2. Fig. 15 shows that the backup signals are sent 70ms after the fault location (10ms more than the nominal operational time of the isolators). Moreover, Fig. 4.15 shows the status of DCCB1, DCCB2, and DIS21, which determines that the study network is restored after almost 160ms.

**Case study 5**

**Occurrence of a PP fault at Bus2.**

In order to investigate the busbar protection, it is assumed that Bus2 is impacted by a solid PP fault. After to the fault occurrence, the fault currents flow from Line12 and Line23 to this bus. Therefore, CIR21 and CIR23 assume negative values for the fault current and do not detect the fault. As mentioned before, due to the inadequacy of the CIRs, the busbar protection is handled by LPUs. Thus, in this case, the busbar protection algorithm of LPU2 has been implemented on the DK60 board. The differential current calculated by LPU2, which is increased rapidly. Once LPU2 detects the fault on Bus2, it sends a fault detection signal to CIR12 and CIR23. CIR21 and CIR23, in turn, send the open command to the associated isolators, after the fault is cleared. The rest of the protection steps and the restoration time are similar to the ones obtained in the case study 1, except for the fact that DCCB2 remains open.

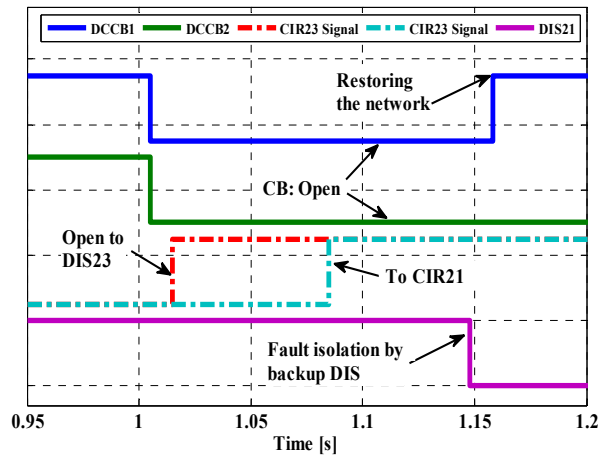


Fig. 4.15. The status of DCCB1, DCCB2, DIS21 and the signals of CIR23 to DIS23 and CIR21.

#### 4.6. Discussion about the network operation

This section investigates the effects of the isolation process and the network restoration on the connected loads. The main protection method restores the network in less than 100ms; while the required time for the backup scheme is less than 500ms. These time delays are in the range of the momentary interruptions in AC distribution systems which happen due to the operation of auto-reclosers, sectionalizers and automatic network restoration process [144, 145]. Therefore, in the worst cases, the proposed method restores the network after a time delay which is in the range of the time delay of the existing system-restoration methods of AC distribution system. It is worth noting that, the power quality of DC distribution systems can be improved by replacing some of the isolators with DCCBs. For example, let's assume that in the network of Fig. 4.5, DIS12 and DIS43 have been replaced with DCCBs. In this case, after the fault occurrence at point F1, it is not necessary to open all the DCCBs. Hence, only the loads and microgrids that are connected to Bus2 and Bus3 sense the momentary interruption. This change can enhance the power quality, however it increases the costs of the protection system.

##### 4.6.1. Evaluation of the main protection method

In order to evaluate the proposed method from the power quality point of view, the effect of the method on both AC and DC system is considered here.

At first, the response of the AC network is studied when the main protection method (i.e., the communication-based) is active. Fig. 4.16 shows a simplified diagram of the study system.

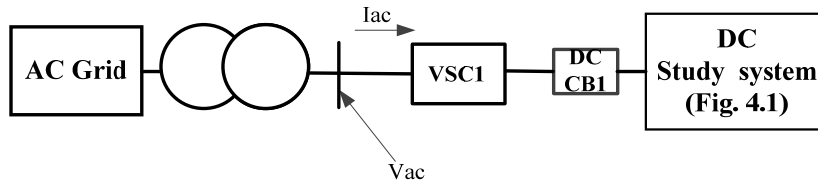


Fig. 4.16. Simplified diagram of the study system.

For the Case study1 of this chapter (i.e., occurrence of a fault between Bus2 and Bus3), the voltage and current of the AC network are shown in Fig. 4.17 and Fig. 4.18, respectively. Fig. 4.17 shows that the voltage reaches the steady state within 2-3 cycles after the fault clearance. On the other hand, the AC-side current of the VSC1 ( $I_{ac}$ ) decays to zero due to the opening of the DCCB1 and recovers after the fault isolation.

This simulation shows that due to the fast fault interruption (in less than 5ms), the AC network remains stable. Moreover, the re-energizing of the DC network does not impact the AC network stability. To provide more clarification, in another test, it is assumed that a 4-MW load was connected to the AC network as well (as it is shown in Fig. 4.19).

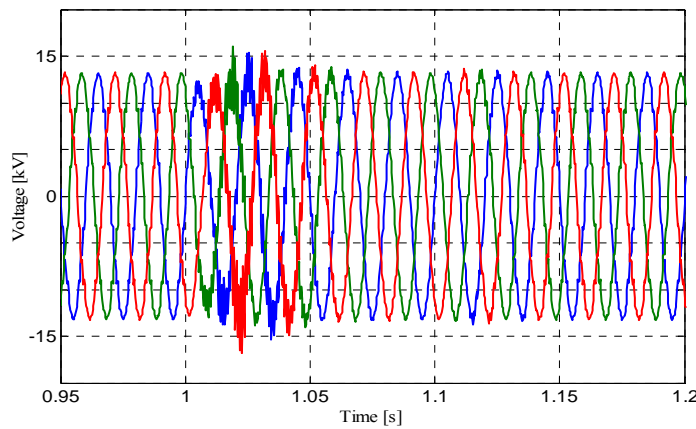


Fig. 4.17. AC network voltage ( $V_{ac}$ )

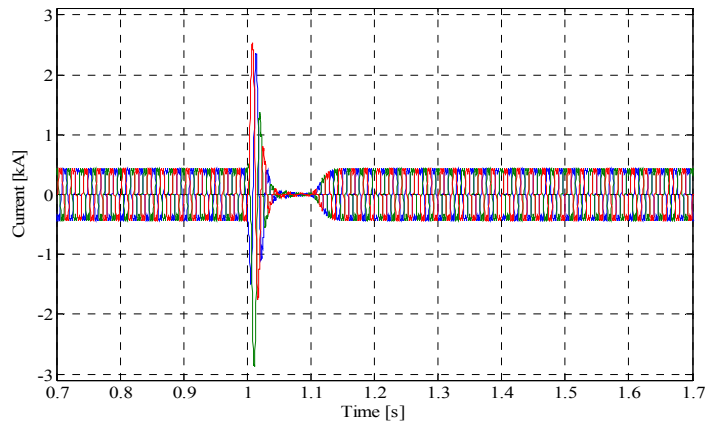


Fig. 4.18. AC network current to VSC1 ( $I_{ac}$ ).

Fig. 4.20 shows the voltage of the AC network ( $V_{ac}$ ) and the total current during and after the fault isolation process. This figure illustrates that the voltage remain stable (as it returns to the nominal value within 2-3 cycles) and hence the AC load can continue its normal operation without any interruption or effective voltage sag. Furthermore, the current of the AC load, shown in Fig. 4.21.a, illustrates the stable operation of this load. Fig. 4.21.b shows the AC-side current of the VSC1; this current is reestablished after the fault isolation.

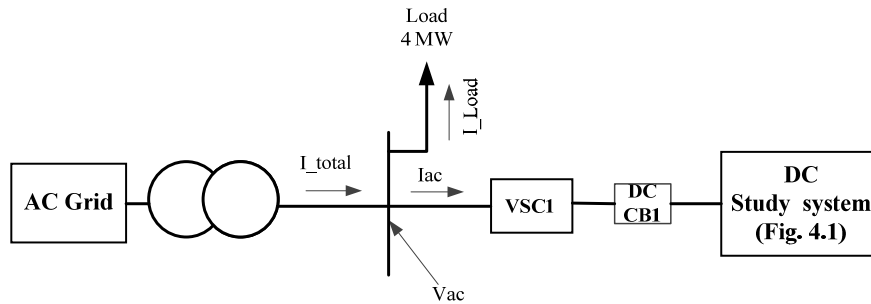


Fig. 4.19. Simplified diagram of the study system and the AC-side load.

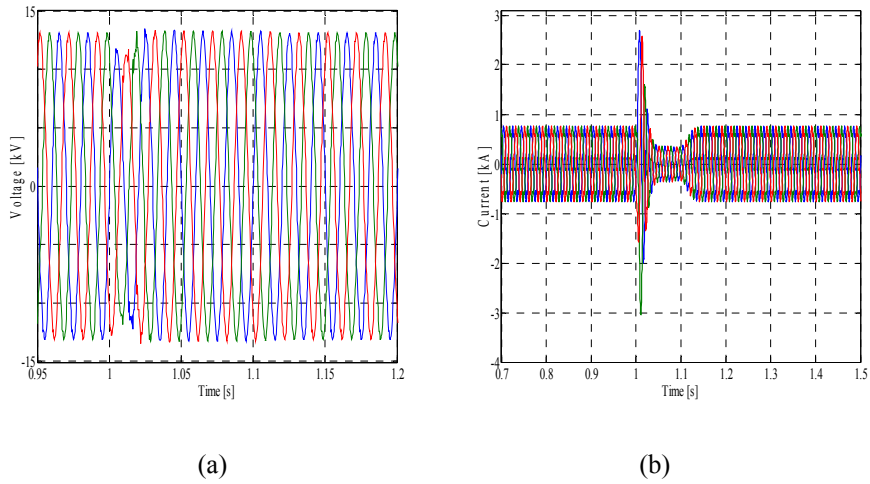


Fig. 4.20. a) Voltage of the AC network; b) total current ( $I_{total}$ )

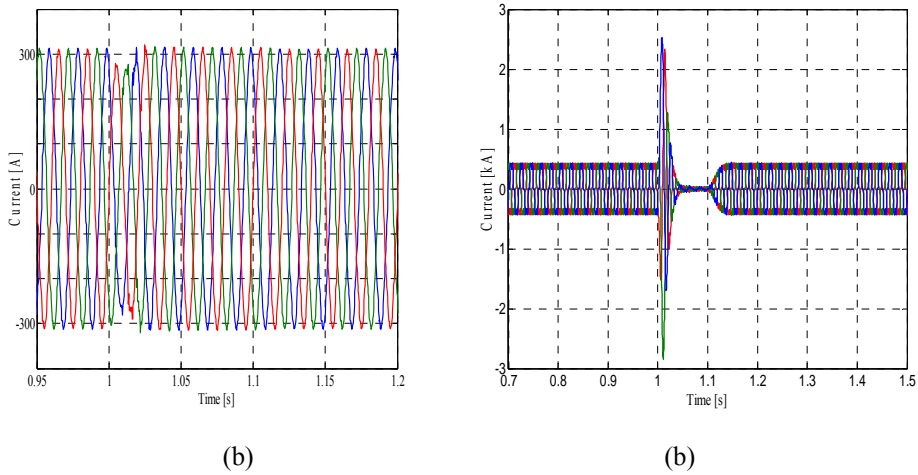


Fig. 4.21. a) Current of the AC load ( $I_{Load}$ ); b) current to VSC1 ( $I_{ac}$ )

#### 4.6.2. Evaluation of the backup method

Similar to the simulations presented above, two other tests were done when the communication fails and the backup method is activated.

The response of the AC network is similar to the above simulation results. For example, Fig. 4.22 and Fig. 4.23 show the performance of  $V_{ac}$  and  $I_{ac}$  in the network of Fig. 4.16 (without AC loads).

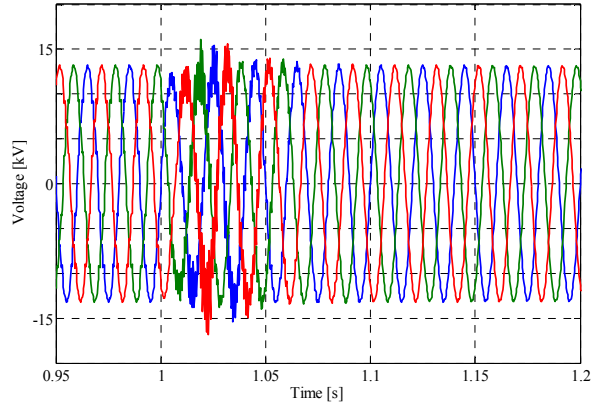


Fig. 4.22. AC side voltage ( $V_{ac}$ ) during the backup protection for the network of Fig. 4.16 .

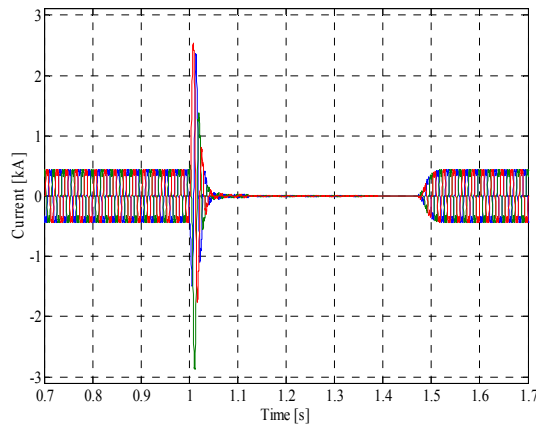


Fig. 4.23. Current ( $I_{ac}$ ) during the backup protection for network of Fig. 4.16.

As another example, Fig. 4.24 shows the performance of  $V_{ac}$ ,  $I_{total}$  for the network of Fig. 4.19. This figure illustrates that due to the fast fault interruption, the AC network remains stable and its connected loads continue their stable operation during the fault isolation process.

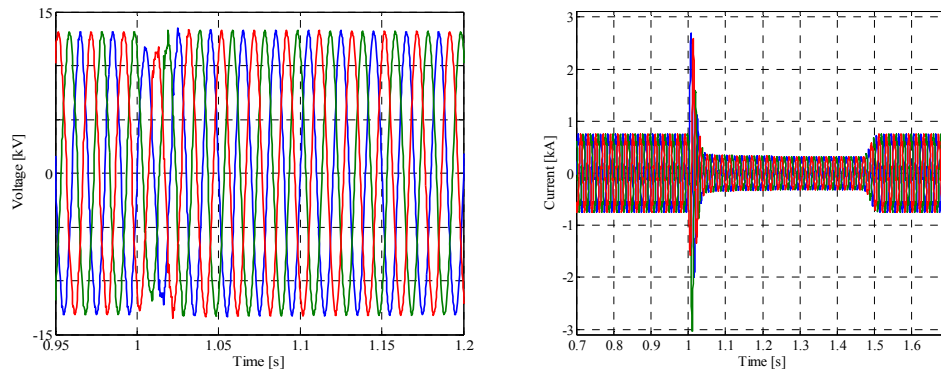


Fig. 4.24. AC side voltage ( $V_{ac}$ ) and the total current ( $I_{total}$ ) during the backup protection for network of Fig. 4.19.

#### 4.6.3. Voltage at the Microgrids’s busses

As mentioned in this chapter, one of the main applications of the MVDC system is the interconnection of different AC microgrids (this application is introduced and explained in [39]). Normally, microgrids integrate different kind of DGs. Therefore, in addition to the grid-connected mode, they can operate in islanded mode during an outage or interruption in the main grid. In fact, the loads inside the microgrid are supported with the corresponding DGs. Therefore, during the restoration process (and its related momentary interruption in the main DC grid) the customers within the microgrid may be able to avoid an extended outage [146].

Therefore, the proposed method does not cause any interruption for loads inside the microgrid; however short-term voltage sag may happen. According to the ITIC curves and IEEE Std 1564-2014[147] the voltage reduction limited to 70% of the nominal voltage is acceptable even for sensitive loads, if the voltage is restored in less than 500ms. (50% of voltage reduction is acceptable for 200ms). Our simulation results show that this goal can be achieved for each microgrid of the study system if Load/Generation ratio of that microgrid is at least 2:1.

For example, to consider the worst case, it is assumed that the communication link failed and the network restores 500ms after the fault occurrence in Line23. It is assumed that the DGs inside the microgrid generate 2.5 MW while 5MW of loads are connected to the network (i.e, Load/Generation is 2:1). Fig. 4.25 and Fig. 4.26 show that the voltage at the point of common coupling (PCC) of the Microgrid-1. This figure illustrates that in the worst

case, the RMS value of the voltage drop to 70% of its nominal value ( $4900/6930=0.707$ ). This voltage returns to its nominal value after the network restoration. Therefore, according to ITIC curves presented in IEEE Std 1564-2014, the sensitive loads do not sense any momentary interruption if the generated power of DGs inside the microgrid reaches to 50% of the connected load's power.

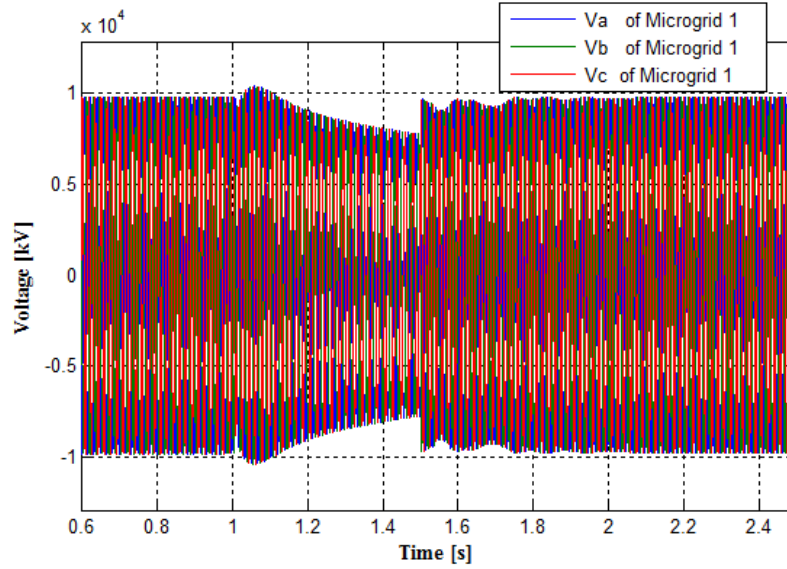


Fig. 4.25. PCC voltage of the Microgrid-1 of the study system: three phase voltages.

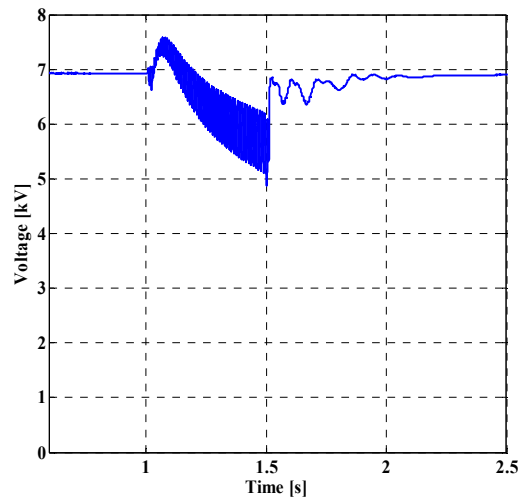


Fig. 4.26. PCC voltage of the Microgrid-1 of the study system: the RMS value of phase A.

---

## Centralized Protection and Self-Healing for DC Distribution Systems and Microgrid

The fault detection/location methods presented in chapters 3 and 4 could be categorized as de-centralized protection methods; while, in this chapter a centralized protection method is presented to address some of the challenges regarding protection in DC distribution systems and microgrids. The proposed protection strategy consists of: 1) a differential based relay which is used to carry out the fault location and detection inside sub-microgrids; 2) an overcurrent-based relay to protect the VSCs of the host network and the DGs; 3) a Centralized Protection Unit (CPU) which supervises the protection devices and adapts them with the operational conditions of the microgrid. This unit also executes a self-healing process to guarantee the supply-adequacy of the islanded microgrids and on-outage sub-microgrids; 4) a combination of DCCBs and isolators to provide a fast and selective fault interruption with the minimum number of the DCCBs. Indeed, the proposed protection and self-healing strategy provides the necessary equipment/methods of the smart operation of DC microgrids.

The proposed technique is complemented by a backup protection mechanism which is activated when the communication link fails. Moreover, the Hardware-In-the Loop (HIL) approach is used to evaluate the performance of the proposed strategy. Using this method errors and delays that do not appear in off-line simulation, such as time delay in data

transferring, are take into consideration.

### 5.1. Study Case System

The performance of the proposed protection technique is explained and evaluated, for a set of case studies which are based on a hypothetical DC distribution network, as shown in Fig. 5.1. The basic configuration and parameters of this network are extracted from the benchmark proposed in [97] and re-designed to operate as a DC microgrid. The network is a VSC-based DC system; consisting of: DGs which are interfaced to the grid through VSCs; residential/industrial loads; and the DC feeders. Two-level  $\pm 10$ -kV VSCs are used to interface the connection to the AC network as well as the RESs to the DC network. Hall-Effect current transducers (CTs) are installed on both ends of the dc lines. The data transfer amongst the dc buses and the centralized protection unit is handled via dedicated communication links.

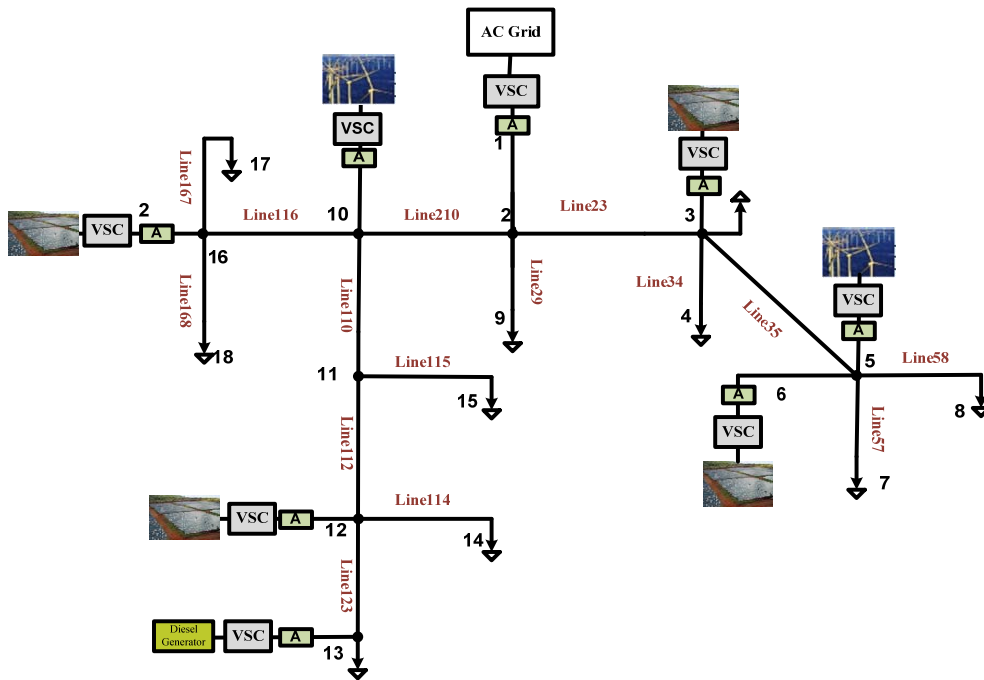


Fig. 5.1. DC microgrid study case.

### 5.2. Components of the proposed protection scheme

The protection systems must be able to detect and locate the various types of faults, interrupt the fault current and isolate the faulty zones before serious damages are inflicted to vital devices. The following subsections describe the method and devices that are used in the proposed strategy to achieve the protection goals.

#### 5.2.1. Fault interruption and isolation.

The fault current should be interrupted by the appropriate DCCBs; however, due to the specification of these CBs, they are relatively more expensive than the counterpart AC breakers. Indeed, installing the DCCBs in both ends of all the DC lines, although provides a selective and reliable protection, it increases substantially the initial cost of the protection scheme. Hence it is not applicable for most DC distribution systems and microgrids. Therefore, in this chapter, a combination of DCCBs and isolator switches are used to provide an economic and selective protection scheme.

After a fault occurrence, the fault is fed by the sources which are connected to the microgrid. Of course, the contribution of each source in the fault current is related to different factors such as the source location and its capacity. As shown in Fig. 5.1, the VSCs are located in the microgrid at the point of connection to the host network as well as at the different connection points of the various DGs. Thus, to interrupt the fault current and to protect the VSCs and the network elements, it is necessary to install the DCCBs at the connection point of the microgrid to the host network and at the connection point of DGs, i.e. points labeled “A”. Solid-state CBs (SSCBs) are the fastest type of DCCBs and they can operate in less than 1ms; however, they are expensive devices. Hence, hybrid DCCBs could be used as the fault interruption devices for the proposed protection scheme. The hybrid DCCB is able to interrupt the fault current in less than 5ms [70].

To provide a selective protection, the faulty line/busbar should be isolated and the rest of the network should continue its normal operation. This can be achieved by installing the appropriate isolator switches at both ends of the DC lines. These switches are cheaper than DCCBs; however they must be opened/ closed only in the no-load condition. Therefore, they isolate the faulty part, but only after the fault current is interrupted by the DCCBs.

#### 5.2.2. Forming sub-microgrids (SMGs)

The use of a combination of DCCBs and isolators results in a “*cut and try*” process. During this process, the entire microgrid is disconnected from the sources and, after the fault is isolated, the rest of the network is reconnected again. In the proposed protection scheme, to prevent the overall outage and to limit the negative effects of the cut and try process, the microgrid is clustered into several sub-microgrids. The sub-microgrids are connected

together using the DCCBs. In other words, the boundaries of the sub-microgrids are determined by the location of the DCCBs. By using this clustering, the cut-and-try process is done only for the faulted sub-microgrid. It should be noted that determining the optimal placement of these CBs (i.e., optimal microgrid clustering) is out of the scope of this chapter; however, as mentioned in [14] factors such as supply-adequacy can be considered to facilitate the operation of the sub-microgrids even if they are disconnected from the rest of the network. These DCCBs also play an important role on the backup protection which is executed when the communication link fails; as it will be explained in Section 5.3.2.

### 5.2.3. Fault detection and location

As mentioned above, the fault current is supplied through the VSC stations of the host grid and of the DGs. These VSCs are vulnerable against faults on their DC sides; hence, fast fault detection is necessary for the VSC stations. This can be achieved by monitoring the current at the connection points of the VSCs and at the microgrid, i.e., points labeled “A” in Fig. 5.1. For this reason the VSC stations are equipped with an overcurrent-based relay which is referenced as Source Protection Relays (SPR). The first stage of the fault current, i.e. the capacitor discharge current, has a high increasing rate. Hence, the SPRs can detect the fault after several microseconds. The thresholds of these relays are determined based on the critical time of the corresponding VSCs and the load current. Other specifications and tasks of the SPRs are explained in Section 5.4.

However, monitoring the currents at the “A” points does not permit to determine the exact location of the fault and cannot provide a selective protection. Moreover, in the case of HIF, the SPR may not detect the fault. For these reasons, in the proposed strategy, the fault location is handled by the current-differential-based method. The differential relays are more accurate than the overcurrent relays and are able to determine the exact faulty line/busbar. Moreover, unlike the time-inverse overcurrent relays, their accuracy is not impacted by the high raising rate of the DC fault current.

In the proposed method, each SMG is protected by a sub-microgrid relay (SMR) which consists on several differential elements. Each differential element of the SMR receives the measured current at both ends of a DC line and calculates the differential current of the protected line according to (5.1).

$$I_{diff,j}[k] = |I_{1,j}[k] - I_{2,j}[k]| \quad (5.1)$$

where  $I_{1,j}$  and  $I_{2,j}$  denote the measured current at both ends of the  $j^{\text{th}}$  line, and  $k$  is the sample number. In normal conditions the calculated value for  $I_{diff}$  should be close to zero; however, to prevent the relay’s mis-operation, the threshold of the differential elements of the SMRs are adjusted considering a restrained current ( $I_r$ ). In other words, it is assumed that

## 5.2. Components of the proposed protection scheme

the  $j^{\text{th}}$  differential element of a SMR operates if  $I_{diff,j}[k] > I_{r,j}$ . The restrained current of each element can be determined according to the smallest current required for the operation of that element; e.g.  $I_{r,j} = KI_{n,j}$ . In which K is a reliability coefficient with a value that can be set to 0.1 to 0.25 and  $I_{n,j}$  is the nominal current of the  $j^{\text{th}}$  line [44]. After a fault occurrence in the  $j^{\text{th}}$  line, the corresponding differential element detects the fault and issues a trip signal. The fact that the difference in equation (5.1) is taken in absolute value shows that bi-directional power flows caused by DGs cannot impact the performance of the differential scheme.

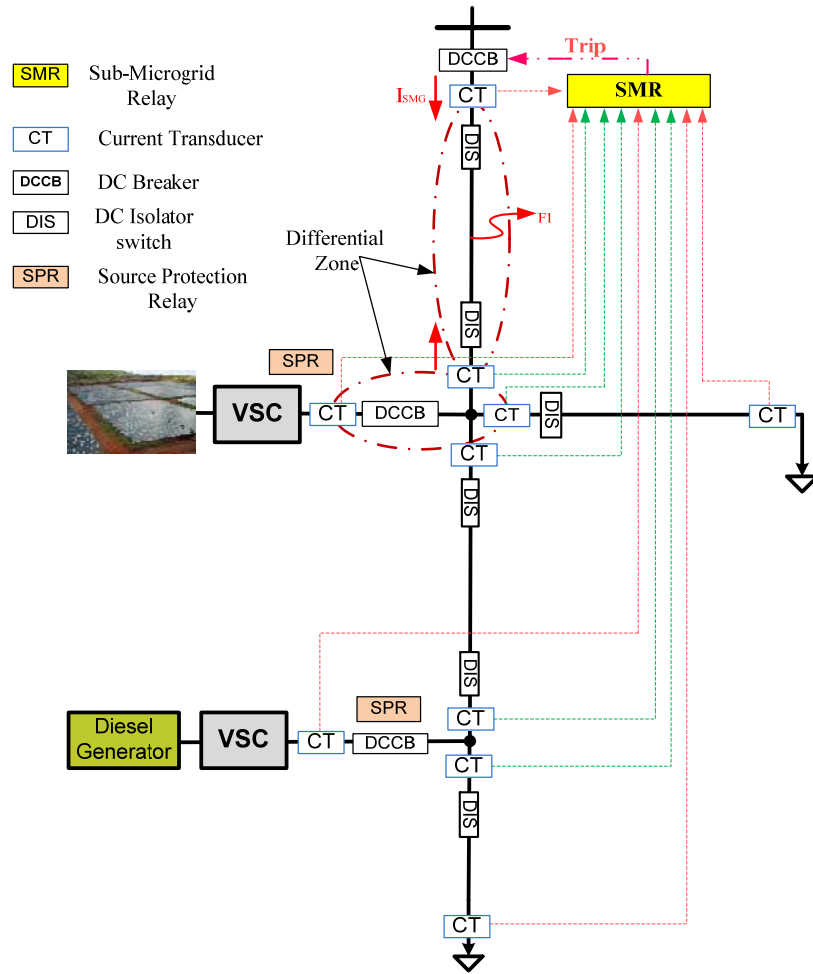


Fig. 5.2. Required data for differential and multi-terminal differential protection for a SMG.

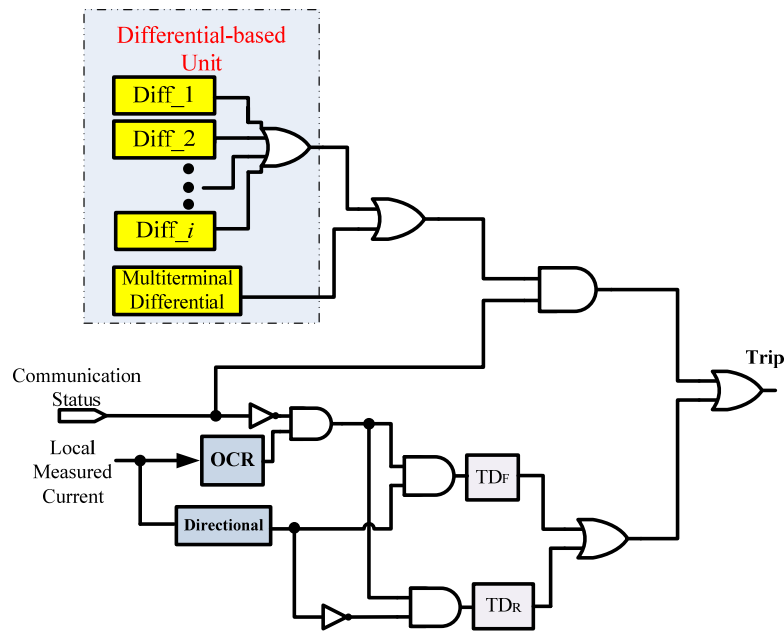


Fig. 5.3. The logic circuit of the SMR.

As shown in Fig. 5.2, the current measured by the CTs which are located inside a SMG are transmitted to the corresponding SMR through the communication links. By using these communication links not only the required data for the differential elements are collected, but also a multi-terminal differential protection can be formed. Indeed, using the measured currents of the SMG's boundaries, transmitted through the red communication links in Fig. 5.2, the differential current of each SMG can be calculated as shown in (2).

$$I_{dSMG}[k] = I_{SMG}[k] - \sum_{i=1}^{n-1} I_{b,i}[k] \quad (5.2)$$

where  $I_{SMG}$ , as shown in Fig. 5.2, and  $I_{b,i}$  denotes the measured currents at the SMG's boundaries, and  $n$  is the number of the SMGs boundaries.

The trip command of the SMR can be generated by both: the two-terminal differential and the multi-terminal element. Thus, the SMRs can provide a more stable and reliable protection when they are equipped with this multi-terminal differential element.

## 5.2. Components of the proposed protection scheme

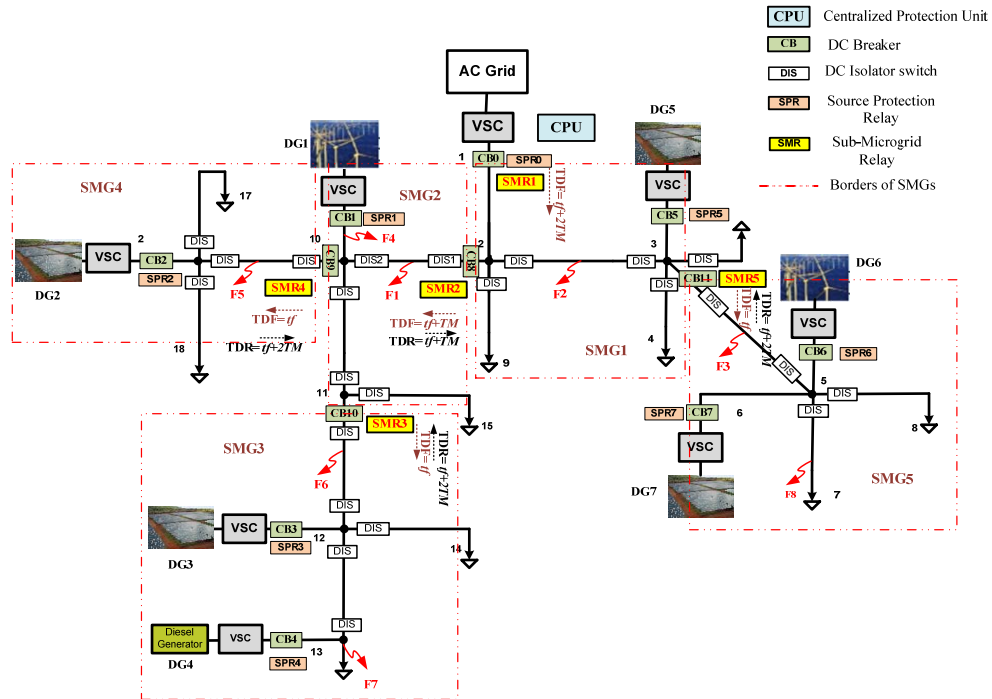


Fig. 5.4. Study microgrid equipped with the protection elements.

The logic circuit of the SMR, which can be implemented on micro-processor-based relays is shown in Fig. 5.3. This figure illustrates that the differential-based unit of SMRs consists of several differential elements. Each of these elements, i.e.,  $Diff_i$ , protect one of the differential zones of the associated SMG. In addition, the multi-terminal differential element is embedded in the differential-based unit that is able to detect faults that occurred inside the SMG. Each of these differential elements is also equipped with a RSG unit to improve its performance. The trip command of the differential-based unit of a SMR is sent to the related DCCB if each of the differential elements detect a fault. Moreover, Fig. 5.3 shows that the SMR is equipped with overcurrent directional elements as well; these elements operate as a backup unit when the communication link fails. The features and specifications of this backup system are explained in Section 5.3.

It should be noted that SMRs which are located at the borders of two SMGs, are enabled to protect both of the SMGs. For example, SMR4 receive measured current from the DC lines of SMG2 and SMG4. This SMR sends the trip command to CB9 if it detects a fault in any of these sub-microgrids.

### 5.2.4. Centralized Protection Unit (CPU)

The CPU includes two independent units; the centralized protection coordinator (CPC) and the self-healing and adapting system (SHA). The SHA receives the status of the DGs, loads, isolators and CBs. Then it estimates the network topology and calculates new settings for the relays. This unit is also equipped with a self-healing strategy that guarantees the supply-adequacy of on-outage zones of the microgrid. Meanwhile, the CPC supervises the operation of the protection elements of the microgrid and coordinates their operation. All the actions of the protection devices as well as measured currents are reported to both of these units.

### 5.3. Proposed Protection Scheme

This section explains the proposed protection strategy considering the elements described in Section 5.2. Both the main and the backup protection strategies are address here. The main protection is communication-assisted; whereas the backup protection is activated when the communication link fails.

#### 5.3.1. Main Protection

Fig. 5.4 shows the placements of the protection devices presented in Section 5.2 into the study microgrid. According to this figure, the following steps are performed after the fault occurrence:

*Step 1*) the fault is detected by the differential elements of the corresponding SMR. At the same time, the SPRs of the DGs which are inside the faulted sub-microgrid detect the fault. Moreover, according to the type and the location of the fault, the other SPRs which are outside of this sub-microgrid may detect the fault as well.

*Step 2*) the SMR sends the trip signal to the corresponding DCCB. It also reports the fault detection to the CPC by sending an appropriate signal. In this stage, the CPC identifies the faulty sub-microgrid. Simultaneously, the SPRs which detected the fault send the trip signal to the corresponding CBs if the fault current is not interrupted before the critical time of the related VSC. Since the SMRs use the differential-based protection, they can also detect the HIFs which might not be detectable by SPRs. Therefore, the SMR will send the trip command to the related SPRs as well.

*Step 3*) the DCCB(s) that received the trip signal operate and interrupt the fault current. Hence, the faulty sub-microgrid is separated from the microgrid. The CBs status then will be reported to the CPU.

*Step 4*) the open command is sent to the isolators in both ends of the faulted line. These isolators are opened when their flowing current decays to zero.

*Step 5*) after the fault isolation, the opened DCCBs are reclosed by the appropriate commands from the SMRs and the rest of the network is reconnected.

Considering the process detailed before, the faults are isolated in Step 4 by opening the isolators at all sides of the faulty zone. Thus, the network restoration of Step 5 is achieved only when the associated isolators operated successfully. However, the isolator's failure may impact this operation. For instance, if an isolator in one side of the faulty line fails in opening, then the line is not isolated and hence the fault will remain in the system. To prevent this issue, an isolator-failure-backup function is introduced for the CPC. Based on this function, when the "open" command is sent to an isolator, the CPC monitors the status of the isolator. If the isolator fails to open within a determined time, then the CPC will send the open command to the isolators located in its neighborhood.

Based on the requirements of the proposed method, the flowchart of the SPR's operation is shown in Fig. 5.5.

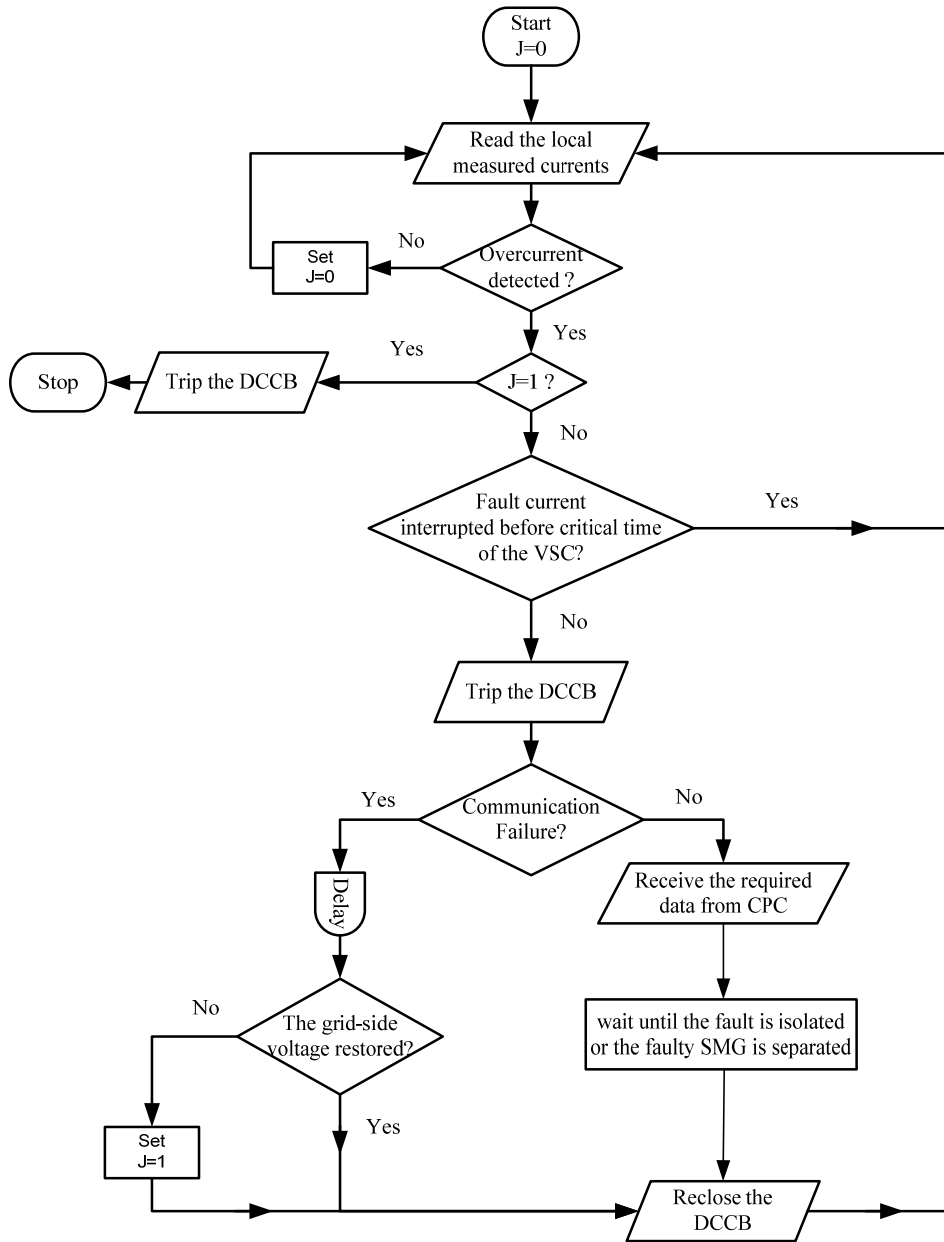


Fig. 5.5. The proposed algorithm for the SPRs.

### 5.3.2. Backup protection

Communication-based protection methods are vulnerable to communication failures. Therefore, the proposed method is supported by overcurrent directional elements to back the differential protection up if the communication network fails. This chapter follows the overcurrent directional protection which has been proposed in [97] for active AC microgrids.

The proposed SMRs switch to the O/C directional-based backup protection if the communication network fails. It should be noted that, according to the specifications of the industrial protocols, the protective devices, are equipped with communication failure detection capability and switch to the backup protection without requirement of any signals from the external supervisory systems [139]. The communication failure detection is handled by exchanging an identification signals between the protection devices. Therefore, if a SMR does not receive the associated identification signals after a predefined period time it will switch to the backup mode, automatically.

As mentioned in Section 5.2., based on the location of the DCCBs, the microgrid is divided into several sub-microgrids. Indeed, each sub-microgrid can be determined as a zone of the backup protection; hence, the directional definite-time overcurrent units are embedded into the SMRs.

As it is shown in Fig. 5.4, the overcurrent directional element of the SMRs have two operating times for forward and reverse faults, i.e.,  $TD_F$  and  $TD_R$ , respectively. If the communication network fails while a forward fault is detected, a trip command is generated after a time delay ( $TD_F$ ). Likewise, for the reverse faults, the trip signal is sent to the corresponding CB after  $TD_R$ .

The operational time of these relays should be determined according to: 1) the requirements of the selective protection through the relay coordination and 2) the critical time of the main VSC station. To provide a selective protection, each relay should operate as a backup for its neighboring relay if the fault was not cleared after a time margin (TM). This time margin should be selected larger than the required time for the operation of the main protection. For example, as illustrated in Fig. 5.4, the maximum operating time of the most upstream relay, i.e., SMR0, is 2TM. Therefore, assuming that the critical time of the main VSC is  $T_C$ , the maximum value of TM is calculated as shown in (5.3).

$$TMD=(T_C - (t_{CT} + t_{det} + t_{CB}))/2 \quad (5.3)$$

Where  $t_{CT}$  denotes the delay associated with current transducers and their corresponding A/D converters (several microseconds);  $t_{det}$  is the fault detection time of the directional overcurrent relay (in the range of several microseconds); and  $t_{CB}$  denotes the operational

time of DCCBs (less than 1ms when the solid-state CBs are used). The operational time of the definite-time overcurrent relays for the backup protection were shown in Fig. 5.4.

On the other hand, the threshold of the overcurrent element of the  $i^{th}$  SMR,  $I_{S,i}$ , is determined according to the nominal current flowing through the corresponding DCCB; i.e.,  $I_{S,i} = RI_{SMG,i}$ , in which  $R$  can be set to values in the range from 1 to 1.2. This current may change after any change occurs in the operational conditions of the microgrid. Therefore, the relay threshold should be changed by a self-regulation method that is explained in Section 5.4.

After any failure in the communication links, the SMRs switch to the backup method and the CPU is disabled. The backup strategy, based on directional overcurrent, is implemented as described in the following steps:

**Step 0)** the SMRs are switched to the backup mode and the CPC is disabled. This step is done once the communication failure is recognized by each relay.

**Step 1)** the fault is detected by SPRs and SMRs. In this step not only the relays of the faulty zone, but also the relays outside of this zone may detect the fault.

**Step 2)** the SMRs send the trip signal to the corresponding DCCBs if the fault current was not interrupted before their predetermined time settings. Simultaneously, the SPRs send the trip command if the fault was not cleared before the critical time of the related VSC.

**Step 3)** the faulted sub-microgrid is isolated and remains separated from the rest of the microgrid.

**Step 4)** some of the SPRs are operated even though their VSCs and DG stations are not located inside a faulty sub-microgrid. In this step, these stations are reconnected after the fault isolation. The flowchart of the proposed SPRs, shown in Fig. 5.5, determines that in the case of communication failure, they try to reconnect the DGs by using the following methods:

- Voltage check: when the DCCB of a DG station is opened, the SPR monitors the voltage of the grid-side busbar and reconnects its DG if this voltage returns to an acceptable range (0.9 of the nominal voltage is selected in this chapter).
- Auto-reclosing: in some cases it is not possible to detect the fault isolation by monitoring the grid-side voltage. For example, when SMG1 of Fig. 5.4 is impacted by a fault and isolated, SMG5 will become separated from the rest of the grid as well. Assuming that the protections of all the DG stations inside this SMG disconnect their DGs, the voltage of this grid cannot return to the acceptable range. Consequently, the

DGs are not reconnected again and a healthy SMG will remain de-energized. To prevent the occurrence of this problem and to facilitate the network restoring, the auto-reclosing ability is embedded into the SPRs. As, shown in Fig. 5.5 the SPR recloses the corresponding DCCB after a time delay. The DCCBs will remain closed if the faulty sub-microgrid was isolated.

It should be noted that the above two methods are executed on all the SPRs; hence, the re-closing process will be executed for those DCCBs which are inside the faulted SMG as well. This can cause an automatic network-restoring, in case of temporary faults, and enhance the reliability.

#### 5.4. Self-healing and adapting unit

Microgrids can operate in grid-connected and islanded modes. Since loads are supplied by the host network and DGs, the load-generation balance is always met in the grid-connected mode. Whereas, in islanded mode, considering the total possible generated power of DGs, the load-generation balance is not necessarily achieved. In this case, the supply-adequacy is the main concern about the successful operation of the microgrid. Indeed, supply-adequacy is the initial condition for the reliable operation of the isolated grids. Forming a supply-adequate microgrid by performing a real-time balancing between the load and generation is known as one of the important features of the network self-healing process[7]. Thus, in this chapter, a centralized self-healing strategy is presented to guarantee the successful operation of the microgrid in various operational conditions. The same self-healing strategy is used for the on-outage SMGs as well. For example, in Fig. 5.4 after the isolation of the line that has been impacted by F1, i.e., Line210, SMG2, SMG3 and SMG4

Furthermore, as mentioned in Section 2 and Section 3, the thresholds of both the main and backup elements of the SMRs are determined according to the nominal currents of the associated lines of the associated SMGs. The nominal current of the lines may vary due to the changes in the microgrid operation modes, load variations or the intermittent behavior of the DGs. Thus, using the fixed relay settings may lead to protection issues such as relays mal-operation and protection blinding [148]. For this reason, in this chapter the thresholds of the SMRs are updated after significant changes in the pre-noted factors.

Briefly, to deal with the above mentioned issues, the microgrid is equipped with the centralized self-healing and adapting (SHA) unit, which its main tasks are:

- Providing network self-healing to guarantee the supply-adequacy when 1) the microgrid works in the islanding mode; and/or 2) SMGs are separated from the grid.

- Adapting the SMRs settings according to the network operational conditions.

These goals are achieved by performing the following steps:

*Step 1)* in the first step, the SHA collects the required information from the isolated microgrid or separated zone. The most important information are the power of the connected loads, the output power of the DGs and the free capacity of the dispatch-able DGs (DDGs) [7]. According to this information, the SHA determines the value of the power which should be disconnected from the on-outage zone. Then, the candidate loads which should be shed are selected based on the pre-determined load priority.

*Step 2)* the appropriate signals are sent to the loads that are selected in Step 1.

*Step 3)* The DDGs are re-dispatched and the settings of the SPRs are adapted based on the new output current of the corresponding VSCs.

*Step 4)* considering the status of the isolators and the DCCBs, the topology of the on-outage zone is estimated.

*Step 5)* new thresholds for the SMRs are calculated according to the load flow equations in DC grids (the method is explained below in Section 5.4.1).

*Step 6)* the new settings are applied to SPRs and SMRs.

### 5.4.1. Re-calculating the SMRs setting

The SHA calculates the new threshold of the SMRs based on the power flow equations of the DC systems presented in [142]. The algorithm that is used for re-calculating the SMR's setting is similar to the method explained in Section 4.4 and based on equation (4.1) to equation (4.6). Therefore, those equations are not repeated here.

The equation (4.6) shows that any change in the network topology, reflected in the  $\mathbf{Y}$  matrix, may impact in the direction and/or the magnitude of the distribution line current. Furthermore, this equation illustrates that the connection/disconnection of DGs or changes in their generated power, reflected in  $\Delta\mathbf{P}$ , may also result in significant changes in the feeders currents.

Thus, in order to calculate the new pickup currents, the SHA monitors: 1) the status of the DCCBs and isolators to estimate the network topology and to update the  $\mathbf{Y}$  matrix; 2) the injected power of the DGs and the load currents; and 3) the voltage of the DC busses. Then, the SHA calculates the new pickup currents and communicates with the SMRs to apply the

new settings. Fig. 5.6 shows the flowchart of the proposed self-healing strategy to be implemented in the SHA unit.

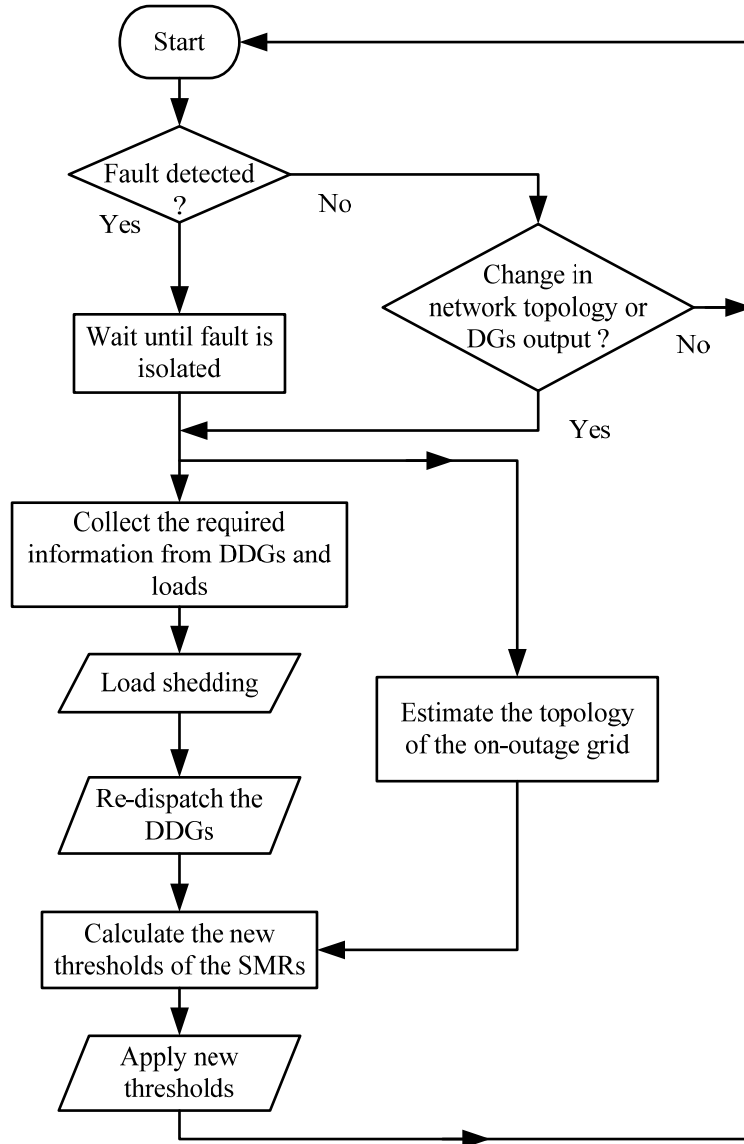


Fig. 5.6. The proposed algorithm of the SHA.

### 5.5. HIL verification and case studies

To validate the proposed protection scheme in the context of the network of Fig. 5.4, the HIL simulation approach was used. The HIL method was introduced to investigate errors and delays that do not appear in the classical off-line simulations. More explanations about the setup test-bed are presented in the Appendix of this thesis.

The operational time of the typical medium voltage CBs is around 55-60ms. Moreover, it is assumed that the SSCBs are used wherever a DCCB is necessary. The operational time of these CBs is less than 1ms.

#### Case Study 1:

##### Operation of the main protection.

In the first case study case it is assumed that at  $t = 1s$  a solid pole to pole (PP) fault impacts the microgrid at the point labeled with F1 in Fig. 5.4. Subsequent to the fault occurrence, SMR2, SMR3 and SMR4 detect the fault and send the trip command to the corresponding DCCBs after 2.4ms ( $\pm 0.2ms$ ).  $\pm 0.2ms$  is the difference between the operational times of these SMRs. The corresponding DCCBs operate and isolate SMG2 around 3.6ms after the fault occurrence. Meanwhile, SPR1 detects the fault 48  $\mu s$  after its occurrence; however it sends the trip command after 3.2ms.

Simultaneously, the relays of the DGs outside the faulty SMG whose critical time of their VSC station is less than the fault clearing time will operate as well. For example, the operating time of SPR2 is set to 2.7ms while the fault current fed from the SMG4 is interrupted after 3.6ms; hence, SPR2 sends the trip command to DCCB2 and isolate DG2. This DG should be re-connected as soon as possible. All these operations and commands are reported to the CPC. When the CPC receives the “open” status of the DCCBs, it will send two important commands. First, the “reclose” command is sent to SPR2 which is not inside the faulty SMG. This command is received at SPR2 in less than 15ms after the fault occurrence. Second, after a time margin, which is set to 10ms, the CPC sends the “open” command to the corresponding isolator switches. Therefore, considering the operational time of these switches, the faulty line is isolated in less than 80ms after the fault occurrence. The open status of these switches is reported to the CPC and considering the time margin for reliable operation the “close” command is sent to SMR2, SMR3, SMR4 and SPR1 93ms after the fault occurrence. The operational time of the various parts of the proposed protection technique is shown in Fig. 5.7. This test illustrates that the proposed protection is able to isolate the faulty part and re-store the sound parts of the microgrid in less than 100ms.

This study case also illustrates that by the use of a minimum number of DCCBs, the method provides a selective protection with the minimum possible interrupted loads and very short interruption duration. In other words, the minimum possible loads are disconnected and

the rest of the faulty sub-microgrid is restored after around 100ms. This behavior enhances the network reliability, and due to the direct relation between the reliability indexes and the economic aspects of the network operation [149, 150], the method reduces the outage costs as well.

### Case Study 2:

#### Operation of the backup protection when communication fails.

After the communication failure, the SMRs switch to their backup mode. In this case, the  $TD_F$  and  $TD_R$  of each SMR is set according to the TM. The method for calculating the TM was explained in Section IV.B. The simulation results show that the critical time of the main VSC station is 8.5ms; then, the TM is set to 3.5ms.

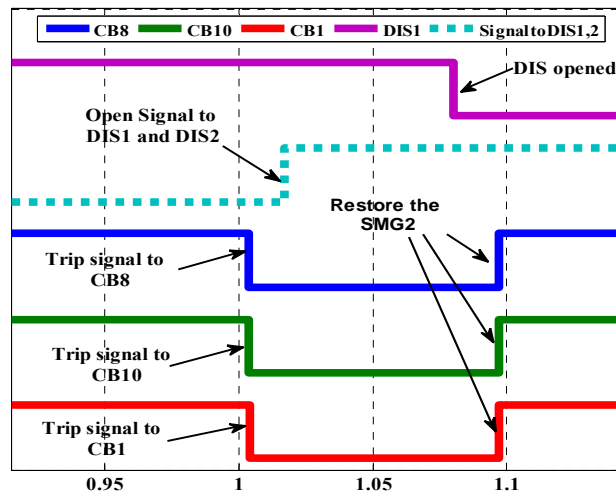


Fig. 5.7. The operation time of the protection elements for case study1.

Now, let's assume that a PG fault occurs at the point labeled with F2 in Fig. 5.4 while the communication link fails. In this case, SPR5, SPR6, SPR7, and SMR5 detect the fault in less than 120  $\mu$ s. SMR5 sends the trip command immediately; consequently SMG5 is isolated from the rest of the network after 1.1ms. Furthermore, SPR5, SPR6 and SPR7 are going to send the trip command after 2.8ms, 2.5ms and 3.1ms respectively. Due to the separation of the SMG5 before the operating time of SPR5, this relay will not send its trip command. By the operation of CB6 and CB7, the DG6 and DG7 are disconnected in less than 4ms after the fault occurrence. It is clear that, although this backup method can provide a fast fault

interruption, the faulty SMG will be separated after any fault occurrence. As it is shown in Fig. 5.8, to facilitate the fast network restoring, all the relays which have been sent the trip command will send the reclosing command after a time delay. For this study case, this time delay is set to 0.3s. Hence, in the case of the temporary fault occurrence, the isolated network may get restored after 0.3s.

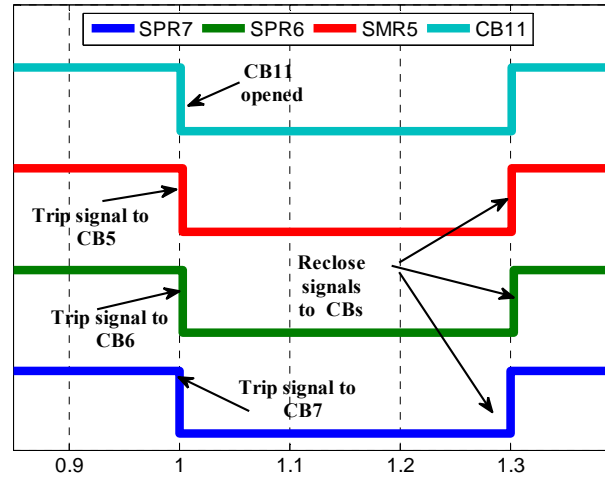


Fig. 5.8. The operation time of the protection elements for case study 2.

To further evaluate the effectiveness of the proposed protection strategy, in addition to the previous two cases, various fault scenarios have also been studied that are reported in Table 5.1. It should be noted that for each case, only the operating time of the relays inside the faulty SMG are reported in Table 5.1.

Table 5.1. Operating times of the main and backup protection for selected fault scenarios.

| Fault Type | Fault Location | Main Protection   |                     |                                | Backup Protection<br>(Communication Failure) |                     |   |     |
|------------|----------------|-------------------|---------------------|--------------------------------|--|---------------------|---|-----|
|            |                | Operated Relay(s) | Operating Time (ms) | Faulty SMG Restored After (ms) | Operated Relay(s)                            | Operating Time (ms) | For Temporary Faults, SMG Restored After (ms) |     |
| PP         | F2             | SMR1              | 2.5                 | 97                             | SMR1   | 5                   | 307   |     |
|            |                | SMR2              | 2.4                 |                                | SMR2   | 2.5                 |   |     |
|            |                | SMR5              | 2.6                 |                                | SMR5   | 5.2                 |   |     |
|            |                | SPR5              | 2.8                 |                                | SPR5   | 2.8                 |   |     |
|            | F7             | SMR3              | 2.4                 | 99                             | SMR3   | 0.12                | 306   |     |
|            |                | SPR3              | 3.8                 |                                | SPR3   | 3.8                 |   |     |
|            |                | SPR4              | 4.2                 |                                | SPR4   | 4.2                 |   |     |
|            | F8             | SMR5              | 2.5                 | 98                             | SMR5   | 0.15                | 307   |     |
|            |                | SPR6              | 2.5                 |                                | SPR6   | 2.5                 |   |     |
|            |                | SPR7              | 3.1                 |                                | SPR7   | 3.1                 |   |     |
|            | PG             | F4                | SMR2                | 2.7                            | 98   | SMR2                | 2.52  | 307 |
|            |                |                   | SMR3                | 2.6                            |  | SMR3                | 5.3   |     |
| SMR4       |                |                   | 2.5                 | SMR4                           |  | 5.35                |   |     |
| SPR1       |                |                   | 3.2                 | SPR1                           |  | 3.2                 |   |     |
| F5         |                | SMR4              | 2.6                 | 97                             | SMR4   | 0.21                | 305   |     |
|            |                | SPR2              | 2.7                 |                                | SPR2   | 2.7                 |   |     |
| F6         |                | SMR3              | 2.8                 | 99                             | SMR3   | 0.25                | 308   |     |
|            |                | SPR3              | 3.8                 |                                | SPR3   | 3.8                 |   |     |
|            |                | SPR4              | 4.2                 |                                | SPR4   | 4.2                 |   |     |



---

## Fault management and self-healing in active distribution systems

An optimized network clustering is presented in this chapter for active distribution systems. In this method after a fault occurrence, the on-outage section of an active distribution network is divided into some microgrids based on the optimum operation and supply-adequacy aspects. To achieve the optimum operation, the borders of microgrids are determined considering the total losses, voltage deviations and minimum load shedding. On the other hand, the equivalent circuit of each zone of the network is calculated based on the measured data by PMUs. Therefore, the proposed clustering method determines the optimum microgrids without requirement to the information about the network topology and components. The performance of the proposed method for AC and hybrid AC/DC grids is evaluated using HIL simulation, in which the study network is simulated in a real time simulator and the proposed algorithm, which is executed in an aggregator, receives the required data from the PMUs.

### 6.1. Introduction

The self-healing is introduced as one of the features of the future smart distribution grids which will serious contribute to increase the network reliability [7]. In order to provide self-healing capabilities, distribution grids should be equipped with advanced control algorithms which enable them to automatically handle and solve problems that may happen during its generic operation [14].

On the other hand, the penetration of conventional and/or renewable distributed generators (DGs) is increasing in distribution grids. During the normal operation of active distribution networks, loads are supplied by the main grid, e.g. transmission networks, and DGs. However, when a disturbance or a fault occurs, the entire or a section of the distribution feeder is disconnected from the main grid. In these conditions the loads inside the on-outage section are supplied only by the DGs. It should be noted that, in this chapter it is assumed that an “on-outage section” is a section of the study grid that is isolated from the host system after a fault or un-expected event. This section may include several zones. In this case, as a self-healing action, the on-outage section can be divided into a set of microgrids and operate individually to continue the reliable supply for the maximum possible loads [7]. Therefore, clustering an on-outage network into a set of microgrids can improve the network operation and reliability [151].

The supply-adequacy is the initial and the essential requirement of each individual microgrid; however, the optimal operation of the on-outage section is achieved by forming the optimal microgrids. Therefore, the optimized network-clustering (ONC) is introduced as a self-healing task to divide the on-outage section to a set of microgrids considering different factors, such as: minimizing the total loss, power quality issues, and DG characteristics.

Most of the advanced network-clustering methods require a certain amount of information about the network topology and its components (e.g. line impedance, etc.) in order to work properly [7, 12-14]. Nevertheless, in this chapter a measurement-based clustering method is presented. In this method, the boundaries of the optimized microgrids are determined based on the analysis of the equivalent circuits which are calculated by a PMU-based method. Therefore, due to the independency of the network parameters, the intermittent behavior of DGs and their connection/ disconnection, possible network reconfiguration or change in the feeders, do not impact on the accuracy of the method.

The proposed method is executed in a central management unit (CMU); hence the measured data by all the PMUs are collected in the CMU. In addition, each zone of the distribution network, determined by the CBs location, is equipped with a zone control unit (ZCU) which is able to monitor DGs inside the zone, as well as to communicate with CMU and to disconnect some of the loads in critical cases.

This chapter presents two different ONC methods which are based on: 1) the admittance matrix of the system and 2) the PMU-based equivalent circuit. However, these methods are applicable for AC distribution systems and hybrid AC/DC grids. If compared to the previous presented works, the main contributions of the proposed method can be summarized as:

1. The proposed method is a measurement-based ONC method that does not require having the exact values of the network parameters and the information about the network topology.

2. In most of the advanced ONC methods, the borders of each cluster are determined assuming that there are suitable switches in each line of the distribution system. However, this is not a realistic assumption for most distribution systems. However, in the proposed method, network clusters are defined considering the location of the existing CBs; indeed, the locations of CBs have been considered as the connection points of microgrids. Therefore, the method can be implemented on the existing distribution systems with no need to add new CBs or assuming that each branch counts on the adequate switches.
3. The method has been implemented in a HIL test-bed including PMUs, real-time simulator, and the controller. Therefore, the issues related to the real implementation of the method have been considered as well.
4. The method not only provides an acceptable performance for active AC distribution systems, but if a suitable equivalent circuit for VSCs is used, it can be implemented for hybrid AC/DC grids too.
5. The clusters of the study network can be modified according to the changes in the loads, the changes in the generated power of DGs and any other changes in the network elements that may affect the operation of the grid. To achieve this goal, the network quantities are continuously monitored and after a significant change occurs, the objective functions of the possible microgrids are re-calculated.

## 6.2. Study Case

Since this chapter was done in the framework of the IDE4L (Ideal Grid for All) project, the study case in this chapter is a 132-bus system that has been designed according to the reference grid of this project presented in [152]. This grid includes different type of DGs that their location, type and rated power are arbitrary selected. Table 6.1 describes the rated power of the DGs.

This grid, as a large distribution networks, can be divided into some zones due to the operation of the CBs that are located at various points of the grid. It should be noted that, in this chapter, it is assumed that “zone” is a section of the study grid which is located between some CBs. Each zone can be isolated form the rest of the grid or can be connected to the host network by operation of its boundary CBs. Each of these zones may count on different types of DGs, loads, energy storages, etc. Therefore, they can be considered a microgrid. When the distribution system is connected to the transmission network, the CBs are normally closed.

It is also assumed that relays corresponding to the CBs shown in Fig. 6.1, are able to measure synchrophasors of voltage and currents; hence, these relays can operate as PMUs as well (See Section 6.5.2).

Table 6.1. The rated power of DGs.

| DG type                              | Rated power  |
|--------------------------------------|--|
| WT                                   | 1000-1500 kW<br>(for average wind speed of 15 m/s) |
| Single-phase residential PV          | 20-50 kW   |
| PV farm                              | 100-200 kW   |
| Diesel generators and micro turbines | 500-1000 kW  |

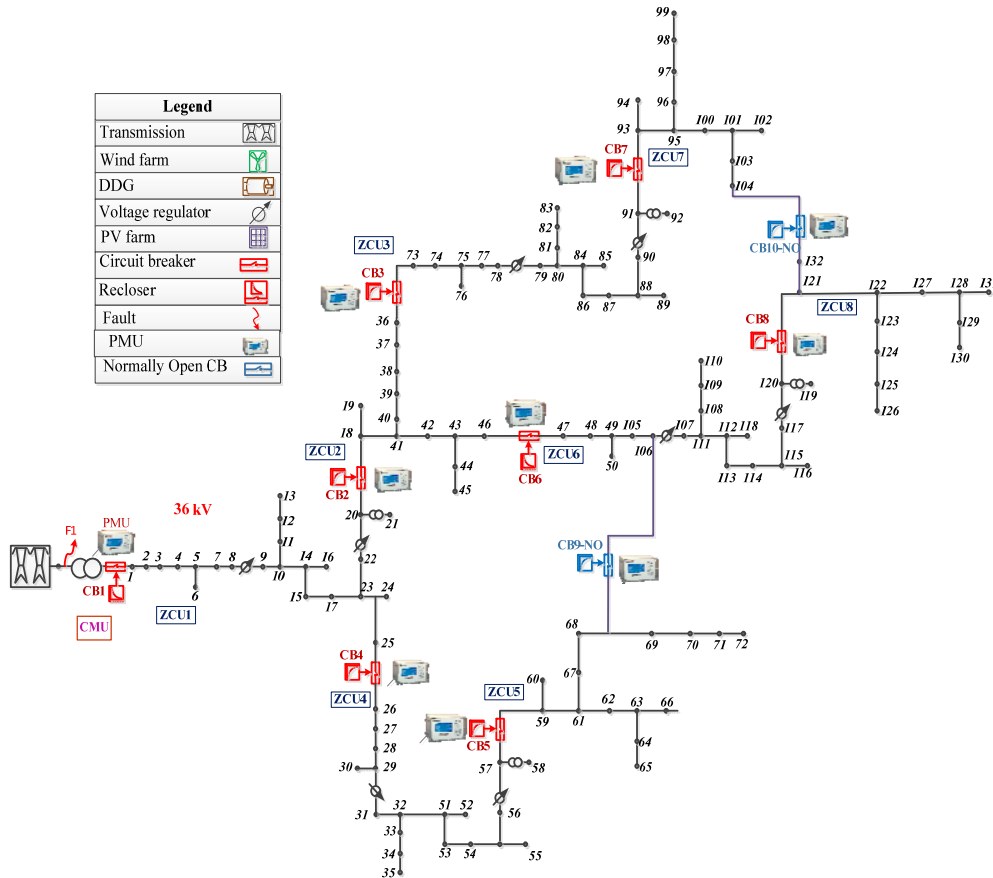


Fig. 6.1. The study distribution network and location of PMUs.

### 6.3. Requirements of the proposed ONC method

In order to apply the proposed ONC method to the network of Fig. 6.1, the following assumptions are required.

#### 6.3.1. Network assumptions

As mentioned above, different types of DG may be placed in each zone. DGs such as micro turbines (MTs) and diesel generators (DIGs) are determined as dispatchable DGs (DDGs) whereas some other types of DGs (e.g. Photovoltaic (PV) generation units) are considered as not dispatchable. In an isolated microgrid the load variation can be handled by performing an appropriated control of the DDGs. Therefore, it is assumed that each zone includes DDGs with a fast response capability to the load variation. Moreover, each zone has an individual Zone Control Unit (ZCU) that monitors the zone's operational conditions; therefore, the operation of each zone can be controlled using the de-centralized control logic. The available capacity of each DG inside the zone and the currents of the zone boundaries, CB locations and status are reported to the ZCU. Furthermore, the type of the DGs, dispatch-able or not, and the load priority is predetermined for the ZCU. In addition, ZCUs send the new setting for the generated power of each DG; this capability is important especially when the zone is isolated and the total generation and loads should be balanced by the local DGs. All the ZCUs are connected to the CMU and exchange the necessary signal through the communication systems to provide a coordinated control to the related distribution system. Table 6.2 shows the exchanged information between the elements of the network.

### 6.4. Proposed Optimized-Network-Clustering (ONC) algorithm

As mentioned before, the main goal of the proposed method is to cluster the whole or a part of a distribution network into a set of individual microgrids to achieve the optimal network operation. The main concepts, constraints, and objective functions of the proposed ONC method are explained in this section.

#### 6.4.1. Constraints for successful operation of an isolated microgrid

The possibility of the successful isolated operation of each zone (namely, as a microgrid) should be evaluated in the first stage of each network-clustering methods. As mentioned above, the supply-adequacy is the initial and the essential requirement for the reliable operation of an isolated microgrid. Therefore, the following constraints should be considered as the initial factors for the reliable operation of each microgrid.

Table 6.2. Information exchange between the network elements.

| Inputs  |       |  | Outputs   |               |   |
|---|-------|--|-----------|---------------|---|
| Name  | Type  | Description  | Name      | Type          | Description   |
| <i>Signal exchanged between ZCUs and elements inside the microgrid.</i> |       |  |           |               |   |
| DgStat  | Bool  | DG connected or not.   | DgCbSt    | Bool          | Send open/close command to CB of a DG.  |
| DgGen   | Float | Generated power of a DG.   | CbsStat   | Bool          | Send open/close command to a CB installed at the borders.                         |
| DgAvaPow  | Float | Available power of a DG.   | LodShed   | Bool          | Send message to a Load to disconnect it form the grid.                            |
| CurBor  | Float | Currents measured at the microgrid's boundaries..                | DgOutSet  | Float         | Determines the generated power of each DG.  |
| <i>Signal exchanged between ZCUs and CMU.</i>                           |       |  |           |               |   |
| CurBond   | Float | Summation of the measured current at the microgrid's boundaries. | IsoCom    | Array of Bool | CMS-Array: determines which CBs on the borders of the microgrid should be opened. |
| FaultDet  | Bool  | A fault has been occurred at the microgrid.                      | ZoOoOut   | Bool          | The zone is located inside an on-outage section.                                  |
| TotDgAvaPow   | Float | The total available power of DGs.                                | ZoCon     | Bool          | The on-outage section has reconnected and the zone connected to the host grid.    |
| <i>Signals transmitted by PMUs at the borders of a microgrid.</i>       |       |  |           |               |   |
| MeasCur   | Float | Measured currents at the PMU location                            | CurSyncPh | Float         | Current synchrophasors to ZCUs and CMU.   |
| MeasVol   | Float | Measured voltages at the PMU location                            | VolSyncPh | Float         | Voltage synchrophasors to ZCUs and CMU.   |
| TimSyncMSg  | Float | Time synchronization message from GPS antenna.                   |           |               |   |

#### A. Load-generation balance

From the supply-adequacy point of view, the load-generation balance is the most important constraint for the autonomous operation of a microgrid. Each zone can operate as an islanded microgrid if [153]:

$$\sum P_{S,i}(t) + \sum P_{W,i}(t) + \sum P_{PV,i}(t) \geq P_L(t) + P_{Loss}(t) \quad (6.1)$$

Where  $P_{S,i}$ ,  $P_{W,i}$  and  $P_{PV,i}$  are the output power of the  $i$ th DDG, wind turbine and PV unit respectively;  $P_L$  and  $P_{Loss}$  are the total load and losses inside the zone. Indeed (6.1) determines the possibility of keeping the load-generation balance inside the microgrid (i.e. DGs power match the total load and losses).

On the other hand, distribution systems normally consist on a high number of busses, lines and loads. However, due to economic reasons, it is not reasonable to use a high number of measurement devices; therefore, normally voltage and current measurements are only available from the main substations (where CBs are installed). Furthermore, the flowing

current into/from a zone are measured and reported to the ZCU; thus, the load/generation balance, before the disconnection from the main grid, can be determined by measuring the input/output currents in the borders of the microgrids. Therefore, the summation of these currents is calculated as shown in (6.2); this equation can be used instead of (6.1).

$$I_{DZ} = \sum_{i=1}^N I_{z,i}(t) \quad (6.2)$$

Where  $I_{z,i}$  denotes the current in the  $i^{\text{th}}$  connection points (boundary) of the zone and  $I_{DZ}$  is the summation of the boundaries current (current flowing into or from the microgrid are assumed as positive and negative current, respectively). If there are enough measurement devices (6.1) can be used; otherwise, (6.2) should be used.

#### B. Generators limits

Each generator has a stable operation if it works between its lowest and highest generation limit [154]. Therefore, the allowed generated power of each DG can be written as:

$$P_i^{\min} \leq P_i(t) \leq P_i^{\max} \quad (6.3)$$

Where  $P_i^{\min}$  and  $P_i^{\max}$  are the lowest and the highest generation limits of  $i^{\text{th}}$  DG.

#### C. Generated Power of DDGs

Due to the intermittent behavior and uncertainties related to renewable DGs and also the dynamic behavior of loads, the microgrid must contain DDGs to match the load by changing their output power. Furthermore, voltage regulation with DDGs can ensure the voltage stability for an isolated microgrid [155]. Therefore, to provide a successful islanding operation, the generated power of the DDGs should be at least 60% of the total load at the time of islanding [156]. For this reason, each zone can be operated as a successful microgrid if:

$$\sum P_{S,i}(t) \geq 0.6 * P_L(t) \quad (6.4)$$

Each zone of the study network which satisfies the three above conditions is considered as a fundamental microgrid (FMG). On the other words, a FMG is a microgrid which has the initial conditions for the successful islanding operation.

### 6.4.2. Objective Functions for Optimal network clustering

The above mentioned criteria determine the feasibility of the islanding operation in a microgrid. However, they cannot guarantee the optimal operation of the on-outage zone when it is clustered to some FMGs. In order to achieve the optimal operation of an on-outage zone various parameters can be introduced as the targets of the optimization process. In this research, in order to achieve the optimized clustering, three objective functions (OFs) are considered. These OFs are: 1) to minimize the total loss, 2) to minimize the voltage deviation, and 3) to minimize the total power of the disconnected loads.

In the following sections it is explained that these OFs are calculated for all the possible combinations of FMG to recognize the optimum arrangement of the network clusters.

#### 6.4.2.1. To minimize the total losses

An on-outage grid can be clustered into various microgrids. According to the topology and the type, size and location of DGs and loads, these various clusters-arrangements may results in various power-flows in the on-outage zone. Consequently, for the various possible clusters-arrangements the current flowing through the lines of the on-outage zone are not necessarily the same. Therefore, through the optimal selection of the network clusters, the total loss of the on-outage zone can be minimized; hence, the first objective function considers the total loss of the on-outage zone for each possible combination of the FMGs:

$$F_1 = \sum_{i=1}^N P_{Loss,i} \quad (6.5)$$

where  $P_{Loss,i}$  is the losses inside the  $i$ th network cluster.

#### 6.4.2.2. To minimize the voltage deviations

Similar to the logic explained for the first function, the total voltage deviations of the on-outage zone is not the same for all the possible clusters-arrangements. Therefore, the second function calculates the summation of the voltage deviations in all the boundaries of the microgrids as presented in (6.6):

$$F_2 = \sum_{k=1}^N |V_k - V_n| \quad (6.6)$$

where  $V_k$  is the voltage magnitude at terminal  $k$  of the on-outage zone and  $V_n$  is the nominal voltage.

It should be also noted that  $F_2$  determines the summation of the voltage deviation in all the buses; however, each bus should individually satisfy the voltage constraints. Thus, clusters-arrangements that do not satisfy the condition presented in (6.7) are omitted from the possible options for network clustering.

$$V_i^{min} \leq V_k(t) \leq V_i^{max} \quad (6.7)$$

##### 6.4.2.3. To minimize the disconnected loads and enhance the reliability indices

Network reliability is one of the most important operational features of distribution systems. IEEE Std 1366-2012 [157] presents several reliability indices to assess the operation of distribution systems. Two of the most important and commonly used indices are the system average interruption frequency index (SAIFI) and the system average interruption duration index (SAIDI). These indices are defined as:

$$SAIFI = \left( \sum_{i=1}^n N_i \right) / N_T \quad (6.8)$$

$$SAIDI = \left( \sum_{i=1}^n U_i N_i \right) / N_T \quad (6.9)$$

where  $N_i$  is the number of loads connected to bus  $i$  that are interrupted after the event,  $n$  is the number of the busses of the on-outage zone,  $N_T$  is the total number of loads connected to the on-outage network and  $U_i$  is the total interruption during.

On the other hand, as mentioned in Section 6.4.1, the load-generation balance is the essential factor for the successful islanding operation of a microgrid. To achieve load-generation balance for each FMG, in some cases, it is necessary to apply the load-shedding on that FMG. According to the above two reliability indices, load shedding increases the number of the disconnected loads and hence impacts the network reliability. Therefore, in order to enhance the network reliability, it is necessary to decrease the number and the total power of the disconnected loads.

Loads which have been shed in the previous stage (i.e., when FMG are formed) can be re-connected if the FMG is integrated with another FMG with enough power capacity. Therefore, selecting the optimum clusters-arrangement can reduce the total disconnected load and enhance the network reliability. As a consequence, the third function is defined in (6.10) to calculate the disconnected load for each possible network clustering option.

$$F_3 = \sum_{i=1}^m P_{Dis,i} \quad (6.10)$$

Where  $P_{Dis,i}$  is the disconnected power inside the  $i$ th network cluster and  $m$  is the numbers of clusters.

### 6.5. Calculation of the optimization functions

In order to calculate the total losses and voltage deviations, two different methods are explained here. In the first method, see Section 6.5.1, the admittance matrix of the study system is used to calculate current and voltage of the buses of the on-outage zone. While, in Section 6.5.2, using a PMU-based method, the equivalent circuit of each FMG is calculated and the power-flow equations are applied on the equivalent circuit instead of the admittance matrix of the grid.

#### 6.5.1. Using network parameters

In order to calculate the objective functions, introduced in Section 6.4.2, it is necessary to calculate the total losses and the total voltage deviations of the on-outage section of the study grid. These two functions can be calculated using the power-flow equations. The basic equations for the power-flow analysis are started by creating a bus admittance matrix ( $Y_{Bus}$ ). For example, for an  $n$  bus grid, the basic equation for power-flow analysis starts by:

$$\begin{bmatrix} Y_{11} & \cdots & Y_{1n} \\ Y_{21} & \ddots & Y_{2n} \\ \vdots & \ddots & \vdots \\ Y_{n1} & \cdots & Y_{nn} \end{bmatrix} \begin{bmatrix} V_1 \\ V_2 \\ \vdots \\ V_n \end{bmatrix} = \begin{bmatrix} I_1 \\ I_2 \\ \vdots \\ I_n \end{bmatrix} \quad (6.11)$$

Where,  $Y_{ij}$  denotes the elements of the admittance matrix;  $V_i$  is the voltage of  $i$ th bus and  $I_i$  is the injected current to the  $i$ th bus. Distribution systems normally consisting of high number of lines and busbars; therefore, the admittance matrix is typically a large matrix.

This equation implies that in order to calculate the total losses and voltage deviations of the grid it is necessary to have the following information:

- Lines' characteristics
- Network topology
- Loads' characteristics

It is worth noting that changes in this information will change the components of the admittance matrix; therefore, such changes should be reported to the central unit of the ONC method. Furthermore, after some type of changes in the network topology, e.g. adding a new line, not only the elements of the  $Y_{Bus}$  matrix, but also its dimension should be modified.

### 6.5.2. PMU-based equivalent circuit

Equation (6.11) illustrates that for solving the basic power-flow equations it is necessary to have an updated admittance matrix of the on-outage zone which is formed based on the information provided in Section 6.5.1. However, it is not always easy/ possible to use the admittance matrix particularly in the following cases:

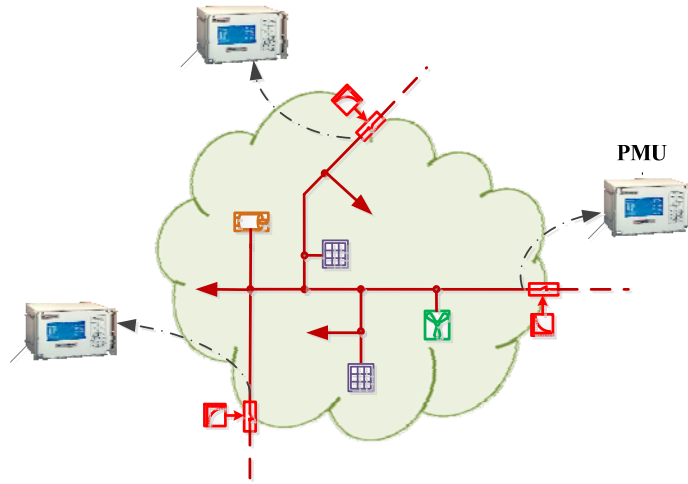
- When there is not enough information about the elements of an existing grid.
- When the network topology changes after the connection/disconnection of a DG.
- When a new line is added to the grid or an existing line which is removed from the network.

Therefore, in such cases, it is necessary to use an estimated model for the power system under study to simulate the steady-state behavior of that system. Moreover, after any change in the study grid, the model should be modified automatically. In this chapter, a phasor-based network-estimation, which was presented in [158], is used. This method provides an updated equivalent circuit for the FMGs of the on-outage zone by using the phasors of voltages and currents in the borders of each FMG. It is noted that For a sinusoidal and periodic voltage, the phasor of the voltage is defined as:  $V = (\frac{V_{max}}{\sqrt{2}})e^{j\varphi}$ ; where  $V_{max}$  is the peak value of voltage and  $\varphi$  is the phasor angle relative to a reference.

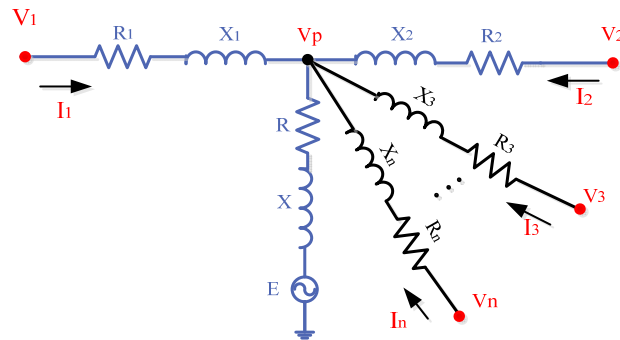
About the application of PMUs, it should be noted that since many of modern protection relays are equipped with the algorithm of synchrophasors calculation, these relays can operate as a PMU as well. Therefore, the required information for the PMU-based model of a grid can be obtained from the PMU applications of the existing relays and it is not necessary to add new PMUs. Moreover, the communication infrastructure of smart grids is used to communicate between the PMUs and the central control units.

6.5.3. Calculation of the PMU-based equivalent circuit

As mentioned above, in order to estimate the steady-state behavior of each FMG, a PMU-based equivalent circuit is used here. Based on this method, each zone of a network can be replaced by an equivalent circuit consisting on a source and several R-L branches.



a.



b.

Fig. 6.2. a. A typical FMG, and b. its equivalent circuit estimated by  $n$  PMUs [158].

The number of branches is determined according to the number of PMUs. However the phasors measured by at least two PMUs are necessary; therefore, the equivalent circuit at

least has three branches (blue branches in Fig. 6.2). It should be noted that in this equivalent circuit these three branches have the same values of R and X [158]; therefore, for  $i$ th phase of each FMG it can be written:

$$R^i = R_1^i = R_2^i \quad (6.12)$$

and

$$X^i = X_1^i = X_2^i \quad (6.13)$$

Fig. 6.2 shows the equivalent circuit of a typical FMG when  $n$  PMUs are installed at its borders. Assuming that  $V_j^i$  and  $I_j^i$  are the voltage and current phasor of phase  $i$  measured by  $j$ th PMU, for each phase of the equivalent circuit it can be written as:

$$V_1^i \angle \delta_1^i - V_2^i \angle \delta_2^i = (R^i + jX^i) (I_1^i \angle \varphi_1^i - I_2^i \angle \varphi_2^i) \quad (6.14)$$

Where  $i$  denotes the phase, which can be a, b, or c. Accordingly, the impedances of the main branches are calculated as:

$$R^i + jX^i = \frac{V_1^i \angle \delta_1^i - V_2^i \angle \delta_2^i}{I_1^i \angle \varphi_1^i - I_2^i \angle \varphi_2^i} \quad (6.15)$$

On the other hand, applying the KVL in the loop formed with the first branch and the voltage source branch, the voltage source of the equivalent circuit can be calculated as:

$$E^i \angle \delta^i = V_1^i \angle \delta_1^i - (R^i + X^i) I_1^i \angle \varphi_1^i - (R^i + X^i) (I_1^i \angle \varphi_1^i + I_2^i \angle \varphi_2^i) \quad (6.16)$$

Using the above two equations, the values of the main branch's impedances (blue impedances in Fig 6.2) and the equivalent voltage source are calculated. In the next step, the impedances of the other branches are also calculated by applying KVL on the corresponding loops as following:

$$V_1^i \angle \delta_1^i - V_n^i \angle \delta_n^i = I_1^i \angle \varphi_1^i (R_2^i + jX_2^i) - I_n^i \angle \varphi_n^i (R_n^i + jX_n^i) \quad (6.17)$$

It is worth noting that, the dimension of the admittance matrix of the estimated equivalent circuit is much smaller than the dimension of the admittance matrix presented in (6.11). Therefore, this method needs less mathematical calculations and hence the power-flow equations can be solved faster and easier.

### 6.6. Steps of the proposed method

Based on the above mentioned constraints for the successful and optimum operation of on-outage grids, in this section the steps of the proposed ONC method is explained in the context of the study grid of Fig. 6.1.

It should be noted that in most of the advanced ONC methods, the on-outage grids were clustered from each line assuming that there are suitable switches (CBs) in each branch; however, it is not a realistic method for most of the distribution systems. Therefore, in the proposed ONC, the zones are defined based on the location of the existing CBs. Indeed, the proposed ONC can be implemented on the existing distribution systems with no need of installing new CBs or assuming that there are the adequate switches installed at all the distribution lines. In other words, in this method, the location of CBs has been considered as the connection point of microgrids. The selection of the CBs location, and consequently PMUs, is out of the scope of this thesis and can be considered as a future work. It is also worth noting that, if all the network parameters are known and CBs are located at all the distribution line, the method presented in Appendix B also can be applicable.

#### Step1. Forming the fundamental microgrids

In the first step, the possibility of the successful autonomous operation is investigated for each zone of the on-outage section. As mentioned in section 6.4.1, to ensure the supply-adequacy is the initial and the essential requirement for the reliable operation of each microgrid. Therefore, in this stage the constraints described by (6.1) to (6.4) are investigated for each zone.

It is clear that for the usual distribution systems these conditions cannot be satisfied by all the zones. Thus, the following tasks are applied on these zones, in order to convert them to a FMG:

- If the initial necessary conditions are not satisfied by a zone but there is more than enough generation (and DDG capacity) inside one of the zones in its neighborhood, the possibility of the integration of these zones is investigated. If this integration can create a zone that satisfies the above mentioned conditions, this new zone can be determined as a FMG. In this case, the possible combinations of the zone with its neighboring zones are investigated to determine a FMG which

includes both zones. Indeed, the FMG created in this stage includes more than one zone.

- If the integration with other zones cannot satisfy the conditions, the zone should be converted to the FMG by load shedding. Although load shedding can be achieved by various methods, such as using frequency relays or PLC-based methods that have been explained in [155], in the proposed ONC method it is assumed that a centralized load-shedding logic is used for each zone. In this case, according to the load priority, predetermined for ZCUs, the load shedding is applied to the zone to reach to the initial conditions of the FMG's successful operation.

Finally, in this stage, using the rules presented in Section 6.4.1 and the above complementary actions, the network is divided into a set of supply-adequacy FMG (see Fig. 6.3). Indeed, in this step the reliable supply is provided for the maximum possible loads inside all the isolated FMGs.

It is also worth to mention that the proposed ONC method can be applied in networks which have been designed accordingly, where the above mentioned conditions have been determined as constraints in the network's design. In this case, each zone operates as a FMG without integrating other zones or performing load shedding.

Furthermore, it should be noted that network clustering is enabled after the fault occurrence and the isolation of the on-outage section of the grid. In such conditions, the most important factor is providing a stable operation for the grid and to guarantee the continuous power supply to the loads; therefore, the economic aspects related to the power generation of the DGs are not in the first level of importance. For this reason, although maybe under normal conditions some of DGs are not generating their maximum possible power, due to economic issues and etc.; it is assumed that after the fault occurrence and network isolation (i.e., when the on-outage zone is in emergency conditions), the economic issues are not considered as critical. Therefore, in this stage, the generated power by DDGs is changed without considering economic factors which are typically investigated under normal conditions.

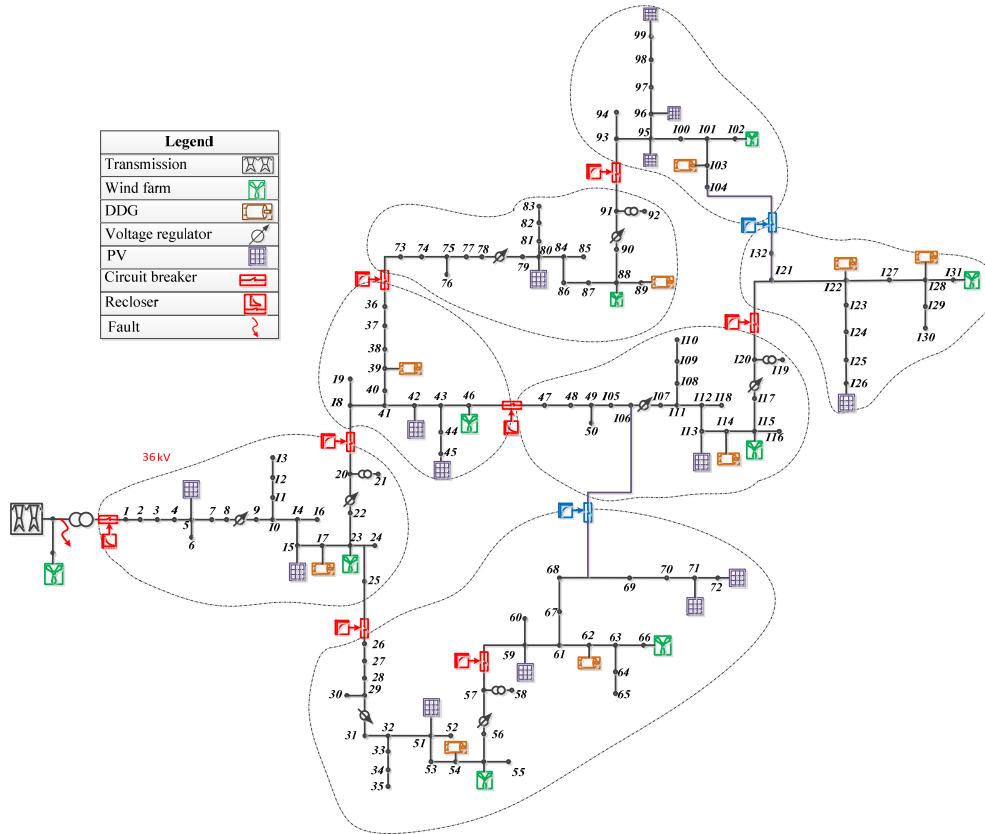


Fig. 6.3. A possible arrangement for FMGs of the study system.

**Step2. Calculating the equivalent circuit of FMGs**

As it was already explained, it is vital to have an equivalent model of each FMG in order to apply the proposed ONC method. Therefore, it is assumed that PMUs are installed at the boundaries of zones in order to derive the equivalent model, as described in Section 6.5.3. Furthermore, since the load-generation-balance of each FMG is controlled by the DDGs, the generated power of DDGs may change during the isolated operation. Therefore, this type of DGs is not included in the equivalent circuit and it is necessary to install PMUs at the connection points of DDG stations and the grid.

The PMUs send the measured values to the CMU. Therefore, in this step, the equivalent circuit of each FMG is calculated in CMU and hence an overall equivalent circuit is calculated for the on-outage section. This circuit is used in Step 4 to determine the optimum clustering.

It should be noted that, the equivalent circuit of each FMG can be generated based on the measured and recorded phasors before the disconnection of the on-outage section (in the normal operation of the system). In this case, the required data is collected before the isolation of the on-outage zone and hence after the operation of the fault occurrence and disconnection of the faulty zone, the self-healing system can operate fast.

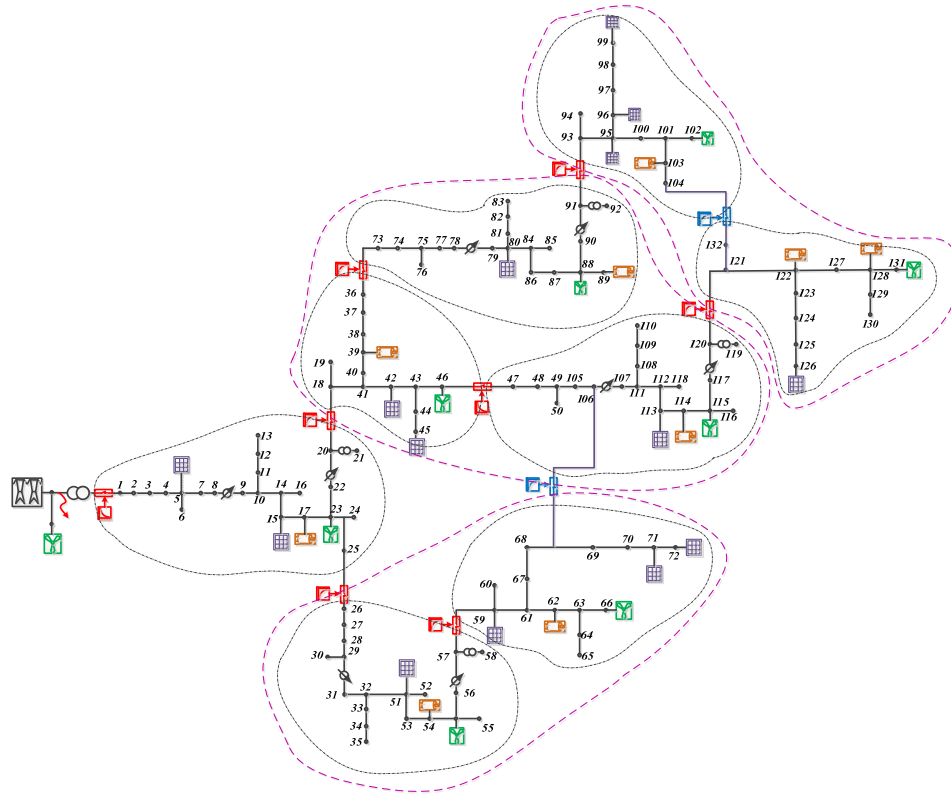


Fig. 6.4. Fundamental Microgrids and a possible arrangement for CMSs.

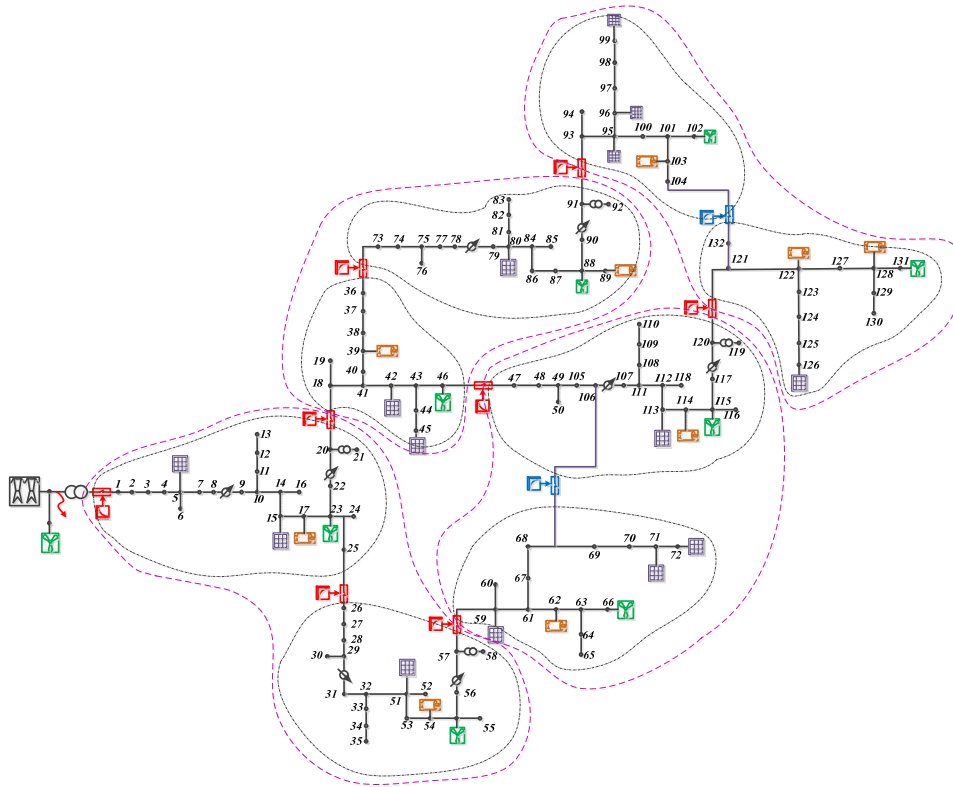


Fig. 6.5. Fundamental Microgrids and another possible arrangement for CMSs.

**Step3. Determining the candidate microgrid sets based on the FMGs**

A FMG is the smallest zone of an on-outage area which can operate successfully considering the conditions presented in (6.2) and (6.3). However, as mentioned in Section 6.4.2, the autonomous operation of FMGs cannot necessarily provide the optimum operation for the on-outage section. Hence, in this step, various scenarios for the interconnection of the FMGs are considered. It means that, in this step, several possible arrangements for the FMGs integration are determined. For each arrangement, the combination of FMGs results in what will be called from now as Candidate Microgrid Set (CMS). For example, two different CMSs for the FMGs of the network of Fig. 6.3 are shown in Fig. 6.4 and Fig. 6.5. Consequently, a list, consisting on CMSs, is created with the ones that satisfy the minimum requirements for conducting a successful autonomous operation.

**Step4. Calculating the optimization objectives**

In this step the objective function presented in Section 6.4.2 is calculated for the CMS. In this stage a feasible solution for the microgrid clustering is selected as the starting point. Here, assumed that the case of autonomous operation of all the FMGs is selected as the starting point. This case has been selected as the starting point because in the previous section it was explained that each FMG can operate autonomously when it is isolated from the main grid. Therefore, the starting point can be presented in form of a “1\*n” array, named as CMS-array, where  $n$  is the number of CBs between the FMGs as shown following:

$$X = [0 \ 1 \ 0 \ \dots \ \dots \ 1 \ 0 \ 1] \quad (6.19)$$

In this array, numbers “0” and “1” demonstrate the “opened” and the “closed” CB, respectively. Indeed, the status of the CBs for each CMS, that has been determined in Step 3, can be shown by a CMS-array. For example, the CMS-array that represents the CMS of Fig. 6.8 is:

$$X = [0 \ 0 \ 1 \ 1 \ 0 \ 0 \ 0 \ 1 \ 1 \ 0] \quad (6.20)$$

Then, for each CMS, according to the equivalent circuit of each FMG, the power losses and the voltage deviation of the on-outage zone is calculated. Furthermore, in this step the possibility of the shed loads re-connection is checked to connect the maximum possible loads that have been disconnected in Step 1. To achieve this goal, the ZCUs of each CMS communicate together and re-dispatch the corresponding DDGs if they have free available capacity.

**Step5. Choosing the optimum MGs**

In the final step, according to the calculations performed in step 4, the optimum CMS is selected. Although all the objective functions, introduced in Section 6.4.2 are important factors in the optimum operation of a grid, the weight of each function may vary from a network to another one. On the other hand, the objective functions of Step 4 are calculated separately; however they can be combined to provide a comprehensive objective function. For this reason, a multi-objective function is used to consider all the above mentioned objective functions together. In this new function, shown in (6.21), each objective function contributes according to its priority and importance [156]:

$$F_m = K_1 * F_1 + K_2 * F_2 + K_3 * F_3 \quad (6.21)$$

where  $K_i$  is the weight of  $F_i$  and determines the importance of this function. It should be noted that normalized values (between 0 and 100) of  $F_1$ ,  $F_2$  and  $F_3$  are calculated and used in (6.19) as explained in [156].

Therefore, in this step, by using (6.21) the value of  $F_m$  is calculated for all the CMS and the optimized clustering is selected. Then, according to the selected CMS, the appropriate command is sent to the FMG's CBs and the on-outage section operates as some independent microgrids.

### 6.6.1. Method Explanation

The flowchart of the proposed ONC method is shown in Fig. 6.6. After the fault occurrence in each line, the method is applied to the on-outage section of the network. In this case, by using a fault locator algorithm, the CMU determines the zones which are located inside the on-outage section and sends a "ZoOnOut" signal to the ZCUs of these zones. Based on the pre-fault saved information, the CMU determines the borders of the FMGs and send the amount of loads which should be disconnected to the ZCUs. Then, the ZCU of each zone re-dispatch the DDGs and applies the required load shedding according to its loads priority. In this stage, the FMGs are determined therefore the CMU receive the required data from the PMUs installed at the boundaries of the FMGs and calculates the equivalent circuit of each FMG. After that, a list of the possible CMSs is generated by CMU and the equivalent circuit of each microgrid of all the CMSs is calculated. Based on the calculated equivalent circuits, the voltage of the microgrid borders is calculated for each CMS. If these voltages do not satisfy the condition presented in (6.7) the CMS cannot be a reliable option for clustering and it will omitted from the candidate list. Otherwise, the objective functions of total losses, total voltage deviation and total disconnected loads are calculated. Then, according to the importance coefficient of each objective function, the main objective function, equation (6.21) is calculated. This process is done for all the possible CMS. Based on the main objective function, the optimized CMS is selected and the status of the CB of each zone is determined. Finally, the CMU sends the appropriate command to the CBs and each microgrid operates in islanded mode.

It is notable that the clustering process should have a dynamic operation to deal with the intermittent behavior of DGS. For example, if it is assumed that the predicted data of the output of the DGs in the next 2 hours is available in 30 minute time step; this assumption implies that: 1) the output of DGs is assumed to be constant during a 30 minute time frame and 2) in each 30 minute the DG output for the next 2 hours is predicted. In this case, after each 30 min it is necessary to investigate the initial conditions of the successful operation of each microgrid and if the microgrid does not satisfy the conditions presented in (6.1) to (6.4), the ONC should be executed again. To reduce the number of the CBs action, if the conditions from (6.1) to (6.4) are satisfied, the other optimization goals should not be considered again. Also, the ONC should be executed again after a huge unpredicted change in the loads

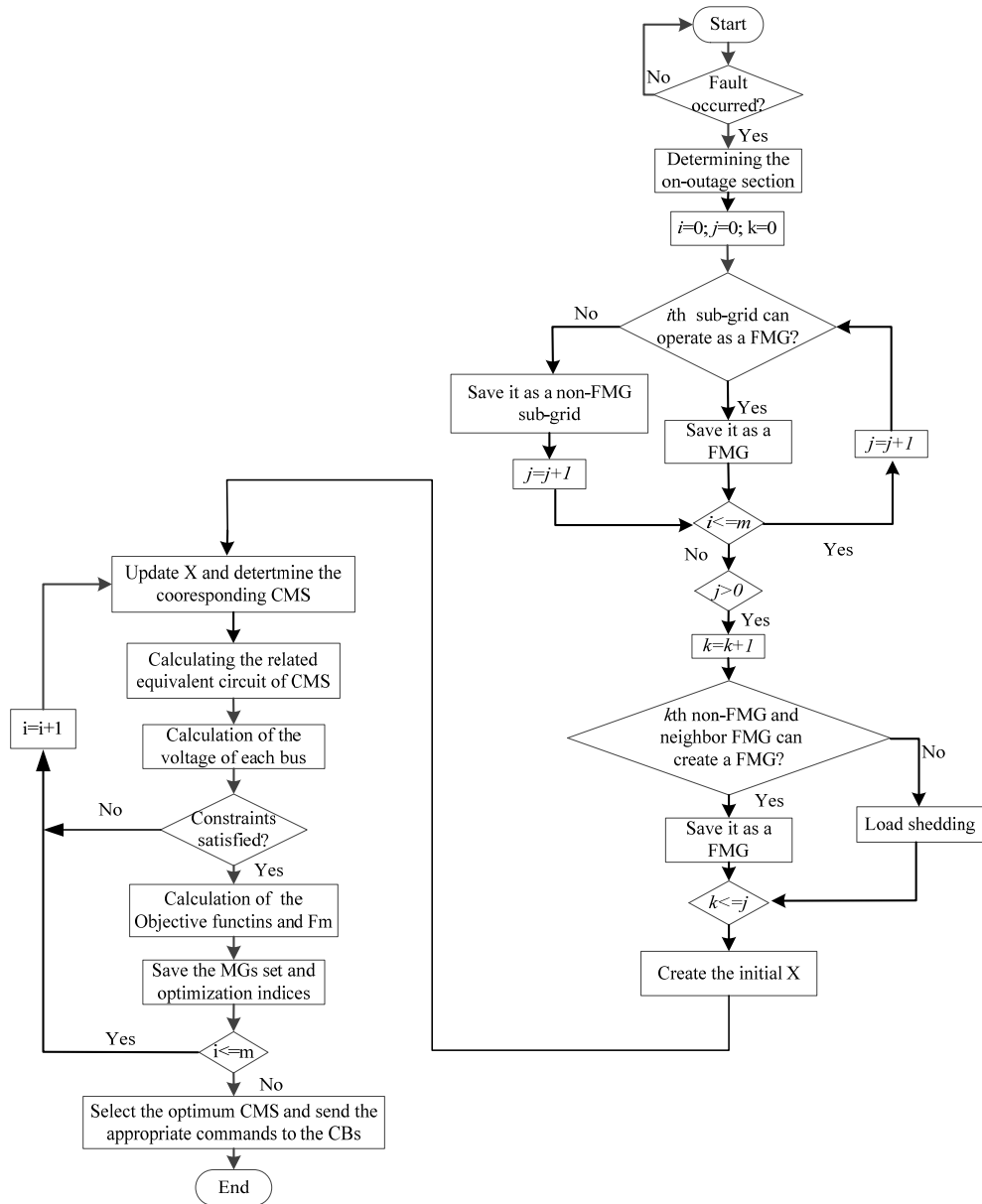


Fig. 6.6. The flowchart of the proposed ONC method.

### 6.7. Converting the study grid to a hybrid AC/DC grid

Although the previous explanation about the proposed ONC method was based on the assumption that the method is applied to an AC active distribution system, the method is also applicable for DC and hybrid AC/DC grid. In order to evaluate the method in a hybrid AC/DC distribution system it is first necessary to add some DC lines to the study network of Fig. 6.1 to convert it into a hybrid grid. Fig. 6.8 shows the modified study grid which is used to evaluate the method for hybrid networks.

The connection point of AC and DC sections includes a bi-directional AC/DC converter. Therefore, these converters have to be considered in the estimated model of the corresponding zone. The key point in the implementation of the ONC in hybrid AC and DC systems is that the bi-directional AC/DC converters can be presented in a  $\pi$ -model as described in [159]. The  $\pi$ -model of the controllable AC/DC converters are merged in the  $Y_{Bus}$  matrix of the corresponding zone; therefore, the PMU-based equivalent model for the zone includes the model of the DC section as well.

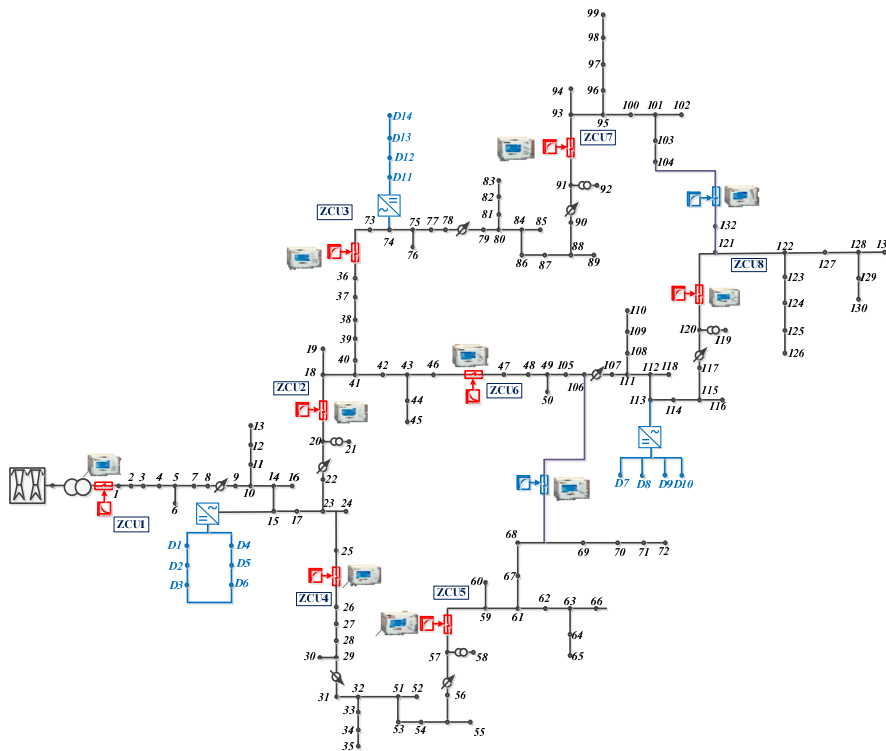


Fig. 6.7. The modified study grid with DC feeders to operate as a hybrid AC/DC system.

## 6.8. HIL validation and Simulation Results

### 6.8.1. Implementation of the proposed ONC

The proposed ONC method has been evaluated by use of the HIL approach on the test-bed of the SmarTS lab, whose structure and features are introduced in the Appendix. Fig. 6.7 shows the structure and general parts of HIL test-bed. In the following case studies, the study distribution network is simulated in Matlab/Simulink and executed in the OPAL-RT real-time simulator. Feeder voltages are monitored with PMUs, to be more specific SEL-421 from Schweitzer Engineering Laboratories (SEL). The PMU data are then sent to a PDC which streams the data over TCP/IP to a workstation computer holding Statnett's Synchrophasor Development Kit (S3DK), which provides a real-time data mediator that parses the PDC data stream and makes it available to the user in the LabVIEW environment.

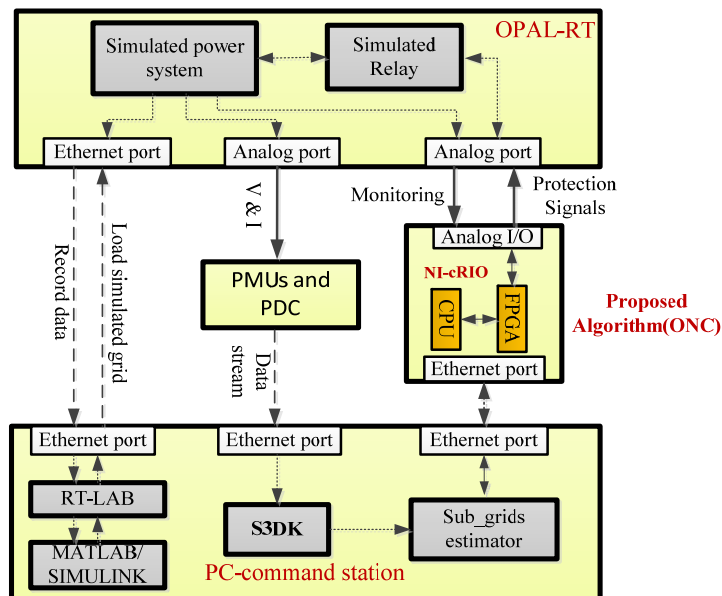


Fig.. 6.8. The structure of the HIL test-bed.

The proposed ONC is implemented on the LabVIEW software and then runs on a Compact Reconfigurable IO systems (cRIO) from National Instruments (NI) Corporation, which is programmed with LabVIEW graphical programming tools. The simulated voltages of the FMGs boundaries are sent to the corresponding PMUs. Then, the outputs of these PMUs

(i.e., phasors of the FMGs boundaries) are collected in the PDC and transferred to the LabVIEW software. The other required data are submitted from OPAL-RT to LabVIEW as well. After that, the proposed algorithm estimates the required equivalent circuits and determines the optimum network clustering. Finally, the statuses of the network's CBs are determined and the close/open command is sent from the NI-cRIO to the simulated CBs inside the real-time simulator. More explanations about the HIL setup are presented in the Appendix of this thesis.

It should be also noted that the proposed ONC should be implemented on a centralized hardware and a fast and reliable communication link is needed to connect the CMU to the PMUs, ZCUs and CBs. Moreover, the method should be equipped with an accurate fault locator to determine the faulty line and the on-outage zone. Furthermore, the control of the DDGs should be able to change the output power according to the remote signals.

**6.8.2. Case Study: when a fault occurs in transmission system**

In this case, it is assumed that after the occurrence of a fault in the transmission system, the distribution system of Fig. 6.1 is isolated from the transmission system. Also, it is assumed that the fault clearance time is one hour and half and during this time the generated power of non-dispatch-able DGs will remain constant (only the DDGs are re-dispatched). Moreover it is assumed that the normally opened CBs (i.e., CB9 and CB10) will remain open; thus, the statuses of these CBs are not reported in the following tests.

Table 6.3 shows the required information from all the zones of the study grid that are reported to the CMU. Based on this information, it is clear that Zone6 cannot operate as an autonomous grid without a load-shedding process or connection to the neighbor zones; therefore, the possibility of connection of Zone6 and Zone8 and also Zone6 and Zone2 are investigated to prevent the load-shedding in this zone.

Table 6.3. Data reported by the ZCUs.

| <b>Data from</b> | <b>Total<br/>connected<br/>power (kW)</b> | <b>Total<br/>installed<br/>DGs (kW)</b> | $\frac{P_{DDG}}{P_L}$ | $\frac{P_{DDG}}{P_{DG}}$ |
|------------------|---|---|-----------------------|--------------------------|
| <b>ZCU1</b>      | 2321                                      | 2630                                    | 0.65                  | 0.57                     |
| <b>ZCU2</b>      | 1336                                      | 1570                                    | 1.12                  | 0.96                     |
| <b>ZCU3</b>      | 1901                                      | 2520                                    | 0.79                  | 0.60                     |
| <b>ZCU4</b>      | 1196                                      | 1530                                    | 1.25                  | 0.98                     |
| <b>ZCU5</b>      | 1631                                      | 2680                                    | 0.92                  | 0.56                     |
| <b>ZCU6</b>      | 1781                                      | 1600                                    | 0.84                  | 0.94                     |
| <b>ZCU7</b>      | 1766                                      | 3240                                    | 0.85                  | 0.46                     |
| <b>ZCU8</b>      | 2056                                      | 3200                                    | 0.73                  | 0.47                     |

As mentioned in Section 6.6, the main multi-objective function ( $F$ ) is formed based on three basic objective functions that the importance of this function is determined by a coefficient ( $K_i$ ). Accordingly, in this section four different cases with different values for  $K_i$  are defined. For each case the optimum clustering using the proposed ONC method will be obtained. These cases are:

- A. Clustering based on the first objective function (minimize the total losses)
- B. Clustering based on the second objective function (minimize the voltage deviations)
- C. Clustering based on the third objective function (minimize the disconnected loads)
- D. Clustering considering all the objective functions (main multi-objective function)

Table 6.4. Various states according to the optimization function.

| Case     | $K_1$ | $K_2$ | $K_3$ | output vector of the ONC                       |
|----------|-------|-------|-------|--|
| <b>A</b> | 1     | 0     | 0     | [0 1 0 0 1 0 1 1]                              |
| <b>B</b> | 0     | 1     | 0     | [0 1 0 1 1 0 1 1]                              |
| <b>C</b> | 0     | 0     | 1     | Various arrangement e.g.,<br>[0 1 1 1 1 1 1 1] |
| <b>D</b> | 1     | 1     | 1     | [0 1 0 0 1 0 1 1]                              |

The output of these cases are reported in Table 6.4 in which the effects of each objective function is defined by a coefficient (i.e.,  $K_i$ ). This table illustrates that for the various objective functions, the optimum clusters are not necessarily the same. Therefore, as an essential stage of the optimized clustering process, it is necessary to determine the appropriate values for the coefficients of (6.19).

For example, Table 6.4, shows that for the main objective function, i.e., when it is assumed that in (6.19) the values of coefficients are:  $K_1 = 1$ ,  $K_2 = 1$ , and  $K_3 = 1$ , the output vector of the proposed ONC determines that CB2, CB5, CB7, and CB8 should remain closed and the other CBs are opened. The status of these CBs are shown in Fig. 6.9 (Open: red; Close: green).

Moreover, the output vector of this case means that the optimum operational condition is achieved by clustering the study grid into 4 microgrids as following:

- MG1: consist of Zone1 and Zone2.
- MG2: consist of Zone4 and Zone5.
- MG3: Zone6 and Zone8.
- MG4: Zone3 and Zone7.

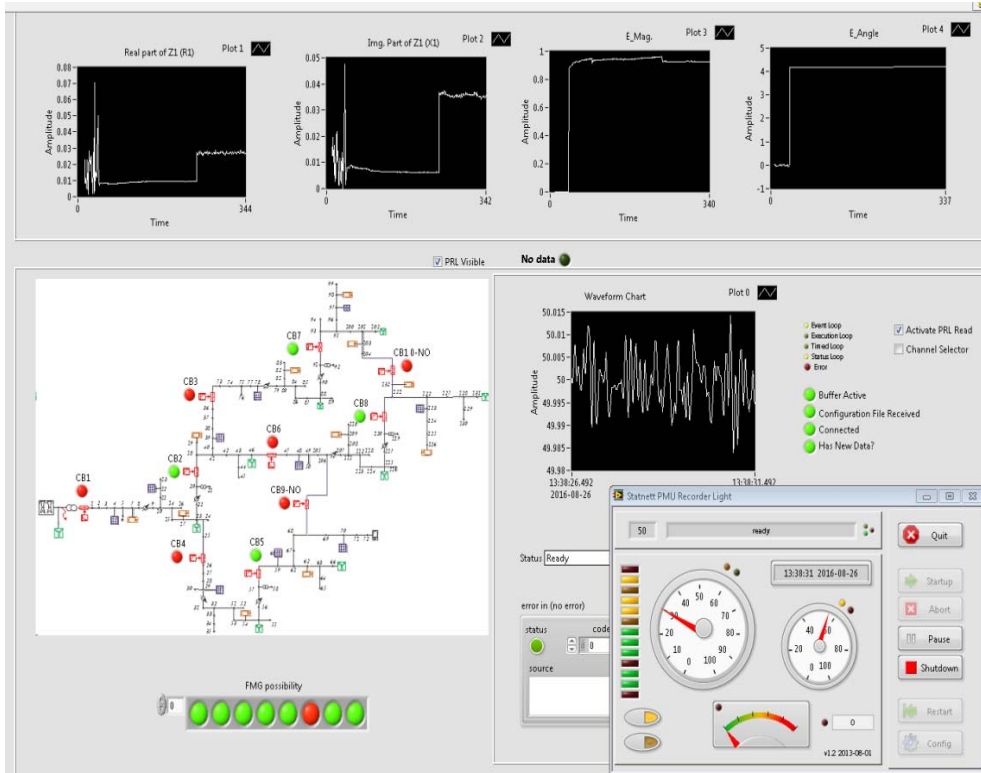


Fig. 6.9. The front-panel of the Lab-View application designed to implement the ONC.

The normalized value for the objective functions for some of the possible CMSs are reported in Table 6.5. This table shows that, the CMS1 and CMS5 can provide the minimum power losses for the study grid; while, the minimum voltage deviation is achieved when CMS6 or CMS2 are selected. Moreover, this table shows that, the CMS10, which is the case that all the zones of the on-outage grid remain connected together, is one of the possible CMSs with the highest values of the power losses. Moreover, since the grid is equipped with enough DGs, all of the reported CMSs can provide the load-generation balance and hence, the load shedding is not necessary.

Finally, as mentioned above, the CMS1 is the best possible option for the network clustering; therefore, as it is shown in Fig. 6.9, the CBs of the study grid receive the related close/open command according to this CMS. The simulation results also show that in compare to the CMS10, the total voltage deviation of CMS1 has been reduced up to 5.6%.

Table 6.5. The objective functions for various CMS cases.

|              | <b>CB statuses</b> | <b>F1</b> | <b>F2</b> | <b>F3</b> | <b>F</b> |
|--------------|--------------------|-----------|-----------|-----------|----------|
| <b>CMS1</b>  | [0 1 0 0 1 0 1 1]  | 0         | 28.32     | 0         | 28.32    |
| <b>CMS2</b>  | [0 0 1 1 1 0 1 1]  | 95.63     | 15.49     | 0         | 111.10   |
| <b>CMS3</b>  | [0 0 0 1 1 1 1 1]  | 58.44     | 25.32     | 0         | 83.76    |
| <b>CMS4</b>  | [0 1 1 0 1 0 1 1]  | 73.96     | 100       | 0         | 173.96   |
| <b>CMS5</b>  | [0 1 0 0 1 1 1 1]  | 0.58      | 52.92     | 0         | 53.50    |
| <b>CMS6</b>  | [0 1 0 1 1 0 1 1]  | 53.84     | 0         | 0         | 53.84    |
| <b>CMS7</b>  | [0 0 1 1 1 1 1 1]  | 100       | 42.24     | 0         | 142.24   |
| <b>CMS8</b>  | [0 1 0 1 1 1 1 1]  | 62.05     | 30.08     | 0         | 92.13    |
| <b>CMS9</b>  | [0 1 1 1 1 0 1 1]  | 95.22     | 20.97     | 0         | 116.19   |
| <b>CMS10</b> | [0 1 1 1 1 1 1 1]  | 99.48     | 48.02     | 0         | 147.50   |



---

## Conclusions and future work

### 7.1. Conclusions

The work presented in this thesis presents protection and fault management methods for active DC and AC distribution systems. In the thesis, after analyzing the differences between protection issues in AC and DC distribution systems, effective protection methods have presented for DC distribution systems and microgrids. These methods are communication-based methods that are equipped with the backup protection to manage the communication failure. Moreover, a fault management and self-healing algorithm has proposed for active distribution systems; the proposed algorithm, presents an optimized network clustering method that enhance the reliability of distribution systems. The performance of the proposed method for DC and AC grids was evaluated using HIL simulation, in which the study networks were simulated in a real time simulator.

The thesis started by the analysis of the fault current characteristics and the performance of conventional protection methods in DC distribution systems. The analyses show that the conventional protection schemes must be modified to provide adequate protection for distribution systems with DGs. The fault detection/location methods in AC systems heavily rely on the processing of local values (current, voltage, phasors, harmonic contents, etc.) that are not necessarily effective for DC systems. Moreover, conventional protection methods, such as directional overcurrent relays and distance protection, must be modified based on the characteristics of DC networks during faults and transient incidents. Therefore, the worldwide application of multi-terminal DC distribution systems requires a fresh look into the traditional protection schemes.

Moreover, due to the special behavior of DC fault currents, which adversely affect the coordination of overcurrent based relays, and also due to the difficulties in the fault location performed by distance-based relays in DC distribution systems, it has been clarified that the use of communication technologies may enhance the performance of DC protection systems and improve the selectivity and reliability of the protection systems. Therefore, a multi-zone differential-based protection strategy has been developed for DC distribution networks. In the framework of this work it has been proven that the proposed method provides a selective protection with a fast and simple algorithm. Therefore, by providing a higher selectivity, the proposed scheme minimizes the interrupted zones and improves the reliability of DC distribution systems. Compared to the conventional differential-based methods, the proposed protection scheme enhances the reliability of the protection by introducing an additional differential backup for the relays located in the neighborhood, and provides a backup protection which will act in case of communication failures. In addition, a significant feature of the proposed method is that its effectiveness is independent of the fault current level, fault impedance, operational mode of the network, as well as the type, size, location, and status of DGs. Furthermore, a relay coordination method, for both the communication-based and backup units, has been presented in this thesis where the operation of the main and backup zones as well as series relays are coordinated considering the critical time of the VSC stations, delay on communication and operating time of DCCBs.

On the other hand, in order to improve the weakness of differential-based protection, an adaptive-communication-assisted fault location method has been presented in this thesis as well. In this method, faults are detected by using the exchanged signals among the relays located at both sides of a DC line. This method does not need to use synchronized measurements. The settings of the overcurrent-based relays used in this method are adapted according to the changes in the network topology and the DGs' generated power; therefore, the intermittent nature of DGs or the possible changes in the network topology do not cause any protection blinding or mal-operation.

Since the use of DCCBs for all the dc lines is not economically feasible for most microgrids and distribution systems, a fault isolation method based on using a minimum number of DCCBs has presented in this thesis. In this method, the fault interruption and faulty section isolation is achieved by a coordinated operation between the DCCBs and the isolator switches. This method is suitable for multi-terminal MVDC systems which are used to connect AC and DC microgrid and RESs. In connection with a fast enough fault detection/location method, the HIL simulation results showed that the proposed fault isolation can restore the network in less than the typical network restoration time in AC distribution systems. Moreover, the effects of the network restoration process on the neighboring AC systems have been studied; the results of this study illustrates that the method does not impact on the performance of AC systems during the fault interruption and network restoration.

Also, a centralized protection and self-healing has been also proposed in this thesis. In this method, a self-healing strategy which can facilitate the network-restoration has been implemented for DC distribution systems and microgrids. The self-healing strategy guarantees that each sub-grid continues its normal operation even if it is isolated from the main source. The simulation results show that using this self-healing system, DC distribution systems can provide a more reliable operation and permits a very fast restoration. Moreover, due to the fast network-restoration, the method reduces the interrupted zone and the interruption time which are reflected in the reduction of outage costs.

In the last chapter of the thesis, in order to enhance the reliability of the active distribution systems, a PMU-based ONC has been also developed. In this method, after the fault occurrence in the upstream grid and the disconnection of a zone in the distribution systems, the on-outage zone is optimally divided into some microgrid that can operate autonomously. The method uses a PMU-based method to estimate the equivalent circuits in various zones of the grid. The HIL simulation results showed that the method is able to minimize the total losses, the total voltage deviations, and the total disconnected loads in the on-outage section of the grid. Indeed, this method illustrates that using the features of modern smart grids, the reliability of active distribution systems can be enhanced with a simple communication-based method. Also, the efficient performance of this method shows that a well-designed measurement-based method can provide a real-time and acceptable estimation for active distribution systems that does not need to know the parameters of the grid (e.g., line impedances), but also can update the estimated model according to the changes in the network topology.

### 7.2. Future works:

Based on the results achieved in this thesis and according to the requirements of the future active AC and DC systems, protection of future distribution systems still needs more attention and effective works. There are several points that each of them can be considered as the future works. One of the most important issues that still needs more works for DC distribution systems is issues related to the grounding of such systems. The grounding method has a significant impact on the fault behavior and, hence, protection performance in DC systems. However, this factor has not been fully investigated in the existing technical literature. It is an important subject that should be addressed in the future studies. Moreover, the effect of fault resistance on AC and DC systems are not exactly the same. Therefore, the proposed methods for high-impedance fault detection in AC systems are not necessarily applicable to DC systems. However, no independent studies have been conducted on the detection and location of high-impedance faults in DC distribution systems.

Also, Due to the characteristics of DC fault currents, ACCBs are not suitable for fault current interruption in DC systems. On the other hand, economical concerns and technical

challenges preclude the widespread use of DCCBs. Therefore, further studies are required to address the issues associated with fault breaking devices in DC distribution systems; the problem particularly manifests itself in medium-voltage level and above.

The proposed protection methods in this work have been presented for DC distribution systems; however, the effective protection methods for future hybrid AC/DC distribution systems should consider the characteristics of both AC and DC systems. In other words, the future protection methods should be able to provide an acceptable performance for both AC and DC systems. Reaching this goal needs to consider the specification of both of these grids simultaneously.

On the other hand, the performance of the proposed ONC can be improved by considering more optimization factors in the network-clustering algorithm. For example, by considering the reliability indices, e.g., system average interruption duration index (SAIDI), it would be possible to provide a more efficient network clustering.

The economic aspects of the proposed methods can be considered with more details. In fact, in order to assess the economic benefits of the proposed ONC method, several aspects should be considered. Therefore, a detailed analysis could be a topic for a future work. Such analysis would require more information from the study grids. For example, to assess the economic features of the proposed ONC, statistical fault data from the grid such as, fault location and type, size of the on-outage area, cost/penalty for each minute of power disconnection should be available.

- 
- [1] A. Karabiber, C. Keles, A. Kaygusuz, and B. B. Alagoz, "An approach for the integration of renewable distributed generation in hybrid DC/AC microgrids," *Renewable Energy*, vol. 52, pp. 251-259, 4// 2013.
  - [2] W. S. Tan, M. Y. Hassan, M. S. Majid, and H. Abdul Rahman, "Optimal distributed renewable generation planning: A review of different approaches," *Renewable and Sustainable Energy Reviews*, vol. 18, pp. 626-645, 2// 2013.
  - [3] S. D. A. Fletcher, P. J. Norman, S. J. Galloway, P. Crolla, and G. M. Burt, "Optimizing the Roles of Unit and Non-unit Protection Methods Within DC Microgrids," *IEEE Transactions on Smart Grid*, vol. 3, pp. 2079-2087, Dec 2012.
  - [4] J. Yang, J. E. Fletcher, and J. O'Reilly, "Multiterminal DC wind farm collection grid internal fault analysis and protection design," *Power Delivery, IEEE Transactions on*, vol. 25, pp. 2308-2318, 2010.
  - [5] F. Dastgeer, "Direct current distribution systems for residential areas powered by distributed generation," PhD thesis, Victoria University, 2011.
  - [6] S. F. Bush, S. Goel, and G. Simard, "IEEE Vision for Smart Grid Communications: 2030 and Beyond " *IEEE Standards Associations* 2013.
  - [7] Z. Wang and J. Wang, "Self-Healing Resilient Distribution Systems Based on Sectionalization Into Microgrids," *Power Systems, IEEE Transactions on*, vol. PP, pp. 1-11, 2015.
  - [8] B. Zeng, J. Wen, J. Shi, J. Zhang, and Y. Zhang, "A multi-level approach to active distribution system planning for efficient renewable energy harvesting in a deregulated environment," *Energy*, vol. 96, pp. 614-624, 2016.
  - [9] K. De Kerf, K. Srivastava, M. Reza, D. Bekaert, S. Cole, D. Van Hertem, *et al.*, "Wavelet-based protection strategy for DC faults in multi-terminal VSC HVDC systems," *Generation, Transmission & Distribution, IET*, vol. 5, pp. 496-503, 2011.

- [10] X. Li, Q. Song, W. Liu, H. Rao, S. Xu, and L. Li, "Protection of nonpermanent faults on DC overhead lines in MMC-based HVDC systems," *Power Delivery, IEEE Transactions on*, vol. 28, pp. 483-490, 2013.
- [11] "IEEE Guide for Design, Operation, and Integration of Distributed Resource Island Systems with Electric Power Systems," *IEEE Std 1547.4-2011*, pp. 1-54, 2011.
- [12] S. A. Arefifar, Y. A. R. I. Mohamed, and T. H. M. El-Fouly, "Optimum Microgrid Design for Enhancing Reliability and Supply-Security," *Smart Grid, IEEE Transactions on*, vol. 4, pp. 1567-1575, 2013.
- [13] S. A. Arefifar, Y. A. R. I. Mohamed, and T. El-Fouly, "Optimized Multiple Microgrid-Based Clustering of Active Distribution Systems Considering Communication and Control Requirements," *Industrial Electronics, IEEE Transactions on*, vol. 62, pp. 711-723, 2015.
- [14] S. A. Arefifar, Y. A. R. I. Mohamed, and T. H. M. El-Fouly, "Comprehensive Operational Planning Framework for Self-Healing Control Actions in Smart Distribution Grids," *Power Systems, IEEE Transactions on*, vol. 28, pp. 4192-4200, 2013.
- [15] C. L. T. Borges, "An overview of reliability models and methods for distribution systems with renewable energy distributed generation," *Renewable and Sustainable Energy Reviews*, vol. 16, pp. 4008-4015, 8// 2012.
- [16] J. J. Justo, F. Mwasilu, J. Lee, and J.-W. Jung, "AC-microgrids versus DC-microgrids with distributed energy resources: A review," *Renewable and Sustainable Energy Reviews*, vol. 24, pp. 387-405, 2013.
- [17] G. M. Joselin Herbert, S. Iniyar, and D. Amutha, "A review of technical issues on the development of wind farms," *Renewable and Sustainable Energy Reviews*, vol. 32, pp. 619-641, 4// 2014.
- [18] M. Abdullah, A. Agalgaonkar, and K. Muttaqi, "Assessment of energy supply and continuity of service in distribution network with renewable distributed generation," *Applied Energy*, vol. 113, pp. 1015-1026, 2014.
- [19] A. K. Marvasti, F. Yong, S. DorMohammadi, and M. Rais-Rohani, "Optimal Operation of Active Distribution Grids: A System of Systems Framework," *Smart Grid, IEEE Transactions on*, vol. 5, pp. 1228-1237, 2014.
- [20] S. Conti, "Analysis of distribution network protection issues in presence of dispersed generation," *Electric Power Systems Research*, vol. 79, pp. 49-56, 2009.
- [21] A. M. El-Zonkoly, "Fault diagnosis in distribution networks with distributed generation," *Electric Power Systems Research*, vol. 81, pp. 1482-1490, 2011.
- [22] V. R. Pandi, H. Zeineldin, and W. Xiao, "Determining optimal location and size of distributed generation resources considering harmonic and protection coordination limits," *Power Systems, IEEE Transactions on*, vol. 28, pp. 1245-1254, 2013.
- [23] T. S. Ustun, C. Ozansoy, and A. Zayegh, "Modeling of a centralized microgrid protection system and distributed energy resources according to IEC 61850-7-420," *Power Systems, IEEE Transactions on*, vol. 27, pp. 1560-1567, 2012.
- [24] E. J. Coster, J. M. Myrzik, B. Kruimer, and W. L. Kling, "Integration issues of distributed generation in distribution grids," *Proceedings of the IEEE*, vol. 99, pp. 28-39, 2011.

- 
- [25] P. Basak, S. Chowdhury, S. Halder nee Dey, and S. Chowdhury, "A literature review on integration of distributed energy resources in the perspective of control, protection and stability of microgrid," *Renewable and Sustainable Energy Reviews*, vol. 16, pp. 5545-5556, 2012.
- [26] S. Ruiz-Romero, A. Colmenar-Santos, F. Mur-Pérez, and Á. López-Rey, "Integration of distributed generation in the power distribution network: The need for smart grid control systems, communication and equipment for a smart city — Use cases," *Renewable and Sustainable Energy Reviews*, vol. 38, pp. 223-234, 10// 2014.
- [27] M. A. Zamani, T. S. Sidhu, and A. Yazdani, "A Protection Strategy and Microprocessor-Based Relay for Low-Voltage Microgrids," *Power Delivery, IEEE Transactions on*, vol. 26, pp. 1873-1883, 2011.
- [28] Y. Firouz, J. Lobry, F. Vallée, and O. Durieux, "Numerical Comparison of the Effects of Different Types of Distributed Generation Units on Overcurrent Protection Systems in MV Distribution Grids," *Renewable Energy: An International Journal*, 2014.
- [29] R. Noroozian, M. Abedi, G. Gharehpetian, and S. Hosseini, "Distributed resources and DC distribution system combination for high power quality," *International Journal of Electrical Power & Energy Systems*, vol. 32, pp. 769-781, 2010.
- [30] A. T. Elsayed, A. A. Mohamed, and O. A. Mohammed, "DC microgrids and distribution systems: An overview," *Electric Power Systems Research*, vol. 119, pp. 407-417, 2015.
- [31] V. Arcidiacono, A. Monti, and G. Sulligoi, "Generation control system for improving design and stability of medium-voltage DC power systems on ships," *IET Electrical Systems in Transportation*, vol. 2, p. 158, 2012.
- [32] D. Nilsson and A. Sannino, "Efficiency analysis of low-and medium-voltage dc distribution systems," in *Power Engineering Society General Meeting, 2004. IEEE*, 2004, pp. 2315-2321.
- [33] M. E. Baran and N. R. Mahajan, "DC distribution for industrial systems: opportunities and challenges," *Industry Applications, IEEE Transactions on*, vol. 39, pp. 1596-1601, 2003.
- [34] D. Salomonsson, L. Soder, and A. Sannino, "Protection of low-voltage DC microgrids," *Power Delivery, IEEE Transactions on*, vol. 24, pp. 1045-1053, 2009.
- [35] D. M. Larruskain, I. Zamora, O. Abarrategui, and A. Iturregi, "VSC-HVDC configurations for converting AC distribution lines into DC lines," *International Journal of Electrical Power & Energy Systems*, vol. 54, pp. 589-597, 1// 2014.
- [36] R. W. De Doncker, C. Meyer, R. U. Lenke, and F. Mura, "Power electronics for future utility applications," in *Power Electronics and Drive Systems, 7th International Conference on*, 2007, pp. K-1-K-8.
- [37] F. Mura and R. W. De Doncker, "Design aspects of a medium-voltage direct current (MVDC) grid for a university campus," in *Power Electronics and ECCE Asia (ICPE & ECCE), 2011 IEEE 8th International Conference on*, 2011, pp. 2359-2366.
-

- [38] E. Planas, J. Andreu, J. I. Gárate, I. M. de Alegría, and E. Ibarra, "AC and DC technology in microgrids: A review," *Renewable and Sustainable Energy Reviews*, vol. 43, pp. 726-749, 2015.
- [39] R. Majumder, "Aggregation of microgrids with DC system," *Electric Power Systems Research*, vol. 108, pp. 134-143, 2014.
- [40] A. Rufer and S. Kenzelmann, "Modular DC/DC Converter for DC Distribution and Collection Networks," PhD, ÉCOLE POLYTECHNIQUE FÉDÉRALE DE LAUSANNE, 2012.
- [41] W. Chen, A. Q. Huang, C. Li, G. Wang, and W. Gu, "Analysis and comparison of medium voltage high power DC/DC converters for offshore wind energy systems," *Power Electronics, IEEE Transactions on*, vol. 28, pp. 2014-2023, 2013.
- [42] D. M. Larruskain, I. Zamora, O. Abarrategui, and Z. Aginako, "Conversion of AC distribution lines into DC lines to upgrade transmission capacity," *Electric Power Systems Research*, vol. 81, pp. 1341-1348, 2011.
- [43] H. Li, W. Li, M. Luo, A. Monti, and F. Ponci, "Design of smart MVDC power grid protection," *Instrumentation and Measurement, IEEE Transactions on*, vol. 60, pp. 3035-3046, 2011.
- [44] P. M. Anderson, *Power system protection* vol. 1307: McGraw-Hill New York, 1999.
- [45] J. J. Grainger and W. D. Stevenson, *Power system analysis* vol. 621: McGraw-Hill New York, 1994.
- [46] P. Kundur, N. J. Balu, and M. G. Lauby, *Power system stability and control* vol. 7: McGraw-hill New York, 1994.
- [47] A. Darwish, A. Abdel-Khalik, A. Elserougi, S. Ahmed, and A. Massoud, "Fault current contribution scenarios for grid-connected voltage source inverter-based distributed generation with an LCL filter," *Electric Power Systems Research*, vol. 104, pp. 93-103, 2013.
- [48] J.-D. Park and J. Candelaria, "Fault Detection and Isolation in Low-Voltage DC-Bus Microgrid System," *IEEE Transactions on Power Delivery*, vol. 28, pp. 779-787, Apr 2013.
- [49] T. N. Jimmy Ehnberg, "Protection system design for MVDC collection grids for off-shore wind farms," [elforsk.se/Rapporter/?download=report&rid=12\\_02\\_2011](http://elforsk.se/Rapporter/?download=report&rid=12_02_2011).
- [50] S. Falcones, X. Mao, and R. Ayyanar, "Topology comparison for solid state transformer implementation," in *Power and Energy Society General Meeting, 2010 IEEE*, 2010, pp. 1-8.
- [51] F. Deng and Z. Chen, "Design of protective inductors for HVDC transmission line within DC grid offshore wind farms," *Power Delivery, IEEE Transactions on*, vol. 28, pp. 75-83, 2013.
- [52] S. Fletcher, P. Norman, S. Galloway, and G. Burt, "Determination of protection system requirements for DC unmanned aerial vehicle electrical power networks for enhanced capability and survivability," *IET Electrical Systems in Transportation*, vol. 1, pp. 137-147, 2011.
- [53] J. Yang, J. E. Fletcher, and J. O'Reilly, "Short-circuit and ground fault analyses and location in VSC-based DC network cables," *Industrial Electronics, IEEE Transactions on*, vol. 59, pp. 3827-3837, 2012.

- 
- [54] J. Candelaria and J.-D. Park, "VSC-HVDC system protection: A review of current methods," in *Power Systems Conference and Exposition (PSCE), 2011 IEEE/PES, 2011*, pp. 1-7.
- [55] L. Tang and B.-T. Ooi, "Protection of VSC-multi-terminal HVDC against DC faults," in *Power Electronics Specialists Conference, 2002. pesc 02. 2002 IEEE 33rd Annual, 2002*, pp. 719-724.
- [56] J. D. Park, J. Candelaria, L. Y. Ma, and K. Dunn, "DC Ring-Bus Microgrid Fault Protection and Identification of Fault Location," *IEEE Transactions on Power Delivery*, vol. 28, pp. 2574-2584, Oct 2013.
- [57] C. Jin, R. A. Dougal, and S. Liu, "Solid-state Over-current Protection for Industrial DC Distribution Systems," *4th International Energy Conversion Engineering Conference and Exhibit (IECEC)*, pp. 26-29, 2006.
- [58] C. Peng and A. Q. Huang, "A protection scheme against DC faults VSC based DC systems with bus capacitors," in *Applied Power Electronics Conference and Exposition (APEC), 2014 Twenty-Ninth Annual IEEE, 2014*, pp. 3423-3428.
- [59] Q. Ai, X. Wang, and X. He, "The impact of large-scale distributed generation on power grid and microgrids," *Renewable Energy*, vol. 62, pp. 417-423, 2014.
- [60] R. M. Kamel, "Effect of wind generation system types on Micro-Grid (MG) fault performance during both standalone and grid connected modes," *Energy Conversion and Management*, vol. 79, pp. 232-245, 2014.
- [61] S. A. M. Javadian, M. R. Haghifam, M. Fotuhi Firoozabad, and S. M. T. Bathaee, "Analysis of protection system's risk in distribution networks with DG," *International Journal of Electrical Power & Energy Systems*, vol. 44, pp. 688-695, 1// 2013.
- [62] A. Girgis and S. Brahma, "Effect of distributed generation on protective device coordination in distribution system," in *Power Engineering, 2001. LESCOPE'01. 2001 Large Engineering Systems Conference on, 2001*, pp. 115-119.
- [63] M. Geidl, *Protection of power systems with distributed generation: state of the art*. ETH, Eidgenössische Technische Hochschule Zürich, EEH Power Systems Laboratory, 2005.
- [64] W. El-Khattam and T. S. Sidhu, "Restoration of directional overcurrent relay coordination in distributed generation systems utilizing fault current limiter," *Power Delivery, IEEE Transactions on*, vol. 23, pp. 576-585, 2008.
- [65] W. L. Li, A. Monti, and F. Ponci, "Fault Detection and Classification in Medium Voltage DC Shipboard Power Systems With Wavelets and Artificial Neural Networks," *IEEE Transactions on Instrumentation and Measurement*, vol. 63, pp. 2651-2665, Nov 2014.
- [66] R. Cuzner, D. MacFarlin, D. Clinger, M. Rumney, and G. Castles, "Circuit breaker protection considerations in power converter-fed DC Systems," in *Electric Ship Technologies Symposium, 2009. ESTS 2009. IEEE, 2009*, pp. 360-367.
- [67] S. A. Gopalan, V. Sreeram, and H. H. Iu, "A review of coordination strategies and protection schemes for microgrids," *Renewable and Sustainable Energy Reviews*, vol. 32, pp. 222-228, 2014.
- [68] "Gas insulated MV circuit-breakers," in *Medium voltage products*, ABB, Ed., ed: [www.abb.com](http://www.abb.com), 2013.
-

## References

---

- [69] M. E. Baran and N. R. Mahajan, "Overcurrent protection on voltage-source-converter-based multiterminal DC distribution systems," *Power Delivery, IEEE Transactions on*, vol. 22, pp. 406-412, 2007.
- [70] A. B. M. Callavik, J. Häfner, B. Jacobson. The Hybrid HVDC Breaker: An innovation breakthrough enabling reliable HVDC grids [Online].
- [71] N. Flourentzou, V. G. Agelidis, and G. D. Demetriades, "VSC-Based HVDC Power Transmission Systems: An Overview," *Power Electronics, IEEE Transactions on*, vol. 24, pp. 592-602, 2009.
- [72] H. Yazdanpanahi, Y. W. Li, and W. Xu, "A new control strategy to mitigate the impact of inverter-based DGs on protection system," *Smart Grid, IEEE Transactions on*, vol. 3, pp. 1427-1436, 2012.
- [73] J. Ma, J. Li, and Z. Wang, "An adaptive distance protection scheme for distribution system with distributed generation," in *Critical Infrastructure (CRIS), 2010 5th International Conference on*, 2010, pp. 1-4.
- [74] E. Sortomme, S. Venkata, and J. Mitra, "Microgrid protection using communication-assisted digital relays," *Power Delivery, IEEE Transactions on*, vol. 25, pp. 2789-2796, 2010.
- [75] J. Tang and P. McLaren, "A wide area differential backup protection scheme for shipboard application," *Power Delivery, IEEE Transactions on*, vol. 21, pp. 1183-1190, 2006.
- [76] S. Dambhare, S. Soman, and M. Chandorkar, "Adaptive current differential protection schemes for transmission-line protection," *Power Delivery, IEEE Transactions on*, vol. 24, pp. 1832-1841, 2009.
- [77] A. Zamani, T. Sidhu, and A. Yazdani, "A strategy for protection coordination in radial distribution networks with distributed generators," in *Power and Energy Society General Meeting, 2010 IEEE*, 2010, pp. 1-8.
- [78] D. Jones and J. Kumm, "Future distribution feeder protection using directional overcurrent elements," in *Rural Electric Power Conference (REPC), 2013 IEEE*, 2013, pp. B4-1-B4-7.
- [79] H. Jiadong, Z. Zeyun, and D. Xiaobo, "The Influence of the Distributed Generation to the Distribution Network Line Protection and Countermeasures," *Physics Procedia*, vol. 24, pp. 205-210, 2012.
- [80] Y. Zhang and R. A. Dougal, "Novel dual-FCL connection for adding distributed generation to a power distribution utility," *Applied Superconductivity, IEEE Transactions on*, vol. 21, pp. 2179-2183, 2011.
- [81] B. Hussain, S. Sharkh, S. Hussain, and M. Abusara, "An Adaptive Relaying Scheme for Fuse Saving in Distribution Networks With Distributed Generation," 2013.
- [82] T. Ghanbari and E. Farjah, "Development of an Efficient Solid-State Fault Current Limiter for Microgrid," *Power Delivery, IEEE Transactions on*, vol. 27, pp. 1829-1834, 2012.
- [83] N. Nimpitiwan, G. T. Heydt, R. Ayyanar, and S. Suryanarayanan, "Fault current contribution from synchronous machine and inverter based distributed generators," *Power Delivery, IEEE Transactions on*, vol. 22, pp. 634-641, 2007.
- [84] T. S. Basso and R. DeBlasio, "IEEE 1547 series of standards: interconnection issues," *Power Electronics, IEEE Transactions on*, vol. 19, pp. 1159-1162, 2004.

- 
- [85] S. M. Brahma and A. A. Girgis, "Development of adaptive protection scheme for distribution systems with high penetration of distributed generation," *Power Delivery, IEEE Transactions on*, vol. 19, pp. 56-63, 2004.
- [86] S. Javadian, M.-R. Haghifam, and N. Rezaei, "A fault location and protection scheme for distribution systems in presence of dg using MLP neural networks," in *Power & Energy Society General Meeting, 2009. PES'09. IEEE*, 2009, pp. 1-8.
- [87] M. Dewadasa, A. Ghosh, G. Ledwich, and M. Wishart, "Fault isolation in distributed generation connected distribution networks," *IET generation, transmission & distribution*, vol. 5, pp. 1053-1061, 2011.
- [88] S. Conti and S. Nicotra, "Procedures for fault location and isolation to solve protection selectivity problems in MV distribution networks with dispersed generation," *Electric Power Systems Research*, vol. 79, pp. 57-64, 2009.
- [89] J. Ma, X. Wang, Y. Zhang, Q. Yang, and A. Phadke, "A novel adaptive current protection scheme for distribution systems with distributed generation," *International Journal of Electrical Power & Energy Systems*, vol. 43, pp. 1460-1466, 2012.
- [90] T. Amraee, "Coordination of directional overcurrent relays using seeker algorithm," *Power Delivery, IEEE Transactions on*, vol. 27, pp. 1415-1422, 2012.
- [91] W. K. Najy, H. H. Zeineldin, and W. L. Woon, "Optimal protection coordination for microgrids with grid-connected and islanded capability," *Industrial Electronics, IEEE Transactions on*, vol. 60, pp. 1668-1677, 2013.
- [92] H. Zayandehroodi, A. Mohamed, H. Shareef, and M. Farhoodnea, "A novel neural network and backtracking based protection coordination scheme for distribution system with distributed generation," *International Journal of Electrical Power & Energy Systems*, vol. 43, pp. 868-879, 2012.
- [93] N. Rezaei and M.-R. Haghifam, "Protection scheme for a distribution system with distributed generation using neural networks," *International Journal of Electrical Power & Energy Systems*, vol. 30, pp. 235-241, 2008.
- [94] S. A. M. Javadian, M. R. Haghifam, S. M. T. Bathaee, and M. Fotuhi Firoozabad, "Adaptive centralized protection scheme for distribution systems with DG using risk analysis for protective devices placement," *International Journal of Electrical Power & Energy Systems*, vol. 44, pp. 337-345, 1// 2013.
- [95] S. Mirsaedi, D. Mat Said, M. Wazir Mustafa, M. Hafiz Habibuddin, and K. Ghaffari, "An analytical literature review of the available techniques for the protection of micro-grids," *International Journal of Electrical Power & Energy Systems*, vol. 58, pp. 300-306, 2014.
- [96] H. Wan, K. Li, and K. Wong, "An adaptive multiagent approach to protection relay coordination with distributed generators in industrial power distribution system," *Industry Applications, IEEE Transactions on*, vol. 46, pp. 2118-2124, 2010.
- [97] M. A. Zamani, A. Yazdani, and T. S. Sidhu, "A communication-assisted protection strategy for inverter-based medium-voltage microgrids," *Smart Grid, IEEE Transactions on*, vol. 3, pp. 2088-2099, 2012.
- [98] N. Perera, A. Rajapakse, and T. Buchholzer, "Isolation of faults in distribution networks with distributed generators," *Power Delivery, IEEE Transactions on*, vol. 23, pp. 2347-2355, 2008.
-

- [99] H. J. Laaksonen, "Protection principles for future microgrids," *Power Electronics, IEEE Transactions on*, vol. 25, pp. 2910-2918, 2010.
- [100] R. Mackiewicz, "Overview of IEC 61850 and Benefits," in *Power Systems Conference and Exposition, 2006. PSCE'06. 2006 IEEE PES*, 2006, pp. 623-630.
- [101] P. CODE, "Communication networks and systems in substations—Part 5: Communication requirements for functions and device models," 2003.
- [102] L. Vanfretti, M. Chenine, M. S. Almas, R. Leelaruji, L. Angquist, and L. Nordstrom, "SmarTS Lab—A laboratory for developing applications for WAMPAC Systems," in *Power and Energy Society General Meeting, 2012 IEEE*, 2012, pp. 1-8.
- [103] D. Ishchenko, A. Oudalov, and J. Stoupis, "Protection coordination in active distribution grids with IEC 61850," in *Transmission and Distribution Conference and Exposition (T&D), 2012 IEEE PES*, 2012, pp. 1-6.
- [104] H. K. Zadeh and M. Manjrekar, "A novel IEC 61850-based distribution line/cable protection scheme design," in *Innovative Smart Grid Technologies (ISGT), 2012 IEEE PES*, 2012, pp. 1-6.
- [105] M. Baran and N. R. Mahajan, "PEBB based DC system protection: opportunities and challenges," in *Transmission and Distribution Conference and Exhibition, 2005/2006 IEEE PES*, 2006, pp. 705-707.
- [106] J. Peralta, H. Saad, S. Denetiere, J. Mahseredjian, and S. Nguefeu, "Detailed and averaged models for a 401-level MMC–HVDC system," *Power Delivery, IEEE Transactions on*, vol. 27, pp. 1501-1508, 2012.
- [107] K. Friedrich, "Modern HVDC PLUS application of VSC in Modular Multilevel Converter topology," in *Industrial Electronics (ISIE), 2010 IEEE International Symposium on*, 2010, pp. 3807-3810.
- [108] P. Cairoli, I. Kondratiev, and R. A. Dougal, "Coordinated control of the bus tie switches and power supply converters for fault protection in dc microgrids," *Power Electronics, IEEE Transactions on*, vol. 28, pp. 2037-2047, 2013.
- [109] L. Tang and B.-T. Ooi, "Locating and isolating DC faults in multi-terminal DC systems," *Power Delivery, IEEE Transactions on*, vol. 22, pp. 1877-1884, 2007.
- [110] J. Shi, Y. Tang, C. Wang, Y. Zhou, J. Li, L. Ren, *et al.*, "Active superconducting DC fault current limiter based on flux compensation," *Physica C: Superconductivity*, vol. 442, pp. 108-112, 2006.
- [111] U. Ghisla, I. Kondratiev, and R. Dougal, "Protection of medium voltage DC power systems against ground faults and negative incremental impedances," in *IEEE SoutheastCon 2010 (SoutheastCon), Proceedings of the*, 2010, pp. 259-263.
- [112] C. K.-C. Mehdi Monadi, Alvaro Luna, Jose Ignacio Candela, Pedro Rodriguez, "A Protection Strategy for Fault Detection and Location for Multi-Terminal MVDC Distribution Systems with Renewable Energy Systems," presented at the ICRERA2014, Milwaukee, USA, 2014.
- [113] M. Farhadi and O. A. Mohammed, "Event-Based Protection Scheme for a Multiterminal Hybrid DC Power System," *Ieee Transactions on Smart Grid*, vol. 6, pp. 1658-1669, Jul 2015.
- [114] C. Yuan, M. Haj-ahmed, and M. Illindala, "Protection Strategies for Medium Voltage Direct Current Microgrid at a Remote Area Mine Site."

- 
- [115] S. Fletcher, P. Norman, S. Galloway, and G. Burt, "Fault detection and location in DC systems from initial di/dt measurement," *Euro Tech Con Conference*, 2012.
- [116] E. Cinieri, A. Fumi, V. Salvatori, and C. Spalvieri, "A New High-Speed Digital Relay Protection of the 3-kVdc Electric Railway Lines," *Power Delivery, IEEE Transactions on*, vol. 22, pp. 2262-2270, 2007.
- [117] A. A. S. Emhemed and G. M. Burt, "An Advanced Protection Scheme for Enabling an LVDC Last Mile Distribution Network," *Ieee Transactions on Smart Grid*, vol. 5, pp. 2602-2609, Sep 2014.
- [118] E. Christopher, M. Sumner, D. W. P. Thomas, W. Xiaohui, and F. de Wildt, "Fault Location in a Zonal DC Marine Power System Using Active Impedance Estimation," *Industry Applications, IEEE Transactions on*, vol. 49, pp. 860-865, 2013.
- [119] J. Descoux, B. Raison, and J.-B. Curis, "Protection strategy for undersea mtde grids," in *PowerTech (POWERTECH), 2013 IEEE Grenoble*, 2013, pp. 1-6.
- [120] M. Hajian, L. Zhang, and D. Jovcic, "DC Transmission Grid With Low-Speed Protection Using Mechanical DC Circuit Breakers," *IEEE Transactions on Power Delivery*, vol. 30, pp. 1383-1391, 2015.
- [121] S. D. A. Fletcher, P. J. Norman, K. Fong, S. J. Galloway, and G. M. Burt, "High-Speed Differential Protection for Smart DC Distribution Systems," *Smart Grid, IEEE Transactions on*, vol. 5, pp. 2610-2617, Sep 2014.
- [122] W. Li, M. Luo, A. Monti, and F. Ponci, "Wavelet based method for fault detection in medium voltage DC shipboard power systems," in *Instrumentation and Measurement Technology Conference (I2MTC), 2012 IEEE International*, 2012, pp. 2155-2160.
- [123] J. Cheng, M. Guan, L. Tang, and H. Huang, "A fault location criterion for MTDC transmission lines using transient current characteristics," *International Journal of Electrical Power & Energy Systems*, vol. 61, pp. 647-655, 2014.
- [124] M. Joorabian, S. M. A. Taleghani Asl, and R. K. Aggarwal, "Accurate fault locator for EHV transmission lines based on radial basis function neural networks," *Electric Power Systems Research*, vol. 71, pp. 195-202, 11// 2004.
- [125] N. K. Chanda and Y. Fu, "ANN-based fault classification and location in MVDC shipboard power systems," in *North American Power Symposium (NAPS), 2011*, 2011, pp. 1-7.
- [126] C. Chang, S. Kumar, B. Liu, and A. Khambadkone, "Real-time detection using wavelet transform and neural network of short-circuit faults within a train in DC transit systems," *Electric Power Applications, IEE Proceedings-*, vol. 148, pp. 251-256, 2001.
- [127] S. Azizi, S. Afsharnia, and M. Sanaye-Pasand, "Fault location on multi-terminal DC systems using synchronized current measurements," *International Journal of Electrical Power & Energy Systems*, vol. 63, pp. 779-786, 2014.
- [128] L. Xiaqing, G. Shuyou, Z. Yiming, L. Yunhua, and F. Shengtao, "Research on Fault Diagnosis and Protect Model for DC Traction Power Supply System Based on Traveling Wave Theory," in *Robotics, Automation and Mechatronics, 2006 IEEE Conference on*, 2006, pp. 1-5.
-

- [129] L. Xiaolei, A. H. Osman, and O. P. Malik, "Hybrid Traveling Wave/Boundary Protection for Monopolar HVDC Line," *Power Delivery, IEEE Transactions on*, vol. 24, pp. 569-578, 2009.
- [130] M. Monadi, M. Amin Zamani, J. Ignacio Candela, A. Luna, and P. Rodriguez, "Protection of AC and DC distribution systems Embedding distributed energy resources: A comparative review and analysis," *Renewable and Sustainable Energy Reviews*, vol. 51, pp. 1578-1593, 2015.
- [131] A. E. B. Abu-Elanien, A. A. Elserougi, A. S. Abdel-Khalik, A. M. Massoud, and S. Ahmed, "A differential protection technique for multi-terminal HVDC," *Electric Power Systems Research*, vol. 130, pp. 78-88, 2016.
- [132] W. Leterme, J. Beerten, and D. Van Hertem, "Non-unit protection of HVDC grids with inductive dc cable termination," *IEEE Transactions on Power Delivery*, vol. PP, pp. 1-1, 2015.
- [133] M. K. Bucher and C. M. Franck, "Fault Current Interruption in Multiterminal HVDC Networks," *Power Delivery, IEEE Transactions on*, vol. 31, pp. 87-95, 2016.
- [134] C. M. Franck, "HVDC Circuit Breakers: A Review Identifying Future Research Needs," *Power Delivery, IEEE Transactions on*, vol. 26, pp. 998-1007, 2011.
- [135] R. Mohanty, U. Mukha Balaji, and A. Pradhan, "An Accurate Non-iterative Fault Location Technique for Low Voltage DC Microgrid," *Power Delivery, IEEE Transactions on*, 2015.
- [136] J. Yang, "Fault analysis and protection for wind power generation systems," University of Glasgow, 2011.
- [137] P. Karlsson, "DC distributed power systems-Analysis, design and control for a renewable energy system," Lund University, 2002.
- [138] S.R.Bhide, *Digital Power System Protection*: PHI Learning Private Limited, 2014.
- [139] "IEC 61850-8-1, Communication networks and systems in substations – Part 8-1: Specific Communication Service Mapping (SCSM) – Mappings to MMS (ISO 9506-1 and ISO 9506-2) and to ISO/IEC 8802-3," ed: IEC, 2004.
- [140] K. Rudion, A. Orths, Z. Styczynski, and K. Strunz, "Design of benchmark of medium voltage distribution network for investigation of DG integration," in *Power Energy Society General Meeting, 2006. IEEE*, 2006, p. 6 pp.
- [141] B. Kasztenny, S. Conrad, P. Beaumont, K. Behrendt, O. Bolado, J. Boyle, *et al.*, "Exploring the IEEE C37.234 Guide for Protective Relay Application to Power System Buses," *Power Delivery, IEEE Transactions on*, vol. 26, pp. 936-943, 2011.
- [142] T. M. Haileselassie and K. Uhlen, "Impact of DC Line Voltage Drops on Power Flow of MTDC Using Droop Control," *Power Systems, IEEE Transactions on*, vol. 27, pp. 1441-1449, 2012.
- [143] "American National Standard for AC High-Voltage Circuit Breakers - Rated on a Symmetrical Current Basis - Preferred Ratings and Related Required Capabilities," *ANSI C37.06-2000*, pp. 1-36, 2003.
- [144] A. Anwar, Z. Yucheng, C. W. Brice, and R. A. Dougal, "Soft Reclosing of an Industrial Power Network Using an Inverter-Controlled Energy-Storage System," *Power Delivery, IEEE Transactions on*, vol. 29, pp. 1111-1119, 2014.

- 
- [145] M. Eriksson, M. Armendariz, O. O. Vasilenko, A. Saleem, and L. Nordstrom, "Multiagent-Based Distribution Automation Solution for Self-Healing Grids," *Industrial Electronics, IEEE Transactions on*, vol. 62, pp. 2620-2628, 2015.
- [146] L. Juan, M. Xi-Yuan, L. Chen-Ching, and K. P. Schneider, "Distribution System Restoration With Microgrids Using Spanning Tree Search," *Power Systems, IEEE Transactions on*, vol. 29, pp. 3021-3029, 2014.
- [147] "IEEE Guide for Voltage Sag Indices," *IEEE Std 1564-2014*, pp. 1-59, 2014.
- [148] M. Monadi, M. A. Zamani, A. Luna, J. I. Candela, and P. Rodriguez, "Protection of AC and DC distribution systems Embedding distributed energy resources: A comparative review and analysis," *Renewable & Sustainable Energy Reviews*, 2015.
- [149] J. F. Prada, "The Value of Reliability in Power Systems - Pricing Operating Reserves -," Energy Laboratory, Massachusetts Institute of Technology 1999.
- [150] R. F. Ghajar and R. Billinton, "Economic costs of power interruptions: a consistent model and methodology," *International Journal of Electrical Power & Energy Systems*, vol. 28, pp. 29-35, 1// 2006.
- [151] !!! INVALID CITATION !!! [11, 151].
- [152] H. Hooshyar, F. Mahmood, L. Vanfretti, and M. Baudette, "Specification, implementation, and hardware-in-the-loop real-time simulation of an active distribution grid," *Sustainable Energy, Grids and Networks*, vol. 3, pp. 36-51, 9// 2015.
- [153] Y. M. Atwa, E. F. El-Saadany, M. M. A. Salama, R. Seethapathy, M. Assam, and S. Conti, "Adequacy Evaluation of Distribution System Including Wind/Solar DG During Different Modes of Operation," *Power Systems, IEEE Transactions on*, vol. 26, pp. 1945-1952, 2011.
- [154] S. Tan, J. X. Xu, and S. K. Panda, "Optimization of Distribution Network Incorporating Distributed Generators: An Integrated Approach," *IEEE Transactions on Power Systems*, vol. 28, pp. 2421-2432, 2013.
- [155] R. Majumder, "Some Aspects of Stability in Microgrids," *IEEE Transactions on Power Systems*, vol. 28, pp. 3243-3252, 2013.
- [156] S. A. Arefifar and Y. A. R. I. Mohamed, "Probabilistic Optimal Reactive Power Planning in Distribution Systems With Renewable Resources in Grid-Connected and Islanded Modes," *Industrial Electronics, IEEE Transactions on*, vol. 61, pp. 5830-5839, 2014.
- [157] "IEEE Guide for Electric Power Distribution Reliability Indices," *IEEE Std 1366-2012 (Revision of IEEE Std 1366-2003)*, pp. 1-43, 2012.
- [158] F. Mahmood, H. Hooshyar, J. Lavenius, P. Lund, and L. Vanfretti, "Real-time Reduced Steady State Model Synthesis of Active Distribution Networks Using PMU Measurements," *IEEE Transactions on Power Delivery*, vol. PP, pp. 1-1, 2016.
- [159] C. Opathella and B. Venkatesh, "Three-Phase Unbalanced Power Flow Using a PI-Model of Controllable AC-DC Converters," *IEEE Transactions on Power Systems*, vol. PP, pp. 1-11, 2016.
-



---

## Laboratory Setup

### A. The Setup of the SEER Research Center

Fig. A.1. shows the structure and the general parts of the HIL test-bed setup of the SEER Research Center, at the Technical University of Catalonia (UPC). The proposed methods detailed in the Chapters 3, 4 and 5 have been implemented and evaluated in this setup. This setup consists of:

- OPAL-RT: real-time simulator that simulate the study systems.
- Programming host; a PC as command station that is used to run the Matlab/Simulink model that will be executed on the OPAL-RT
- DK60 board; a development board that is used to implement the proposed protection algorithms.
- Router; is used to connect all the setup devices in the same sub-network.

In this test-bed, the OP5600 HIL box from OPAL is used as real time (RT) simulator which takes care of running the simulations with a multi-processor configuration to provide a fast computation. A FPGA controller is used inside the OPAT-RT to connect the PCI bus of the processors to the digital and analogue inputs/outputs. Moreover, the board of this simulator is equipped with multiple analog and digital inputs/outputs for connecting different hardware providing thus a powerful tool for HIL testing.

## Appendix A. Laboratory Setup

---

To develop the real-time applications for the OPAL-RT, the RT-LAB software is used. This software is fully integrated with Matlab/Simulink. RT-LAB processes the Matlab/Simulink models, converts them to C-codes and uploads finally the converted model to the OPAL-RT. Moreover, it provides additional Simulink libraries, including an IEC61850 implementation that allows the exchange of two types of messages, defined by the standard: GOOSE (for sending status messages, e.g. trip commands) and Sampled Values (SV, used for transmitting current and voltage measurements).

The OPAL-RT is connected to the DK60 board through an Ethernet port. The DK60 board provides communication capabilities through various ports and protocols, including Ethernet, SPI, and CAN. For the processor running on the board, an IEC61850 stack implementation is available from SystemCORP that provides functionalities for all the three communication messages (MMS, GOOSE, and SV) of the IEC61850 protocol. This makes possible the development of custom applications using the IEC61850 communication protocol. This board embed an application developed in C++ and involved the implementation of the relay's algorithm. During the experiment tests, messages are exchanged between the OPAL-RT, and the DK60, running the proposed protection methods.

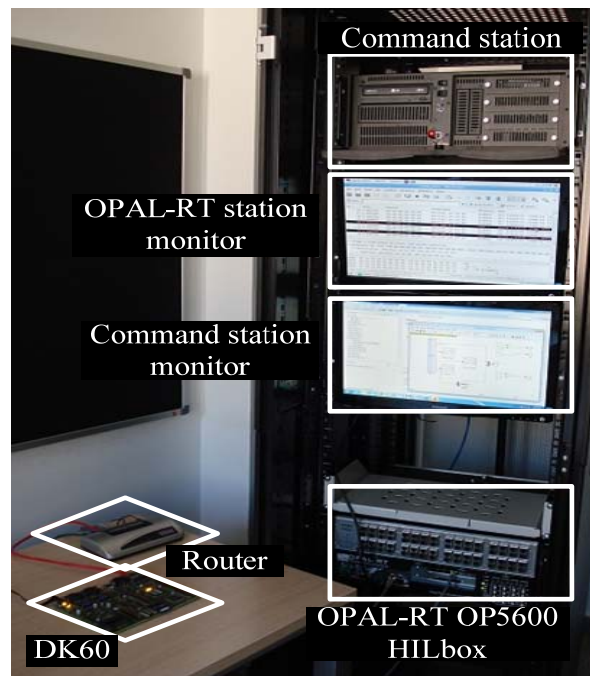


Fig. A.1. The HIL test-bed at the SEER Research Center (UPC)

### B. The setup of the SmarTS group

Fig. A.2 shows the architecture of the HIL simulation setup of the SmarTS group, KTH University. The optimized network clustering method, presented in Chapter 6 has been implemented and evaluated in this setup. Moreover, a novel adaptive autoreclosing scheme has been tested using this setup which has not addressed in this thesis.



Fig. A.2. The HIL test-bed (SmarTS Lab, KTH University)

**The components of this setup are:**

- Real time simulator, consisting of two OPAL-RT units (Target1 and Target2) each with 12 Intel i7 3.3 GHz cores.
- Protection relays from Schweitzer Engineering Laboratories (SEL); these relays have been used as PMUs.

## Appendix A. Laboratory Setup

---

- PMU data concentrator (PDC); to generate the required streams.
- WorkStation computers; the software that has been executed on these PCs are:
  - Matlab 2011/Simulink
  - RT-Lab 11.05
  - LabVIEW
- Compact Reconfigurable IO controllers (cRIO) from National Instruments (NI) Corporation consisting of:
  - Controller 9081,
  - 25ns FPGA execution rate,
  - 1.06 GHz dual-core Intel Celeron processor (RT); 16 GB nonvolatile storage,
  - 2 GB DDR3 800 MHz RAM,
  - 8-slot Spartan-6 LX75 FPGA chassis for custom I/O timing, control, and processing,
  - NI 9264 Analogue Voltage Output Module: 16 channel analogue voltage out,
  - This controller has been used to implement the proposed ONC method.
- GPS antenna.
- Amplifiers; to boost the output voltage and current of the simulators.

---

## A Conventional ONC method

If it is assumed that all the lines of the study systems are equipped with CBs, then a conventional ONC method can be presented with the following steps:

### **Step1: Finding the starting points**

In the first step, a starting point is determined for each possible microgrid. The locations of the dispatchable DGs (DDGs) are selected as the starting points. These points are selected to meet one of the main constraints (in each MG, the rated capacity of DDGs have to be at least 60% of the total DGs output).

### **Step2: Forming the fundamental microgrids (FMGs)**

From each DDG, its corresponding FMG is formed based on the two main constraints i.e., load/Gen balance and generation control as determined in (6.1) to (6.4).

### **Step3: Forming the candidate Microgrid sets (CMGS)**

A FMG is the smallest zone of an on-outage area which can operate successfully considering the conditions presented in (6.1) and (6.4). However, the autonomous operation of FMGs cannot necessarily provide the optimum operation for the on-outage section. Hence, in this step, various scenarios for interconnection of the FMGs are considered. It means that, in this step, several possible arrangements for the FMGs integration are determined. For each arrangement, the combination of FMGs results in creating a candidate microgrid set (CMS). Consequently, a list consist of CMSs is created which all of them satisfy the minimum requirement for the successful autonomous operation. It should be noted

that, in this stage, the loads that are not located inside a FMG will be connected to one of the neighbor FMGs and the load shedding process is applied to the related FMG if it is necessary.

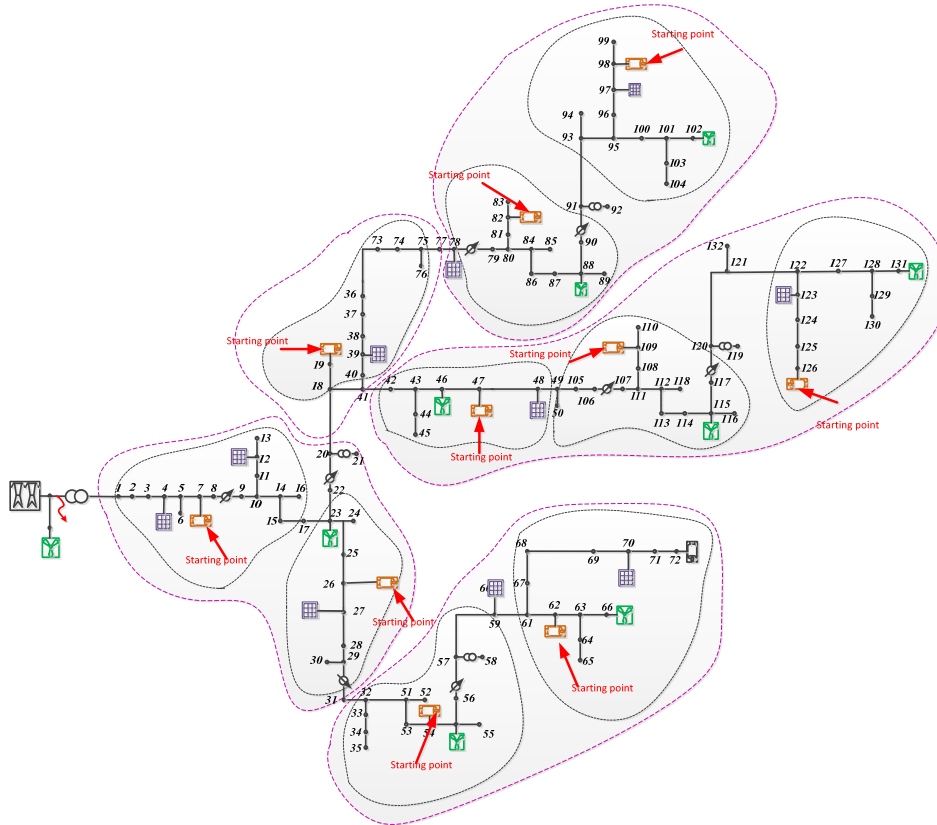


Fig. B.1. Fundamental Microgrids and a possible arrangement for CMSs.

#### Step 4: Calculating the optimization objectives

In order to achieve the optimal operation of an on-outage zone various parameters can be introduced as the goals of the optimization process. In this research, in order to achieve the optimized clustering, three objective functions (OFs) are considered. These OFs are:  $F_1$ : to minimize the total loss,  $F_2$ : to minimize the voltage deviation, and  $F_3$ : to minimize the total power of the disconnected loads. Therefore, in this stage for each CMS, the power loss and the voltage deviation of the on-outage zone is calculated.

### Step5. Choosing the optimum MGs

In the final step, according to the calculations in step 4, the optimum CMS is selected. To provide a comprehensive objective function, a multi-objective function is used to consider all the above mentioned objective functions together. In this new function, shown below, each objective function contributes according to its priority and importance [156]:

$$F_m = K_1 * F_1 + K_2 * F_2 + K_3 * F_3 \quad (B.1)$$

where  $K_i$  is the weight of  $F_i$  and determines the importance of this function.